

**KANSAS RIGID PAVEMENT ANALYSIS FOLLOWING NEW
MECHANISTIC-EMPIRICAL DESIGN GUIDE**

By

TASLIMA KHANUM

B.S., Bangladesh University of Engineering and Technology, 2002

A THESIS

**Submitted in partial fulfillment of the
Requirements for the degree**

MASTER OF SCIENCE

**Department of Civil Engineering
College of Engineering**

**KANSAS STATE UNIVERSITY
Manhattan, Kansas
2005**

Approved by:

**Major Professor
Dr. Mustaque Hossain**

ABSTRACT

The AASHTO Guide for Design of Pavement Structures is the primary document used by the state highway agencies to design new and rehabilitated highway pavements. Currently the Kansas Department of Transportation (KDOT) uses the 1993 edition of the AASHTO pavement design guide, based on empirical performance equations, for the design of Jointed Plain Concrete Pavements (JPCP). However, the newly released Mechanistic-Empirical Pavement Design Guide (MEPDG) provides methodologies for mechanistic-empirical pavement design while accounting for local materials, environmental conditions, and actual highway traffic load distribution by means of axle load spectra.

The major objective of this study was to predict pavement distresses from the MEPDG design analysis for selected in-service JPCP projects in Kansas. Five roadway sections designed by KDOT and three long term pavement performance (LTPP) sections in Kansas were analyzed. Project-specific construction, materials, climatic, and traffic data were also generated in the study. Typical examples of axle load spectra calculations from the existing Weigh-in-Motion (WIM) data were provided. Vehicle class and hourly truck traffic distributions were also derived from Automatic Vehicle Classification (AVC) data provided by KDOT. The predicted output variables, IRI, percent slabs cracked, and faulting values, were compared with those obtained during annual pavement management system (PMS) condition survey done by KDOT. A sensitivity analysis was also performed to determine the sensitivity of the output variables due to variations in the key input parameters used in the design process. Finally, the interaction of selected

significant factors through statistical analysis was identified to find the effect on current KDOT specifications for rigid pavement construction.

The results showed that IRI was the most sensitive output. For most projects in this study, the predicted IRI was similar to the measured values. MEPDG analysis showed minimal or no faulting and was confirmed by visual observation. Only a few projects showed some cracking. It was also observed that the MEPDG outputs were very sensitive to some specific traffic, material, and construction input parameters such as, average daily truck traffic, truck percentages, dowel diameter, tied concrete shoulder, widened lane, slab thickness, coefficient of thermal expansion, compressive strength, base type, etc. Statistical analysis results showed that the current KDOT Percent Within Limits (PWL) specifications for concrete pavement construction are more sensitive to the concrete strength than to the slab thickness. Concrete slab thickness, strength, and truck traffic significantly influence the distresses predicted by MEPDG in most cases. The interactions among these factors are also almost always evident.

TABLE OF CONTENTS

TABLE OF CONTENTS.....	i
LIST OF FIGURES.....	iv
LIST OF TABLES.....	viii
ACKNOWLEDGEMENTS.....	xi
CHAPTER 1.....	1
1.1 Introduction.....	1
1.2 Pavement Types.....	2
1.3 Problem Statement.....	3
1.4 Objectives.....	7
1.5 Organization of the Thesis.....	7
CHAPTER 2.....	9
LITERATURE REVIEW.....	9
2.1 Types of Concrete Pavement.....	9
2.2 Jointed Plain Concrete Pavement (JPCP).....	12
2.2.1 Geometric Design.....	12
2.2.2 Drainage.....	14
2.2.3 Concrete Slab.....	17
2.2.4 Concrete mixture.....	18
2.2.4.1 Cement Content and Type.....	19
2.2.4.2 Coarse Aggregate.....	19
2.2.4.3 Fine Aggregate.....	20
2.2.4.4 Admixtures and Air Content.....	21
2.2.4.5 Concrete Consistency.....	21
2.2.4.6 Water-Cement Ratio.....	21
2.2.4.7 Concrete Mixing and Delivery.....	22
2.2.5 Shoulder and Widened lane.....	22
2.2.6 Base/Subbase.....	24
2.2.6.1 Granular Base.....	25
2.2.6.2 Asphalt-treated Base.....	25
2.2.6.3 Cement-treated Base.....	26
2.2.6.4 Lean Concrete Base.....	26
2.2.6.5 Permeable Base.....	27
2.2.7 Subgrade.....	27
2.2.8 Joints in JPCP.....	29
2.2.8.1 Load Transfer Devices.....	31
2.2.9 PCCP Construction.....	35
2.3 JPCP Design Methods.....	39
2.4 Framework for the Mechanistic-Empirical Design Method.....	41
2.4.1 Basic Design Concept.....	41

2.4.2	Advantages over Empirical Design procedure	41
2.4.3	Design Overview	42
2.5	NCHRP Mechanistic-Empirical Pavement Design Guide (MEPDG)	49
2.5.1	Design Approach	49
2.5.2	Overview of the Design Process for JPCP.....	50
2.5.3	Key JPCP Distresses and Critical Responses	52
2.5.4	Smoothness (IRI) prediction.....	55
2.5.5	JPCP Performance Prediction Models	56
2.5.5.1	Cracking Model	56
2.5.5.2	Faulting Model.....	57
2.5.5.3	Smoothness Model.....	58
2.6	JPCP Evaluation and Management in Kansas	59
2.6.1	Profile/Roughness Data Collection.....	60
2.6.2	Faulting	62
2.6.3	Joint Distress.....	63
2.6.4	Definition of Pavement Condition	63
2.7	Mechanistic-Empirical Pavement Design Guide (MEPDG) Software.....	65
2.7.1	MEPDG Software Layout.....	66
2.8	Summary	75
CHAPTER 3		76
TEST SECTIONS AND DESIGN ANALYSIS INPUTS		76
3.1	Test Sections	76
3.2	Inputs.....	78
3.3	Hierarchical Design Inputs	78
3.4	Development of Kansas-Specific MEPDG Inputs.....	79
3.4.1	General.....	80
3.4.1.1	General Information.....	80
3.4.1.2	Site Identification.....	82
3.4.1.3	Analysis Parameters.....	82
3.4.2	Traffic	83
3.4.2.1	MEPDG Hierarchical Traffic Inputs.....	84
3.4.2.2	Kansas Traffic Monitoring System for Highways (TMS/H)	87
3.4.2.3	Base Year Input.....	88
3.4.2.4	Traffic Volume Adjustments	89
3.4.2.5	General Traffic Input	106
3.4.3	Climate.....	109
3.4.3.1	Climatic file generation.....	110
3.4.4	Structure.....	111
3.4.4.1	Design Features of JPCP.....	112
3.4.4.2	Drainage and Surface Properties.....	117
3.4.4.3	Pavement Layers.....	118
CHAPTER 4.....		136
DESIGN AND SENSITIVITY ANALYSIS		136

4.1	Prediction and Comparison of Distresses from Design Analysis	136
4.1.1	Smoothness or IRI.....	136
4.1.2	Faulting	139
4.1.3	Percent Slabs Cracked.....	141
4.2	Sensitivity Analysis	142
4.2.1	Traffic Input.....	143
4.2.2	Material.....	149
4.2.3	Design and Construction Features	160
4.2.4	Alternative Design	180
CHAPTER 5.....		184
EFFECT OF JPCP PERFORMANCE ON PCC QC/QA SPECIFICATIONS.....		184
5.1	Introduction.....	184
5.2	KDOT QC/QA Specification for PCC.....	185
5.2.1	Overview.....	185
5.3	KDOT PCCP PWL Pay Factor Computation Inputs	187
5.4	MEPDG-Predicted Performance and Corresponding PWL Results.....	188
5.5	Statistical Analysis.....	189
5.6	Effect of Thickness and Strength on Predicted Distresses.....	194
5.7	Interaction of Thickness and Strength on Predicted Distresses Based on Bonferroni Adjustment	204
5.8	Interaction of Strength-Traffic Based on With and Without Bonferroni Adjustment.....	211
5.9	Thickness-Traffic Interaction Based on With and Without Bonferroni Adjustment.....	212
CHAPTER 6.....		213
CONCLUSIONS AND RECOMMENDATIONS.....		213
6.1	Conclusions.....	213
6.2	Recommendations.....	217
REFERENCES.....		218
APPENDICES.....		223
	Appendix-A.....	223
	Appendix-B.....	243

LIST OF FIGURES

Figure 1.1	Components of (a) Flexible and (b) Rigid pavements.....	3
Figure 2.1	Types of Concrete pavements (ACPA 2005).....	10
Figure 2.2	Typical cross-section of a two lane highway (AASHTO 1984).....	13
Figure 2.3	Typical cross-section of a divided highway in Kansas.....	13
Figure 2.4	Basic component of a concrete pavement (ACPA 2005).....	18
Figure 2.5	Short steel dowel bars.....	32
Figure 2.6	Typical dowel layout.....	33
Figure 2.7	Deformed tie bars.....	34
Figure 2.8	PCCP paving operation in Kansas.....	37
Figure 2.9	Typical joint sawing operation in Kansas.....	37
Figure 2.10	Curing operations using liquid membrane forming curing compound.....	39
Figure 2.11	Prediction of distress over time.....	47
Figure 2.12	PCC mechanistic-empirical design framework (NCHRP 2004).....	50
Figure 2.13	Overall design process for JPCP.....	52
Figure 2.14	Critical loading and structural response location for JPCP bottom-up transverse cracking.....	53
Figure 2.15	Critical loading and structural response location for JPCP top-down transverse cracking.....	54
Figure 2.16	Schematic of faulting.....	54
Figure 2.17	Critical loading and structural response location for JPCP faulting analysis.....	55
Figure 2.18	KDOT South Dakota-type profilometer.....	60
Figure 2.19	Quarter Car simulation of road roughness (Sayers 1985).....	61

Figure 2.20	KDOT fault calculation algorithm.....	62
Figure 2.21	Opening screen for MEPDG software.....	66
Figure 2.22	Program layout.....	67
Figure 2.23	Color-coded inputs.....	67
Figure 2.24	Traffic screen.....	68
Figure 2.25	Monthly adjustment factors screen.....	69
Figure 2.26	Vehicle class distribution screen.....	69
Figure 2.27	Hourly distribution screen.....	70
Figure 2.28	Axle load spectra screen.....	70
Figure 2.29	Climatic screen.....	71
Figure 2.30	JPCP design features screen.....	72
Figure 2.31	JPCP layers screen.....	72
Figure 2.32	Output summaries for IRI.....	74
Figure 2.33	Output summaries for Faulting.....	74
Figure 3.34	Output summaries for Cracking.....	75
Figure 3.1	Illustration of the FHWA vehicle classes for MEPDG (Milestones 2002).....	86
Figure 3.2	Comparison of monthly adjustment factor distribution for Kansas input and MEPDG default.....	93
Figure 3.3	Comparison of MEPDG default truck class distribution with Kansas input for Principal Arterials (urban).....	95
Figure 3.4	Typical hourly distribution for Rural Interstate compare to MEPDG default input.....	97
Figure 3.5	Typical axle configurations for vehicle Class 9.....	104
Figure 3.6	Comparison of axle load distribution for Class 9 vehicle with MEPDG default distribution.....	104

Figure 3.7	Gradation for permeable and semi-permeable base materials.....	131
Figure 4.1	Predicted and measured JPCP distresses on Interstate sections.....	137
Figure 4.2	Predicted and measured JPCP distresses on Non-Interstate sections.....	138
Figure 4.3	Predicted JPCP distresses at varying levels of AADT.....	145
Figure 4.4	Predicted JPCP distresses at varying levels of truck traffic.....	147
Figure 4.5	Predicted JPCP distresses at varying levels of class 9 truck type.....	148
Figure 4.6	Predicted JPCP distresses for varying PCC strength.....	150
Figure 4.7	Predicted JPCP distresses for different CTE input.....	153
Figure 4.8	Predicted JPCP Distresses for different Shrinkage Strain input.....	155
Figure 4.9	Predicted JPCP distresses for different pavement construction months.....	157
Figure 4.10	Predicted JPCP distresses for different Subgrade Soil Type.....	159
Figure 4.11	Predicted JPCP distresses on KDOT sections for varying thickness.....	161
Figure 4.12	Predicted JPCP distresses on SPS-2 Sections for varying thickness.....	163
Figure 4.13	Predicted JPCP distresses for different dowel diameters.....	167
Figure 4.14	Predicted JPCP distresses for different dowel spacing.....	169
Figure 4.15	Predicted JPCP distresses for different shoulder type.....	171
Figure 4.16	Predicted JPCP Distresses for different lane widths.....	174
Figure 4.17	Predicted JPCP distresses for curing type.....	175
Figure 4.18	Predicted JPCP distresses for different granular bases.....	177
Figure 4.19	Predicted JPCP distresses for stabilized bases.....	179
Figure 4.20	Predicted JPCP distresses for alternative designs.....	181
Figure 5.1	Cross section of the pavements studied.....	190

Figure 5.2 Variation of predicted distresses with thickness for I-70 Shawnee county
and K-7 Johnson county projects..... 200

LIST OF TABLES

Table 2.1	Gradation for Coarse Aggregate for Pavement Concrete (KDOT 1990)..	20
Table 2.2	Grading Requirements for Fine Aggregate (KDOT 1990).....	21
Table 3.1	Project Features of the Study Sections.....	77
Table 3.2	Recommended Design Reliability for MEPDG (NCHRP 2004).....	83
Table 3.3	Summarization of Base Year Input.....	89
Table 3.4	Adjustment Factors Report for Rural Interstate Highways (KDOT 2003)	91
Table 3.5	Adjustment Factors Report for Other Urban Roadways (KDOT 2003)...	91
Table 3.6	Adjustment Factors Report for Other Rural Roadways (KDOT 2003)....	92
Table 3.7	Vehicle Class Distribution based on Functional Classification of Roadways.....	94
Table 3.8	Vehicle Classification Record (“C”- Card) File Code.....	96
Table 3.9	Hourly Truck Traffic Distribution Values Based on the Functional Classification of the Roadways.....	98
Table 3.10	Function Used in Computing/ Forecasting Truck Traffic Over Time (NCHRP 2004).....	99
Table 3.11	Truck Weight Record (“W”-Card) for Axle Load Distribution Factor...	102
Table 3.12	Typical Example of Axle Load Spectra Calculation for Vehicle Class 9.....	105
Table 3.13	Frequency Distribution of Tandem axle for Month of January.....	105
Table 3.14	Default Distribution for Number of Axles/ Truck (NCHRP 2004).....	107
Table 3.15	Summarization of the Project Specific Latitude, Longitude, Elevation and Water Table Depth.....	111
Table 3.16	Structural Input Parameters for MEPDG Rigid Pavement Design Analysis.....	120
Table 3.17	Strength and Modulus of Elasticity Inputs for JPCP and CRCP Design.....	122

Table 3.18	Approximate Relationship between Shrinkage and Indirect Tensile Strength of PCC.....	128
Table 3.19	Inputs for Different Base type.....	130
Table 4.1	Comparison of Predicted Response.....	140
Table 4.2	Measured Responses.....	141
Table 4.3	Effect of Traffic (AADT) on Predicted Responses.....	146
Table 4.4	Comparison of Predicted Response Corresponding to Different Coefficient of Thermal Expansion.....	152
Table 4.5	Comparison of Predicted Response Corresponding to Varying Different Dowel Diameter.....	166
Table 4.6	Comparison of Predicted Responses Corresponding to Tied and Untied Shoulders.....	170
Table 4.7	Comparison of Predicted Response Corresponding to Varying Lane Width.....	173
Table 4.8	Comparison of Predicted Responses Corresponding to Different Design Strategy.....	180
Table 5.1	Predicted Distresses and PWL for the Projects.....	189
Table 5.2	Analysis of Variance for the Effect of Strength, Thickness and Traffic.....	193
Table 5.3	Effect of Interaction of Thickness (T) and Strength (S) on Predicted IRI for SPS-2 Control Section.....	195
Table 5.4	Effect of Interaction of Thickness (T) and Strength (S) on Predicted IRI for I-70, Shawnee County.....	198
Table 5.5	Effect of Interaction of Thickness (T) and Strength (S) on Predicted for K-7, Johnson County.....	202
Table 5.6	Effect of Interaction of Thickness and Strength on Predicted IRI for SPS-2 Control Section (with Bonferroni adjustment).....	207
Table 5.7	Effect of Interaction of Thickness (T) and Strength (S) on Predicted IRI for I-70, Shawnee County (With Bonferroni adjustment).....	208

Table 5.8	Effect of Interaction of Thickness (T) and Strength (S) on Predicted IRI for K-7, Johnson County (with Bonferroni adjustment).....	210
-----------	--	-----

ACKNOWLEDGEMENTS

I wish to express my deepest gratitude and sincere appreciation to Dr. Mustaque Hossain, for his constant guidance, dedication, and encouragement throughout the course of the study. His systematic guidance, moral support, constant persuasion, motivation, and encouragement helped me at all stages to complete this thesis. I would also like to thank Dr. Stefan Romanoschi for being on my thesis committee and for his valuable suggestions and comments. Special thanks are due to Dr. Jim Neill for being a committee member and also for his valuable guidance in the statistical analysis for this study. Thanks are also due to Mr. Ke Zhang of the Department of Statistics for his help in SAS coding and output interpretation.

I gratefully acknowledge the financial support provided by the Kansas Department of Transportation (KDOT). I wish to thank Mr. Richard Barezinisky, P.E., and Mr. Greg Schiber, E.I.T. who served as the project monitors. I would also like to thank Mr. Andrew. J. Gisi, P.E. of KDOT for his review of this work. Assistance of Mr. Jose Villarreal of the Department of Civil Engineering at Kansas State University in this thesis is highly appreciated. Special thanks are also due to Mr. Cody Gratny for his help in traffic classification and load analysis.

Finally, I am grateful to my parents, siblings, and my husband, Nazrul Islam, for their affection and love toward my work and for all their sacrifices that they have made to pave a smooth path for me leading to the present.

CHAPTER 1

1.1 Introduction

The most widely used procedure for design of concrete pavements is specified in the *Guide for Design of Pavement Structures*, published in 1986 and 1993, by the American Association of State Highway and Transportation Officials (AASHTO 1986; AASHTO 1993). A few states use the 1972 American Association of State Highway Officials (AASHTO) Interim Guide procedure, the Portland Cement Association (PCA) procedure, their own empirical or mechanistic-empirical procedure, or a design catalog (Hall 2003). The 1986 and 1993 Guides contained some state-of-practice refinements in materials input parameters and design procedures for rehabilitation design. In recognition of the limitations of earlier Guides, the AASHTO Joint Task Force on Pavements (JTTFP) initiated an effort in the late nineties to develop an improved Guide by 2002. The major long-term goal identified by the JTTFP was the development of a design guide based as fully as possible on mechanistic principles. The National Cooperative Highway Research Program (NCHRP) sponsored project 1-37A to develop a user-friendly procedure capable of doing mechanistic-empirical design while accounting for local environment conditions, local highway materials, and actual highway traffic distribution by means of axle load spectra. The overall objective of the NCHRP guide for the Mechanistic-Empirical Design of New and Rehabilitated Pavement Structures (now known as MEPDG) is to provide the highway community with a state-of-the-practice tool for the design of new and rehabilitated pavement structures, based on mechanistic-empirical principles.

1.2 Pavement Types

Paved roads are an integral part of our transportation system. Currently, there are over 3.96 million public centerline road miles (8.28 million lane miles) in the U.S. and of this 2.5 million miles (or about 63% percent) are paved (FHWA 2002). Historically, pavements have been divided into two broad categories, either flexible (asphalt concrete) pavements, constructed from bituminous materials, or rigid (concrete) pavements, constructed from Portland cement concrete (PCC) (Yoder & Witczak 1975). The flexible pavement may consist of a relatively thin wearing surface built over a base course and subbase course. The entire pavement structure, which is constructed over the subgrade, is designed to support the traffic load and distribute the load over the roadbed (Yoder & Witczak 1975). In contrast, the rigid pavement may or may not have a base course between the pavement slab and the subgrade. Base courses are used under rigid pavements for various reasons such as: (1) control of pumping, (2) control of frost action, (3) drainage, (4) control of shrink and swell potential of the subgrade soil, and (5) expedient construction. Base course in rigid pavements also provides some structural capacity, however it has no significant impact on the load-carrying capacity of the pavement slab.

The essential difference between the two major types of pavements is the mechanics of load distribution on the subgrade. In case of rigid pavement, the applied load tends to be distributed over a relatively wide area of soil due to the rigidity and high modulus of elasticity of the PCC slab. These pavements are called “rigid” because they are substantially stiffer than flexible pavements due to the high stiffness of the concrete slab. Rigid pavements comprise about seven percent of all paved roads in the U.S.

Flexible pavement structure “bends” or “deflects” due to traffic load. This pavement type is generally composed of several layers of materials that can accommodate this “flexing.” About 93 percent of the U.S paved roads are flexible. In general, both flexible and rigid pavements can be designed for longer life (e.g., in excess of 30 years). Both types have been used for just about every functional classification of highways. There are many different reasons for choosing one type of pavement or the other, some practical, some economical, and some political (NCHRP 2004). Figure 1.1 shows the typical cross section of flexible and rigid pavements.

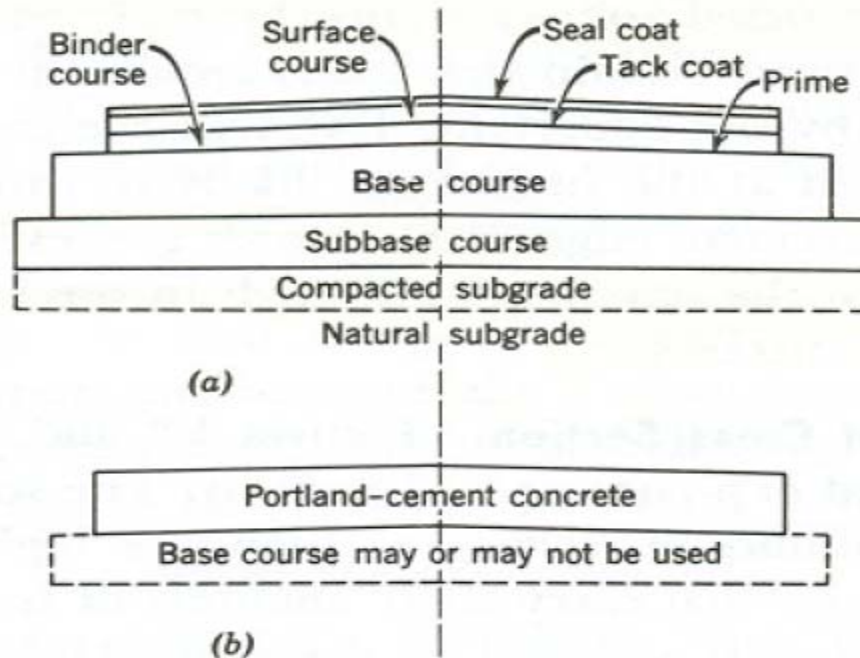


Figure 1.1 Components of (a) Flexible and (b) Rigid pavements (Yoder & Witczak 1975)

1.3 Problem Statement

The *AASHTO Guide for the Design of Pavement Structures* is the primary document used by the state highway agencies to design new and rehabilitated highway pavements. The

National Pavement Design Review conducted by the Federal Highway Administration (FHWA) during 1995-1997 found that some 80% of the states make use of either the 1972, 1986, or 1993 AASHTO Pavement Design Guide (KSU Proposal 2003). The Kansas Department of Transportation (KDOT) is currently using the 1993 AASHTO pavement design guide. All AASHTO Design Guide versions are based on empirical performance equations developed using the AASHO (now AASHTO) Road Test data from the late 1950's. Although various editions of the AASHTO Design Guide have served the pavement community well for several decades, many serious limitations exist for their continued use as primary pavement design procedures. The limitations are described as follows (NCHRP 2004):

- ◆ One of the serious limitations of the AASHO Road Test is the traffic loading deficiency. Heavy truck traffic design volume levels have increased tremendously (about 10 to 20 times) since the design of the pavements used in the Interstate system in the 1960's. The original Interstate pavements were designed for 5 to 15 million trucks over a 20 year period, whereas today these same pavements must be designed for 50 to 200 million trucks and sometimes, for even longer design life (e.g., 30-40 years).
- ◆ Pavement rehabilitation was not included in the Road Test experimental design. The rehabilitation design procedures described in the 1993 Guide are completely empirical and limited, especially in consideration of heavy traffic.
- ◆ Since the Road test was conducted at one geographic location, it is very difficult to address the effects of different climatic conditions on the pavement performance equation developed.

- ◆ Only one type of subgrade soil was used for all test sections at the Road Test.
- ◆ During the Road Test, only one type of surface material was used for each of the different pavement type, such as hot mix asphalt (HMA) mixture for flexible and one Portland cement concrete (PCC) mixture for concrete pavements. Currently, different types of mixture, such as Superpave, Stone Mastic Asphalt (SMA), high-strength PCC, etc., are available.
- ◆ Only unstabilized, dense graded granular bases were included in the main pavement sections (limited use of treated base was included for flexible pavements). Currently, most pavements are constructed over stabilized base or subbase, especially for heavier traffic loading.
- ◆ Vehicle suspension, axle configuration, and tire types and pressures were representatives of the vehicles used in the late 1950's. Most of those are outmoded today.
- ◆ Pavement designs, materials and construction were representative of those at the time of the Road Test. For example, no sub-drainage was included in the Road Test sections, but positive subdrainage has become common in today's highways.
- ◆ The Road Test only lasted approximately two years, and has been used for the design of pavements that are supposed to last for 20 years. Therefore, significant interpolation is required to ensure the design life reliability.
- ◆ Earlier AASHTO procedures relate the thickness of the pavement surface layers (asphalt layers or concrete slab) to serviceability. However, research and observations have shown that many pavements need rehabilitation for

reasons that are not related directly to the pavement thickness (e.g., rutting, thermal cracking, and faulting). These failure modes are not considered directly in the previous versions of the AASHTO Guide.

- ◆ According to the 1986 AASHTO Guide, desired reliability level can be achieved through a large multiplier of design traffic loading and this has never been validated. The multiplier increased greatly with the design level of reliability and may result in excessive layer thickness for pavements carrying heavier traffic.

These limitations have long been recognized by the pavement design community. Beginning in 1987 with the NCHRP Project 1-26, formal steps were taken to include mechanistic principles in the AASHTO design procedures. An NCHRP report published in 1990 first recommended the inclusion of the mechanistic procedures in the AASHTO guide. This research proposed two programs, ILLI-PAVE and ILLI-SLAB for flexible and rigid pavement design, respectively. In turn, mechanistic design procedures for the rigid pavement were included as a supplement to the *1993 Guide* (NCHRP 1990).

The AASHTO Joint Task Force on Pavements (JTTFP) initiated an effort to develop an improved design guide in 1997. NCHRP project 1-37 was the initial step toward developing this new guide. Finally the objective was accomplished through developing MEPDG itself, which is based on the existing mechanistic-empirical technologies. User-oriented computational software and documentation based on the MEPDG procedure have also enhanced the objective. Since the resulting procedure is very sound and flexible, and it considerably surpasses any currently available pavement design and analysis tools, it is expected it will be adopted by AASHTO as the new AASHTO design

method for pavements structures (NCHRP 2004). It is also expected that KDOT will adopt the new AASHTO design method to replace the 1993 AASHTO design method currently in use.

1.4 Objectives

The major objective of this study was to predict distresses from the MEPDG design analysis for selected in-service Jointed Plain Concrete Pavement (JPCP) projects in Kansas. The predicted distresses were then to be compared with the available measured distresses. Sensitivity analysis was also to be performed for determining the sensitivity of the output variables due to variations in the key input parameters used in the design process. For this task, project-specific material, climatic, and traffic inputs also needed to be generated. Typical examples of axle load spectra calculation from the existing Weigh-in-Motion (WIM) data were done. Vehicle class and hourly truck traffic distributions needed to be derived from the KDOT-provided Automatic Vehicle Classification (AVC) data. The final objective was to identify the interactions of some significant factors through statistical analysis to find the effect on the current KDOT specifications for rigid pavement construction process.

1.5 Organization of the Thesis

The thesis is divided into six chapters. Chapter 1 is an introduction to the problem. Chapter 2 presents an overview of the Jointed Plain Concrete Pavements (JPCP). It also describes the framework for the Mechanistic-Empirical pavement design method and the new MEPDG software. Chapter 3 describes the study sections and input data generation

process. Chapter 4 presents the MEPDG design analysis of some existing JPCP projects in Kansas and the sensitivity analysis of the factors that significantly affect predicted JPCP distresses. Chapter 5 presents the statistical analysis to identify the interactions of some significant factors and the effect on current KDOT specifications for rigid pavement construction process. Finally Chapter 6 presents the conclusions based on this study and recommendations for future research.

CHAPTER 2

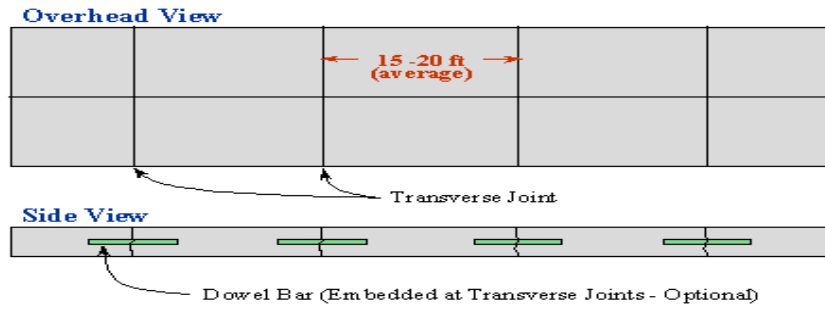
LITERATURE REVIEW

This chapter presents an overview of the Jointed Plain Concrete Pavement, the framework for the Mechanistic-Empirical pavement design method, and an introduction to the new Mechanistic-Empirical Design Guide software developed by the National Cooperative Highway Research Program (NCHRP).

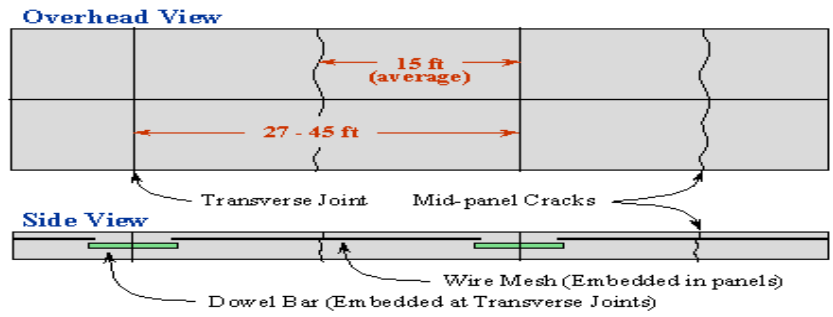
2.1 Types of Concrete Pavement

According to the American Concrete Pavement Association (ACPA 2005), concrete pavement can be classified into three types: jointed plain concrete pavement (JPCP), jointed reinforced concrete pavement (JRCP), and continuously reinforced concrete pavement (CRCP). This classification was done based on the joint spacing and use of reinforcement. Figure 2.1 shows the plan and side views of these pavement types.

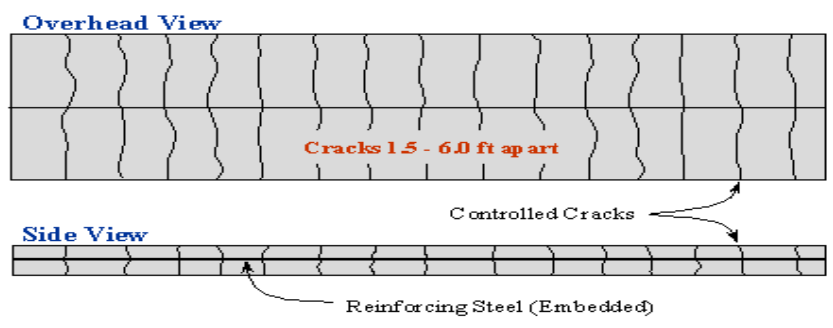
Jointed plain concrete pavements (JPCP) have sufficient number of joints to control the locations of all expected cracks. The concrete cracks at the joint locations and not elsewhere in the slabs. Jointed plain pavements do not contain any steel reinforcement. However, there may be smooth dowel bars at the transverse joints and tie bars at the longitudinal joints. The spacing between the transverse joints is typically about 15 feet for slabs 7 to 12 inches thick. Today, a majority of the U.S. state agencies build jointed plain concrete pavements (ACPA 2005).



a) Jointed Plain Concrete Pavement (JPCP)



b) Jointed Reinforced Concrete Pavement (JRCP)



c) Continuously Reinforced Concrete Pavement (CRCP)

Figure 2.1 Types of Concrete Pavements (ACPA 2005)

Jointed reinforced concrete pavements (JRCP) contain steel mesh reinforcement (sometimes called distributed steel). In JRCP, designers increase the joint spacing purposely, and include reinforcing steel to hold together intermediate cracks in each slab. The spacing between the transverse joints is typically 30 feet or more. In the past, some agencies used spacing as large as 100 feet. During construction of the interstate system, most agencies in the Eastern and Midwestern U.S. built jointed-reinforced concrete pavement. Today only a handful of agencies employ this design.

Continuously reinforced concrete pavements (CRCP) do not require any transverse contraction joints. Transverse shrinkage cracks are expected in the slab, usually at intervals of 3 to 5 ft. CRC pavements are designed with enough steel, 0.6 to 0.7% by cross-sectional area, so that cracks are held together tightly. An appropriate spacing between the cracks is determined in the design process.

CRCP designs generally cost more than jointed reinforced or jointed plain designs initially due to increased quantities of steel. However, they can demonstrate superior long-term performance and cost-effectiveness. A number of agencies choose to use CRCP designs in their busy, urban corridors carrying heavy traffic.

2.2 Jointed Plain Concrete Pavement (JPCP)

2.2.1 Geometric Design

The principal elements of a roadway cross section consist of the travel lanes, shoulder, and medians (for some multilane highways). Marginal elements include median and roadside barrier, curbs, gutters, guard rails, sidewalks, and side slopes. Figure 2.2 shows a typical cross section for a two-lane highway.

Travel lane widths usually vary from 9 to 12 ft, with a 12-ft lane being predominant on most high-type highways (AASHTO 2004). It is generally accepted that lane widths of 12 ft should be provided on main highways. Widened lane of 14 ft width is also used in Kansas, for some experimental purposes, though this lane width is not a very common practice nation wide.

A shoulder is the portion of the roadway contiguous with the traveled way for accommodation of stopped vehicles, for emergency use, and for lateral support of subbase, base, and surface courses (AASHTO 2004). Shoulder width varies from only 2 ft or so on minor rural roads to about 12 ft on major roads. Shoulder can be tied or untied. Tie bars are used to construct tied shoulder. Shoulder width in Kansas is governed by the shoulder design policy. Full-width shoulders for a 2-lane pavement are 10 ft wide. For 4-lane highways, the outside shoulders are 10 ft wide and the inside shoulders are 6 ft wide. Lower volume highways may have shoulders from 3 to 10 ft widths. Some shoulders may be composite with the 3 ft shoulder adjacent to the traveled way being paved and the shoulder outside this may be turf or aggregate surfaced.

The right lane in a four-lane divided highway section is designated as the driving lane. The left lane is the passing lane. Two lane and wider undivided pavements on

tangents or on flat curves have a crown or high point in the middle, and slope downward toward both edges. This provides a cross slope, whose cross section can be either curved or plane or a combination of the two. AASHTO recommended (2004) cross slope rates are 1.5 percent to 2.0 percent for high-type pavements, 1.5 percent to 3.0 percent for intermediate-type of pavements, 2.0 to 6.0 percent for low-type pavements. In Kansas, the traveled way has a typical cross slope of 1.6 percent (3/16 inch per ft) as shown in Figure 2.3. The shoulders have a cross slope of 4.2 percent. The shoulder side slope is 1:6.

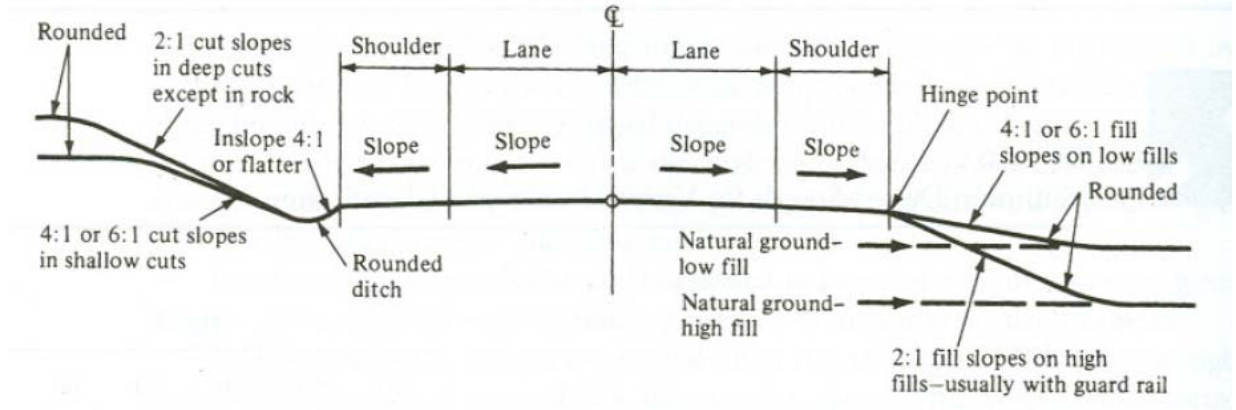


Figure 2.2 Typical cross-section of a two-lane highway (AASHTO 1984)

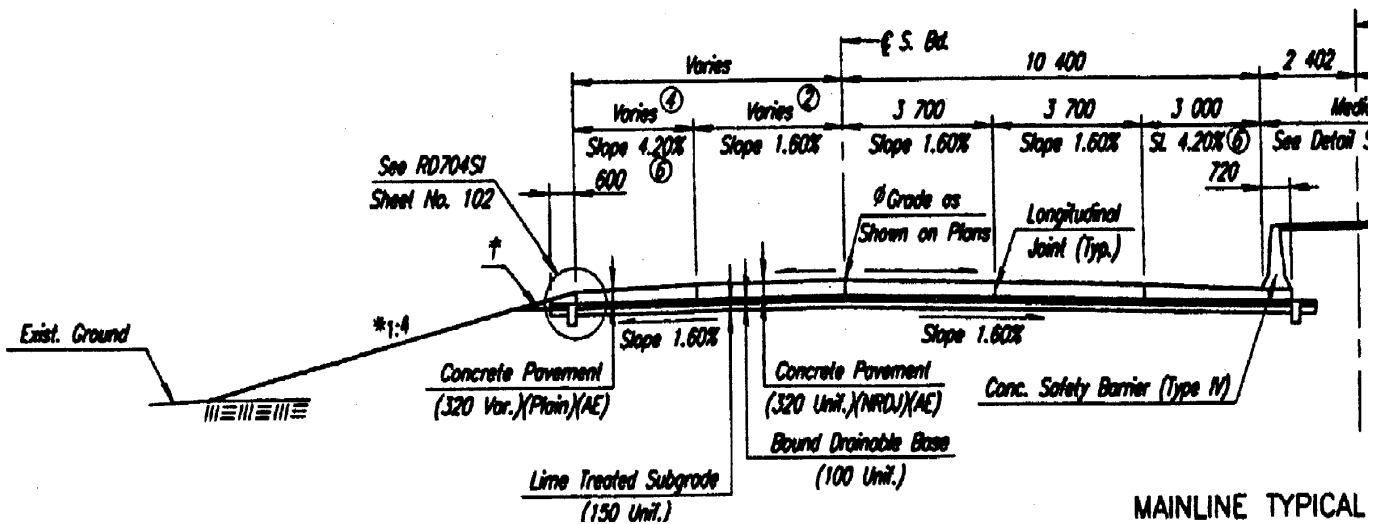


Figure 2.3 Typical cross-section of a divided highway in Kansas

2.2.2 *Drainage*

Pavement drainage systems may be grouped into three general classes based on their geometry: (1) longitudinal drains, (2) drainage blankets, and (3) transverse drains (NHI 1992).

Longitudinal drains are usually located near the pavement or shoulder edge and run parallel to the roadway centerline. *Drainage blankets* are layers of highly permeable material that normally extend across the entire pavement width for an appreciable length along the pavement centerline. *Transverse drains* are generally placed laterally under the pavement, usually at right angles to the pavement centerline.

Most sub-drainage systems consist of some combination of the drainage layers, filter layers, water collection systems, and outlet systems. *Drainage layers* are usually constructed of granular material whose gradation has been selected and controlled to ensure a high degree of permeability. Asphalt stabilized, open-graded material and porous concrete can also be used as drainage layers. The drainage layer may serve as a part of the drainage system and as the pavement base or subbase. *Filter layers* consist of either specially graded granular material or commercial filter fabric. *Collector systems* serve to gather the water from drainage layers or surrounding materials. They often consist of perforated pipes placed in the permeable granular drainage layer. *Outlet systems* convey the water from the collector system to some suitable discharge point.

The addition of drainable base layer in the design of PCC pavements has been recommended practice by FHWA since 1992. KDOT, along with many other state agencies, has been using this design practice since 1988 to help elevate moisture-related

damage to the pavement structure. When the drainage layers are properly designed, constructed and maintained, this damage can be minimized.

Based on the precipitation intensity data for the United States, Kansas averages 1.4 in/hr in the West and 1.8 in/hr in the East based on a two-year, one-hour rainfall event. However, majority of the PCC pavements in Kansas do not incorporate a drainable base because the traffic volume is low to medium, the pavement is dowelled, and shoulders are concrete, and are tied to the mainline pavement. The exception is in the more heavily traveled highways in Kansas.

Until 2000, the KDOT design guidelines were as follows for the dowelled Portland Cement Concrete Pavements: less than 275 Equivalent Single Axle Loads (ESAL)/day in the design lane an unbound, dense-graded aggregate base is used. From 275 to 650 ESAL/day in the design lane, a bound dense graded base (either with Portland cement or asphalt cement) is used. For loads greater than 650 ESAL/day a bound drainable base (BDB) with edge drains, as shown in Figure 2.3, is used. BDB are designed to have a minimum permeability of 1000 ft/day. The 7-day required compressive strength for 6 in. x 6 in. cylinders of concrete mixes bound with fly ash or Portland cement shall be in the range of 595 psi to 1,200 psi and a Marshall stability of 400 psi for bases bound with asphalt cement. The water carried into the BDB layer can be removed by the edge drains and outlets, or on a case-by-case basis, BDB may be daylighted to the shoulder slope (KDOT 1990).

The contractor chooses the aggregate gradations based on the mix design required to obtain the minimum permeability. However, the contractors are allowed to crush and recycle the existing concrete pavement to be used in the drainable base layer. Typically,

the contractors use 70 to 100% of the crushed concrete sweetened with sand-sand gravel, two to three percent of cement, and four to five percent of fly ash. A minimum water/cement ratio of 0.45 is recommended to increase the workability (NHI 1998).

The longitudinal grade also facilitates the surface drainage of PCC pavements. AASHTO recommends a minimum of 0.2% to 0.3% longitudinal grade for adequate drainage of most high-type pavements with recommended cross slope.

The normal cross slope used by KDOT is a crown at the center of the highway. Thus, water flows toward both sides of the pavement. The edge drains are constructed longitudinally down the highway, on both sides of the concrete shoulder. The edge drain pipe is placed in a (8 in x 8 in) trench which is wrapped with a geosynthetic to avoid contamination from the fine-grained soils. The pipe is perforated and is generally 4 inches in diameter. The material around the pipe in the trench is the same aggregate as used in BDB but without any binder.

An outlet pipe is placed every 500 ft that carries the water from the edge drain pipe to the ditch. The outlet pipe is also 4 inches in diameter and is not perforated. Since a high percentage of these pipes get crushed, the stiffness of these pipes is much greater than the stiffness of the edge drain pipe.

When a pavement is superelevated, the edge drain pipe is discontinued on the high side of the superelevation and continued again when coming out of the superelevation. Because of the potentially increased flow of water within the base due to the single cross-slope, the outlet spacing on the low side of the superelevation should be reduced to 200 ft.

2.2.3 Concrete Slab

This is the topmost layer of the PCCP system as shown in Figure 2.4. The desirable characteristics include friction, smoothness, noise control, and drainage. In addition, it serves as a waterproofing layer to the underlying base and subgrade layers. The slab must have a thickness that is adequate to support the loads, to be applied during its service life, and the design must be economical. Several design methods are available to determine the required thickness of the PCCP slab. The Portland Cement Association (PCA 1984) method is one such design process. According to PCA, design considerations that are vital to the satisfactory performance and long life of a PCCP are: reasonably uniform support for the pavement, elimination of pumping by using a thin treated or untreated base course, adequate joint design, and a thickness that will keep load stresses within safe limits. Thickness is determined based on two criteria: erosion analysis, and fatigue analysis. Fatigue analysis recognizes that pavements can fail by the fatigue of concrete, while in erosion analysis pavements fail by pumping, erosion of foundation, and joint faulting. Several tables and nomographs are available to determine thickness based on material properties (modulus of rupture of concrete and modulus of subgrade reaction of subgrade) and traffic (in terms of actual single and tandem axle load distributions).

The AASHTO (1993) method is another widely used method. The procedure uses empirical equations obtained from the AASHO Road Test with further modifications based on theory and experience. Unlike the PCA method, the AASHTO method is based on the 18-kip equivalent single-axle load (ESAL) applications. KDOT currently uses the 1993 AASHTO Design Guide for JPCP design. The minimum PCC slab thickness on

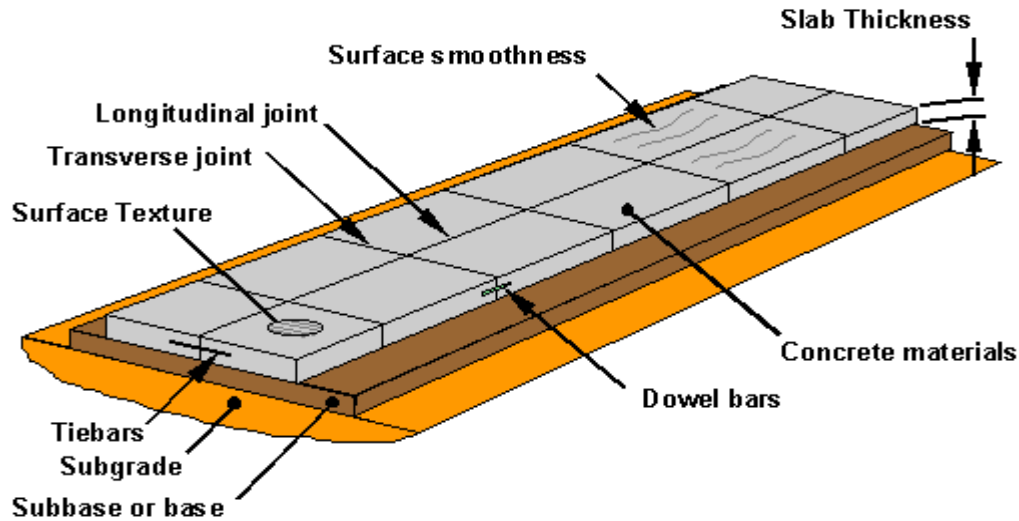


Figure 2.4 Basic component of a concrete pavement (ACPA 2005)

Kansas highways are 8 inch (200 mm). Normally, rigid pavements in Kansas have 2-stage construction since an overlay is planned after 20 years of service life for the initial design.

2.2.4 Concrete mixture

The process of determining required and specified characteristics of a concrete mixture is called mix design. Concrete is a mixture Portland cement, water, and aggregates (coarse and fine) with or without air entraining or other admixtures. Desirable concrete characteristics include: (1) fresh/plastic concrete properties; (2) required mechanical properties of hardened concrete such as, strength and durability requirements; and (3) the inclusion, exclusion, or limits on specific ingredients. Mix design leads to the development of a concrete specification (PCA 2002).

2.2.4.1 Cement Content and Type

According to the KDOT standard specifications, either Type IP Portland–Pozzolan cement, Type I (PM) Pozzolan-Modified Portland cement or Type II Portland cement shall be used for the construction of concrete pavement. The cementations material content is usually determined from the selected water-cementitious materials ratio and water content, although minimum cement content frequently is included in specifications in addition to maximum water-cementitious materials ratio (KDOT 1990). According to the Portland Cement Association (PCA), minimum cement content varies from 470 to 610 pound per cubic yard based on the nominal maximum aggregate size of 1 ½ inch to 3/8 inch, respectively. KDOT standard specification specifies minimum 602 pounds of cement per cubic yard of concrete, prepared with coarse and fine aggregate. Concrete with mixed aggregates (mostly siliceous) will require minimum 620 lbs of cement per cubic yard.

2.2.4.2 Coarse Aggregate

Two characteristics of aggregates, grading and nature of particles (shape, porosity, and surface texture), have an influence on proportioning concrete mixtures to affect the workability of fresh concrete. KDOT uses Siliceous Gravel, Chat or Calcite Cemented Sandstones as coarse aggregates for concrete pavement with minimum soundness of 0.90. In addition to the above stated aggregates, crushed Limestone or Dolomite is also commonly used for pavement construction. Maximum loss in the Los Angeles (L.A.) wear test for all these aggregates is 50%. Table 2.1 summarizes the typical gradation for coarse aggregates for concrete pavement in Kansas.

Table 2.1 Gradation for Coarse Aggregate for Pavement Concrete (KDOT 1990)

Sieve size	Percent Retained
1 1/2"	0
1"	0-10
3/4"	30-65
1/2"	-
3/8"	70-93
No.4	-
No.8	95-100
No.30	-

KDOT also uses mixed aggregates which are naturally occurring predominant siliceous aggregates or may be a sweetened basic aggregate with a minimum soundness of 0.90 and maximum L.A. wear of 50%. Total mixed aggregate may not be used in concrete for pavement, unless a sample of a total mixed aggregate from the source has met the desired modulus of rupture and expansion requirements. Current KDOT special provisions require that mixed aggregate should have a minimum 60-day modulus of rupture of 550 psi and expansion should not exceed more than 0.070% at 365 days (KDOT 1990).

2.2.4.3 Fine Aggregate

KDOT uses two types of fine aggregates: *FA-A* and *FA-B*. *FA-A* consists of natural sand resulting from the disintegration of siliceous and/or calcareous rocks or manufactured sand produced by crushing predominantly siliceous materials or a combination of natural and manufacture sand. *FA-B* consists of fine granular particles resulting from the crushing of zinc and lead ores. Typical grading requirements are shown in Table 2.2.

Table 2.2 Grading Requirements for Fine Aggregate (KDOT 1990)

Sieve size	Percent Retained
3/8"	0
No.4	0-5
No.8	0-24
No.16	15-50
No.30	40-75
No.50	70-90
No.100	90-100

2.2.4.4 Admixtures and Air Content

Entrained air must be used in all concrete that will be exposed to freezing and thawing and de-icing chemicals. Air entrainment also improves workability. Air entrainment is accomplished by using an air entraining Portland cement or by adding an air-entraining admixture at the mixer. KDOT specifies about 6 ± 2 percent of entrained air by volume for JPCP slab concrete.

2.2.4.5 Concrete Consistency

The consistency of the concrete when delivered to the paving train is usually designated by the Engineer. According to KDOT specification, the tolerance permitted from the designated slump shall be plus or minus $\frac{3}{4}$ of an inch. The maximum slump allowable shall be 2 1/2 inches. When the designated slump is greater than 1 $\frac{3}{4}$ inches, the upper limit will be determined by the maximum slump.

2.2.4.6 Water-Cement Ratio

In mix design, the water cement ratio is simply the mass of water divided by the mass of total cement content. The water content should be the minimum necessary to

maintain the required workability. KDOT specifies a maximum water cement ratio of 0.49 for paving concrete.

2.2.4.7 Concrete Mixing and Delivery

Concrete is mixed in quantities required for immediate use. Most specifications require that concrete should not be used when it has developed initial set or is not in place ½ hour after the water has been added for non-agitated concrete. Concrete may be mixed at the site of the work, in a central-mix plant, or in truck mixers. Finally, concrete shall be discharged without delay. For the delivery purpose, approved covers shall be provided for protection against the weather as per requirements.

2.2.5 *Shoulder and Widened lane*

Shoulder in concrete pavement is considered as a safety area for errant or wandering vehicles. It also serves as an auxiliary area for emergency stopping. Structurally, the shoulder may provide lateral support to a mainline concrete pavement as in the case of widened slabs and/or tied concrete shoulders. Two basic types of shoulder are used in concrete pavements: (1) Tied concrete shoulder and (2) Asphalt shoulder.

Tied concrete shoulder is a paved slab that is tied to a mainline concrete pavement. The concrete shoulder provides lateral support to the shoulder by shear load transfer (ties bars and if, paved with the mainline, aggregate interlock) as well as by increased bending resistance. A tied shoulder will have the same thickness as the mainline pavement if the two are paved together. In rural areas, a tied shoulder is

sometimes constructed to a lesser thickness than the mainline pavement, with a dense granular fill material below. Tie bars can be placed on chairs or inserted during paving. Both the tie bar and the aggregate interlock at the lane/shoulder joint provide shear load transfer. The tie bar should be deformed steel, at least No. 5 [0.625 in] bars, spaced at no more than 30 in center to center. Transverse joints in the concrete shoulder should match those in the mainline pavement (NHI 2001).

Asphalt shoulders are commonly used adjacent to the concrete mainline pavements because they are less expensive than the concrete shoulder. They may be asphalt concrete or an asphaltic surface treatment. In general, they do not provide lateral support to the mainline pavement.

The 1986/1993 AASHTO Guide procedure takes a tied concrete shoulder into consideration in the assignment of a lower “J” factor, an important factor in rigid pavement design. Kansas PCC pavements, which are dowel jointed and usually have tied PCC shoulders, have a J factor of 2.8. If the pavement does not have tied shoulders or doweled joints, then the J factor is increased. The maximum value is typically 4.0 when there is very poor load transfer across joints and the shoulders are not tied PCC. In Kansas, all new rigid pavements will have tied PCC shoulders or in the case of a 3 ft paved shoulder, it may be considered as a widened lane. These pavements will have a J value of 2.8.

Widened slabs are paved slightly wider (1 to 3 ft) than the conventional slabs, but the travel lane is striped at a width of 12 ft. This keeps trucks from encroaching near the edge of the slab, thereby greatly reducing slab stresses and deflections at the edges and corners. Lane widening is typically done for the outside traffic lane, which usually carries

more traffic. In field studies, excellent performance has been observed with widened slab which will reduce the faulting and cracking in JPCP, although excessive widening may lead to longitudinal cracking (NHI 2001).

2.2.6 Base/Subbase

Subbase is the layer between the concrete slab and the foundation layer or subgrade. Experimental work has indicated that subbases play a minor role in increasing the structural capacity of a concrete pavement, which obtains its load carrying capacity mainly from the structural rigidity of the slab. Experiments have also indicated that one inch of concrete is equivalent to about six inches of subbase, and unless suitable subbase material can be obtained economically it will usually be economical to increase the thickness of the slab in order to increase the load carrying capacity (Sharp 1970). In practice, a subbase is used under a concrete slab mainly for construction purposes, i.e., to protect the subgrade soil and to facilitate the paving operation. There are, however, one or two exceptions. Some clayey and silty subgrades tend to exhibit the phenomenon called “pumping.” Under repeated heavy traffic and with ingress of water, these materials readily assume the consistency of mud and are sometimes pumped out through the joints and cracks in concrete slabs. In such cases, a subbase is essential to prevent pumping unless traffic is light. It may also be necessary to provide a subbase to insulate frost-susceptible subgrade soils from frost penetration. Subbase may also be used as a drainage layer in the pavement. It also reduces the bending stress in the slab and deflections at the joints and cracks. Improved joint/crack load transfer is also obtained for dowelled JPCP with treated subbases.

The stabilization of natural soils and aggregates is now widely used in the construction for road bases. Traditional base construction methods using mechanically stable material are not suitable for present day heavy traffic intensities and loadings, but they can be readily improved by incorporating some type of binder. Soil cement has been used in the United States since 1935 (Sharp 1970). The use of lean concrete on a large scale started as a development from soil cement, being a material more suited to the pavements carrying heavy traffic. Cement bound granular material is a further development from lean concrete where some relaxation of gradation of the constituent aggregates is permitted (Croney and Croney 1991). In the United States, the use of lean concrete as a subbase layer for JPCP is a common practice.

2.2.6.1 Granular Base

Granular base consists of untreated dense-graded aggregate, such as crushed stone, crushed slag, crushed or uncrushed gravel, sand, or a mixture of any of these materials. Granular bases have historically seen the most use beneath concrete pavements, but because of their susceptibility to pumping and erosion, may not be suitable for pavements subjected to high traffic levels (NHI 2001).

2.2.6.2 Asphalt-treated Base

Asphalt treated bases use the same aggregates as in the granular bases, but mixed with an asphaltic binder. Typically three to five percent asphalt has been added, but PIARC recommends five to six percent to provide resistance to erosion (NHI 2001).

2.2.6.3 Cement-treated Base

Cement-treated bases consist of conventional dense-graded aggregates mixed with Portland cement (typically about 3 to 6 percent). About four to five percent cement should produce a 28 day strength of about 750 psi for a cement-treated base. PIARC studies have shown that in order for the base to be erosion resistant, six to eight percent cement is required (NHI 2001). However, some cement-treated bases constructed with these cement contents have been responsible for increased slab cracking, in cases where the bases and the slab were not bonded and the slab experienced high curling stresses. In such cases, shorter joint spacing should be employed. KDOT standard specification requires that the minimum cement content will be five percent by weight of dry aggregate and the maximum will be ten percent by weight. In Kansas, the Portland cement treated base (PCTB) is constructed two ft wider than the pavement surface. This provides the contractor with a solid surface for the paver's track line.

2.2.6.4 Lean Concrete Base

Lean concrete is similar to paving concrete, but contains less cement (typically about 200 lbs/cubic yd). Thus, it is lower in strength than the conventional paving concrete (about 20 to 50% of strength of paving concrete). The greatest structural contribution of a lean concrete base is achieved with a high degree of friction (resistance to horizontal sliding) and bond (resistance to vertical separation) between the slab and the base (NHI 2001).

2.2.6.5 Permeable Base

Permeable bases are open graded materials, constructed using high quality crushed stone, with high permeabilities that allow rapid removal of water from the pavement structure. A collector system and a separator layer are required. The base may be treated or untreated. Treated bases are preferred for higher traffic volumes and also to facilitate construction. Stabilized permeable bases also contribute to the bending stiffness of the pavement structure. Theoretically, compared to a dense-graded asphalt-treated base, permeable asphalt-treated base should be less susceptible to stripping and debonding at the slab/base interface (NHI 2001).

In Kansas, Portland cement-treated base (PCTB), asphalt-treated base (ATB), bound drainable base (BDB) and granular subbase are commonly used for rigid pavements. Base types are selected based on the traffic on the route. BDB has a very open graded gradation. The water infiltrating the base is meant to move to the edge drain system. To stabilize the base, a small percentage of binder is added. This can be either Portland cement or asphalt cement. The required permeability of the base is 1000 ft/day (KDOT 1990).

2.2.7 *Subgrade*

The term “subgrade” is commonly used to refer to the foundation upon which the base and concrete layers are constructed. The foundation consists of the natural soil at the site, possibly an embankment of improved material, a rigid layer of bedrock or hard clay at a sufficiently shallow depth. Although a pavement’s top layer is the most prominent, the success or failure of a pavement is more often dependent upon the underlying

subgrade-the material upon which the pavement structure is built (NHI 2001). Subgrades are composed of a wide range of materials although some are better than others. The subgrade performance generally depends upon three of its basic characteristics: load bearing capacity, moisture content, and shrinkage and/or swelling (WSDOT 2003). These characteristics are interrelated to each other. The properties of soil that are important for pavement construction are: volume stability, strength, permeability, and durability (Ingles and Metcalf 1972). Subgrade needs to be characterized for concrete pavement design purposes. Both dense liquid (k) and elastic solid (E) models attempt to describe the elastic portion of soil response. However, real soil also exhibits plastic (permanent deformation), and time-dependent responses; slow dissipation of pore water pressures under static loading results in larger deflections than rapid dynamic loading (NHI 2001).

To ensure satisfactory concrete pavement performance, the subgrade must be prepared to provide the stiffness which was assumed in design, uniformity, long-term stability, and a stable platform for construction of the base and slab. Poor subgrade should be avoided if possible, but when it is necessary to build over weak soils there are several methods available to improve subgrade performance. Poor subgrade soil can simply be removed and replaced with high quality fill, although it can be expensive. Other methods are soil stabilization, mixing with coarse material, reinforcement with geosynthetics. Subgrade stabilization includes stabilizing fine-grained soils in place (subgrade) or borrow materials, which are used as subbases, such as hydraulic clay fills, or otherwise poor quality clay and silty materials obtained from cuts or borrow pits (Little 1995). The presence of highly expansive clay soils, subject to wide fluctuations in moisture content and resulting shrink-swell phenomenon, has clearly been proven to be

detrimental to the pavements. Stabilization has been alone found to be most beneficial for these soils. Different binders are used for stabilization, such as, lime, Portland cement, and emulsified asphalt. The selection of the binder depends on the subgrade soil. Lime is the most popular binder used now. By adding an appropriate quantity of lime to the subgrade soils, which are suitable for lime stabilization, the engineering properties of these soils can be improved. The stronger, stiffer, and more stable (volumetrically) lime-treated subgrade provides better protection for the pavement. KDOT uses pebble quick lime or hydrated lime for lime treatment of potentially expansive subgrade soils. Soils with more than 2% swell potential require the top six inches of the subgrade be treated with 5% hydrated lime. Soils that do not have over 2% swell potential, or are silty sized particles shall have the top 6 inches of the subgrade treated with approximately 12% fly ash by weight assuming the density of soil at 110 pcf. The top six inch of sandy soils shall be treated with 7% cement by weight. For natural subgrade, the top 18 inches are usually compacted at the density of the soil is equal to or greater than 95% of the standard density.

2.2.8 Joints in JPCP

Joints are installed in concrete pavements to control the stresses induced by volume change in concrete and to allow for a break in construction at the end of the day's work. These stresses may be produced in a concrete slab because of: (1) its contraction due to uniform temperature drop or a decrease in moisture; (2) its expansion due to a uniform temperature increase; and (3) the effects of warping of pavements due to a vertical temperature and/or moisture differential in the slab (Wright and Paquette 1987).

Joints must fulfill a number of functions. They must permit slabs to move without restraint but they must not unduly weaken the road structurally. The joints need to be effectively sealed so as to exclude water and fine matters such as grit, and yet must not detract from the appearance or riding quality of the road (Sharp 1970). Joints can be of four types: transverse contraction joints, transverse construction joints, transverse expansion joints, and longitudinal joints. Contraction joints are called weakened plane joints, created by forming notch in the surface of the slab pavement to create a weak area where the pavement will crack. This type of joint is used to control cracking of the slab resulting from contraction and to relieve warping stresses. Joint spacing varies from agency to agency and depends on the amount of reinforcement used in the pavement. Generally spacing from 12 to 20 ft is used, although thicker slabs can have longer joint spacing. Dowel bars are used under the joint as load transfer device. Construction joints may be placed at the end of the day's run or when work ceases due to some other interruption.

Expansion joints are provided to allow expansion of concrete. Dowel bars are usually used for this type of joint. A longitudinal joint in a concrete pavement is a joint running continuously the length of the pavement. The joint divides, for example, a two-lane pavement into two sections, the width of each being the width of the traffic lane. The purpose of longitudinal joints is simply to control the magnitude of temperature warping stresses in such a fashion that longitudinal cracking of the pavement will not occur. Longitudinal cracking has been almost completely eliminated in concrete pavements by the provision of adequate longitudinal joints (Wright and Paquette 1987). In two-lane

pavements, the two slabs are generally tied together by means of steel tie bars extending transversely across the joint and spaced at intervals along the length of the joint.

Joints may be placed either at fixed interval or at variable spacing [12-15-13-14 ft]. Another variation in joint design is the layout of the joints. Joints can be placed perpendicular to the centerline of the pavements or at an angle to the pavement in a counterclockwise view (known as skewed joint). Skewed joints may be beneficial in reducing faulting of non-doweled pavements, although effectiveness is questionable for doweled pavements. Kansas uses 15 ft joint spacing for new Jointed Plain Concrete Pavement (JPCP).

2.2.8.1 Load Transfer Devices

Load transfer may be defined as the transfer or distribution of load across the discontinuities such as joints or cracks (AASHTO 1993). When a load is applied at a joint or crack, both loaded slab and adjacent unloaded slab deflect. The amount the unloaded slab deflects is directly related to the joint performance. If a joint performs perfectly, both loaded and unloaded slabs deflect equally. Load transfer efficiency depends on temperature, joint spacing, number and magnitude of load applications, foundation support, aggregate particle angularity, and the presence of mechanical load transfer devices, such as, dowel bars (WSDOT 2003). Load transfer is accomplished through aggregate interlock or by dowel bars. In some cases, base courses also contribute to load transfer but are not considered a formal load transfer method.



Figure 2.5 Short steel dowel bars

Dowel bars are short steel bars (as shown in Figure 2.5) that provide a mechanical connection between slabs without restricting horizontal joint movement. They increase load transfer efficiency by allowing the leave slab to assume some of the load before the load is actually over it. This reduces joint deflection and stress in the approach and leave slabs. Dowel bars are recommended for all medium and high traffic facilities (pavements that are thicker than 8 inch). Dowel bar diameter (commonly one-eighth of the slab thickness) typically varies from $\frac{5}{8}$ to $1\frac{1}{2}$ in with lengths varying from 10 to 20 in. Bar spacing generally is 12 to 15 inches from center to center and are usually placed at mid-slab depth on baskets. Figure 2.6 shows the typical dowel layout.



Figure 2.6 Typical dowel layout

Dowels are not bonded to the concrete on one side, and freedom of movement is ensured by painting or lubricating one end of the dowel, by enclosing one end in a sleeve, or by other similar methods. It is essential that the freedom of movement be ensured in the design and placing of the dowel bars, since the purpose of the joint will be largely destroyed if the movement is prevented. Because the concrete is cracked at the joint, the dowels also provide vertical transfer of the load from one slab to the next. The dowels are either placed on baskets or implanted into the plastic concrete. Where a widened slab exists, some agencies may place a dowel bar in the outside widened area, depending on the width of the widening. Currently steel dowels are coated with a corrosion inhibitor to prevent corrosion and subsequent lock up of the dowels. Epoxy is the most commonly used corrosion inhibitor.

In Kansas, joints are doweled with a dowel spacing of 1 ft. Dowel bars in Kansas are smooth, rounded steel bars with a diameter one-eighth of the slab thickness in inches. The length of the dowel bar is 18 inch. The opposite sides of adjacent dowels are coated

with a bond breaker to ensure the joint is a working joint, i.e., the dowels permit the concrete to expand and contract freely.

Tie bars (Figure 2.7) are either deformed steel bars or connectors used to hold the faces of abutting slabs in contact (AASHTO 1993). Although they may provide some minimal amount of load transfer, they are not designed to act as load transfer devices and should not be used as such (AASHTO 1993). Tie bars are typically used at longitudinal joints or between an edge joint and a curb or shoulder. Kansas uses steel tie bars that are typically #5 deformed bars placed perpendicular to the pavement's centerline. They are used to tie adjacent lanes or shoulders to the slab. Tie bars are generally spaced 2 ft apart and are 2 ft long.



Figure 2.7 Deformed tie bars

2.2.9 PCCP Construction

Prepaving Activities

The main construction activities that precede the actual paving of the concrete slab are subgrade preparation, base preparation, and joint layout.

Subgrade Preparation includes any needed mixing of coarser material or stabilizer, grading and compaction to the required density, accurate trimming to establish grade and setting grade stakes for later base/ slab paving (NHI 2001). Both the subgrade and the granular or treated base/subbase are required to be brought to the grade lines according to the designated plan (KDOT 1990). The entire subgrade and granular or treated subbase should be thoroughly compacted. Before placing any surfacing material on any section, the ditches and drains along that section should be completed to drain the highway effectively.

The base course is placed on the finished roadbed, and is often used as a haul road to facilitate construction. For slipform slab paving, a minimum base width of 2 ft on each side beyond the traffic lane width is recommended to accommodate the slipform tracks.

Prior to paving, all transverse and longitudinal joints must be laid out in conformance with details and positions shown on the plan. Tie bars for longitudinal joints and dowel bars for transverse joints are placed on the base in chairs, if not inserted during paving. Epoxy coated dowels are placed with care and sometimes, a metal cap is fitted on one end to allow for expansion of the concrete. Dowels are placed in baskets to control their depth, spacing, and alignment. The baskets are pinned down so that they will not be shoved out of position during concrete placement. Accurate and horizontal alignments of the dowels are essential to the correct functioning of the joints (NHI 2001).

Paving Activities

Paving activities include mixing and transporting concrete to the job site, placing the concrete, and consolidating the concrete. The main goal in mixing and transporting concrete is to optimize workability and finishability while avoiding segregation. The concrete is spread, consolidated, screeded, and float finished in one pass of the paving train. Slipform pavers are used to perform the paving operation. Figure 2.8 shows a PCCP paving operation in Kansas. Since the paving concrete is stiff, it must be effectively consolidated to remove entrapped air and distribute the concrete uniformly around the dowels and reinforcement (NHI 2001). When concrete is placed in more than one layer or full depth, consolidation of each layer is done by vibrators. The concrete should be sufficiently and uniformly vibrated across the full width and depth of the pavement to ensure the density of the pavement concrete not less than 98 percent of the rodded unit weight (KDOT 1990). This density requirement may be eliminated on such miscellaneous areas as entrance pavement, median pavement, gore areas, etc. PCC paving in Kansas is done with the slip form pavers.

Postpaving Activities

Postpaving activities include finishing, texturing, and curing the concrete, and after the concrete hardens, sawing and sealing the transverse and longitudinal joints. Figure 2.9 shows the sawing of joints. Joints are sawed immediately upon hardening of concrete.



Figure 2.8 PCCP paving operation in Kansas



Figure 2.9 Typical joint sawing operation in Kansas

Finishing consists of screeding off the concrete surface level to the desired height and machine floating the surface to fill in low spots. For thicker pavements, additional spreaders are employed. In Kansas, concrete consolidation is accomplished with the gang vibrators on the paver. Initial texturing provides microtexture, which contributes to

surface friction by adhesion with the vehicle tires. Initial texturing is usually accomplished by a burlap or Astroturf drag directly behind the paver. Final texturing provides macrotexture, which contributes to the surface friction by tire deformation, and also channels surface water out from between the pavement and the tire (NHI 2001). Final texturing should be done as soon as possible as the bleed water sheen disappears.

Curing is done to enhance hydration and strength gain by retaining moisture and heat in the concrete immediately after placement and finishing (NHI 2001). Curing can be accomplished by wet burlap cover, liquid membrane-forming compounds, white polyethylene sheeting, concrete curing blanket or reinforced white polyethylene sheeting. In Kansas, liquid membrane-forming curing compound is extensively used for concrete pavements as shown in Figure 2.10.

Joint sawing (Figure 2.9) is done to establish transverse and longitudinal contraction joints and thereby control the cracking that inevitably occurs in a new concrete pavement as it dries (NHI 2001). With conventional equipment, sawcuts are made to a depth of one fourth to one third of the slab thickness, and 1/8 to 3/8 in. wide. After the sealant reservoir is sawed, it must be cleaned by abrasives (i.e., sandblasting) to remove the sawing residue so that the sealant will adhere well to the reservoir wall. After sandblasting, the reservoir is cleaned by air blowing, and the backer rod is installed. The sealant is then installed in the joint. Most of the newer JPCP's in Kansas are sealed with preformed neoprene seals.



Figure 2.10 Curing operation using liquid membrane forming curing compound

2.3 JPCP Design Methods

There are two basic approaches to the thickness design of rigid pavements; the empirical approach and the mechanistic approach (also called the mechanistic-empirical approach, since it incorporates some aspects of both approaches).

Empirical design approaches are based upon the previous experience or measures of field performance, often without consideration of any structural theory (NHI 1992). There are several rigid pavement thickness design procedures that utilize empirical design concepts. The most widely-used major rigid pavement design procedure that is based entirely upon empirical design concepts is the AASHTO rigid pavement design procedure (AASHTO 1986). The method is based upon a full-scale road test, the AASHTO Road Test. The latest versions of this guide are the 1986 and 1993 AASHTO Design Guides, based on the in-service performance of the Road test pavements and take into account numerous design and behavioral factors under test loads, such as soil

conditions, material properties, load transfer devices, and axle loading and configuration. The AASHTO approach is empirical and is based on the ability of the pavement to serve traffic over the design period—that is, its functional performance. Although empirical pavement design models have historically taken forms that are as simple as “rules of thumb,” it is now more common for these models to be developed using pavement performance database and statistical and/or multiple regression analysis techniques.

There are several limitations of the AASHTO Road Test such as, one soil type and one climate, constant traffic load magnitude and configuration, serviceability concept for roughness and distress measurement, etc. Thus the applications of the empirical models are limited as they are applicable only within the limits of the data from which they have been derived. Despite these limitations, empirical design procedures are often very useful in providing indications of relative performance trends and in evaluating the effects of different design features on pavement performance (NHI 1992).

Mechanistic design approach indicates a design method where the principles of engineering mechanics will be applied. This approach begins with the determination of the critical stresses that the pavement will experience due to traffic loads, temperature and moisture effects, and foundation movements. These stresses are typically estimated using a slab stress model such as Westergaard’s equations or finite element analysis techniques (NHI 1992). These analysis techniques use theories of material behavior and mechanics to predict pavement response (i.e., stresses, strains, and /or deflections) to external effects (i.e., load and environmental effects) for a given specific pavement and foundation material properties (e.g., thickness, stiffness and Poisson’s ratio of each pavement layer).

2.4 Framework for the Mechanistic-Empirical Design Method

2.4.1 Basic Design Concept

Mechanistic-empirical (M-E) design combines the elements of mechanical modeling and performance observations in determining required pavement thickness for a given set of design inputs. The mechanical model is based on elementary physics and determines pavement response to the wheel loads or environmental condition in terms of stress, strain, and displacement. The empirical part of the design uses the pavement response to predict the life of the pavement on the basis of actual field performance (Timm, Birgisson, and Newcomb 1998). Mechanistic-empirical procedures were not practical until the advent of high-speed computers. The reason is the computational demands associated with the differential equations and finite element matrix solutions employed by various analysis models. The choice of a model and how it was applied often were functions of the computational requirements and how much time was required to accomplish those computations (Proposal 2003).

2.4.2 Advantages over Empirical Design procedure

There are some specific advantages of M-E design over traditional empirical procedures.

Those are outlined below:

- Consideration of changing load types;
- Better utilization and characterization of available materials;
- Improved performance predictions;
- Better definition of the role of construction by identifying parameters that influence pavement performance;

- Relationship of the material properties to actual pavement performance;
- Better definition of existing pavement layer properties; and
- Accommodation of environmental and aging effects of materials.

In essence, M-E design has the capability of changing and adapting to new developments in pavement design by relying primarily on the mechanics of materials. For example, M-E design can accurately examine the effect of new load configuration on a particular pavement. Empirical design, however, is limited to the observations on which the procedure was based (e.g., single axle load). Additionally, since the M-E design process is modular, new advances in pavement design may be incorporated without disrupting the overall procedure (Timm, Birgisson and Newcomb 1998).

2.4.3 *Design Overview*

The major components of the mechanistic-empirical JPCP pavement design are as follows (NHI 2002):

- Inputs—Materials, traffic, climate and structure.
- Structural response model – to compute critical responses.
- Performance models or transfer functions – to predict pavement performance over the design life.
- Performance criteria – to set objective goals by which the pavement performance will be judged.
- Design reliability and variability.

The inputs to the M-E design process include those related to the pavement structure, pavement materials, climactic conditions, season, soil conditions, and traffic loading. In

an M-E design approach, the user has the complete flexibility over all design factors while designing a structure. For this reason, the M-E design approach is not just a thickness design procedure.

Structural response modeling was one the weakest links in the M-E design process prior to the advent of modern computers and computational power. However, this situation has changed considerably due to the availability of numerous computer programs, capable of solving complex pavement problems. In the M-E design process, critical pavement responses for each distress type are estimated from the structural response models based on the loadings applied, pavement layer thicknesses and material properties. However, the accuracy of the responses will be a function of the underlying assumptions of each approach and the theoretical pavement model. Due to the finite nature of concrete pavement slabs and the presence of discontinuities in the form of transverse and longitudinal joints, elastic layer programs, which assume infinite extents in the horizontal direction, are not usually applicable for response calculation. Three methods have been traditionally used to determine stresses and deflections in concrete pavements: closed-form equations, influence charts, and finite element computer programs. Several finite element programs have also been developed over the years to perform rigid pavement analysis. They include ILLI-SLAB, JSLAB, WESLIQID, WESLAYER, RISC, and 3-D EVERFE. Today the use of finite element programs to analyze rigid pavements is fast becoming a norm due to the geometric complexities of such pavements (NHI 2002).

As pavement sections age and traffic and climatic loads act on them, they undergo functional and structural deterioration. This is manifested in terms of pavement

distresses. The progression of pavement distress is directly tied to the pavement responses; therefore, in M-E design, the goal is to keep the critical stresses and strains in the pavement below acceptable limits. In this design process, the focus is on load-associated distresses because they can be controlled directly by changing the structural section to reduce critical pavement stresses and strains. Common load-related distresses for the JPC pavements are fatigue cracking, faulting, etc.

Distress transfer functions relate pavement responses determined from the structural response models to pavement performance as measured by the type and severity of distresses. Pavement responses are computed using structural response models and the pavement performance over time is predicted using transfer functions or distress models. In that sense, transfer functions are a vital component in the overall mechanistic-empirical design process. While several advancements have been made in developing accurate models to compute pavement structural responses, pavement transfer functions are a subject of continuous refinement. Transfer functions used in M-E design are developed relating a phenomenological distress progression function (i.e., a model based on a plausible theoretical correlation between a relevant mechanistic structural response and the distress parameter under question) to observed performance of actual pavement test sections through statistical calibration procedures. The calibration process introduces other relevant pavement variables of interest to the performance equation in addition to the primary mechanistic independent variable, such as, pavement structural properties and climatic variables. Not all pavement distress types can be included in the M-E design process because: (1) lack of a mechanistic basis for the distress under question (e.g., distresses caused by functional inadequacies or material-related failures

that cannot be easily modeled); (2) lack of adequate observational data required to establish a clear statistical relationship between the dependent and the explanatory variables; and (3) inadequate statistical modeling. For rigid pavements, models to predict faulting, transverse cracking, and pumping exist (NHI 2002). Two types of transfer functions can be found in the literature:

- Functions that directly calculate the magnitude of the surface distress at any given time or traffic based on structural response parameters and other pertinent variables.
- Functions that first calculate a damage index based on structural responses and then use damage to distress correlations to assess the distress progression over time.

Pavement deterioration due to traffic and environmental factors (temperature cycles) is termed “damage.” Damage can be defined as an alteration of the physical properties of the pavement structure due to application of wheel loads. A refinement of the damage concept is the incremental damage accumulation. Pavements are loaded incrementally in the field, i.e., every hour a number of axle loads travel over the traffic lane and cause stress, strains, and deformations in the pavement and subgrade. Damage occurs in increments hourly, daily, monthly, and yearly. During these times, many of the key variables that affect pavement performance vary or change. The most obvious are climatic conditions (temperature and moisture) that vary daily and seasonally. Others would be differences in day and night time traffic loadings and seasonal traffic loadings, joint load transfer (for PCC pavements) varying over the day and seasonally (NHI 2002).

According to the incremental approach, damage is not accumulated equally over time. Damage accumulation is higher when critical structural and climatic factors that negatively influence pavement structural responses act in unison, and vice versa. An incremental damage accumulation process breaks up the design period into smaller time increments (e.g., months, seasons) and computes damage for each applied traffic category (truck class, traffic path, and so on) within each time increment. The number of load applications allowed within each time increment is typically referred to as N . Damage at any point in time, D , is defined as the ratio of the accumulated load applications, n , to the total allowable number based on the structural responses within that increment, N , or

$$D = n/N \quad (2.1)$$

Miner's hypothesis (Miner 1945) is commonly used to sum damage over time in pavements. An example of the form of Miner's equation to compute fatigue-related damage in PCC pavements is presented below:

$$FD = \sum_{k=1}^o \sum_{j=1}^m \sum_{i=1}^n \frac{n_{ijk}}{N_{ijk}} \quad (2.2)$$

Where,

FD= Fatigue Damage;

n = Number of applied 80-kN (18 kip) single axles;

N = Number of allowable 80-kN (18 kip) single axles; and

i, j, k = Categories over which damage will be summed.

Once damage over a given time increment is computed in this manner, pavement distress of interest can be determined using the damage-distress transfer function. An

example of the general nature of the fatigue damage correlation to slab cracking is shown in the equation below:

$$\text{PercentSlabsCracked} = f(FD) \quad (2.3)$$

The damage-distress correlation can then be converted to distress-time or distress-traffic correlation. Figure 2.11 illustrates the typical scheme adopted in the incremental damage approach to predict distresses over time or traffic.

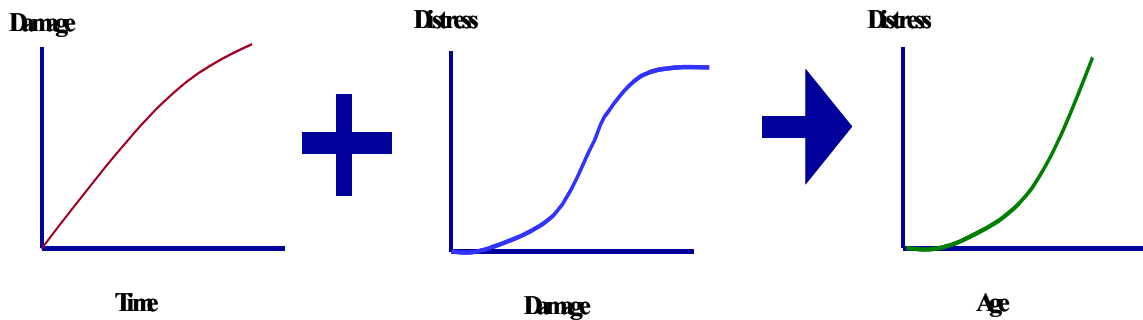


Figure 2.11 Prediction of distress over time

Using pavement structural distresses as measures of performance is unique to the M-E design. This allows performance to be expressed in objective and measurable quantities that engineers can relate to.

Although the M-E approach will require the prediction of specific distress types such as fatigue cracking and faulting, it is still highly desirable to continue with the original serviceability criterion developed at the AASHO Road Test. This will assure the traveling public of a safe and comfortable ride during the pavement's design life. However, since Present Serviceability Rating (PSR) is not a parameter directly measured in the field, it is necessary to use another parameter that is routinely measured and that correlates well with this index value. It has been found from numerous research studies conducted since the AASHO Road Test that pavement smoothness, measured in terms of

the International Roughness Index (IRI), correlates extremely well with PSR. Pavement smoothness information is routinely collected in the field and is a viable alternative for measuring the functional quality of pavements. It is an objective indicator of the ride quality of the pavement, which is the most important parameter from a road user's perspective. However, there are no models to predict pavement profile over time based on the M-E concepts. The present technology uses correlations between the pavement distresses, smoothness immediately after construction (initial IRI), and other related parameters to predict smoothness. Since pavement distresses are predicted using mechanistic methods, and they form inputs to the IRI equation, it can be argued that the prediction of IRI is quasi-mechanistic at this point (NHI 2002).

Reliability of a given design is the probability that the performance of the pavement predicted for that design will be satisfactory over the time period under consideration. Reliability analysis is a requirement in pavement design due to the stochastic nature of the inputs to the design as well as the predicted outputs from the design (e.g., pavement distress or smoothness).

Before a given design is accepted, the probabilistically predicted pavement distresses and smoothness for that design are checked against a set of failure criteria to verify its adequacy. These criteria are preset by agencies based on their maintenance and rehabilitation policies. In M-E design, a number of failure criteria, each directed to a specific distress type, must be established. This is in contrast to the current AASHTO method where the Present Serviceability Index (PSI), which indicates the general pavement condition, is used. In addition to setting failure thresholds for each distress type, a threshold value for IRI is also important because it is quite possible that a

pavement exhibiting low amounts of structural distresses can have an unacceptable ride quality. The following are the example of failure criteria:

- Fatigue cracking – Maximum percent of cracked slabs.
- Faulting – Maximum amount of mean joint faulting/km.
- Smoothness, IRI – Maximum IRI, m/km.

The designer may choose to check for all the distress types and smoothness, or any possible combinations thereof.

2.5 NCHRP Mechanistic-Empirical Pavement Design Guide (MEPDG)

Yoder and Witczak (1975) pointed out that for any pavement design procedure to be completely rational in nature, three elements must be fully considered: (i) the theory used to predict the assumed failure or distress parameter; (ii) the evaluation of the materials properties applicable to the selected theory; and (iii) the determination of the relationship between the magnitude of the parameter in question to the performance level desired. The NCHRP MEPDG considered all three elements.

2.5.1 Design Approach

The design approach followed in MEPDG is summarized in Figure 2.12. The format provides a framework for future continuous improvement to keep up with the changes in truck traffic technology, materials, construction, design concepts, computers, and so on. As shown in the figure, in this guide, the designer first considers site conditions (traffic, climate, material and existing pavement condition, in case of rehabilitation) and construction conditions in proposing a trial design for a new pavement or rehabilitation.

The trial design is then evaluated for adequacy against some predetermined failure criteria. Key distresses and smoothness are predicted from the computed structural responses of stress, strain and deflection due to given traffic and environmental loads, such as temperature gradient across the PCC slab. If the design does not meet desired performance criteria at a preselected level of reliability, it is revised and the evaluation process is repeated as necessary (NCHRP 2004). This approach makes it possible to optimize the design and to more fully insure that specific distress types will not develop.

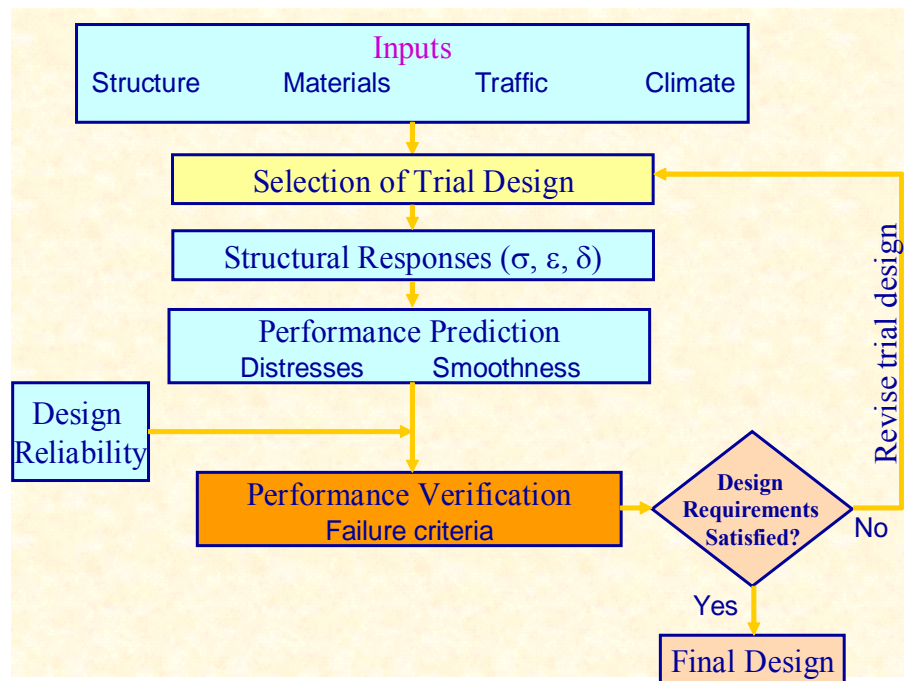


Figure 2.12 PCC mechanistic-empirical design framework (NCHRP 2004)

2.5.2 Overview of the Design Process for JPCP

The overall JPCP design process is illustrated in Figure 2.13. In the first step, a trial design is assembled for specific site conditions including traffic, climate, and foundation.

Foundation includes different layer arrangement, PCC and other paving material properties and design and construction feature inputs are also needed. Then failure criteria are established based on the acceptable pavement performance at the end of the design period (i.e., acceptable levels of faulting, cracking and IRI for JPCP). Reliability levels are also selected for each of these performance indicators. Then these inputs are processed and structural responses are computed using finite element-based rapid solution models for each axle type and load and for each damage-calculation increment throughout the design period. ISLAB 2000, an enhanced 2-D finite element program, was used to make millions of calculations involving typical JPCP pavements. Then neural network technology was incorporated in this Guide for structural response calculation based on these ISLAB 2000 results. Key distresses, faulting and cracking, and smoothness are predicted month by month throughout the design period using the calibrated mechanistic-empirical performance models, provided in MEPDG. Predicted smoothness is a function of the initial IRI, distresses that occur over time, and site factors at the end of each time increment. Expected performance of the trial design is evaluated at the given reliability level. If the design does not meet the established criteria, then it needs to be modified and therefore, iteration continues.

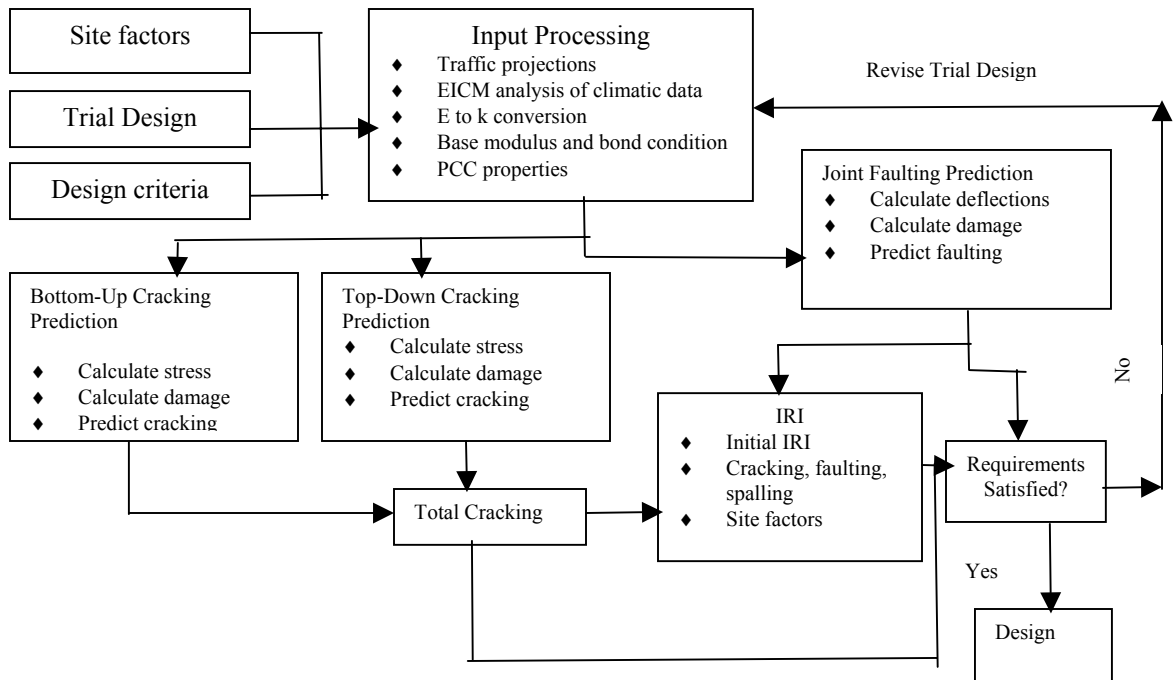


Figure 2.13 Overall design process for JPCP (NCHRP 2004)

2.5.3 Key JPCP Distresses and Critical Responses

The structural distresses considered for JPCP design are fatigue-related transverse cracking of the PCC slabs and differential deflection-related transverse joint faulting. *Transverse cracking* of PCC slabs can initiate either at the top surface of the PCC slab and propagate downward (top-down cracking) or vice versa (bottom-up cracking) depending on the loading and environmental conditions at the project site, as well as material properties, design features, and the conditions during construction (NHI 2002).

Bottom-up cracking is induced by fatigue that accumulates due to repeated loading from truck axles near the longitudinal edge of the slab midway between the transverse joints. This results in critical edge stresses at the bottom of the slab, as shown in Figure 2.14, that increases greatly when there is a high positive temperature gradient across the slab. Repeated loadings from heavy axles result in fatigue damage along the

edge of the slab that eventually results in micro-cracks that propagate to the slab surface and transversely across the slab.

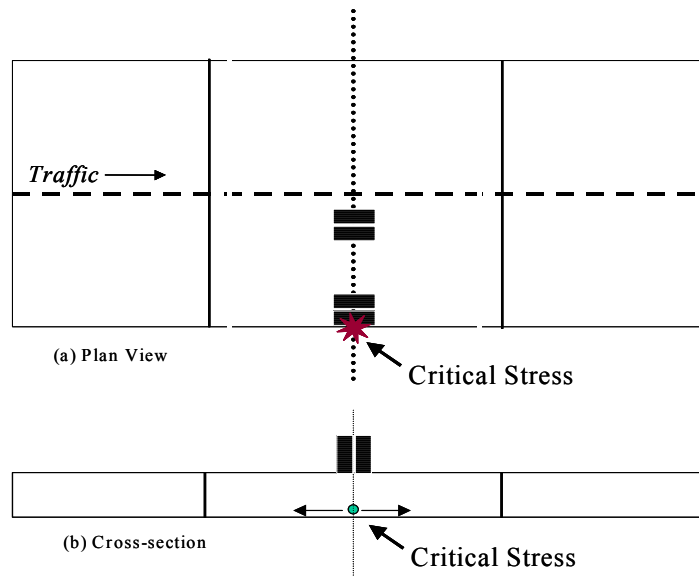


Figure 2.14 Critical loading and structural response location for JPCP bottom-up transverse cracking

When the truck steering axle is near the transverse joint and the drive axle is within 10 to 20 feet away and still on the same slab, a high tensile stress occurs at the top of the slab between axles, some distance from the joint as shown in Figure 2.15. This stress increases when there is a negative temperature gradient through the slab, a built-in negative gradient from construction, or significant drying shrinkage at the top of the slab (all of these conditions are common). Repeated loading of heavy axles results in fatigue damage at the top of the slab, which eventually results in micro-cracks that propagate downward through the slab and transversely or diagonally across the slab.

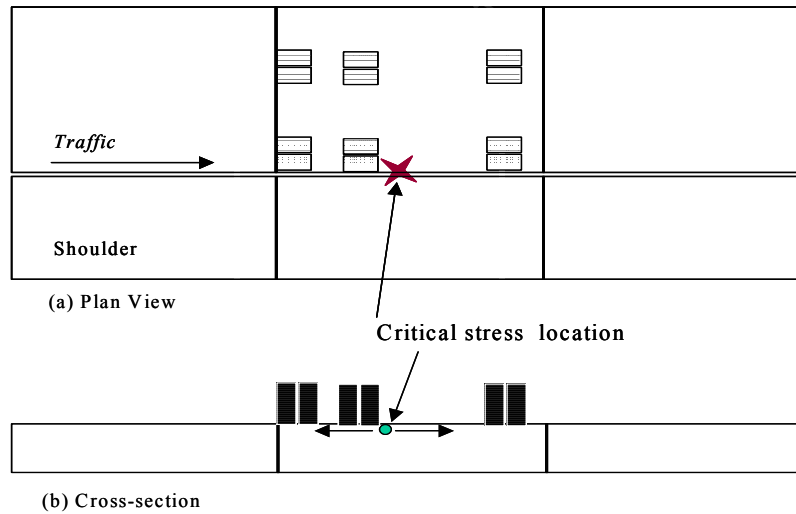


Figure 2.15 Critical loading and structural response location for JPCP top-down transverse cracking

Faulting is the difference of elevation across joints or cracks. Faulting is considered an important distress of JPCP because it affects ride quality. If significant joint faulting occurs, there will be a major impact on the life-cycle costs of the pavement in terms of rehabilitation and vehicle operating costs. Faulting is caused in part by a build-up of loose materials under the trailing slab near joint or crack as well as the depression of the leading slab. Lack of load transfer contributes greatly to faulting (Huang 2003). Figure 2.16 shows the schematic of faulting.

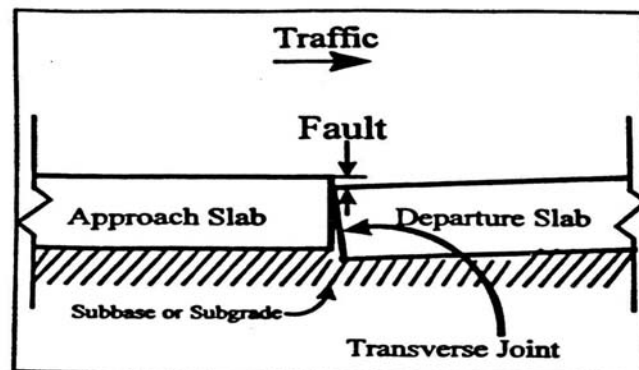


Figure 2.16 Schematic of faulting

Repeated heavy axle load crossing transverse joints create the potential for joint faulting. If there is less than 80 percent joint load transfer efficiency, an erodible base, subbase, shoulder, or subgrade or free moisture beneath the slab, then faulting can become severe and may cause loss of ride quality triggering early rehabilitation (NHI 2002). Figure 2.17 shows the critical loading and response location for faulting. The critical pavement response computed at this location is corner deflection.

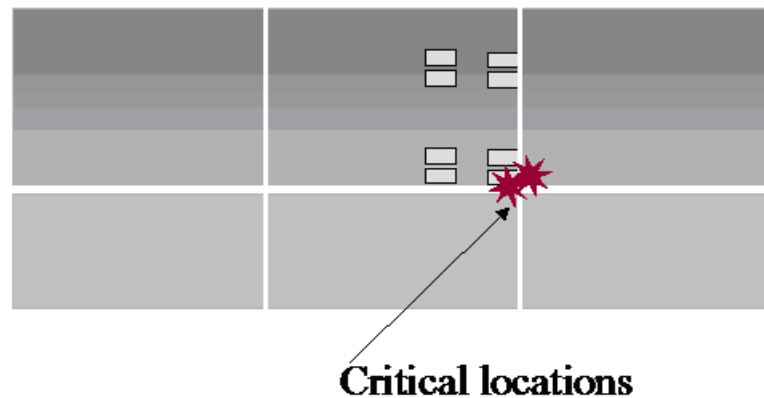


Figure 2.17 Critical loading and structural response location for JPCP faulting analysis

2.5.4 Smoothness (IRI) prediction

The IRI over the design period depends upon the initial as-constructed IRI and the subsequent development of distresses over time. These distresses include transverse slab cracking, joint faulting, and joint spalling for JPCP. The calibrated model for JPCP relates IRI at any time to the as-constructed initial IRI and to the change in IRI due to occurrence of the previously described distresses. These models also include subgrade and climatic calibration factors. Finally IRI is estimated incrementally over the entire design period on a monthly basis.

2.5.5 JPCP Performance Prediction Models

2.5.5.1 Cracking Model

For JPCP transverse cracking, both bottom-up and top-down modes of cracking are considered (NCHRP 2004). The percentage of slabs with transverse cracks in a given traffic lane is used as the measure of transverse cracking and is predicted using the following model for both bottom-up and top-down cracking:

$$CRK = \frac{1}{1 + FD^{-1.68}} \quad (2.4)$$

($R^2 = 0.68$, $N = 521$ observations, and $SEE = 5.4\%$)

Where,

CRK= Predicted amount of bottom-up or top-down cracking (fraction); and

FD= Calculated fatigue damage.

The general expression for fatigue damage is:

$$FD = \sum \frac{n_{i,j,k,l,m,n}}{N_{i,j,k,l,m,n}} \quad (2.5)$$

Where, FD= Fatigue damage;

$n_{i,j,k,l,m,n}$ = Applied number of load application at condition i, j, k, l, m, n ;

$N_{i,j,k,l,m,n}$ = Allowable number of load applications at condition i, j, k, l, m, n ;

i = age, j =month, k =axle type, l =load level, m = temperature difference, and

n =traffic path.

The allowable number of load applications is determined using the following fatigue model:

$$\log(N_{i,j,k,l,m,n}) = C_1 \cdot \left(\frac{MR_i}{\sigma_{i,j,k,l,m,n}} \right) + 0.4371 \quad (2.6)$$

Where, $N_{i,j,k,...}$ = Allowable no. of load applications at condition i,j,k,l,m,n.

MR = PCC modulus of rupture at age i , psi;

$\sigma_{i,j,k,...}$ = Applied stress at condition i, j, k, l, m, n ;

C_1 = Calibration constant=2.0; and

C_2 = Calibration constant=1.22.

2.5.5.2 Faulting Model

The faulting at each month is determined as a sum of faulting increments from all previous months in the pavement life since the traffic opening using the following model:

$$Fault_m = \sum_i^m Fault_i \quad (2.7)$$

$$\Delta Fault_i = C_{34} * (FAULTMAX_{i-1} - Fault_{i-1})^2 * DE_i \quad (2.8)$$

$$FAULTMAX_i = FAULTMAX_0 + C_7 * \sum_{j=1}^m DE_j * \log(1 + C_5 * 5.0^{EROD})^{C_6} \quad (2.9)$$

$$FAULTMAX_0 = C_{12} * \delta_{curling} * \left[\log(1 + C_5 * 5.0^{EROD}) * \log\left(\frac{P_{200} * WetDays}{P_s}\right) \right]^{C_6} \quad (2.10)$$

The model statistics are: ($R^2=0.71$, $SEE=0.029$, and $N=564$)

Where,

$Fault_m$ = Mean joint faulting at the end of month m , in;

$\Delta Fault_i$ = Incremental change in mean transverse joint faulting in month i , in;

$FAULTMAX_i$ = Maximum mean transverse joint faulting for month i , in;

$FAULTMAX_0$ = Initial maximum mean transverse joint faulting, in;

$EROD$ = Base/subbase erodibility factor;

DE_i = Differential deformation energy accumulated during month i ;

$\delta_{curling}$ = Maximum mean monthly slab corner upward deflection PCC due to temperature curling and moisture warping;

P_S = Overburden on subgrade, lb;

P_{200} = Percent subgrade material passing US No.200 sieve;

$WetDays$ = Average annual number of wet days (greater than 0.1 in rainfall);

FR = Base freezing index defined as the percentage of time the temperature of the base top is below freezing (32°F) temperature

C_1 through C_8 and C_{12} , C_{34} are national calibration constants:

$$C_{12} = C_1 + C_2 * FR^{0.25} \text{ and } C_{34} = C_3 + C_4 * FR^{0.25}$$

$$C_1 = 1.29, C_2 = 1.1, C_3 = 0.001725, C_4 = 0.0008, C_5 = 250, C_6 = 0.4, \text{ and } C_7 = 1.2$$

2.5.5.3 Smoothness Model

Smoothness is the most important pavement characteristic valued by the highway users. In MEPDG, smoothness is defined by IRI. The IRI model was calibrated and validated using Long Term Pavement Performance (LTPP) and other field data. The following is the final calibrated model:

$$IRI = IRI_I + C1 * CRK + C2 * SPALL + C3 * TFAULT + C4 * SF \quad (2.11)$$

The model statistics are: ($R^2=0.60$, $SEE=27.3$, and $N= 183$)

Where, IRI = Predicted IRI, in/mi;

IRI_I = Initial smoothness measured as IRI, in/mi;

CRK = Percent slabs with transverse cracks (all severities);

$SPALL$ = Percentage of joints with spalling; and

$TFAULT$ = Total joint faulting cumulated per mi, in.

$$SF = \text{Site factor} = AGE (1 + 0.5556 * FI) (1 + P_{200}) * 10^{-6} \quad (2.12)$$

Where, AGE = Pavement age, yr;

FI = Freezing index, °F-days; and

P_{200} = Percent subgrade material passing No.200 sieve.

The constants evaluated in the calibration process are:

$C1 = 0.8203$, $C2 = 0.4417$, $C3 = 1.4929$, and $C4 = 25.24$

2.6 JPCP Evaluation and Management in Kansas

KDOT uses a comprehensive, successful pavement management system (PMS) for all pavement types in Kansas. The network level PMS of KDOT is popularly known as the Network Optimization System (NOS). In support of NOS, annual condition surveys are conducted based on the methodologies proposed by Woodward Clyde consultants (now URS Corp.) and subsequently, refined by the KDOT Pavement Management Section. Current annual condition surveys include roughness (IRI), faulting and joint distresses for rigid pavements. Different severity levels and extent are measured in the survey. While the roughness and faulting data are collected using automated methods, joint distress surveys are done manually. These survey results constitute basic inputs into the NOS system. The performance prediction methodology in the NOS system is based on the Markov process. The technique uses transition matrices to predict future condition based on current condition for multi-year programming (Kulkarni et al. 1983).

2.6.1 Profile/Roughness Data Collection

Pavement profile data consists of elevation measurements at discrete intervals along a pavement surface. Profile data is collected on both wheel paths (left and right) of driving and passing lanes on the pavement sections using an International Cybernetics Corporation (ICC) South Dakota-type profiler (Figure 2.18) with a three-sensor configuration. The profiler is operated at highway speeds (usually 50 mph or 80 km/h). These sensors measure the vertical distance from the front bumper to the pavement surface, and the profiler is equipped with accelerometers at each of the wheel path sensors to compensate for the vertical motion of the vehicle body. The KDOT ICC profiler has three Selcom 220 laser sensors. The outer two sensors are spaced at about 66 in. apart. The third sensor is located in the middle. KDOT profiler aggregates profile elevation data at every 3 inch from the laser shots taken at the rate of 3200 per second (Miller et al. 2004).

A number of summary statistics are available to represent road roughness using road profile data. International Roughness Index (IRI) is most commonly used by many agencies because of its acceptance by FHWA.



Figure 2.18 KDOT South Dakota-type profilometer

The IRI is a profile-based statistic that was initially established in a study by the World Bank (Sayers 1985). It is used worldwide as the index for comparing pavement roughness. The IRI mathematically represents the response of a single tire on a vehicle suspension (quarter-car) to roughness in the pavement surface (Figure 2.19), traveling at 50 mph. The model, shown schematically in Figure 2.19, includes one tire, represented with a vertical spring, the mass of the axle supported by the tire, a suspension spring and a damper, and the mass of the body supported by the suspension for that tire. The quarter-car filter calculates the suspension deflection of a simulated mechanical system with response similar to a passenger car. The simulation suspension motion is accumulated and divided by the distance traveled to give an index with units of slope (Sayers 1985). IRI is expressed in mm/km (inches/mile).

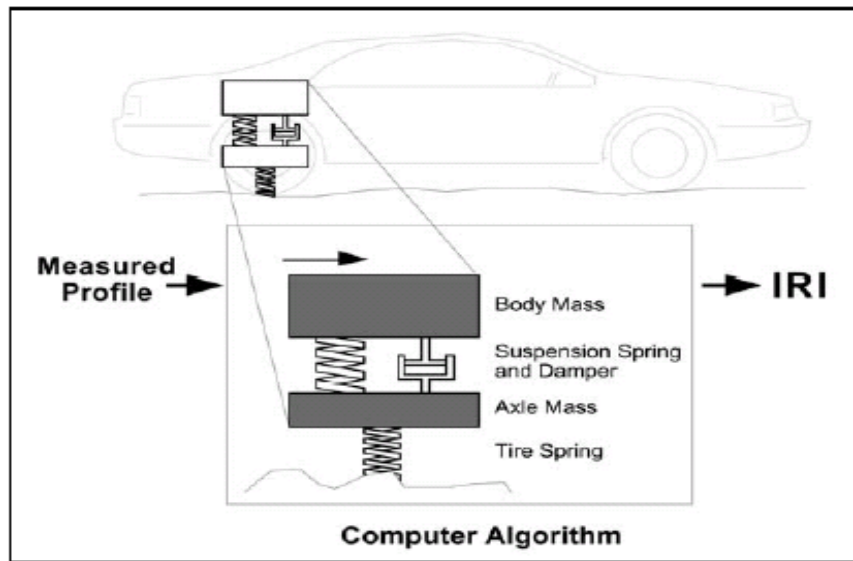


Figure 2.19 Quarter Car Simulation of road roughness (Sayers 1985)

2.6.2 Faulting

The fault values are calculated from the profile data using an algorithm developed by KDOT internally. In this process, anytime the absolute relative elevation difference between two points at 6 in. intervals for the right sensor from the output of profile elevation data processing software exceeds 0.09 inch, then the relative elevation difference (fault) values are algebraically summed until either three consecutive fault values are less than 0.09 in or 3 ft has been traversed. The calculated fault value would be the algebraic sum of the points divided by two as illustrated in Figure 2.20. Once a fault has been detected, the next fault must be located at least 10 ft away. A 0.1-mile aggregation is used for the data analysis (Miller et al. 2004).

MP	Relative Elevation	
	Left Sensor/ Wheel Path	Right Sensor/ Wheel Path
1.41548	0.02	0.03
1.41543	-0.02	-0.03
1.41538	-0.03	0.04
1.41534	0.05	0.07
1.41529	0.08	0.15
1.41524	0.01	0.15
1.41519	-0.04	0.11
1.41515	-0.04	0.05
1.41510	-0.02	-0.02
1.41505	-0.02	-0.08
1.41501	-0.02	-0.10
1.41496	0.00	-0.08
1.41491	0.00	-0.06
1.41487	0.01	-0.04

$\Sigma = 0.36$
 Fault = $0.36/2 = 0.18''$

$\Sigma = -0.28$
 $-0.28/2 = -0.14''$

Not 10' displacement

Figure 2.20 KDOT fault calculation algorithm

2.6.3 *Joint Distress*

For *Joint Distress*, three 100-ft randomly selected test sections are used to determine the expected condition for any 100-ft portion of the PMS pavement section under survey (usually one mile) (NOS 2004). The distress severity is done manually by comparing the condition observed with a set of photographs showing different severity levels. However, this distress is not compatible with the JPCP distresses predicted in the MEPDG analysis.

2.6.4 *Definition of Pavement Condition*

In Kansas, pavement condition is represented by the pavement performance level. This performance level is defined by Distress State and type of pavement. Distress State is the condition of the segment at the time of survey and is represented by a three-digit number. For rigid pavements, the first digit indicates roughness, the second digit indicates the joint distress and the third digit indicates faulting. Each digit thus represents a level of the pavement condition parameters, roughness, faulting, and joint distress. This level ranges from 1-3 with 1 being the best condition and 3 being the worst, resulting in a total of nine different distress states. Three performance levels (level 1, level 2 and level 3) are obtained by combining these nine distress states with the pavement type. Performance level 1 represents segments that appeared to require no corrective action at the time of the survey and is denoted “Good” or “Acceptable” condition. Performance level 2 represents segments that appeared to require at least routine maintenance at the time of survey and is denoted “Deteriorating” or “Tolerable” condition. Performance level 3 represents segments that appeared to require rehabilitative action beyond routine maintenance at the

time of the survey and is denoted “Deteriorated” or “Unacceptable” condition (Vedula et al. 2004).

Roughness

The first component of the JPCP Distress State discussed earlier is roughness. Roughness is expressed in KDOT PMS in ranges of IRI as follows (KDOT 2004):

- “1” indicates an IRI value of less than 105 inches per mile.
- “2” indicates an IRI value of 105 to 164 inches per mile.
- “3” indicates an IRI value of more than 164 inches per mile.

Faulting

There are three faulting severity codes (KDOT 2004):

F1: >0.125" and <0.25"

F2: 0.25" to 0.5"

F3: >0.5"

With these codes a "Fault Score" is generated by:

Fault Score = [percentage of joints in a segment exhibiting F1 faulting] + 2* [percentage of joints in a segment exhibiting F2 faulting] + 4* [percentage of joints in a segment exhibiting F3 faulting]

Using the Fault Score, the Fault Code (F) is assigned as:

1: $4 < \text{Fault Score} \leq 45$ 2: $45 < \text{Fault Score} \leq 100$ 3: $100 < \text{Fault Score}$

Then severity levels, F1, F2, and F3 in percentages are expressed as the weighted average percent of codes 1,2 and 3 faults per mile based on 352 joints per mile (15 ft joint spacing).

Joint Distress

The severity codes for joint distress are (KDOT 2004):

- J1: Noticeable staining and/or minimal cracking at each joint.
- J2: Staining and/or hairline cracking with minimum spalling.
- J3: Significant cracking and spalling. Some patching done or necessary.
- J4: Advanced cracking and severe spalling. Patching deteriorated, and 2 to 3 feet wide along joint.

Minimal cracking or spalling is defined as *less than 2 feet* along the joint length. *Significant* cracking or spalling is defined as *more than 2 feet* along the joint length. More than one severity level may be coded per test section. Extent is the number of full width joints in each severity code (KDOT 2004).

2.7 Mechanistic-Empirical Pavement Design Guide (MEPDG) Software

The MEPDG software is the primary tool used for the design of new and rehabilitated pavement structures using MEPDG algorithm. The software provides an interface to the input design variables, computational engines for analysis and performance prediction, and results and outputs from the analyses in formats suitable for use in an electronic document, such as, Excel or for making hardcopies (NCHRP 2004).

MEPDG software is a user-friendly program. It has a tree-structured layout most suitable for novices as well as experienced users. The software (runs on Windows 98, 2000, NT, and XP) handles both U.S. customary and SI units. Figure 2.21 shows the opening screen for the NCHRP MEPDG software. In this study, all analysis was done from April 2005 to August 2005, using the on-line release of the MEPDG software.

2.7.1 MEPDG Software Layout

Figure 2.22 shows a typical layout of the program. To open a new project, select “New” from the “File” menu on the tool bar. The user first provides the software with the General Information of the project and inputs in three main categories, Traffic, Climate, and Structure. All inputs for the software program are color coded as shown in Figure 2.23. Input screens that have not been visited are coded “red”. Those that have default values are coded “yellow” and those that have complete inputs are coded “green”.

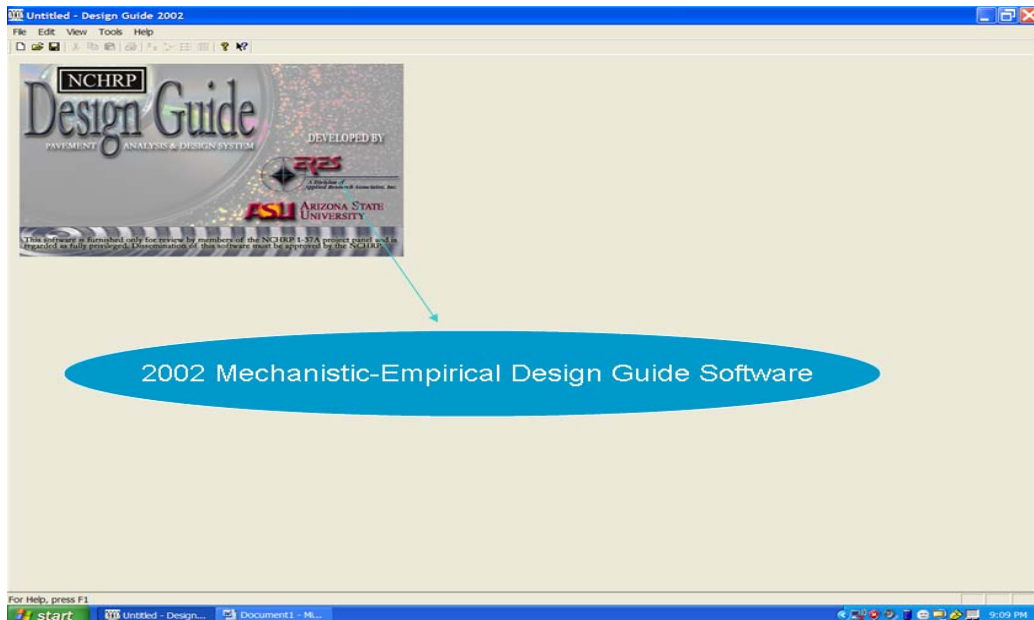


Figure 2.21 Opening screen for MEPDG software

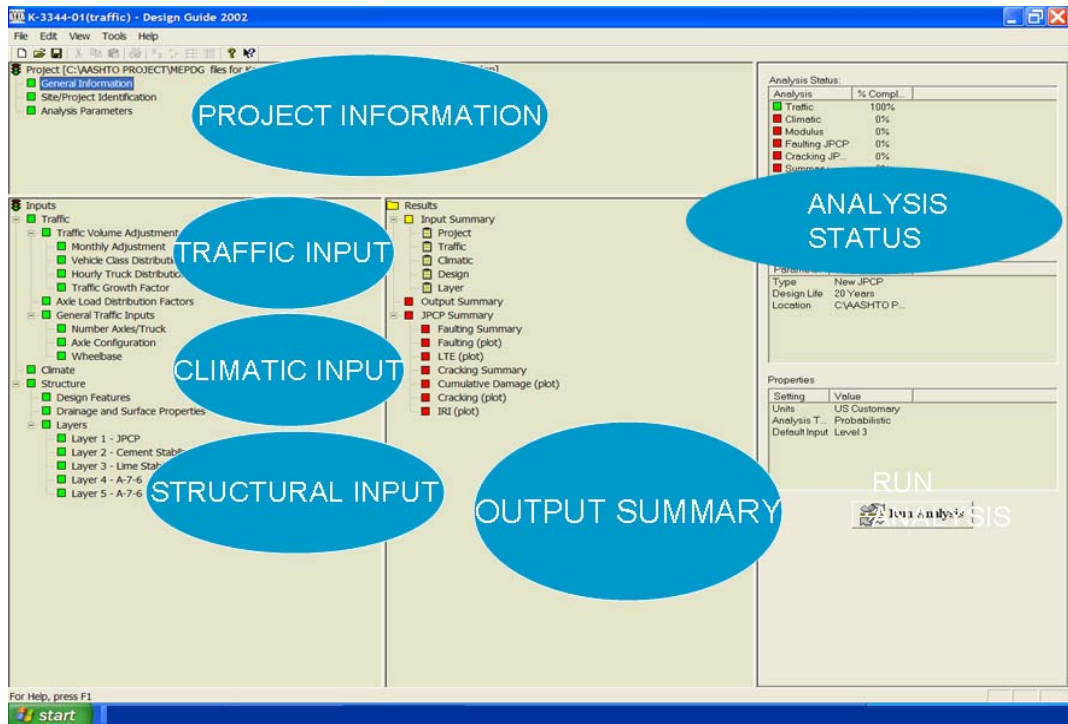


Figure 2.22 Program layout

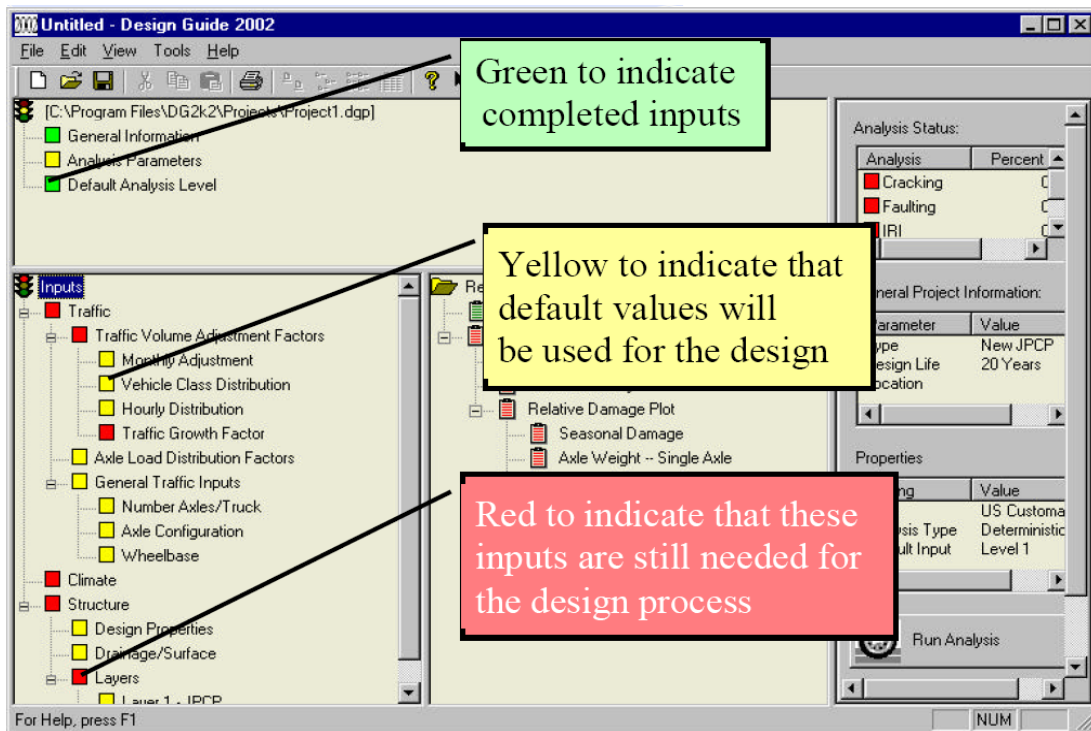


Figure 2.23 Color-coded inputs

Project related information such as, design life of the pavement, construction date, traffic opening month, site identification, mile-post limit and direction of traffic. It also includes analysis parameters such as, initial IRI and the target distress limits with corresponding reliability levels.

Figures 2.24 through 2.28 show the screens for traffic data input. Traffic screen window allows the user to make general traffic volume inputs and provides a link to other traffic screens for Volume Adjustments, Axle Load Distribution Factors, and General Inputs. It requires some general information such as, initial two-way AADT, number of lanes in the design direction, percent of trucks in the design direction and on the design lane, operational speed and traffic growth factor, etc. Monthly adjustment factors, vehicle class distribution, hourly truck traffic distribution and load spectra are also required traffic inputs.

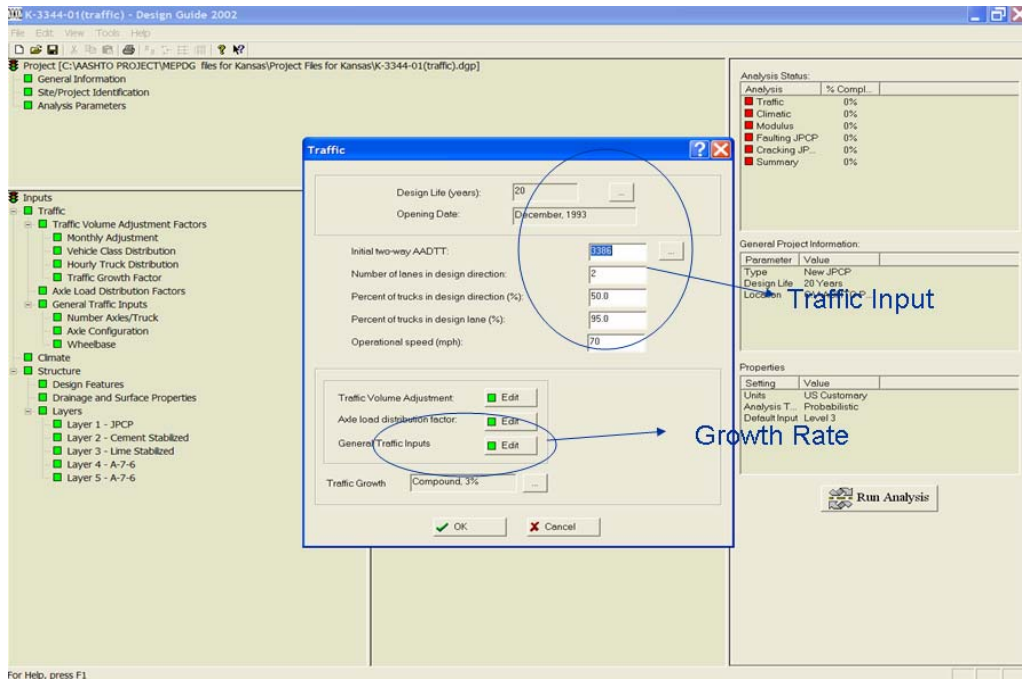


Figure 2.24 Traffic screen

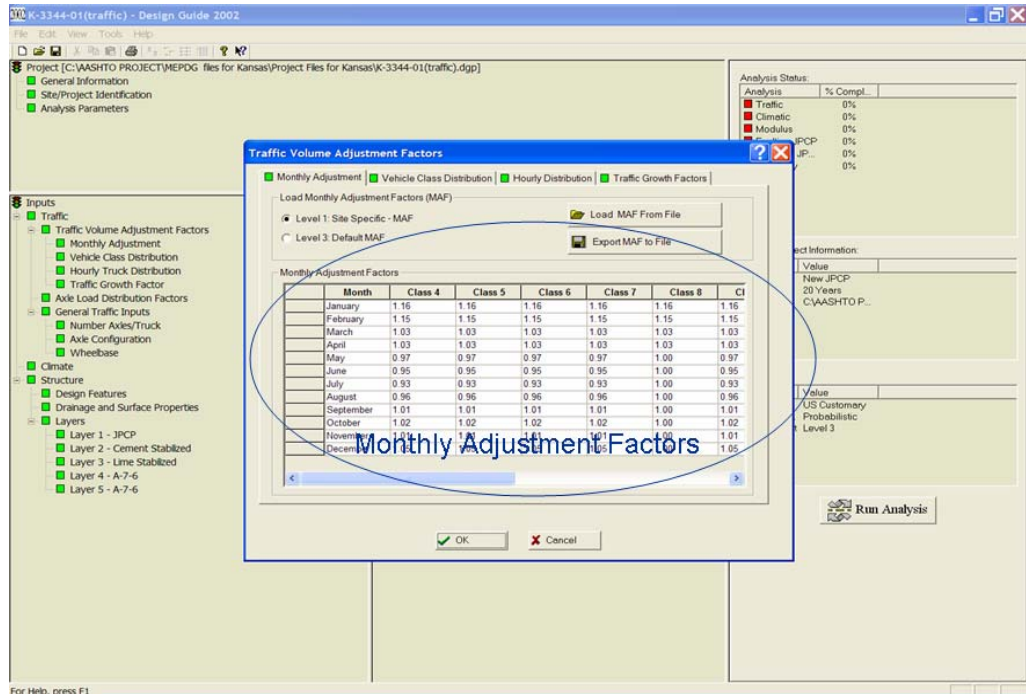


Figure 2.25 Monthly adjustment factors screen

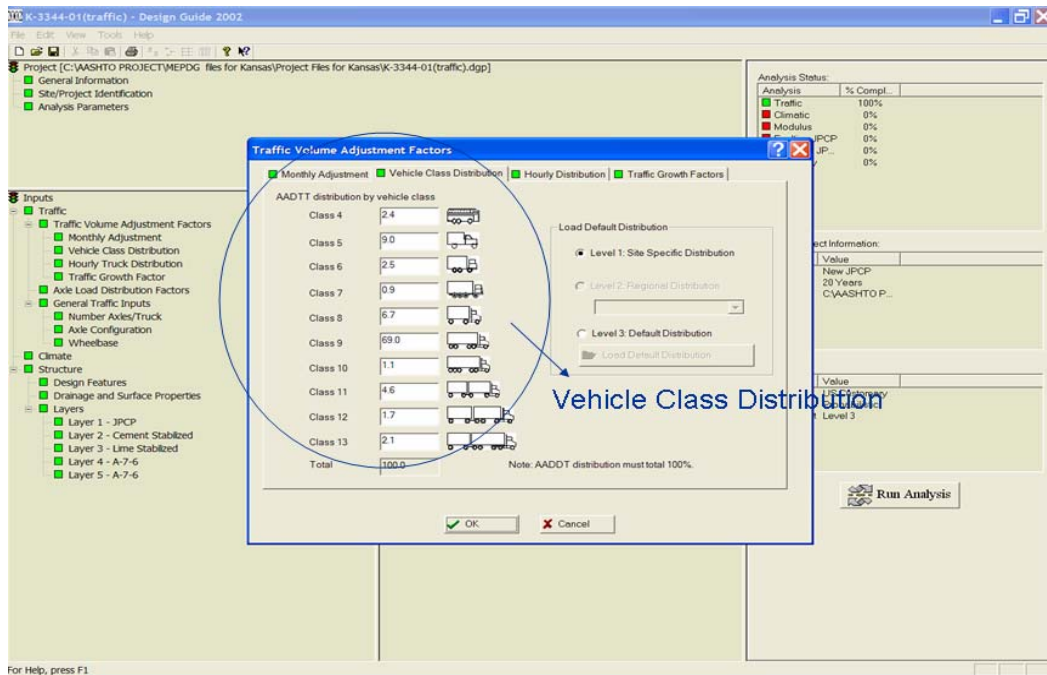


Figure 2.26 Vehicle class distribution screen

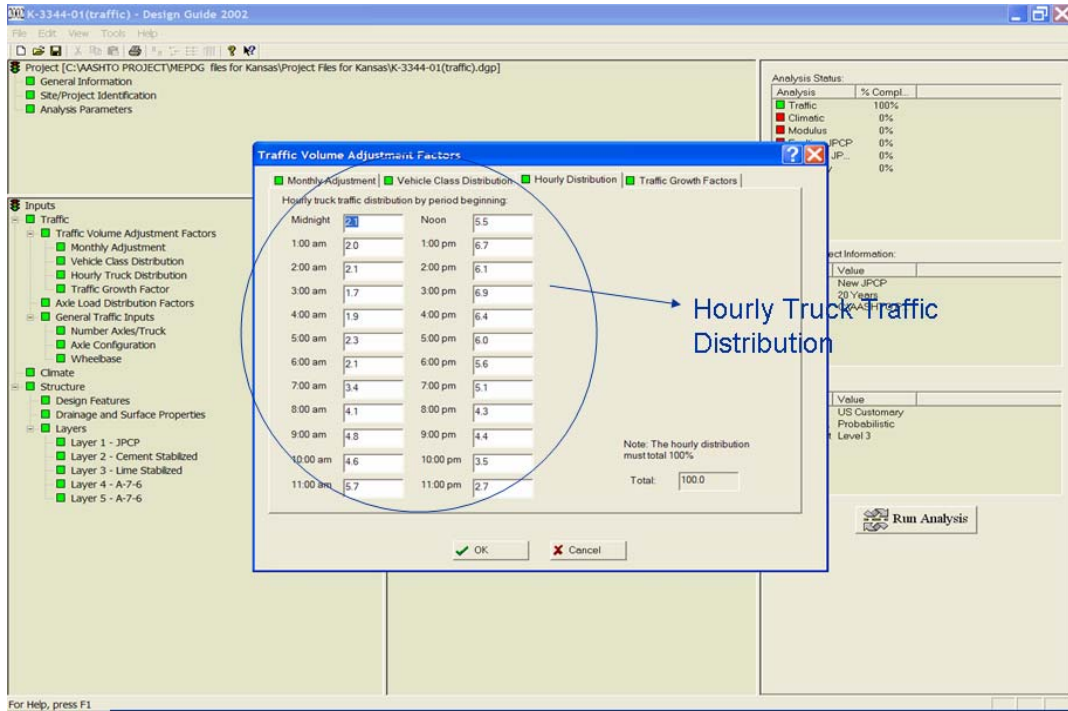


Figure 2.27 Hourly distribution screen

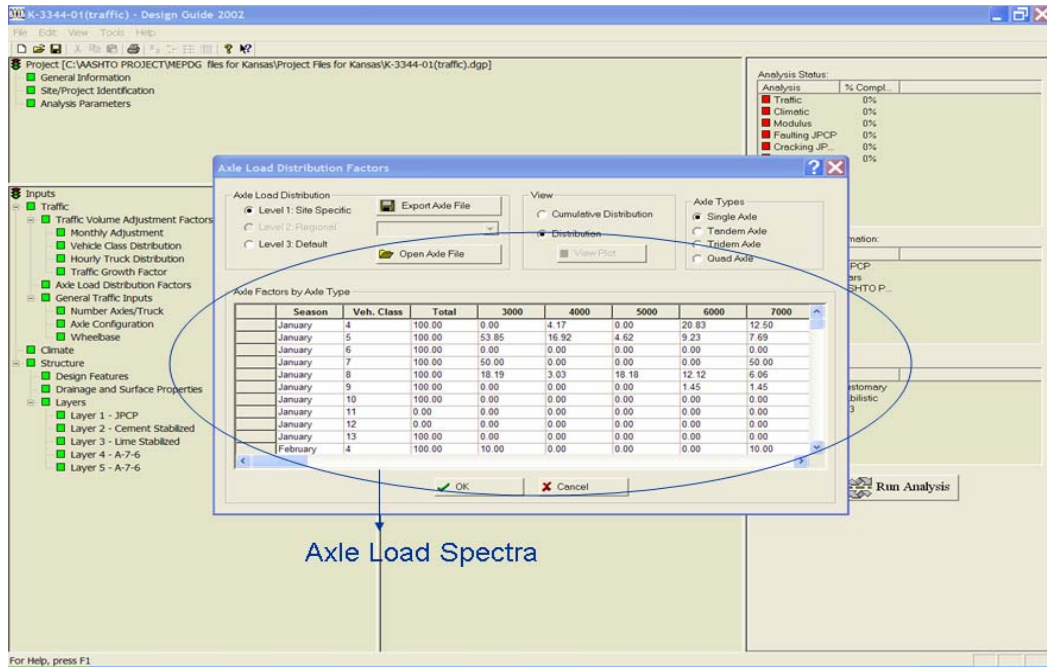


Figure 2.28 Axle load spectra screen

Figure 2.29 shows the climatic input screen. MEPDG recommends the weather inputs based on the pre-generated weather station, near the specific project site. The

software includes a database of 800 weather stations throughout the United States. This database can be accessed by specifying the latitude, longitude, and elevation of the project location.

Figures 2.30 and 2.31 show the structural input screens. Figure 2.30 shows the project specific design features inputs such as, type of design, dowel/undoweled joint, joint spacing, dowel diameter, etc. Figure 2.31 shows the inputs related to the layers in the pavement structure. Inputs for the PCC layer include PCC thickness, unit weight, compressive-strength, Poisson ratio, modulus of rupture, cement content and type, etc. If the PCC structure has a base or subbase layer, layer properties such as, elastic modulus, Poisson ratio, etc are also required inputs. Subgrade layer inputs include soil gradation, resilient modulus, etc.

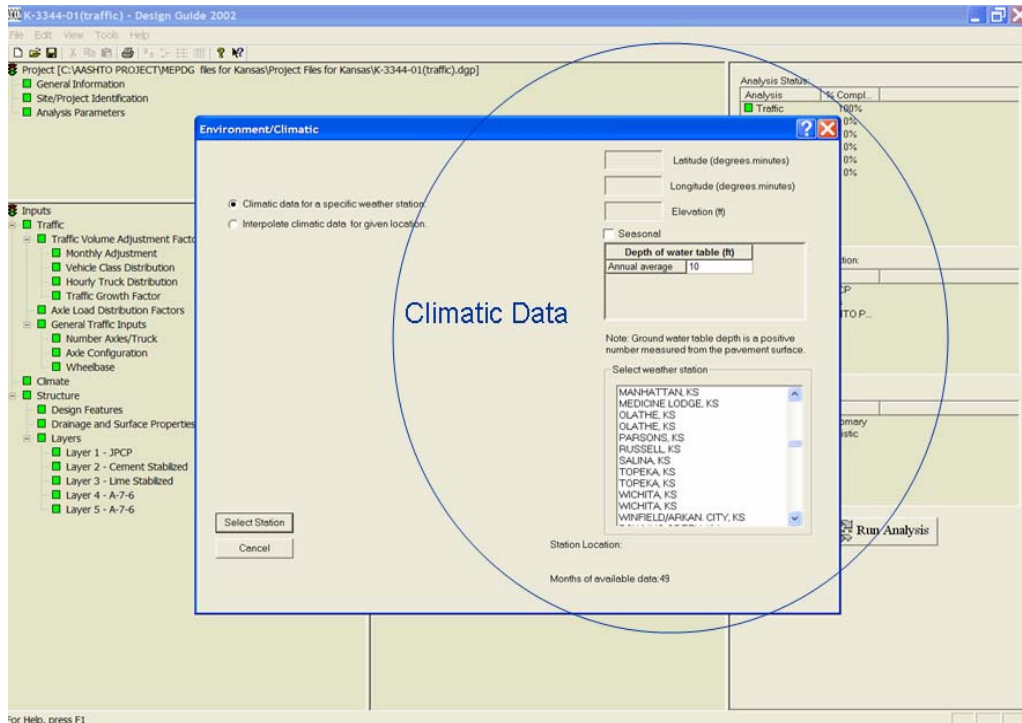


Figure 2.29 Climatic screen

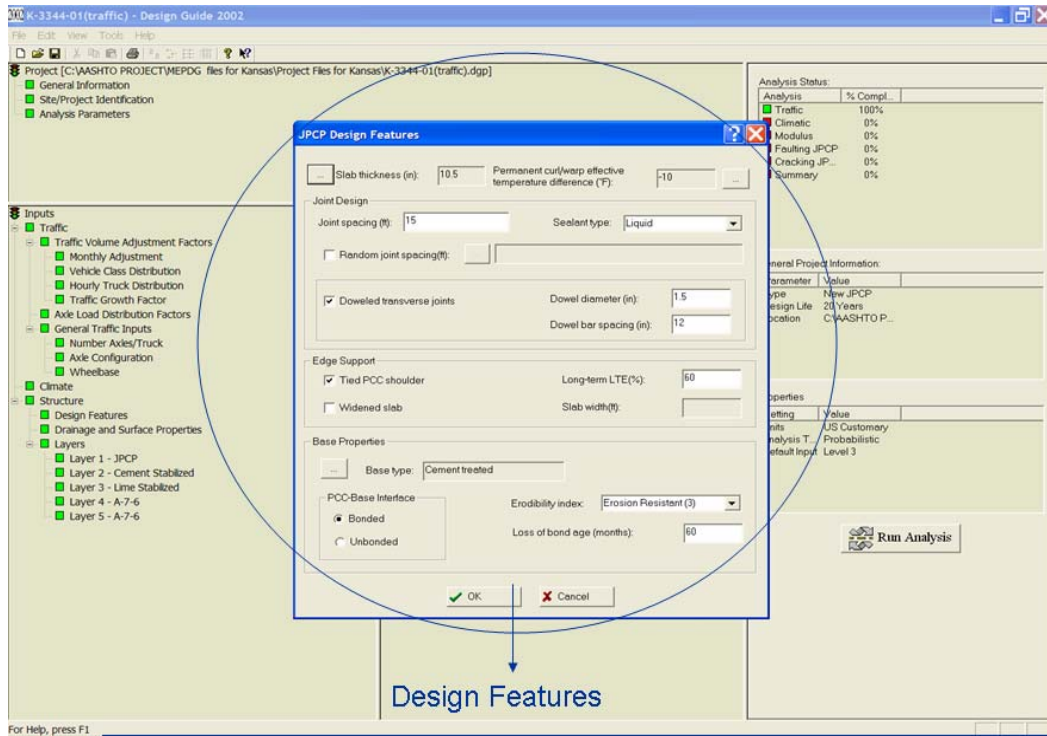


Figure 2.30 JPCP design features screen

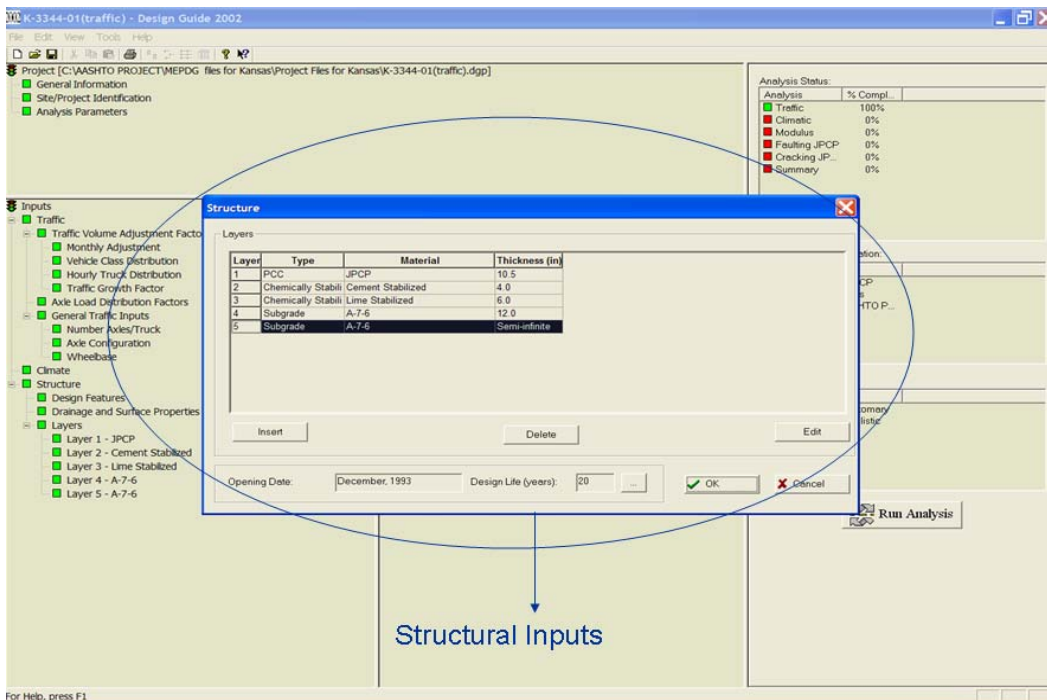


Figure 2.31 JPCP layers screen

After providing all design inputs and by clicking the *Run Analysis* button, the Design Guide software runs the analysis process to predict the performance of the trial design over the design life of the pavement. During running, the program reports the analysis status on the upper right hand corner of the screen. The software executes the damage analysis and the performance prediction engines for the trial design inputs. At the end of analysis, the program creates a summary file and other output files in the project directory. The files are in the MS Excel format. The summary file contains an input summary sheet, reliability summary sheet, distress, faulting, and cracking summary sheets in a tabular format, and the predicted faulting, Load Transfer Efficiency (LTE), differential energy, cumulative damage, cracking, and IRI in a graphical format.

For a given trial design, IRI, transverse cracking, and faulting are predicted over the design period at a certain selected reliability level. Figures 2.32 through 2.34 show the output summary tables for the predicted distresses in JPCP. Figure 2.32 shows the distress summary table that includes the predicted IRI. It also predicts the PCC modulus, base modulus, the cumulative heavy trucks and IRI at the specified reliability level for every month of the design life.

As shown in Figure 2.33, faulting summary table shows the k-value, relative humidity, joint opening, LTE, loaded/unloaded slab deflection, predicted faulting and faulting at specified reliability level, month-by-month and year-by-year. Figure 2.34 shows the cracking summary that includes the top-down and bottom-up cracking for different axle-type and traffic wheel load distribution and percent slabs cracked at the specified reliability for the whole design life of the pavement.

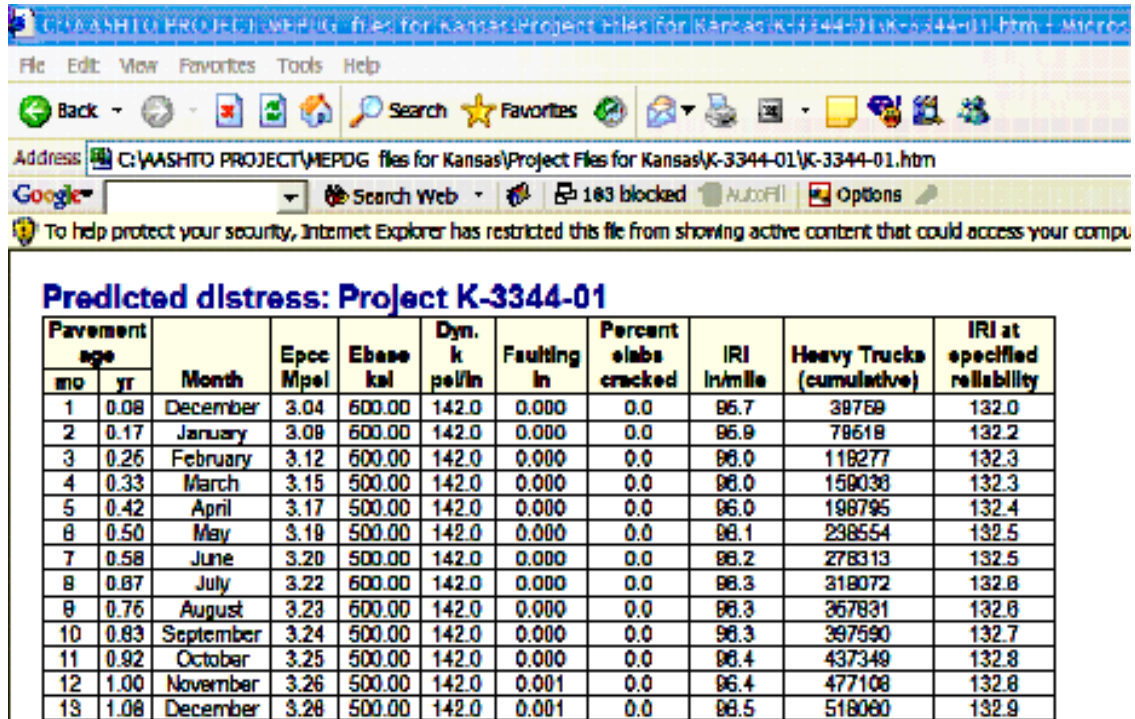


Figure 2.32 Output summaries for IRI

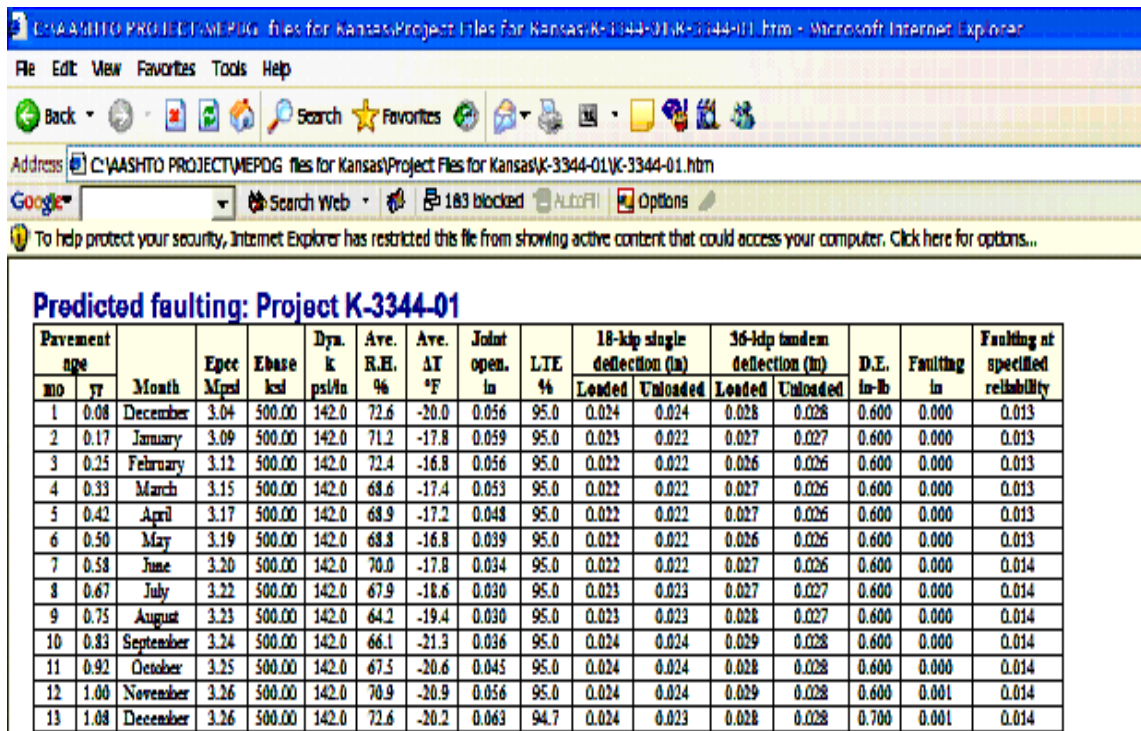


Figure 2.33 Output summaries for faulting

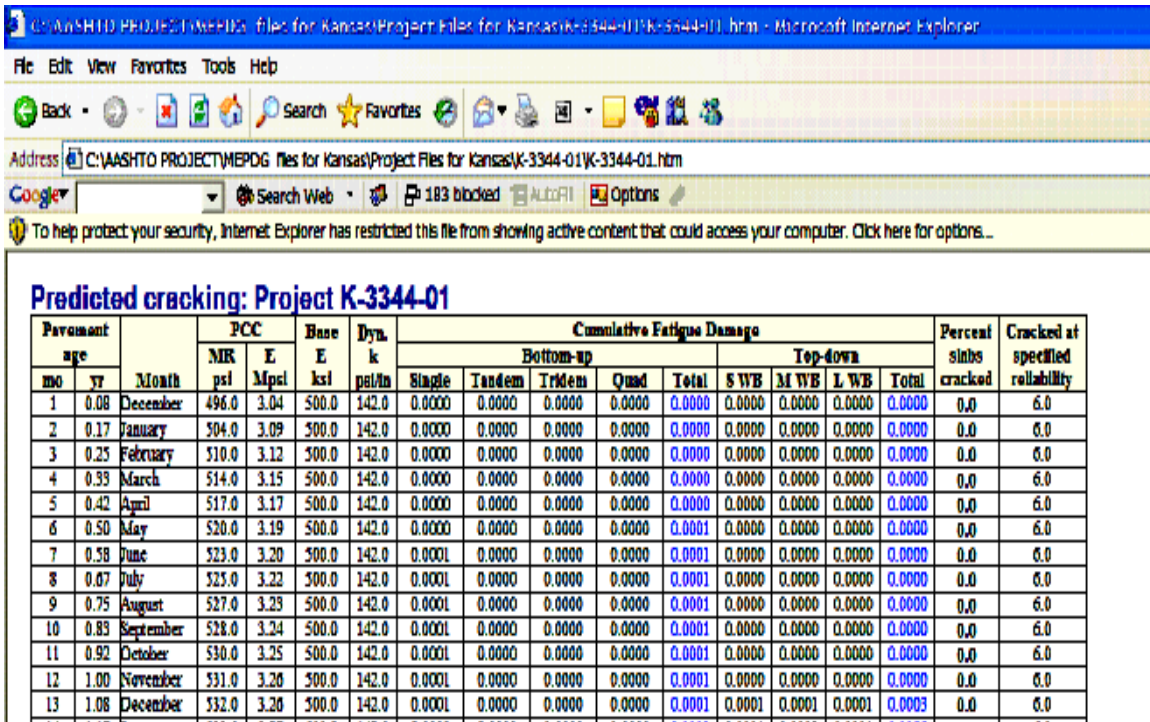


Figure 2.34 Output summaries for cracking

2.8 Summary

The new Mechanistic Empirical Design Guide has significant influence on the performance of the JPCP. Deficiency in different design and construction features of JPCP contributes to the pavement smoothness (IRI), faulting and cracking. Identification of these distresses can help to figure out different alternative design strategy to compensate the distresses. Current AASHTO Design Guide (1993) is based on empirical performance equations, for the design of Jointed Plain Concrete Pavements (JPCP). That Guide ignores a number of important design features. However, the newly released Mechanistic-Empirical Pavement Design Guide (MEPDG) provides methodologies for mechanistic-empirical pavement design while accounting for local materials, environmental conditions, and actual highway traffic load distribution by means of axle load spectra.

CHAPTER 3

TEST SECTIONS AND DESIGN ANALYSIS INPUTS

This chapter describes the test sections selected and the material characteristics required for the mechanistic-empirical (M-E) design analysis described in MEPDG. It also outlines the Kansas-specific input data generation process.

3.1 Test Sections

Eight in-service JPCP projects were selected for the MEPDG design analysis. Three of these projects were the experimental sections chosen from the Kansas Specific Pavement Studies -2 (SPS-2) projects located on Interstate route 70. Two other projects are located on I-70, two on US-50 and one on route K-7. Table 3.1 tabulates the general features of these sections. The SPS-2 sections were each 500 ft long, and the rest are one to several miles long.

All sections have 15 ft joint spacing with dowelled joints. Three of the experimental sections have 1.5-in diameter steel dowels and other sections have dowel diameters varying from 1.125 in to 1.375 in. All sections have 12 ft lanes with tied concrete shoulders except the SPS-2 Section 6. That section has a widened lane of 14 ft with tied PCC shoulder. The sections were constructed on a stabilized base and a treated subgrade. Base stabilization was done with Portland cement. Depending upon the cement content and gradation, the bases were designated as Portland cement-treated base (PCTB), bound drainable base (BDB) or lean concrete base (LCB). Base thickness ranged from 4 to 6 inches as shown in Table 3.1. The projects have primarily silty clay as subgrade. The top six inches of the natural subgrade were treated with lime or fly ash to reduce the plasticity and/or control the moisture during construction. PCC slab

thickness, designed according to the 1986 or 1993 AASHTO Design Guide, ranged from 9 to 12 inches. The strength (modulus of rupture or compressive strength) values shown in Table 3.1 are the actual average values obtained during construction. The as-constructed International Roughness Index (IRI) values on these projects varied from 59 in/mile to 122 in/mile.

The annual average daily traffic (AADT) on these sections ranged from 2,080 for a US-50 Chase County project to 36,000 for the I-70 Shawnee County project. Very high percentage (45.5%) of truck traffic was observed on the US-50 projects and the lowest percentage (5%) was on the I-70 Shawnee County project.

Table 3.1 Project Features of the Study Sections

Project ID	Route	County	Year Built	Mile post Limit	Traffic Direction	PCC Thickness (in)	PCC 28-day Strength (psi)	Initial IRI (in/mi)	Subgrade Soil Type
K-2611-01*	I-70	Geary	Nov 1990	0 – 7	WB	11	690	60	A-6
K-3344-01**	I-70	Shawnee	Oct 1993	9 – 10	WB	10.5	473	96	A-7-6
SPS-2 (Sec-5)†	I-70	Dickinson	July 1992	20 – 22.61	WB	11	945	122	A-6
SPS-2 (Sec-6)†	I-70	Dickinson	July 1992	20 – 22.61	WB	11	617	98	A-6
SPS-2 (Control)*	I-70	Dickinson	July 1992	20 – 22.61	WB	12	647	95	A-6
K-3216-02***	US-50	Chase	Dec 1997	0 – 9	WB	10	5,569	59	A-7-6
K-3217-02***	US-50	Chase	Dec 1997	9 – 19	WB	10	4,362	68	A-7-6
K-3382-01**	K-7	Johnson	Sep 1995	12 – 15	SB	9	537	81	A-7-6

*6" Portland Cement-Treated Base (PCTB)

** 4" Portland Cement-Treated Base (PCTB)

*** 4" Bound Drainable Base (BDB)

† 6" Lean Concrete Base (LCB)

3.2 Inputs

One of the most important aspects of mechanistic-empirical pavement design is the set of inputs required to perform the analysis and design. These inputs define the conditions under which a particular pavement structure is designed to perform.

As the desired project-specific information is not generally available at the design stage and mostly estimated several years in advance of construction, difficulty arises in obtaining adequate design inputs. Therefore, the designer needs to obtain as much data as possible on material properties, traffic, and other inputs for use in design to ensure as realistic data as possible.

The primary design inputs required for MEPDG are listed below:

- ◆ Designer/user selected inputs for pavement structures, such as layer thickness, material types, joint spacing, etc.
- ◆ Design inputs under which a pavement structure is designed to perform, such as, traffic, subgrade/foundation, and environment/climate.
- ◆ Input for the material / mix design properties of the layers.

3.3 Hierarchical Design Inputs

The hierarchical approach is used for the design inputs in MEPDG. This approach provides the designer with several levels of "design efficacy" that can be related to the class of highway under consideration or to the level of reliability of design desired. The hierarchical approach is primarily employed for traffic, materials, and environmental inputs (NCHRP 2004). In general, three levels of inputs are provided:

Level 1 - Level 1 is a "first class" or advanced design procedure and provides for the highest practically achievable level of reliability and recommended for design in the heaviest traffic corridors or wherever there are dire safety or economic consequences of early failure. The design inputs also are of the highest practically achievable level and generally require site-specific data collection and/or testing. Example is the site-specific axle load spectra for traffic input.

Level 2 - Level 2 is the input level expected to be used in routine design. Level 2 inputs are typically user selected, possibly from an agency database. The data can be derived from a less than optimum testing program or can be estimated empirically. Estimated Portland cement concrete elastic modulus from the compressive strength test results is an example of Level 2 input in the material input data category.

Level 3 - Level 3 typically is the lowest class of design and should be used where there are minimal consequences of early failure. Inputs typically are user-selected default values or typical averages for the region. An example would be the default value for the Portland cement concrete coefficient of thermal expansion for a given mix class and aggregates used by an agency.

For a given design, it is permissible to mix different levels of input.

3.4 Development of Kansas-Specific MEPDG Inputs

The inputs required for the MEPDG software can be classified into four categories:

- ◆ General
- ◆ Traffic

- ◆ Climate
- ◆ Structural Inputs.

The following sections will summarize all inputs required for the design analysis of Jointed Plain Concrete Pavements (JPCP) using MEPDG and their relationships to the design process.

3.4.1 *General*

The general inputs consist of information required by the MEPDG software that describes the nature of the project, the timeline, the design criteria that the agency specifies, and miscellaneous information that can serve to identify the project files. The General project information can be entered in to the MEPDG software from three individual screens of General Information, Site/Project Identification, and Analysis Parameters.

3.4.1.1 General Information

This part allows the user to make broad choices about the design options. The MEPDG software considers two pavement types, “flexible” and “rigid. Rigid pavement design offers two alternatives for the surface layer, JPCP and CRCP. All pavement design projects can be classified under three main categories as New Design, Restoration, and Rehabilitation or Overlay.

The following inputs define the analysis period and type of design analysis for JPCP:

- ◆ Design Life
- ◆ Pavement Construction Month

- ◆ Traffic Opening Month
- ◆ Pavement Type

The *Design life* is the expected service life of the pavement in years. Pavement performance is predicted over the design life from the month the pavement is opened to traffic to the last month in design life.

Pavement construction month is the month when the surface (PCC) layer is placed. Due to time and environmental conditions, changes to the surface layer material properties are considered from the pavement construction month. This input is required to estimate the “zero-stress” temperature in the PCC slab at construction which affects the faulting in JPCP.

Traffic opening month and year are also required inputs for MEPDG to estimate the pavement opening date to traffic after construction. This parameter defines the climatic condition at that time that relates to the temperature gradients and the layer moduli, including that of the subgrade. This input also determines the PCC strength at which traffic load is applied to the pavement for damage calculation purposes.

Pavement type can be JPCP or CRCP. This input determines the method of design evaluations and the applicable performance models.

Project-specific “General” details are described in Table 3.1. All test sections selected in this study are JPCP with a design life of 20 years. All SPS-2 sections were constructed in July 1992 and opened to traffic in August. The I-70 Geary County project had the earliest construction year of 1990 and the Chase County projects were the latest, constructed in 1997.

3.4.1.2 Site Identification

This screen in the MEPDG software allows the user to provide information that are typically useful for identification and documentation purposes only. This information will not affect the analysis or design process but will help identify the location and stationing of the project. Typical inputs include Project location, Project ID, Section ID, begin and end mile posts, and traffic direction (EB, WB, SB, NB).

In this study, typical site identification information for the test sections are shown in Table 3.1. Five of the projects are Rural Principal Arterial Interstate, one is Principal Arterial others (Urban), and two are Rural Principal Arterial (others).

3.4.1.3 Analysis Parameters

This part includes the analysis type and the basic criteria for performance prediction. The project specific inputs for this section includes Initial IRI and performance criteria or failure criteria for verification of the trial design.

The Initial IRI defines the expected level of smoothness in the pavement soon after the completion of construction, expressed in terms of International Roughness Index (IRI). Typical value, suggested by MEPDG, ranges from 50 to 100 in/mi. In this study, initial IRI for the test sections varied from 59 in/mile to 122 in/mile and are presented in Table 3.1.

Depending on the pavement type, the appropriate performance criteria need to be specified in the design analysis. Performance criteria form the basis for acceptance or rejection of a trial design being evaluated using MEPDG. In the MEPDG analysis, the key outputs are the individual distress quantities. For JPCP, MEPDG analysis predicts

faulting, transverse cracking, and smoothness or IRI. Failure criteria are associated with certain design reliability for each distress type. Table 3.2 summarizes the MEPDG suggested reliability levels, based on the functional class of the roadway.

In this study, the projects were functionally classified as Rural Interstate or Principal Arterials (Urban and Rural). Therefore, a design reliability of 90% was used for all projects based on the MEPDG recommendations. The corresponding failure criteria chosen for IRI were 164 in/mile, 0.12 inch for faulting, and 15% for slab cracking. The IRI level was based on the roughness level 2 of the KDOT pavement Management System, NOS.

Table 3.2 Recommended Design Reliability for MEPDG (NCHRP 2004)

Functional Classification	Recommended Reliability	
	Urban	Rural
Interstate/ Freeways	85-97	80-95
Principal Arterials	80-95	75-90
Collectors	75-85	70-80
Local	50-75	50-75

3.4.2 Traffic

Traffic data is a key element in the design/analysis of pavement structures. Traffic data are expressed in terms of equivalent single axle loads (ESALs) in the AASHTO Design Guides since 1972 and also in most other pavement design procedures. As MEPDG does design and performance analysis based on the principles of engineering mechanics, therefore it requires the estimation of axle loads that a pavement is expected to serve. (Milestones 2002)

3.4.2.1 MEPDG Hierarchical Traffic Inputs

MEPDG defines three broad levels of traffic data input. Regardless of the level, the same pavement analysis procedure is followed. As mentioned before, the full axle-load spectrum data are need for MEPDG for new pavement and rehabilitation design analyses. MEPDG recognizes the fact that detailed traffic data over the years to accurately characterize future traffic for design may not be available (NCHRP 2004). Thus, to facilitate the use of MEPDG regardless of the level of detail of available traffic data, a hierarchical approach has been adopted for developing required traffic inputs. MEPDG outlines three broad levels of traffic data input (Levels 1 through 3) based on the amount of traffic data available:

Level 1 – There is a *very good* knowledge of past and future traffic characteristics. At this level, it is assumed that the past traffic volume and weight data have been collected along or near the roadway segment to be designed. Thus, the designer will have a high level of confidence in the accuracy of the truck traffic used in design. Thus, Level 1 requires the gathering and analysis of historical site-specific traffic volume and load data. Level 1 is considered the most accurate because it uses the actual axle weights and truck traffic volume distributions measured over or near the project site.

Level 2 – There is a *modest* knowledge of past and future traffic characteristics. At this level, only regional/state-wide truck volume and weights data may be available for the roadway in question. In this case, the designer will have the ability to predict with reasonable certainty the basic truck load pattern. Level 2 requires the designer to collect enough truck volume information at a site to measure truck

volumes accurately. The data collection should take into account any weekday/weekend volume variation, and any significant seasonal trends in truck loads.

Level 3 – There is a *poor* knowledge of past and future traffic characteristics. At this level, the designer will have little truck volume information (for example, Average Annual Daily Traffic [AADT] and a truck percentage). In this case, a regional or state-wide or some other default load distribution must be used (NCHRP 2004).

State highway agencies often collect two major types of traffic data:

- ◆ Weigh-in-motion (WIM) data, which provide information about the number and configuration of axles observed within a series of load groups.
- ◆ Automatic vehicle classification (AVC) data for information about the number and types of vehicles, as shown in Figure 3.1, that uses a given section of roadway.

WIM data are a tabulation of the vehicle type and number, spacing and weight of axles for each vehicle weighed over a period of time. This information is used to determine normalized axle load distribution or spectra for each axle type within each truck class. This needs to be done external to the MEPDG software. AVC data are used to determine the normalized truck class distribution. This also needs to be done external to the MEPDG software. Classification is based on the specific location at which data are collected such as, site-specific, regional/statewide, or national. Another commonly collected traffic data item is vehicle count. It consists of counting of the total number of vehicles over a period of time. Counts can be continuous, seasonal, or short duration.

MEPDG makes two major assumptions with regard to the truck and axle load and vehicle class distribution (NCHRP 2004):

1. The axle load distribution by axle type and vehicle class remains constant from year to year, whereas the vehicle class distribution can change from year to year.
2. The axle load distribution does not change throughout the day or over the week (weekday versus weekends, and night versus day). However, the vehicle class or truck distributions can change over the time of day or day of the week.














1-2 axles		1	Motorcycles
		2	Passenger cars
		3	Two axles and tire single units
		4	Buses
3-5 axles		5	Two axles and tire single units
		6	Three axles single units
		7	Four or more axle single units
		8	Four or less axle single trailers
6+ axles		9	Five axle single trailers
		10	Six or more axle single trailers
		11	Five or less axle multi-trailers
		12	Six axle multi-trailers
		13	Seven or more axle multi-trailers

Figure 3.1 Illustration of the FHWA vehicle classes for MEPDG (Milestones 2002)

3.4.2.2 Kansas Traffic Monitoring System for Highways (TMS/H)

Kansas TMS/H provides traffic data for the Kansas Department of Transportation (KDOT) for project selection, traffic modeling, traffic forecast, transportation studies, pavement design, and air quality analysis (KDOT 2003). The TMS/H also provides traffic data to Federal Highway Administration (FHWA) for their reporting requirements. The TMS/H was developed following the concepts in FHWA's Traffic Monitoring Guide (TMG) published in February 1995 and May 2001. The 1995 TMG recommended a sample size of 300 vehicle classification sites and 90 truck weight sites which KDOT adopted. Currently, KDOT is adopting 2001 TMG recommendations of increasing number of short-term and continuous classification locations (KDOT 2003). The components of TMS/H that are important for developing traffic inputs for MEPDG are: (1) Continuous traffic counting, (2) Vehicle classification, and (3) Truck weight.

Continuous Traffic Counting

In Kansas, there are about 102 sites throughout the state on most roadway functional classes to do hourly traffic counts using permanent, roadway mounted equipment. About 12,000 24 or 48-hour counts (approximately 5,500 on the State Highway System and 6,500 off the State system) are collected each year for the short-term traffic count. Traffic counts on the State System are collected every two years except on the Interstates, ramps and freeways where data is collected annually. The permanent site data is used to develop temporal adjustment factors for the short-term traffic counts.

Vehicle Classification

Kansas uses FHWA's 13-category, Scheme F for vehicle classification. Classification surveys are done at 300 locations on a three-year cycle or 100 locations per year. Duration of regular survey is 48 hours. Most data are collected by machine, though some is done visually. Some locations cannot be accurately classified using portable classification equipment. Therefore, visual or manual counts are the only possible way to count vehicle types, though counts are limited to 16 hours (6 A.M. to 10 P.M.). At some locations, machine counts are satisfactorily implemented to supplement this limitation and obtain a full 24-hour count. Kansas is in the process of preparing continuous classification data and as of December 2003, there are five locations for collection of continuous classification data (KDOT 2003).

As of now, at very limited sites, Kansas collects information on the speed, class, time, axle weights and axle spacings for each commercial vehicle that crosses the equipment. Around eleven permanent and 73 portable sites provide truck weight data in the State.

A summary of the traffic data required for JPCP design is presented below along with the basic definitions of the variables and references to the default values.

3.4.2.3 Base Year Input

The base year for the traffic inputs is defined as the first year that the roadway segment under design is opened to traffic. The following pieces of base year information are required:

- ◆ Annual Average Daily Truck Traffic (AADTT) for the base year, which

includes the total number of heavy vehicles (FHWA classes 4 to 13 as shown in Figure 3.1) in the traffic stream.

- ◆ Number of lanes in the design direction.
- ◆ Percent trucks in the design direction (directional distribution factor).
- ◆ Percent trucks in the design lane (lane distribution factor).
- ◆ Operational speed of the vehicles.

In this study, AADT ranged from 2,080 to 36,000 for the test sections. Truck percentages in the design direction varied from 47% (provided by LTPP for the three SPS-2 sections) to 50%. Ninety-five percent trucks were assigned in the design lane for the 4-lane divided highways based on the default level 3 inputs. Table 3.3 summarizes the base inputs.

Table 3.3 Base Year Input Summary

Project ID	Initial Two-way AADT	Truck Traffic (%)	No. of lane in Design Direction	% of Truck in Design Direction	Operational Speed (mph)	Linear Growth Rate (%)
K-2611-01	9,200	18	2	50	70	1.2
K-3344-01	36,000	5	2	50	70	3
SPS-2 (Sec-5)	11,970	22.3	2	47	70	3.5
SPS-2 (Sec-6)	11,970	22.3	2	47	70	3.5
SPS-2 (Control)	11,970	22.3	2	47	70	3.5
K-3216-02	2,080	45.5	1	50	70	2.0
K-3217-02	3,480	40.5	1	50	70	2.0
K-3382-01	13,825	7	2	50	60	6.7

3.4.2.4 Traffic Volume Adjustments

In order to characterize traffic, the following truck-traffic volume adjustment factors are required:

- ◆ Monthly adjustment factors
- ◆ Vehicle class distribution factors
- ◆ Hourly truck distribution factors
- ◆ Traffic growth factors

Monthly adjustment factors

Truck traffic monthly adjustment factors (MAF) simply represent the proportion of the annual truck for a given truck class that occurs in a specific month. These values are the ratio of the monthly truck traffic to the AADTT.

$$MAF_i = \frac{AMDTT_i}{\sum_{i=1}^{12} AMDTT_i} * 12 \quad (3.1)$$

Where, MAF_i = monthly adjustment factor for month i ; and

$AMDTT_i$ = average monthly daily traffic for month i .

The sum of MAF_i for all months in a year must equal 12.

The truck monthly distribution factors are used to determine the monthly variation in truck traffic within the base year. Several other factors such as, adjacent land use, location of industries and roadway location (urban or rural) have the influence on MAF_i .

In this study, monthly adjustment factors were extracted from the Traffic Monitoring Guide guidelines followed by KDOT (KDOT 2003). Weekly and monthly adjustment factors were developed based on the functional class of the roadways. Tables 3.4, 3.5 and 3.6 show KDOT-reported monthly and weekly adjustment factors for different functional classifications.

Table 3.4 Adjustment Factors Report for Rural Interstate Highways (KDOT 2003)

Month	Class 4	Class 5	Class 6	Class 7	Class 8	Class 9	Class 10	Class 11	Class 12	Class 13
January	1.164	1.164	1.164	1.164	1.164	1.164	1.164	1.164	1.164	1.164
February	1.152	1.152	1.152	1.152	1.152	1.152	1.152	1.152	1.152	1.152
March	1.034	1.034	1.034	1.034	1.034	1.034	1.034	1.034	1.034	1.034
April	1.034	1.034	1.034	1.034	1.034	1.034	1.034	1.034	1.034	1.034
May	0.973	0.973	0.973	0.973	0.973	0.973	0.973	0.973	0.973	0.973
June	0.948	0.948	0.948	0.948	0.948	0.948	0.948	0.948	0.948	0.948
July	0.93	0.93	0.93	0.93	0.93	0.93	0.93	0.93	0.93	0.93
August	0.956	0.956	0.956	0.956	0.956	0.956	0.956	0.956	0.956	0.956
September	1.012	1.012	1.012	1.012	1.012	1.012	1.012	1.012	1.012	1.012
October	1.022	1.022	1.022	1.022	1.022	1.022	1.022	1.022	1.022	1.022
November	1.011	1.011	1.011	1.011	1.011	1.011	1.011	1.011	1.011	1.011
December	1.048	1.048	1.048	1.048	1.048	1.048	1.048	1.048	1.048	1.048

Table 3.5 Adjustment Factors Report for Other Urban Roadways (KDOT 2003)

Month	Class 4	Class 5	Class 6	Class 7	Class 8	Class 9	Class 10	Class 11	Class 12	Class 13
January	1.012	1.012	1.012	1.012	1.012	1.012	1.012	1.012	1.012	1.012
February	0.981	0.981	0.981	0.981	0.981	0.981	0.981	0.981	0.981	0.981
March	0.957	0.957	0.957	0.957	0.957	0.957	0.957	0.957	0.957	0.957
April	0.904	0.904	0.904	0.904	0.904	0.904	0.904	0.904	0.904	0.904
May	0.901	0.901	0.901	0.901	0.901	0.901	0.901	0.901	0.901	0.901
June	0.889	0.889	0.889	0.889	0.889	0.889	0.889	0.889	0.889	0.889
July	0.907	0.907	0.907	0.907	0.907	0.907	0.907	0.907	0.907	0.907
August	0.904	0.904	0.904	0.904	0.904	0.904	0.904	0.904	0.904	0.904
September	0.938	0.938	0.938	0.938	0.938	0.938	0.938	0.938	0.938	0.938
October	0.923	0.923	0.923	0.923	0.923	0.923	0.923	0.923	0.923	0.923
November	0.943	0.943	0.943	0.943	0.943	0.943	0.943	0.943	0.943	0.943
December	0.981	0.981	0.981	0.981	0.981	0.981	0.981	0.981	0.981	0.981

Table 3.6 Adjustment Factors Report for Other Rural Roadways (KDOT 2003)

Month	Class 4	Class 5	Class 6	Class 7	Class 8	Class 9	Class 10	Class 11	Class 12	Class 13
January	1.075	1.075	1.075	1.075	1.075	1.075	1.075	1.075	1.075	1.075
February	1.047	1.047	1.047	1.047	1.047	1.047	1.047	1.047	1.047	1.047
March	1.009	1.009	1.009	1.009	1.009	1.009	1.009	1.009	1.009	1.009
April	0.942	0.942	0.942	0.942	0.942	0.942	0.942	0.942	0.942	0.942
May	0.921	0.921	0.921	0.921	0.921	0.921	0.921	0.921	0.921	0.921
June	0.907	0.907	0.907	0.907	0.907	0.907	0.907	0.907	0.907	0.907
July	0.916	0.916	0.916	0.916	0.916	0.916	0.916	0.916	0.916	0.916
August	0.928	0.928	0.928	0.928	0.928	0.928	0.928	0.928	0.928	0.928
September	0.947	0.947	0.947	0.947	0.947	0.947	0.947	0.947	0.947	0.947
October	0.961	0.961	0.961	0.961	0.961	0.961	0.961	0.961	0.961	0.961
November	0.972	0.972	0.972	0.972	0.972	0.972	0.972	0.972	0.972	0.972
December	1.028	1.028	1.028	1.028	1.028	1.028	1.028	1.028	1.028	1.028

MEPDG default distribution assumes even distribution, i.e. an MAF of 1.0 for all months for all vehicle classes. Figure 3.2 presents a comparison of MEPDG default monthly adjustment factor distribution for all functional classes of highways with that for the Kansas Rural Interstate highways. It is evident from the figure and the above tables that although MEPDG default input shows no monthly variation of truck traffic within the year, Kansas input shows significant variation within the year. Tables 3.4, 3.5 and 3.6 show that the distribution ratio is greater than 1.0 for the winter months. In general, traffic is heavier in Kansas during the winter and spring months (December through April) partly due to hauling of grains and crops from the elevators to different destinations. The same monthly distribution was used for all classes of vehicles for a particular functional class of roadways.

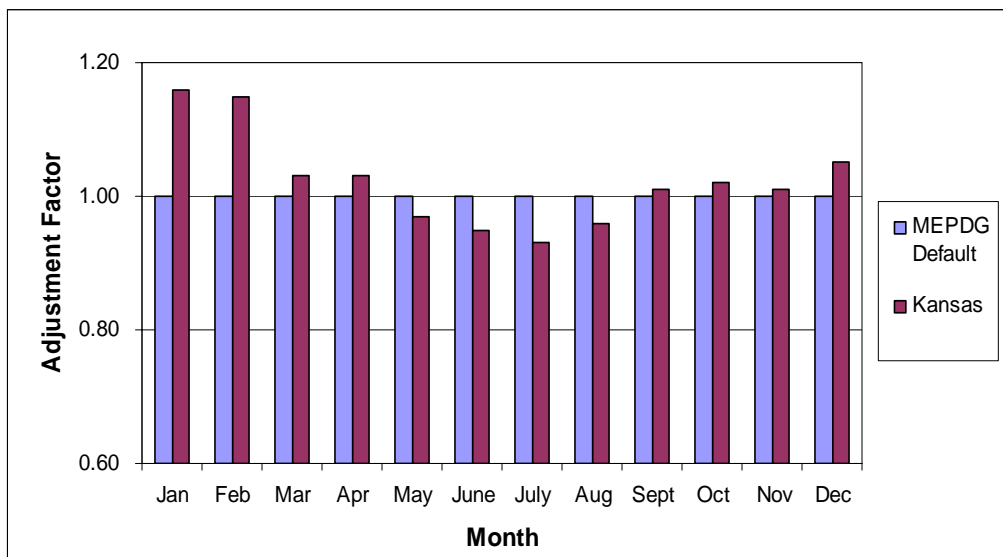


Figure 3.2 Comparison of monthly adjustment factor distribution for Kansas input and MEPDG default

Vehicle Class Distribution

Vehicle class distribution represents the percentage of each truck class (Classes 4 through 13) within the Annual Average Daily Truck Traffic (AADTT) for the base year. The base year for the traffic inputs is defined by MEPDG as the first year that the roadway segment under design is opened to traffic. The sum of the percent AADTT of all truck classes should be equal to 100. Usually WIM, AVC and vehicle count programs are used for the computation of vehicle class distribution. If the site-specific (Level 1) or regional data (Level 2) data are not available, truck traffic classification (TTC) can be used in conjunction with the functional class of the roadway to estimate the vehicle class distribution. MEPDG also has the option for default class distribution based on the roadway functional class and the best combination of Truck Traffic Classification (TTC) groups that describe the traffic stream expected on a given roadway. A typical comparison of the default vehicle class distribution for the Principal Arterials (urban)

with the Kansas-generated input based on TMG is shown in Figure 3.3.

In this study, vehicle class distribution was generated based on the 2000-2003 Traffic Monitoring Guide (TMG) vehicle classification for regular sites as shown in Table 3.7. Project specific distribution was developed based on the functional class. Total counted vehicles from Classes 4 to 13 were added and frequency distribution was developed so that total AADTT distribution by vehicle classes would be equal to 100%.

Table 3.7 Vehicle Class Distribution based on Functional Classification of Roadways

VEHICLE CLASS	Rural Interstate Highways	Principal Arterials Others (Urban)	Principal Arterials Others (Rural)	MEPDG Default (Interstate/ Principal Arterials)
4	2.4	6.6	2.6	1.3
5	9	42.7	17.6	8.5
6	2.5	9.8	5.6	2.8
7	0.9	2.3	1.6	0.3
8	6.7	9.4	7.9	7.6
9	69	25.2	58.2	74
10	1.1	1.4	2.1	1.2
11	4.6	1.1	2.7	3.4
12	1.7	0.4	0.6	0.6
13	2.1	1.1	1.1	1.3

The vehicle class distribution for the Rural Interstate Highway is similar to the MEPDG default distribution for that particular functional class. But the urban arterial is different than the default. The urban arterial shows a lower percentage of Class 9 trucks but a higher percentage of Class 5 trucks (delivery trucks). This trend seems to be very consistent with the location of this particular site (K-7, Johnson County).

For Rural Principal Arterial roadways, MEPDG default distribution for Class 9 vehicle is higher compared to the Kansas generated input for that particular class. Figure 3.3 shows the typical differences between MEPDG default inputs compare to the Kansas

input for a particular functional class.

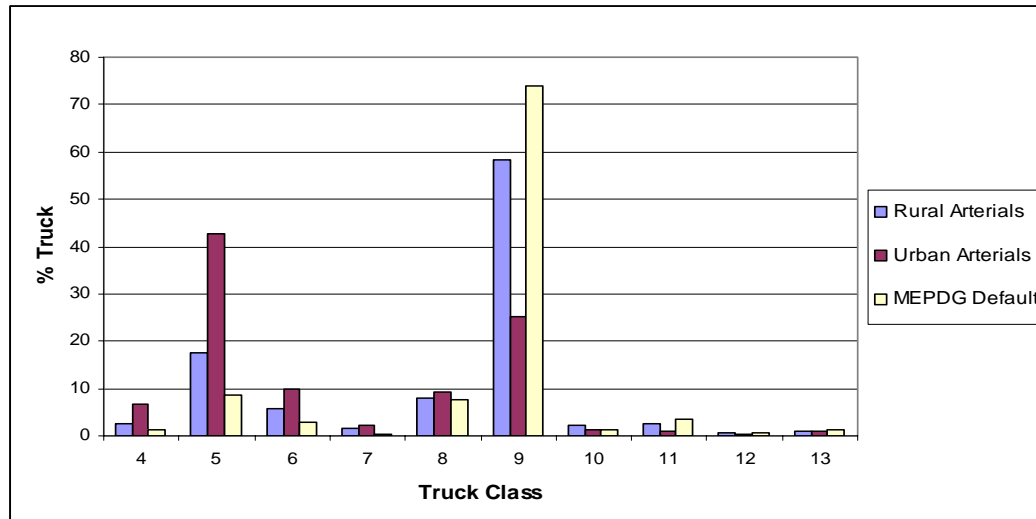


Figure 3.3 Comparison of MEPDG default truck class distribution with Kansas input for Principal Arterials (urban)

Hourly Truck Traffic Distribution

The hourly distribution factors (HDF) represent the percentage of the AADTT within each hour of the day (NCHRP 2004). Hourly distribution factors are used to distribute the monthly average daily truck traffic (MADTT) volumes by the hour of the day. The average hourly distribution of traffic is needed for incremental damage computations for different thermal gradients during the day (NCHRP 2004). For all level of input, HDF was computed in this study based on the truck traffic data collected continuously over a 24-hour period.

Kansas functional class-specific hourly traffic distribution was generated from the KDOT provided AVC data or C- card files for 2002 in the following manner:

- ◆ For a particular site the C-card, files were first processed according to the file coding shown in Table 3.8.
- ◆ The total numbers of trucks (Classes 4 to 13) were added for each hour of the

day and the sum total for a 24-hour period was derived.

- ◆ Hourly data was divided by the sum total from the previous step. For that particular site, some other sets of hourly classification data were also generated in the same manner for a different day within the same month or for different months within the same year.
- ◆ Finally all hourly distribution values were averaged.

Table 3.8 Vehicle Classification Record (“C”- Card) File Code

Field	Columns	Length	Description
1	1	1	Record Type
2	2-3	2	FIPS State Code
3	4-9	6	Station ID
4	10	1	Direction of Travel Code
5	11	1	Lane of Travel
6	12-13	2	Year of Data
7	14-15	2	Month of Data
8	16-17	2	Day of Data
9	18-19	2	Hour of Data
0	20-24	5	Total Volume
11	25-29	5	Class 1 Count
12	30-34	5	Class 2 Count
13	35-39	5	Class 3 Count
14	40-44	5	Class 4 Count
15	45-49	5	Class 5 Count
16	50-54	5	Class 6 Count
17	55-59	5	Class 7 Count
18	60-64	5	Class 8 Count
19	65-69	5	Class 9 Count
20	70-74	5	Class 10 Count
21	75-79	5	Class 11 Count
22	80-84	5	Class 12 Count
23	85-89	5	Class 13 Count
End the record here if the FHWA 13 class system is being used.			

The process was repeated for some other sites with the same functional classification. Average distribution factors were then computed for that particular functional class. The sum of the distribution must add up to 100 percent.

Table 3.9 tabulates the project specific HDF values used in the MEPDG analysis in this study. Figure 3.4 shows the hourly truck traffic distribution for a rural Interstate (I-70) in Kansas and compares with the MEPDG default distribution. It appears that more truck travel happens in Kansas during the afternoon, evening, and night hours than during the early morning and morning hours. It is anticipated that this will have a significant impact on the calculated slab stresses.

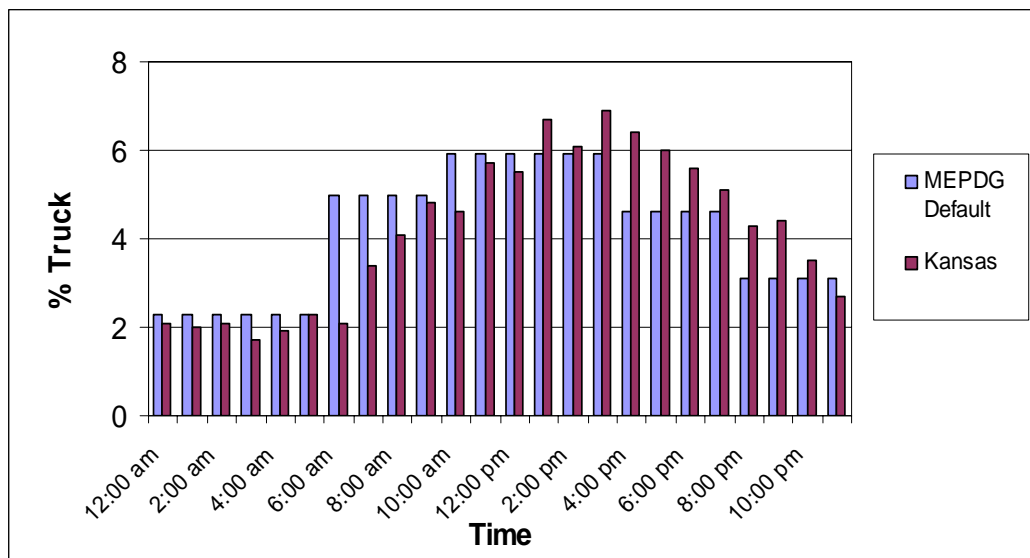


Figure 3.4 Typical hourly distribution for Rural Interstate compare to MEPDG default input

Table 3.9 shows the Kansas generated hourly distribution for different functional classes of roadways. For MEPDG default distribution, the distribution remains constant for a certain hour of the day, whereas in Kansas input, distribution varies for every hour of the day for each functional class.

Table 3.9 Hourly Truck Traffic Distribution Values Based on the Functional Classification of the Roadways

Hours	Rural Interstate Highways	Principal Arterials Others (Urban)	Principal Arterials Others (Rural)	MEPDG Default (Interstate/ Principal Arterials)
Midnight	2.1	0.5	1.4	2.3
1.00 am	2	0.4	1.1	2.3
2.00 am	2.1	0.3	1.4	2.3
3.00 am	1.7	0.3	1.6	2.3
4.00 am	1.9	0.6	2	2.3
5.00 am	2.3	1.6	2.8	2.3
6.00 am	2.1	3.9	4.1	5
7.00 am	3.4	6.2	5.1	5
8.00 am	4.1	7.5	6.2	5
9.00 am	4.8	8.3	6.5	5
10.00 am	4.6	8.1	6.7	5.9
11.00 am	5.7	8.1	6.8	5.9
Noon	5.5	7.8	6.3	5.9
1.00 pm	6.7	7.8	6.4	5.9
2.00 pm	6.1	8.3	6.2	5.9
3.00 pm	6.9	9	6	5.9
4.00 pm	6.4	8	6.1	4.6
5.00 pm	6	4.8	5.3	4.6
6.00 pm	5.6	3.6	4.1	4.6
7.00 pm	5.1	1.8	3.6	4.6
8.00 pm	4.3	1.1	3.3	3.1
9.00 pm	4.4	0.8	2.8	3.1
10.00 pm	3.5	0.8	2.5	3.1
11.00 pm	2.7	0.4	1.7	3.1

Traffic Growth Factors

All traffic input levels require an estimate of future traffic growth, which allows for the growth or decay in traffic over time. MEPDG allows users to use three different traffic growth functions to compute the growth rate over time as shown in Table 3.10. Different growth functions may be used for different functional classes based on several other factors such as, opening date of the roadway to traffic, pavement design life, etc. In this study, traffic growth rate was assumed to be linear based on the project-specific

AADT forecast. Project-specific linear traffic growth rates varying from two to about seven percent were used in this study and summarized in Table 3.3.

Table 3.10 Function Used in Computing/ Forecasting Truck Traffic Over Time (NCHRP 2004)

Function Description	Model
No growth	$AADTT_X = 1.0 * AADTT_{BY}$
Linear growth	$AADTT_X = GR * AGE + AADTT_{BY}$
Compound growth	$AADTT_X = AADTT_{BY} * (GR)^{AGE}$

Where $AADTT_X$ is the annual average daily truck traffic at age X, GR is the traffic growth rate and $AADTT_{BY}$ is the base year annual average daily truck traffic

Axle Load Distribution Factors

In order to use MEPDG effectively, the percentage of the total axle load applications within each load interval (normalized axle load distribution) for a specific axle type (single, tandem, tridem, and quad) and vehicle class (Classes 4 through 13) for each month of the year, must be computed externally. MEPDG software allows input for axle load distribution for each axle type at certain load intervals. For single axles, load distribution is from 3,000 lb to 40,000 lb at 1,000-lb intervals. For tandem axle, distribution ranged from 6,000 lb to 80,000 lb at 2,000 lb intervals, and for tridem axles, distribution interval varies from 12,000 lb to 102,000 lb at 3,000 lb intervals.

The axle load distributions were obtained in this study by analyzing the “W” card files from the WIM data provided by KDOT. The present Kansas truck weight program was established in 1990 with the acquisition of Weigh-In-Motion (WIM) equipment. KDOT has 90 sites for monitoring purposes. Thirty sites are being monitored each year on a 3-year rotation. Nine of those sites are Long Term pavement Performance (LTPP) monitoring sites. The Portable Weigh-In-Motion equipment, incorporating a capacitance mat weight sensor, is currently used for classification and weighing purposes in Kansas.

This system is attached directly to the pavement surface and positioned perpendicular to the normal traffic flow and extends across the traveled lane in order to have only one path contact of the weight sensor. Forty-eight hours of truck weight data are collected at each site once every three years. In order to set up this portable weighing equipment at a particular site, traffic lane closure is essential. After complete setup of the roadway components, truck weight data processor, connected to the weight sensor, collects the data. At the end of one session, other lane is also closed to remove the sensor. Collected data are processed for three types of correction: one for weight and other two are for speed and magnetic length, respectively. The equipment is also required to be calibrated for good results. Original data is stored in specific format and edited according to the machine-specific criteria and processed as “W” card files Individual vehicle records are also reviewed manually to correct any errors. Typically software is used for this review process. Finally with the data file adjusted and edited the “W” card data formats are created for year end data submittal to the Federal Highway Administration (FHWA). This is usually done using in-house and Vehicle TTravel Information System (VTRIS) software packages (KDOT 2003).

In Kansas, permanent scales have been installed at eleven LTPP sites and at least in one traveled lane. Nine of them are equipped with piezo-electric (PE) weighing systems. Among two other sites, one is equipped with a high speed load cell system from Toledo Scale and the other site is equipped with the IRD 1060 bending plate system. To comply with the LTPP requirements, data are collected at many of these 11 sites continuously. These sites are usually calibrated semi-annually (KDOT 2003).

In this study, the following steps were followed for deriving axle load spectra

manually using KDOT-provided WIM data.

1. To get the axle loads, first the KDOT- provided “W” card file was assembled and processed according to the codes of the vehicles provided by TMG as shown in Table 3.11. Nine years of portable WIM data (48-hour counts, 1995-2003) years of annual was provided by KDOT. Because of lack of continuous data NCHRP 1-39 traffic analysis software TrafLoad could not be used. TrafLoad requires uninterrupted hourly data for 365 days to generate all volume adjustment factors and axle load spectra needed by MEPDG. For the portable WIM data, truck weights were not available at any particular site for all months of a year. NCHRP MEPDG research has shown using data from a GPS-5 section in Marion County, Indiana that the variations in axle load spectra across the months within a year and along the years are insignificant (Tam and Von Quintus 2004). Thus it was decided to use different monthly data for different years from different sites and to develop a state-wide axle load distribution. MEPDG also recommends the sample size to estimate the normalized axle load distribution from the WIM data for a given level of confidence and percentage of expected error. The following months were used in this study: 1995 (February), 1996 (January), 1998 (March), 1999 (April), 2000 (May), 2002 (November), 2003 (June, July, August, September, October, and December). At least 24 hours of data were analyzed for each month of the year. Thus the expected error for the generated axle load spectra in this study would be $\pm 10\%$ error at close to 90% confidence interval.

Table 3.11 Truck Weight Record (“W”-Card) for Axle Load Distribution Factor

Field	Columns	Length	Description
1	1	1	Record Type
2	2-3	2	FIPS State Code
3	4-9	6	Station ID
4	10	1	Direction of Travel Code
5	11	1	Lane of Travel
6	12-13	2	Year of Data
7	14-15	2	Month of Data
8	16-17	2	Day of Data
9	18-19	2	Hour of Data
0	20-21	2	Vehicle Class
11	22-24	3	Open
12	25-28	4	Total Weight of Vehicle
13	29-30	2	Number of Axles
14	31-33	3	A-axle Weight
15	34-36	3	A-B Axle Spacing
16	37-39	3	B-axle Weight
17	40-42	3	B-C Axle Spacing
18	43-45	3	C-axle Weight
19	46-48	3	C-D Axle Spacing
20	49-51	3	D-axle Weight
21	52-54	3	D-E Axle Spacing
22	55-57	3	E-axle Weight
23	58-60	3	E-F Axle Spacing
24	61-63	3	F-axle Weight
25	64-66	3	F-G Axle Spacing
26	67-69	3	G-axle Weight
27	70-72	3	G-H Axle Spacing
28	73-75	3	H-axle Weight
29	76-78	3	H-I Axle Spacing
30	79-81	3	I-axle Weight
31	82-84	3	I-J Axle Spacing
32	85-87	3	J-axle Weight
33	88-90	3	J-K Axle Spacing
34	91-93	3	K-axle Weight
35	94-96	3	K-L Axle Spacing
36	97-99	3	L-axle Weight
37	100-102	3	L-M Axle Spacing
38	103-105	3	M-axle Weight

2. After processing one file, for a particular vehicle class, the axles were identified according to their default spacings provided by KDOT. It is also to be noted that “W” Card file also identifies the vehicle class and the order in which the axles were weighted. If the spacing between two axles is low then the axles were grouped together to form a tandem axle, otherwise they were treated as single axles. According to the KDOT practice, two axles 4.6 ft apart are in a tandem. In this study, in some cases, if the spacing between two axles is less than 2.5 ft, they were treated as tandem, when the spacing is greater than 30 inches they were treated as singles. Although the spacing is very short for a typical tandem axle, but it is possible with low-profile tires. “W” Card file also identifies the vehicle class and the order in which the axles were weighted. For example, in a Class 9 vehicle with five axles, the front axle is leveled as “A”, and the first tandem axle is leveled as “B” and so on, as shown in Figure 3.5. Tridem and Quad axle distributions were generated based on the same algorithms. A typical example of axle load spectra calculation for a particular vehicle Class 9 is presented in Table 3.12. This vehicle class is the predominant truck type in Kansas and commonly termed as 18-wheeler.
3. In this step, the total number of axles for each load interval was calculated and the frequency distribution was generated. For a specific axle-type and truck class, the summation of calculated percentages of the total number of axle applications within each load range, should be equal to 100%. A typical frequency distribution for a particular axle type (Tandem axle) and for the month of January is shown in Table 3.13. The above process was repeated for each class of vehicle

for the year and for all axle types.

Figure 3.6 illustrates the distribution of Class 9 vehicles in Kansas and compares it with the MEPDG default input. MEPDG default input shows more truck distribution in the high axle load categories. Therefore it is expected that damage would be higher for MEPDG default traffic input compared to the Kansas traffic input.

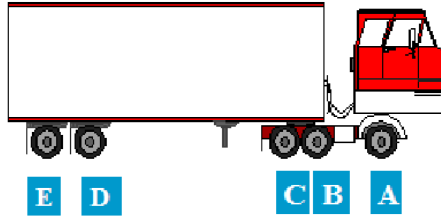


Figure 3.5 Typical axle configurations for vehicle Class 9

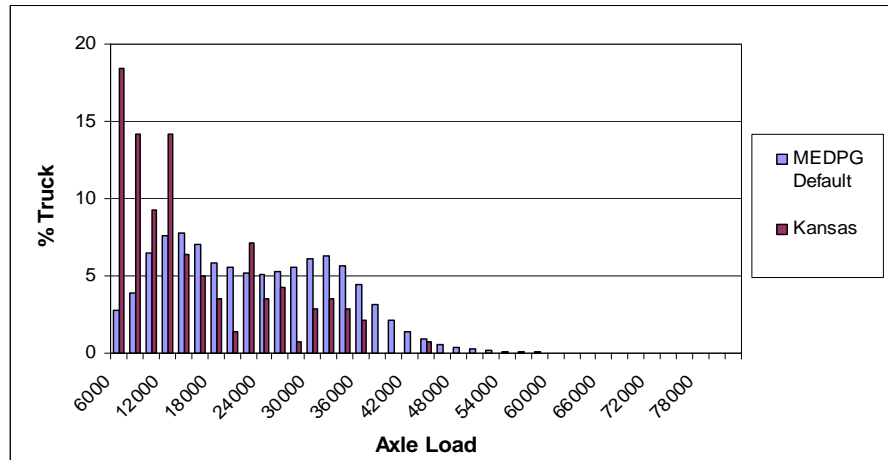


Figure 3.6 Comparison of axle load distribution for Class 9 vehicle with MEPDG default distribution

Table 3.12 shows the typical axle load spectra calculation for Class 9 vehicle. Class 9 vehicle is a five-axle truck, however the axle load distribution will depend up to the axle spacing. Whenever the spacing is less than 30 inch, especially for low profile tires, they were added together for tandem or tridem axle distribution. In this table, it is observed that most of the axle spacing between two axles is around one ft, therefore those axles were added together for tandem or tridem axle distribution.

Table 3.12 Typical Example of Axle Load Spectra Calculation for Vehicle Class 9

Vehicle Class	A-axle weight(lb)	(A-B) axle spacing	B-axle weight(lb)	(B-C) axle spacing	C-axle weight(lb)	(C-D) axle spacing	D-axle weight (lb)	(D-E) Axle Spacing	E-axle weight (lb)
9	9460	50	9680	12	9460	93	8360	12	7480
9	12100	43	16500	13	14960	63	19800	30	19360
9	10120	50	11660	11	11000	93	13860	11	11220
9	11660	35	18260	12	19140	77	18700	12	20900
9	9900	43	8800	12	9900	86	7480	12	8140
9	4180	38	9900	74	5280	8	5280	8	6380
9	11440	49	17160	13	16500	94	17600	12	18040
9	8800	47	18700	13	19140	96	20240	12	18480
9	11000	42	16500	13	15400	62	19360	30	19580
9	11220	36	19800	12	18920	79	16720	12	20460
9	14960	48	14520	13	15620	60	13860	30	15400
9	10120	50	13860	13	12980	73	18040	12	15620

Table 3.13 Frequency Distribution of Tandem Axle for Month of January

Mean Axle Load (lbs)	Vehicle/Truck Class									
	4	5	6	7	8	9	10	11	12	13
6000	0.00	0.00	0.00	0.00	60.00	18.44	0.00	0.00	0.00	0.00
8000	0.00	0.00	12.50	0.00	0.00	14.18	0.00	0.00	0.00	0.00
10000	0.00	0.00	12.50	0.00	0.00	9.22	20.00	0.00	0.00	0.00
12000	0.00	0.00	12.50	0.00	20.00	14.18	0.00	0.00	0.00	0.00
14000	0.00	0.00	37.50	0.00	0.00	6.38	0.00	0.00	0.00	0.00
16000	100.00	0.00	0.00	0.00	20.00	4.96	0.00	0.00	0.00	0.00
18000	0.00	0.00	0.00	0.00	0.00	3.55	40.00	0.00	0.00	0.00
20000	0.00	0.00	0.00	0.00	0.00	1.42	20.00	0.00	0.00	0.00
22000	0.00	0.00	0.00	0.00	0.00	7.09	0.00	0.00	0.00	0.00
24000	0.00	0.00	0.00	0.00	0.00	3.55	0.00	0.00	0.00	0.00
26000	0.00	0.00	0.00	0.00	0.00	4.26	0.00	0.00	0.00	0.00
28000	0.00	0.00	0.00	0.00	0.00	0.71	20.00	0.00	0.00	0.00
30000	0.00	0.00	12.50	0.00	0.00	2.84	0.00	0.00	0.00	0.00
32000	0.00	0.00	0.00	0.00	0.00	3.55	0.00	0.00	0.00	0.00
34000	0.00	0.00	12.50	0.00	0.00	2.84	0.00	0.00	0.00	0.00
36000	0.00	0.00	0.00	0.00	0.00	2.13	0.00	0.00	0.00	0.00
38000	0.00	0.00	0.00	0.00	0.00	0.00	0.00	0.00	0.00	0.00
40000	0.00	0.00	0.00	0.00	0.00	0.00	0.00	0.00	0.00	0.00
42000	0.00	0.00	0.00	0.00	0.00	0.00	0.00	0.00	0.00	0.00
44000	0.00	0.00	0.00	0.00	0.00	0.71	0.00	0.00	0.00	0.00
46000 & High	0.00	0.00	0.00	0.00	0.00	0.00	0.00	0.00	0.00	0.00

It can be observed from Table 3.13 that most of the distributions for the tandem axles exist for Vehicle Class 6, 8, 9 and 10, whereas the default distribution accounts for tandem axle distribution for FHWA Class 5, 7, 11, which should not have any tandem axle.

3.4.2.5 General Traffic Input

Most of the inputs under this category define the axle load configuration and loading details for calculating pavement responses. The “Number of Axle Types per Truck Class” and “Wheelbase” inputs are used in the traffic volume calculations.

Mean wheel location is the distance from the outer edge of the wheel to the pavement marking. For this study, since no state-specific information was not available, a default mean wheel location of 18 inches provided in the MEPDG Software was used.

Traffic Wander Standard Deviation is the standard deviation of the lateral traffic wander used to estimate the number of axle load repetitions over a single point in a probabilistic manner for predicting distresses and performance. A default traffic wander standard deviation of 10 inches was used in this study.

Design lane width, which is not the slab width, is the actual width of the lane as defined by the distance between the lane markings on either side of the design lane. The default value for the standard-width lanes is 12 ft, and this value was used in this study for all projects.

Number of Axles/Truck

These inputs specify the average number of axles for each truck class (Classes 4 to 13) for each axle type (single, tandem, tridem, and quad). It is usually calculated from the WIM data and generated over time by dividing the total number of a specific axle type

measures for a truck class by the total number of trucks in that class. The traffic module assumes that the number of axles for each axle-type is constant with time. The MEPDG Software contains a default set of values derived from the LTPP data. The default data used in this study are presented in Table 3.14.

Table 3.14 Default Distribution for Number of Axles/ Truck (NCHRP 2004)

Vehicle Class	Single	Tandem	Tridem	Quad
4	1.62	0.39	0	0
5	2.0	0	0	0
6	1.02	0.99	0	0
7	1.0	0.26	0.83	0
8	2.38	0.67	0	0
9	1.13	1.93	0	0
10	1.19	1.09	0.89	0
11	4.29	0.26	0.06	0
12	3.52	1.14	0.06	0
13	2.15	2.13	0.35	0

Axle Configuration

These inputs allow the user to make broad inputs regarding the configuration of the typical axle and tire. A series of data are usually required to elaborate the typical tire axle and axle load configuration in order to compute the pavement responses. These data can be obtained from the manufacturer’s database or measured directly in the field. The following elements are in this category:

Average axle-width

Distance between the two outside edges of an axle. A default width of 8.5 ft was used in this study.

Dual Tire Spacing

This is the center-to-center transverse spacing between dual tires of an axle. A default spacing of 12 inch was used in this study.

Axle Spacing

Axle spacing is the distance between the two consecutive axles of a tandem, tridem, or quad. Guide recommended spacings of 51.6, 49.2 and 49.2 inches were used for tandem, tridem and quad axles, respectively.

Tire Pressure

This is the hot inflation pressure of the tire. The tire pressure needs to be input for both single and dual tires. Guide recommended input of 120 psi was used for both types of tire.

Wheelbase

This information is important for determining the JPCP top-down cracking. The top-down cracking is associated with the critical loading by a particular combination of axles and the steering and drive axles of trucks. The user has to specify the percentage of trucks that have short, medium, and long spacings, and these information are used by the MEPDG software for computing pavement responses.

Average axle spacing

This is the average longitudinal distance between two consecutive axles that fall under the short, medium, and long axle spacing category. Axle spacing is applicable to only trucks in Class 8 and above. MEPDG default inputs for average axle spacing were 12 ft for short axle, 15 ft for medium axle and 18 ft for long axle.

Percentage of Trucks

This is the percentage of trucks that have short, medium, and long axle spacings specified above. A default input of 33% was used for the short and long axle spacing trucks whereas 34% was used for the long spacing ones.

3.4.3 *Climate*

This is one of the four required, major categories of inputs. Environmental conditions have significant effects on the performance of rigid pavements. Factors such as, precipitation, temperature, freeze-thaw cycles, and depth to water table affect temperature and moisture contents of unbound materials which, in turn, affect the load carrying capacity of the pavement. Further, the temperature gradients induce stresses and deformations in the concrete slab. The seasonal damage and distress accumulation algorithms in the MEPDG design methodology require hourly data for five weather parameters: air temperature, precipitation, wind speed, percentage sunshine, and relative humidity (NCHRP 2004). Temperature and moisture profiles in the pavement and subgrade are modeled using the Enhanced Integrated Climatic Model (EICM) software, which is integrated into the MEPDG Software. The EICM software is linked to the MEPDG software as an independent module through interfaces and design inputs. EICM is a one-dimensional coupled heat and moisture flow program that simulates changes in the behavior and characteristics of pavement and subgrade materials in conjunction with the climatic conditions over several years of operation.

The temperature and moisture effects that are directly considered in the design of JPCP are as follows:

- ◆ The permanent built-in curling that occurs during construction is combined with the permanent warping due to differential shrinkage, and expressed as “permanent curl/warp.” This parameter is a direct and influential input in the design analysis of JPCP.
- ◆ Transient hourly negative and positive non-linear temperature differences

caused by solar radiation are computed using EICM.

- ◆ Transient hourly negative moisture shrinkage at the top of the slab caused by changes in relative humidity during each month of the year is converted to an equivalent temperature difference for every month.

All three above stated effects on the PCC slab are predicted and combined with the axle loads to compute critical slab stresses in order to accumulate damage through monthly increments.

MEPDG recommends that the weather inputs be obtained from weather stations located near the project site. At least 24 months of actual weather station data are required for computation (Barry and Schwartz 2005). The MEPDG software includes a database of appropriate weather histories from nearly 800 weather stations throughout the United States. This database can be accessed by specifying the latitude, longitude, elevation and depth of water table of the project location. Depth of water table in this context is the depth of the ground water table from the top of the subgrade. Specification of the weather inputs is identical at all three hierarchical input levels in MEPDG.

3.4.3.1 Climatic file generation

The MEPDG software offers two options to specify the climate file for individual project. This file can be imported or generated. Import option is for the previously-generated climat.icm-file. This is achieved by clicking “Import” option and pointing the file location. For “Generate” option, weather data can be updated from a single weather station or virtual weather station can be created by interpolating climatic data for that specific location based on available data at six closest weather stations.

In this study, project-specific virtual weather stations were created by interpolation of climatic data from the selected physical weather stations. For this purpose, project specific latitude, longitude, elevation and water table depth at the given location were provided. Then the MEPDG software listed six closest weather stations in the vicinity of the project, and the weather stations were interpolated for generating those climatic files. EICM interpolates the weather data from the selected locations inversely weighted by the distance from the location. The depth of the water table was found from the soil survey report for each county. For all projects, water table depth was greater than 10 ft or close to 10 ft. Table 3.15 summarizes the basic inputs for the climatic data generated for all projects in this study.

3.4.4 Structure

This is the fourth set of inputs required by the MEPDG software. This category allows the user to specify the structural, design, and material aspects of the trial design chosen for performance evaluation. The category allows specifying the “Design Features of JPCP,” “Drainage” and “Surface” properties for that particular pavement. Furthermore it also provides an access to the input screens for different layers chosen in the structure.

Table 3.15 Summarization of the Project Specific Latitude, Longitude, Elevation and Water Table Depth

Project ID	Latitude(Deg.min)	Longitude(Deg.min)	Elevation (ft)
K-2611-01	39.38	-97.16	1070
K-3344-01	39.04	-95.38	880
SPS-2 (Sec-5)	38.97	-97.09	1194
SPS-2 (Sec-6)	38.97	-97.09	1194
SPS-2 (Control)	38.97	-97.09	1194
K-3216-02	38.15	-95.93	1200
K-3217-02	38.15	-95.93	1200
K-3382-01	38.78	-94.99	1000

3.4.4.1 Design Features of JPCP

Design features have significant effects on the mechanistic response calculated for JPCP as well as on its performance (NCHRP 2004). The inputs for JPCP design features can be broadly classified as: 1) Effective Equivalent Built-in Temperature and Moisture Difference, which directly affects the resulting critical stresses in the slab; 2) Joint Design, which directly affects the corner deflections, slab length, and resulting stresses; 3) Edge Support, which affects the magnitude of stresses depending on the location of the wheel load from the slab edge; and 4) Base Properties, which affects faulting as a result of base erosion and the levels of stresses due to bonded/unbonded condition. These features are described as follows:

(1) Permanent Cur/Warp Effective Temperature Difference

This is the equivalent temperature differential between the top and bottom layers of the concrete slab that can quantitatively describe the locked in stresses in the slab due to construction temperatures, shrinkage, creep and curing conditions. This temperature difference is typically a negative number, i.e. effectively represents a case, when the top of the slab is cooler than the bottom of the slab. The magnitude of permanent curl/warp is a sensitive factor that affects JPCP performance. MEPDG recommended value of -10°F was used in this study for permanent curl/warp. This value was obtained through optimization and applicable to all new and reconstructed rigid pavements in all climatic regions.

(2) Joint Design

Joint Spacing

This is the distance between two adjacent joints in the longitudinal direction and is equal to the length of the slab. The joint spacing is a critical JPCP design factor that affects structural and functional performance of JPCP, as well as construction and maintenance cost. The stresses in JPCP increase rapidly with increasing joint spacing. To a lesser degree, joint faulting also increases with increasing joint spacing. In this study, a joint spacing of 15 ft was used for all projects.

Sealant Type

The sealant type is to be chosen from the options offered in the drop-down menu. The sealant options are liquid, silicone, and preformed. Sealant type is an input to the empirical model used to predict spalling. Spalling is used in smoothness predictions, but it is not considered directly as a measure of performance in MEPDG. In this study, all projects were assumed to have liquid sealant.

Random Joint Spacing

MEPDG offers the designer the option of using random joint spacings, and up to four different values. In this case, the user needs to click on the radio button referring to random joint spacing and enter four different values. If random joint spacing is used, the MEPDG software uses the average joint spacing for faulting analysis and the maximum joint spacing for cracking analysis. In this study, the joint spacing was ordered, not random.

Doweled Transverse Joint

MEPDG has the capability to evaluate the effects of dowels across transverse joints, especially in reducing faulting. If dowels are used to achieve positive load transfer, the user needs to click the button corresponding to the doweled transverse joints and to make further inputs about the size and spacing of the dowels.

Dowel Diameter

This is the diameter of the round dowel bars used for load transfer across the transverse joints. The larger the dowel diameter, the lower the concrete bearing stress and joint faulting. The MEPDG software accepts any dowel diameter from 1 inch to 1.75 inch. Project specific inputs are provided in Table 3.16.

Dowel Bar Spacing

This is the center-to-center distance between the dowels used for load transfer across the transverse joints. The allowable spacings are from 10 to 14 inches.

MEPDG suggests that with increasing slab thickness (in order to reduce slab cracking for heavier traffic), dowel diameter be increased to control joint faulting. This may result in a small increase in predicted joint faulting due to a reduction in effective area of the bar relative to the slab thickness (NCHRP 2004). In this study, a 12-inch dowel spacing was used for all projects.

(3) Edge Support

Tied PCC Shoulder

Tied PCC shoulders can significantly improve JPCP performance by reducing critical deflections and stresses. The shoulder type also affects the amount of moisture infiltration into the pavement structure. The effects of moisture infiltration are

considered in the determination of seasonal moduli values of the unbound layers. The structural effects of the edge support features are directly considered in the design process. For tied concrete shoulders, the long-term Load Transfer Efficiency (LTE) between the lane and the tied shoulder must be provided.

Long-term LTE

LTE is defined as the ratio of the deflection of the unloaded to that of the loaded slab. The higher the LTE, the greater the support provided by the tied shoulder to reduce critical responses of the mainline slabs. Typical long-term deflection LTE values are:

- ◆ 50 to 70 percent for monolithically constructed tied PCC shoulder.
- ◆ 30 to 50 percent for separately constructed tied PCC shoulder.

In this study, 60 percent LTE was considered for the projects with monolithically constructed tied PCC shoulder.

Widened Slab

The JPCP slab can be widened to accommodate the outer wheel path further away from the longitudinal edge. For widened slab cases, the width of the slab has to be specified. In this study, only one project, SPS-2 Section 6, had widened lane of 14 ft.

Slab Width

This is the selected width of the slab and this is not same as the lane width. All projects in this study, except SPS-2 Section 6, had 12 ft lanes.

(4) Base Properties

PCC-Base Interface

This allows the user to specify the interface type and the quality of bond between the slab and the base. Structural contribution of a bonded stabilized base is significant compared to an unstabilized base. The interface between a stabilized base and the PCC slab is modeled either completely bonded or unbonded for the JPCP design. However, the bond tends to weaken over time around the edges. For unbonded base layer, the layer is treated as a separate layer in the analysis. In this study, since all projects have stabilized bases, the PCC-base interface was considered as bonded.

Erodibility Index

This is an index, on a scale of 1 to 5, to rate the potential for erosion of base material. The potential for base or subbase erosion (layer directly beneath the PCC layer) has a significant impact on the initiation and propagation of pavement distresses. Different base types are classified based on this long-term erodibility behavior as follows:

- ◆ Class 1 – Extremely erosion-resistant materials.
- ◆ Class 2 – Very erosion-resistant materials.
- ◆ Class 3 – Erosion resistant materials.
- ◆ Class 4 – Fairly erodible materials.
- ◆ Class 5 – Very erodible materials.

In this study, Class 3 option was chosen for all projects since all had stabilized bases.

Loss of Bond Age

The JPCP design procedure includes the modeling of changes in the interface bond condition over time. This is accomplished by specifying pavement age at which the

debonding occurs. Up to the debonding age, the slab-base interface is assumed fully bonded. After the debonding age, the interface is assumed fully unbonded. The design input is the pavement age at debonding, in months. In general, specifying debonding age greater than 5 years (60 months) is not recommended and was not used in calibration. Therefore, this default value was considered for all projects in this study.

3.4.4.2 Drainage and Surface Properties

This feature allows the user to make inputs for the drainage characteristics of the pavement. Information required under this category are:

- ◆ Pavement surface layer (PCC) shortwave absorptivity
- ◆ Potential for infiltration
- ◆ Pavement cross slope
- ◆ Drainage path length

PCC pavement Shortwave Absorptivity is a measure of the amount of available solar energy that is absorbed by the pavement surface. The lighter and more reflective the surface, the lower the surface shortwave absorptivity. The suggested range for the PCC layer is 0.70 to 0.90. A Shortwave Absorptivity value of 0.85 (default) was used in this study.

Infiltration defines the net infiltration potential of the pavement over its design life. In the MEPDG approach, infiltration can assume four values – none, minor (10 percent of the precipitation enters the pavement), moderate (50 percent of the precipitation enters the pavement), and extreme (100 percent of the precipitation enters the pavement). Based on this input, the EICM determines the amount of water available

at the top of the first unbound layer beneath the PCC slab. A moderate infiltration (50%) value was chosen for all the projects.

Drainage Path Length is the resultant length of the drainage path, i.e., the distance measured along the resultant of the cross and longitudinal slopes of the pavement. It is measured from highest point in the pavement cross-section to the point where drainage occurs. A default drainage path length of 12 ft was used in this project.

Pavement Cross Slope is the percentage vertical drop in the pavement for unit width, measured perpendicular to the direction of traffic. This input is used in computing the time required to drain a pavement base or subbase layer from an initially wet condition. Site-specific cross slope was chosen based on the individual project plan. In this study, most projects had a cross slope of 1.6%.

3.4.4.3 Pavement Layers

PCC Layer

MEPDG requires input values for the following four groups of PCC material properties for JPCP design analysis. Material property data inputs and material test requirement for these properties are briefly discussed below:

1. General Properties:
 - Layer Thickness
 - Unit Weight
 - Poisson's Ratio
2. Strength Properties:
 - Flexural Strength (Modulus of Rupture)

- Modulus of Elasticity
 - Compressive Strength
3. Thermal Properties:
- Coefficient of Thermal Expansion
 - Thermal Conductivity
 - Heat Capacity
 - Surface Short Wave Absorptivity
4. Mixture and Shrinkage Properties:
- Cement type, content, w/c ratio, Aggregate Type
 - Ultimate Shrinkage
 - Reversible Shrinkage
 - Time to Develop 50% of Ultimate Shrinkage

General Properties

Surface layer thickness is the thickness of the PCC slab, which is one of the important parameters needed for concrete pavement performance. In this study, this information was available from each project plan sheet.

Unit weight is the weight of the concrete mix design per unit volume of the mix. This information was obtained from the project mix design.

Poisson's ratio is defined as the ratio of the lateral strain to the longitudinal strain for an elastic material. It is a required input for the structural response models, although its effect on computed pavement responses is not great. Its value for normal concrete typically ranges between 0.11 and 0.21. In this study, the Poisson's ratio was chosen as 0.20 for all projects. Project-specific input values are summarized in Table 3.16.

Table 3.16 Structural Input Parameters for MEPDG Rigid Pavement Design Analysis

INPUT PARAMETERS	Input Value							
	(I-70 GE)	(I-70 SN)	SPS (Sec 5)	SPS (Sec 6)	SPS (Control)	(US-50- CS1)	(US-50- CS2)	(K-7 JO)
<i>Design Features</i>								
Dowel Diameter (in)	1.375	1.375	1.5	1.5	1.5	1.25	1.25	1.125
Design Lane Width (ft)	12	12	12	14	12	12	12	12
<i>PCC Layer</i>								
PCC Layer thickness (in)	11	10.5	11	11	12	10	10	9
Material Unit Weight (pcf)	140	142	143	139.2	146	136.9	138.5	142
Cement Type	II	I	II	II	II	II	II	II
Cement Content (Lb/yd ³)	653.4	630	862	532	600	622.1	626.3	622.9
Poisson's ratio	0.20	0.20	0.20	0.20	0.20	0.20	0.20	0.20
Coeff of thermal Expansion (X 10 ⁻⁶ /°F)	5.5	5.5	5.5	5.5	5.5	5.5	5.5	5.5
Water-cement ratio (w/c)	0.44	0.411	0.35	0.35	0.42	0.42	0.43	0.46
Aggregate Type	Limestone	Limestone	Quartzite	Quartzite	Quartzite	Limestone	Limestone	Limestone
PCC 28-day Strength (psi)	690	473	945	617	647	5,569	4,362	537
Derived ultimate shrinkage (µm)	621	727	596	423	456	554	593	507
Computed Ultimate Shrinkage (µm)	300	600	200	350	386	450	555	507
Derived PCC Zero Stress temperatures (°F)	63	86	130	111	115	48	48	102
<i>Base Material</i>								
Base Type	PCTB	PCTB	LCB	LCB	PCTB	BDB	BDB	PCTB
Base Thickness (in)	6	4	6	6	6	4	4	4
Poisson's ratio	0.15	0.15	0.15	0.15	0.15	0.15	0.15	0.15
Base material unit wt. (pcf)	135	135	135.4	135.4	135	135	135	135
Base Modulus (psi)	500,000	500,000	2,000,000	2,000,000	500,000	500,000	500,000	500,000
<i>Treated Subgrade</i>								
Subgrade type	N/A	LTSG	FASG	FASG	FASG	LTSG	LTSG	LTSG
Subgrade modulus (psi)	N/A	50,000	50,000	50,000	50,000	50,000	50,000	50,000
Poisson's ratio	N/A	0.20	0.15	0.15	0.15	0.20	0.20	0.20
Unit weight (pcf)	N/A	125	125	125	125	125	125	125
Poisson's ratio	N/A	0.20	0.15	0.15	0.15	0.20	0.20	0.20
<i>Compacted Subgrade</i>								
Subgrade soil type	A-6	A-7-6	A-6	A-6	A-6	A-7-6	A-7-6	A-7-6

Table 3.16 Structural Input Parameters for MEPDG Rigid Pavement Design Analysis (Continued)

INPUT PARAMETERS	Input Value							
	(I-70 GE)	(I-70 SN)	SPS (Sec 5)	SPS (Sec 6)	SPS (Control)	(US-50- CS1)	(US-50- CS2)	(K-7 JO)
*Subgrade Modulus (psi)	9746	6268	6928	6928	7523	6300	6098	7262
Plasticity index, PI	15.8	25.7	26	26	23	25.7	27.3	19.9
Percent passing # 200 sieve	71.8	93.3	78.1	78.1	76.9	92.5	91.9	94.3
% passing # 4 sieve	100	100	100	100	98	100	100	100
D ₆₀ (mm)	0.001	0.001	0.001	0.001	0.001	0.001	0.001	0.001
Poisson's ratio	0.35	0.35	0.35	0.35	0.35	0.35	0.35	0.35
<i>Derived Parameters Physicals properties</i>								
MDD (pcf)	107.8	88.3	90.5	90.5	92.2	88.4	87.7	91.5
G _s	2.73	2.75	2.75	2.75	2.74	2.75	2.75	2.75
Hydraulic conductivity (ft/hr)	3.25e-005	3.25e-005	3.25e-005	3.25e-005	3.25e-005	3.25e-005	3.25e-005	3.25e-005
OMC	18.7	24.2	22.7	22.7	21.6	24.1	24.7	22.1
Calculated degree of Sat.(%)	87.6	88.8	88.5	88.5	88.3	88.8	88.8	88.4

* computed by MEPDG

Strength Properties

PCC strength properties that are input in to the MEPDG software are based on the hierarchical level of input selected. The strength parameters considered in the structural and material models for JPCP are the modulus of elasticity, flexural strength, and compressive strength. Table 3.17 provides the required inputs at different hierarchical levels.

Table 3.17 Strength and Modulus of Elasticity Inputs for JPCP and CRCP Design

Input Level	JPCP
Level 1	<ul style="list-style-type: none"> ▪ Modulus of Elasticity (E_c) and Flexural Strength (Modulus of Rupture, MR) at 7, 14, 28, 90 days ▪ Estimated ratios for 20-year to 28-day values of E_c and MR
Level 2	<ul style="list-style-type: none"> ▪ Compressive Strength (f_c) at 7, 14, 28, 90 days ▪ 20-year to 28-day f_c ratio estimate
Level 3	<ul style="list-style-type: none"> ▪ MR or f_c at 28 days ▪ E_c at 28 days (optional)

According to the level 1 input, MEPDG recommends the maximum values for the ratios of 20-year and 28-day values of the strength (MR) and modulus (E). Recommended maximum ratio of the 20-year to the 28-day E_c is 1.20. The same maximum value of 1.20 is also recommended for the ratios of the 20-year to the 28-day MR and E values.

For level 2 input, the compressive strength data at various ages are first converted to the modulus of elasticity and flexural strength at those ages using correlation models for the properties shown in Equations 3.2 and 3.3.

$$E_c = 33\rho^{3/2}(f_c')^{1/2} \quad (3.2)$$

Where, E_c = concrete modulus of elasticity, psi;

ρ = unit weight of concrete, pcf; and

f_c' = compressive strength of concrete, psi.

$$MR = 9.5 (f_c')^{1/2} \quad (3.3)$$

Where, MR = concrete modulus of rupture, psi; and

f_c' = compressive strength of concrete, psi.

Level 3 input requires only the 28-day strength either determined for the specific mix or an agency default. It offers the user the choice of either specifying the 28-day modulus of rupture or the 28-day compressive strength. If 28-day MR is estimated, its value at any given time, t , is determined using:

$$MR(t) = 1.0 + 0.12 \log_{10} (AGE/0.0767) - 0.01566 [\log_{10} (AGE/0.0767)]^2$$

Where, $MR(t)$ = modulus of rupture at a given age t ;

$MR(28)$ = modulus of rupture at 28 days; and

AGE = concrete age of interest in years.

In this study, level 3 input was used for all projects. For Shawnee, Johnson, and Geary county projects, including all SPS-2 projects, 28-day MR value was used whereas for the two Chase county projects, 28-day compressive strength values were used. Shawnee county project has the lowest modulus of rupture of 473 psi, whereas SPS-2 Section 5 has the highest value of 945 psi. Project-specific values are presented in Table 3.16.

Thermal Properties

Coefficient of Thermal Expansion, Thermal Conductivity, and Heat Capacity are the required inputs for the JPCP design analysis, using the MEPDG software.

Coefficient of Thermal Expansion (CTE) is a measure of the expansion or contraction that a material undergoes with the change in temperature. CTE is considered to be a very critical parameter in the calculation of curling stresses developed and therefore, in the prediction of all distresses. Aggregates have CTE values in the range of 2.2 to 7.2×10^{-6} in/in/deg F and the resulting CTE of concrete can range between 4.1 and 7.3×10^{-6} in/in/deg F. This parameter can be determined at different hierarchical levels of

input. In this study, the CTE value was determined from the TP-60 tests on the Kansas cores and the average value was 5.5×10^{-6} in/in/deg F. This value was used for all projects. This value also was a recommended MEPDG default for CTE.

Thermal conductivity is a measure of the ability of the material to uniformly conduct heat through its mass when two faces of the material are under a temperature differential. This value typically ranges from 1.0 to 1.5 Btu/(ft)(hr)(°F).

Heat capacity is defined as the amount of heat required to raise a unit mass of material by a unit temperature and usually ranges from 0.2 to 0.28 Btu/(lb)(°F). In this study, recommended calibrated values of 1.25 BTU/hr-ft-°F and 0.28 BTU/lb-°F were used for thermal conductivity and heat capacity, respectively.

Mixture and Shrinkage Properties

This option allows the user to provide the MEPDG software with mix design parameters and inputs for computing concrete shrinkage. Mix design related inputs are Cement type, Cement Content, Water/cement ratio, Aggregate type, PCC Zero-Stress Temperature, etc.

Three types of cement are identified in the MEPDG software. Cement content is the weight of cement per unit volume of concrete as per the mix design. The water/cement ratio (w/c) is the ratio of the weight of water to the weight of cement used in the mix design. Aggregate type is also a required input for the shrinkage strain calculation. Project specific mix design properties are used in this study and summarized in Table 3.16.

PCC Zero-stress temperature, T_z , is defined as the temperature (after placement and during the curing process) at which PCC becomes sufficiently stiff that it develops

stress if restrained (NCHRP 2004). This is the temperature at which the slab would de-stress itself from all the built-in stresses, i.e. no thermal stresses are present. If the PCC temperature is less than T_z , tensile stresses occur at the top of the slab and vice-versa. Again the T_z is not actually a single temperature but varies throughout the depth of the slab (termed a zero-stress gradient). This value is computed based on the cement content and the mean monthly ambient temperature during construction. The user can, however, choose to provide this input directly into the MEPDG Software. This will require selecting the corresponding box and entering the PCC zero-stress temperature.

As mentioned earlier, *PCC zero-stress temperature*, T_z , is an important parameter that affects the stress buildup in the PCC slab immediately after construction. This parameter is also related to the time of construction since it is computed based on the cement content and the mean monthly temperature (MMT) during construction as shown below (NCHRP 2004):

$$T_z = (CC*0.59328*H*0.5*1000*1.8/ (1.1*2400) + MMT) \quad (3.4)$$

where,

T_z = Temperature at which the PCC layer exhibits zero thermal stress;

CC = Cementitious material content, lb/yd³;

H = $-0.0787+0.007*MMT-0.00003*MMT^2$; and

MMT = Mean monthly temperature for the month of construction, ° F.

Two types of curing method are specified in this software: (1) Curing compound and (2) Wet curing. Curing compound was used as a curing method in this study.

Drying shrinkage of hardened concrete is an important factor affecting the performance of PCC pavements. For JPCP, the principal effect of drying shrinkage is

slab warping caused by the differential shrinkage due to the through-thickness variation in moisture conditions leading to increased cracking susceptibility. For JPCP faulting performance, both slab warping and the magnitude of shrinkage strains are important. The magnitude of drying shrinkage depends on numerous factors, including water per unit volume, aggregate type and content, cement type, ambient relative humidity and temperature, curing, and PCC slab thickness. Drying shrinkage develops over time when PCC is subjected to drying.

Ultimate Shrinkage at 40% relative humidity (RH) is the shrinkage strain that the PCC material undergoes under prolonged exposure to drying conditions and is defined at 40 percent humidity. This input can be site specific, based on some correlation, or typical recommended value. The correlation to estimate the ultimate shrinkage is:

$$\epsilon_{su} = C1 \cdot C2 \cdot [26 w^{2.1} fc^{-0.28} + 270] \quad (3.5)$$

Where, ϵ_{su} = ultimate shrinkage strain ($\times 10^{-6}$);

C1 = cement type factor (1.0 for Type I cement, 0.85 and 1.1 for Type II and Type III cement, respectively);

C2 = curing condition factor (0.75 if steam cured, 1.0 if cured in water or 100% RH or wet burlap and 1.2 if cured by curing compound);

w = water content (lb/ft^3); and

fc' = 28-day compressive strength.

Typical value for the Ultimate Shrinkage can be used based on experience or the following equation can be used to estimate the ultimate shrinkage:

$$\epsilon_{su} = C1 \cdot C2 \cdot \epsilon_{ts} \quad (3.6)$$

Where, ϵ_{su} = ultimate shrinkage strain;

ε_{ts} = typical shrinkage strain;

600×10^{-6} for conventional PCC with $f_c' < 4,000$ psi

650×10^{-6} for high-strength PCC with $f_c' > 4,000$ psi

C1 = cement type factor; and C2 = curing condition factor.

In this study, correlated ultimate shrinkage strain was used based on the mixture properties such as, chosen cement type, water content, w/c ratio, aggregate type, curing method, etc. and the derived values are tabulated in Table 3.16.

Reversible shrinkage is the percentage of ultimate shrinkage that is reversible in the concrete upon rewetting. For reversible shrinkage, a recommended default value of 50% was used in this study.

Time to develop 50 percent of the ultimate shrinkage refer to the time taken in days to attain 50 percent of the ultimate shrinkage at the standard relative humidity conditions. The ACI-suggested default value of 35 days was used in this study.

In the MEPDG software, shrinkage strain ranges from 300 to 1000 micro-strains. In this study, software-predicted ultimate shrinkage was compared with these extreme values. The strain was also computed based on the tensile strength of concrete. The indirect tensile strength of concrete is determined based on AASHTO T198 or ASTM C496 protocol. Shrinkage strain is strongly related to the strength, which is a function of the water-cement ratio. Therefore, the computed shrinkage strain in this study was based on the relationship with the PCC tensile strength as shown in Table 3.18 (AASHTO 1993):

Table 3.18 Approximate Relationship between Shrinkage and Indirect Tensile Strength of PCC

<i>Indirect tensile strength (psi)</i>	<i>Shrinkage (in/in.)</i>
300 or less	0.0008
400	0.0006
500	0.00045
600	0.0003
700 or greater	0.0002

The project-specific tensile strength was computed based on the following equations:

$$f_t = 0.86 * S_c \quad (3.7)$$

$$f_t = 6.5\sqrt{f_c'} \quad (3.8)$$

Where, f_t = Tensile Strength (psi);

S_c = Modulus of rupture (psi); and

f_c' = 28-day PCC compressive strength (psi).

Equations 3.7 and 3.8 were based on the AASHTO and ACI recommendations, respectively. Project-specific computed values are summarized in Table 3.16.

In this study, derived (correlated) ultimate shrinkage strain, based on the mixture properties such as, chosen cement type, water content, w/c ratio, aggregate type and curing method etc., was also used. These values are also tabulated in Table 3.16.

Stabilized Base/Subbase Material

Chemically stabilized materials are used in the pavement base or subbase to achieve design properties. Stabilizing agents are either cementitious or lime. The stabilized materials group consists of lean concrete, cement stabilized, open graded cement stabilized, soil cement, lime-cement-flyash, and lime treated materials. Required

design inputs for all these materials are the same for this design procedure. Layer properties can be further classified as layer material properties, strength properties, and thermal properties. For strength properties, the rigid pavement analysis requires the elastic or resilient modulus and Poisson's ratio (NCHRP 2004).

Unit weight is the weight per unit volume of the stabilized base material. Poisson's ratio is the ratio of the lateral to longitudinal strain of the material and is an important required input for the structural analysis. Values between 0.15 and 0.2 are typical for the chemically stabilized materials.

The required modulus (elastic modulus [E] for lean concrete, cement stabilized, and open graded cement stabilized materials and resilient modulus [Mr] for soil-cement, lime-cement-flyash, and lime stabilized soils) is the 28-day modulus value and is a measure of the deformational characteristics of the material with applied load. This value can be determined either in the laboratory testing, correlations, or based on defaults. All projects in this study have stabilized bases. The inputs required for these bases were layer thickness, mean modulus of elasticity, unit weight of the material, Poisson's ratio, etc. Layer thickness ranged from 4 to 6 inches. The modulus of elasticity for the cement-treated bases (PCTB) and Bound Drainable bases (BDB) were 500,000 psi. The lean concrete base modulus was taken as 2 million psi. All projects have 6-inch lime or fly-ash treated subgrade (LTSG/FASG) with an input modulus of 50,000 psi. Project specific details are presented in Table 3.16.

Table 3.19 Inputs for Different Base Type

Input Parameters	Input Value
<i>DGAB</i>	
Type of materials	Crushed Stone
Derived Modulus (psi)	31,114
Plasticity index, PI	5
Percent passing # 200 sieve	14
% passing # 4 sieve	53
D ₆₀ (mm)	8
<i>PERMEABLE BASE</i>	
Type of materials	Crushed Stone
Derived Modulus (psi)	39,543
Plasticity index, PI	0
Percent passing # 200 sieve	5.6
% passing # 4 sieve	15
D ₆₀ (mm)	14
<i>SEMI-PERMEABLE BASE</i>	
D ₆₀ (mm)	14
Type of materials	A-1-b
Derived Modulus (psi)	37,417
Plasticity index, PI	0
Percent passing # 200 sieve	14.9
% passing # 4 sieve	52.4
D ₆₀ (mm)	11
<i>BDB</i>	
Base Thickness (in)	4
Base material unit wt. (pcf)	145
Base Modulus (psi)-Low	656,000
Base Modulus (psi)-High	1460,000
<i>ATB</i>	
Superpave Binder Grade	PG 64-22
<i>Aggregate Gradation</i>	
Cumulative % retained 3/4" Sieve	33
Cumulative % retained 3/8" Sieve	96
Cumulative % retained #4 Sieve	96
% Passing # 200 Sieve	1.8
<i>Asphalt General</i>	
Reference Temperature (°F)	68
Effective Binder content (%)	2.0%
Air Void (%)	15%
Total Unit weight (pcf)	136
Poisson's ratio	0.35

The permeable and semi-permeable bases are used on top of the lime-treated subgrade. Permeable bases consist of open graded materials, and are constructed with

high quality crushed stone. The gradation for the KDOT permeable base material CA-5 is shown in Figure 3.7. The semi-permeable base is also a granular base, similar to the permeable one. The gradation for such a base used by the Missouri Department of Transportation (MODOT) is also shown in Figure 3.7. For semi-permeable base, the percent materials passing No. 4 and 200 sieves are higher compared to the Kansas CA-5 permeable base (Melhem et.al. 2003). Table 3.19 shows the required MEPDG inputs for different base types studied.

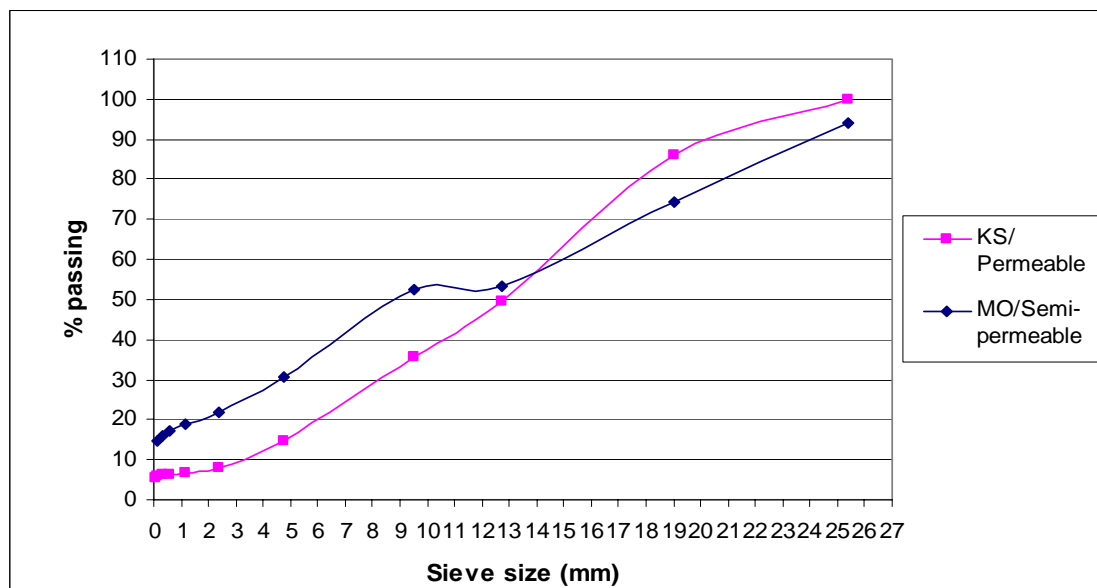


Figure 3.7 Gradation for permeable and semi-permeable base materials

Subgrade

Subgrade materials are commonly termed as unbound materials. The input information is common for all unbound layers, regardless of whether it functions as a base or a subgrade layer in the pavement structure. For this design procedure, unbound granular materials are defined using the AASHTO classification system or Unified Soil Classification (USC) system. In addition to that, unbound base can also be categorized as

crushed stone, crushed gravel, river gravel, permeable aggregate, and cold recycled asphalt. Subgrade materials are defined using both the AASHTO and USC classifications and cover the entire range of soil classifications available under both systems.

The material parameters required for the unbound materials (both granular and subgrade) may be classified into three major groups:

- Pavement response model material inputs.
- EICM material inputs.
- Other material properties

These inputs are, however, grouped into two property pages of the unbound layers screen and are identified as "Strength properties" and "ICM" properties. The inputs provided on the strength properties page, and appropriate inputs on the ICM property page would be essential to make seasonal adjustments to the strength values for seasonal changes. The user also has the option of disregarding the ICM page and making "user-input" seasonal strength values, or specifying that the program disregard seasonal changes and use only the representative values provided on the strength screen.

The strength inputs for the unbound layers can be made in three hierarchical levels. At Level 1, resilient modulus values for the unbound granular materials, subgrade, and bedrock are determined from cyclic triaxial tests on prepared representative samples.

Level 2 analysis requires the use of resilient modulus, M_r . Level 2 inputs in MEPDG use general correlations between the soil index and the strength properties and the resilient modulus to estimate M_r . The relationships could be direct or indirect. For the indirect relationships, the material property is first related to CBR and then CBR is

related to M_r . MEPDG allows the user to use either of the following soil indices to estimate M_r from the aforementioned correlation:

- ◆ CBR
- ◆ R-value
- ◆ Layer coefficient
- ◆ Penetration from DCP
- ◆ Based up on Plasticity Index and Gradation

For level 2, the MEPDG software allows users the following two options:

- ◆ Input a representative value of M_r or other soil indices, and use EICM to adjust it for seasonal climate effects (i.e., the effect of freezing, thawing, and so on).
- ◆ Input M_r or other soil indices for each month (season) of the year (total of 12 months).

Level 3 inputs simply require a default value for the resilient modulus of the unbound material. For this level, only a typical representative M_r value is required at optimum moisture content. EICM is used to modify the representative M_r for the climatic effect.

For ICM properties, inputs provided by the unbound layers are used by the EICM model of the MEPDG software in predicting the temperature and moisture profile throughout the pavement structure. Key inputs include gradation, Atterberg limits, and hydraulic conductivity. Regardless of the input level chosen for the unbound layer, the input parameters required are the same.

The plasticity index, PI, of a soil is the numerical difference between the liquid limit and the plastic limit of the soil, and indicates the magnitude of the range of the

moisture contents over which the soil is in a plastic condition. The AASHTO test method used for determining PI is AASHTO T-90.

The sieve analysis is performed to determine the particle size distribution of unbound granular and subgrade materials and is conducted following AASHTO T27. The required distribution includes percentage of particles passing US No.200 and No.4 sieves, and the diameter of the sieve in mm at which 60 percent of the soil material passes (D60).

In this study, natural subgrade modulus was calculated by the MEPDG software from a correlation equation involving the project-specific plasticity index and soil gradation. The correlations are shown in Equation 3.9 and 3.10. Project-specific inputs are shown in Table 3.16 (NCHRP 2004).

$$CBR = \frac{75}{1 + 0.728(wPI)} \quad (3.9)$$

$$M_r = 2555(CBR)^{0.64} \quad (3.10)$$

Where, $wPI = P_{200} * PI$;

P_{200} = Percent passing No. 200 sieve size;

PI = Plasticity index, percent;

CBR = California Bearing Ratio, percent; and

M_r = Resilient Modulus (psi).

The parameters maximum dry unit weight (MDD), specific gravity of solids (Gs), saturated hydraulic conductivity, optimum gravimetric moisture content (OMC), and calculated degree of saturation can be either input by the user or calculated internally by the MEPDG software. These parameters are used by the EICM model in predicting the moisture profile through the pavement structure. In this study, these parameters were

derived from the MEPDG level 3 default values or determined based on correlations. Table 3.16 lists these values.

MEPDG also has the option for indicating type of compaction achieved for the unbound layer during the construction process. MEPDG internally makes adjustments to the coefficient of lateral pressure to account for the level of compaction provided to the layer and this, in turn, influences the deformational characteristics undergone by the layer for the same level of applied loads. In this study, compacted phase was indicated for the top 12 inches of the natural subgrade material and uncompacted phase was chosen for the rest of the depth of subgrade soil.

CHAPTER 4

DESIGN AND SENSITIVITY ANALYSIS

This chapter describes the Mechanistic-Empirical Pavement Design Guide (MEPDG) design analysis of eight in-service JPCP in Kansas, and sensitivity analysis of the factors that significantly affect the pavement distresses.

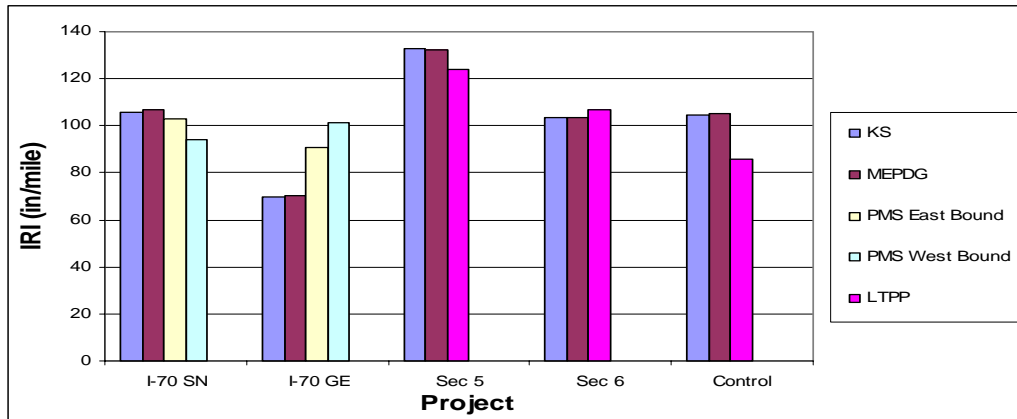
4.1 Prediction and Comparison of Distresses from Design Analysis

As mentioned earlier, key rigid pavement distresses predicted for JPCP from the MEPDG analysis are IRI, faulting, and percent slabs cracked.

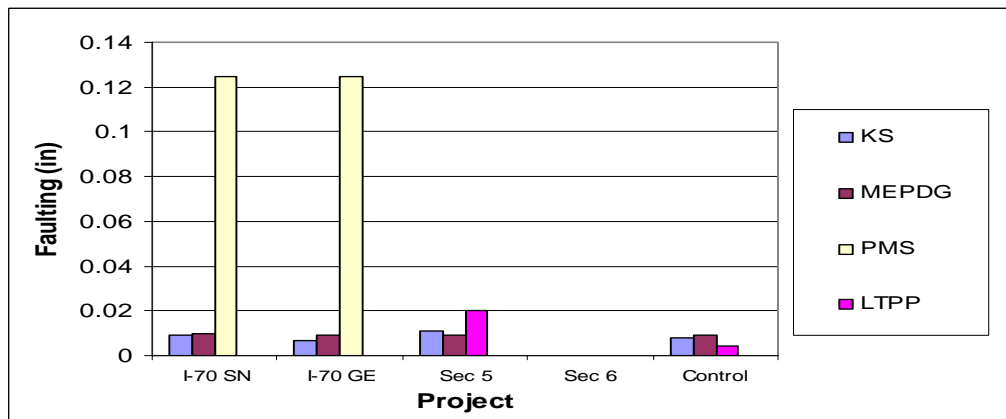
4.1.1 Smoothness or IRI

In this study, MEPDG predicted IRI for the JPCP sections were compared with the KDOT-measured and LTPP DataPave (online database) values for 2003. MEPDG prediction was done with both default and Kansas-specific traffic inputs (truck traffic distribution and axle load spectra). The average IRI, obtained from the left and right wheel path measurements on the travel lane, was used in the comparison. The profile survey for the KDOT Pavement Management System was done on both eastbound and westbound directions for the I-70 Geary and I-70 Shawnee county projects, and on northbound and southbound directions for the K-7 Johnson County project. For the SPS-2 sections, measured values were obtained from the LTPP database. Figure 4.1(a) and 4.2(a) show the comparison between the predicted and the measured IRI values for 2003 for all projects. The values are also summarized in Table 4.1. MEPDG-predicted IRI's with default and Kansas-specific traffic inputs are almost similar on all projects except on the K-7 Johnson County project. It has been previously shown that truck traffic distribution on this section (urban arterial others functional class) is completely different

(a) IRI



(b) Faulting



(c) % Slabs Cracked

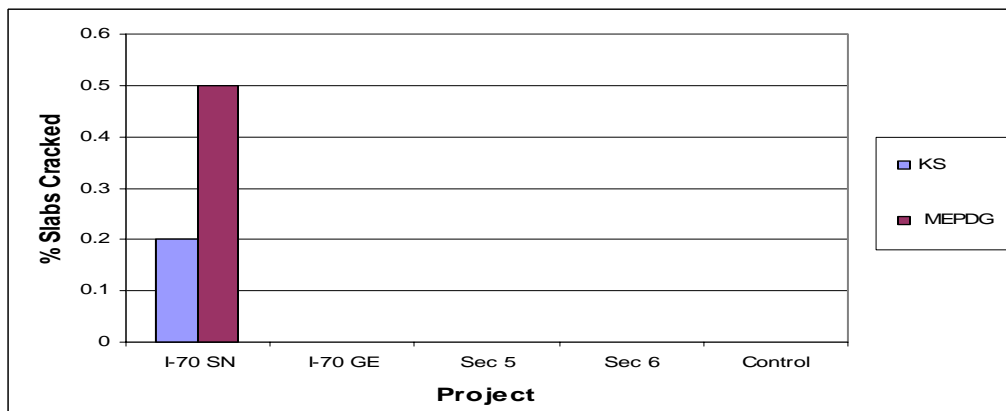
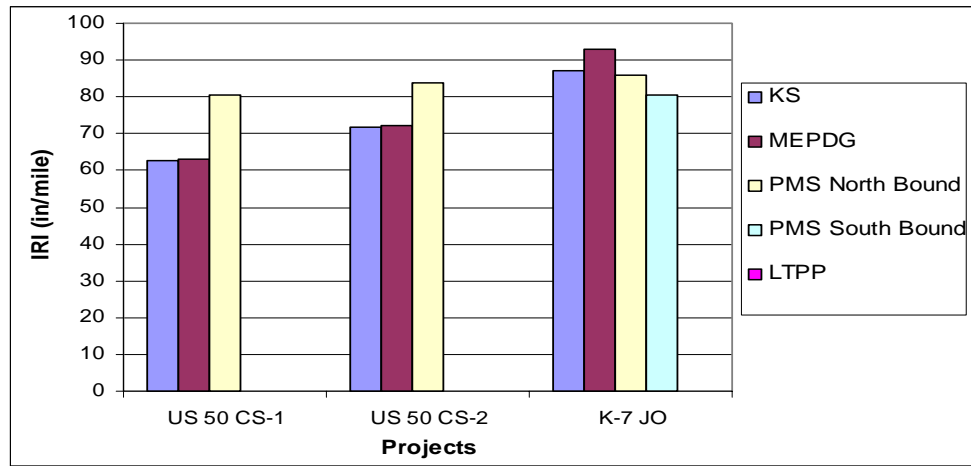
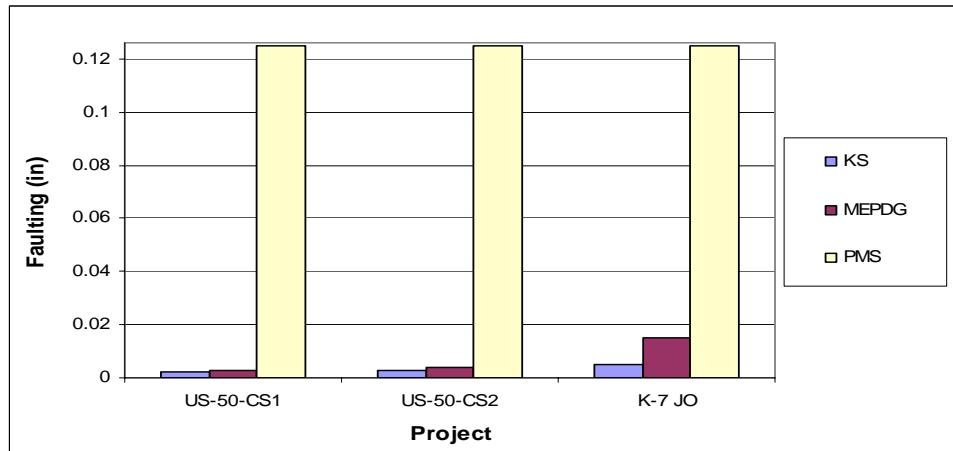


Figure 4.1 Predicted and measured JPCP distresses on Interstate sections

(a) IRI



(b) Faulting



(c) % Slabs Cracked

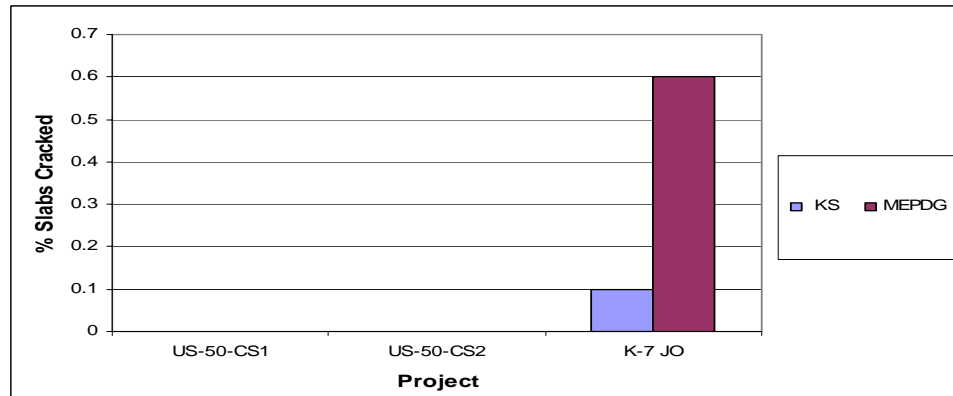


Figure 4.2 Predicted and measured JPCP distresses on Non-Interstate sections

from that used in the MEPDG default traffic input. The predicted IRI values for all Interstate sections are fairly similar to the measured values summarized in Table 4.2, except for the I-70 Geary County and SPS-2 Control Section projects. With Kansas-generated traffic input, SPS Section 5 has the highest predicted IRI of 133 in/mi and the I-70 Geary county project has the lowest. The predicted IRI for the Geary county project is 70 in/mi compared to the measured values of 91 in/mi and 102 in/mi for the eastbound and westbound directions, respectively. For the non-interstate sections, shown in Figure 4.2(a), NOS-measured IRI values are almost similar to the predicted values for the K-7 Johnson County project. For K-7 Johnson County project, the MEPDG predicted IRI is 87 in/mi and 93 in/mi for the Kansas-specific traffic input and MEPDG default traffic input, respectively. These values are almost similar to the measured values of 86 in/mi and 81 in/mi for the northbound and southbound directions, respectively. For the non-interstate sections, NOS-measured IRI values are higher than the predicted values for both Chase county projects.

4.1.2 Faulting

Figures 4.1(b) and 4.2(b) show the comparison between the predicted faulting and the NOS or LTPP-measured values. Tables 4.1 and 4.2 tabulate the values. As shown in Figure 4.1(b), no faulting was observed for the SPS-2 Section 6 that has a widened lane of 14 ft width. Good agreement was also observed for the other SPS-2 section. SPS-2 Section 5 has higher measured faulting of 0.02 in. compared to the Kansas-specific and default traffic values. For the KDOT projects, some discrepancies were observed between the predicted and the measured faulting. However, both measured and predicted values in 2003 were negligible for all practical purposes. For example, with the Kansas-

specific traffic input, the K-7 Johnson County project was projected to show faulting of 0.005 inch in 2003 as shown in Figure 4.2(b). The discrepancies between the NOS-measured and MEPDG-predicted faulting at a few locations were partly due to the way faulting is interpreted in the NOS survey. During NOS reporting, measured faulting is coded as F1, F2 or F3 depending upon the severity of faulting. F1 describes the faulting of greater than 0.125 in but less than 0.25 in. and this is the only severity observed at a few locations on some projects. Also, in NOS faulting is rated on a per mile basis and computed from the profile elevation data. No numerical value of faulting is reported by NOS. Thus the MEPDG analysis showed minimal faulting and it was confirmed by actual observation.

Table 4.1 Comparison of Predicted Response

Project	IRI (in/mi)		Faulting (in)		% Slabs Cracked	
	MEPDG Default Traffic	Kansas Traffic	MEPDG Default Traffic	Kansas Traffic	MEPDG Default Traffic	Kansas Traffic
K-2611-01, I-70 Geary	71	70	0.009	0.007	0	0
K-3344-01, I-70 Shawnee	107	106	0.01	0.009	0.5	0.2
20-0208, SPS-2 (Sec 5)	132	133	0.009	0.011	0	0
20-0207, SPS-2 (Sec 6)	104	104	0	0	0	0
20-0259, SPS-2 Control	105	105	0.009	0.008	0	0
K-3382-01, K-7, Johnson	93	87	0.015	0.005	0.6	0.1
K-3216-01, US-50 Chase	623	63	0.003	0.002	0	0
K-3217-01, US-50 Chase	72	72	0.004	0.003	0	0

Table 4.2 Measured Responses

Project	IRI (in/mi)		Faulting (in)
K-2611-01, I-70 Geary	91 (EB)	101 (WB)	F1 (0.125 in)
K-3344-01, I-70 Shawnee	103 (EB)	94 (WB)	F1 (0.125 in)
20-0208, SPS-2 (Sec 5)	124.2 (LTPP)	-	0.02
20-0207, SPS-2 (Sec 6)	107.0 (LTPP)	-	0
20-0259, SPS-2 Control	86.0 (LTPP)	-	0.004
K-3216-01, US-50, Chase	81 (NB)	-	F1 (0.125 in)
K-3217-01, US-50 Chase	84 (NB)	-	F1 (0.125 in)
K-3382-01, K-7 Johnson	86 (NB)	81 (SB)	F1 (0.125 in)

4.1.3 Percent Slabs Cracked

One of the structural distresses considered for JPCP design in MEPDG is fatigue-related transverse cracking of the PCC slabs. Transverse cracking can initiate either at the top surface of the PCC slab and propagate downward (top-down cracking) or vice versa (bottom-up cracking) depending on the loading and environmental conditions at the project site, material properties, design features, and conditions during construction. The parameter indicates the percentage of total slabs that showed transverse cracking. Figures 4.1(c) and 4.2(c) show the MEPDG-predicted percent slabs cracked values that are tabulated in Table 4.1. With the Kansas-specific traffic input, only I-70 Shawnee and K-7 Johnson county sections showed some insignificant amount of cracking. The percent slabs cracked values for these projects are 0.2% and 0.1%, respectively. The predictions are insignificantly higher for the Shawnee County (0.5%) and K-7 Johnson County (0.6%) projects with the MEPDG default traffic input. It has been previously observed

that the MEPDG-default traffic input has higher percentage of trucks distributed in the higher axle load categories compared to the Kansas input.

No measured cracking values were available from the Kansas NOS condition survey report and LTPP database for comparison with the MEPDG-predicted cracking. In NOS, no cracking survey is done on rigid pavements. In the LTPP survey, cracking is measured in terms of longitudinal and transverse crack lengths that cannot be interpreted as percent slabs cracked. Of course, an average value can be computed. It is to be noted that none of the SPS-2 sections in this study showed any cracking up to 2003 in the MEPDG analysis.

4.2 Sensitivity Analysis

Previous research has shown that the design features that influence JPCP performance include layer thicknesses, joint spacing, joint and load transfer design (Owusu-Antwi et al.1998; Khazanovich et al. 1998). The strength of Portland cement concrete (PCC) mix is also a basic design factor that is often controlled by the designer and is interrelated with the PCC slab thickness. Nantung et al. (2005) and Coree et al. (2005) have shown that PCC compressive strength and slab thickness have significant effects on the predicted distresses. In this part of the study, the sensitivity of the predicted performance parameters in the MEPDG analysis toward the material input (design and construction) parameters has been done for all projects except the projects in Chase County (these projects have shown localized failures, some premature distresses due to erosion of inadequately lime-treated subgrade). The following input parameters were varied:

1. Traffic (AADT, % Truck and Truck Type)

2. Material (PCC Compressive Strength, Coeff. of Thermal Expansion, Shrinkage Strain, PCC-Zero Stress Temperature, and Soil Class)

3. Design and Construction Features (PCC Thickness, Dowel Diameter, Dowel Spacing, Tied/Untied Shoulder, Widen Lane, Curing Type, Granular and Stabilized Base type, etc.)

4. Alternative Design

The JPCP distresses were predicted by the NCHRP MEPDG analysis for a 20-year design period. All other input parameters were project specific as shown in Table 3.16. Typical JPCP distresses-IRI, faulting, and percent slabs cracked, were calculated and compared at various levels of the input parameter chosen.

4.2.1 Traffic Input

In this part of the study, the sensitivity of the predicted performance parameters in the MEPDG analysis toward selected traffic input parameters was studied. The following input parameters were varied at the levels shown and the predicted IRI, faulting, and percent slabs cracked were calculated.

1. AADT [2,080(Low); 12,562 (Medium); 36,000 (High)]

2. Truck (%) [5 (Low); 23.2 (Medium); 47 (High)]

3. Class 9 Truck Type (MEPDG default [74%]; 40%; 50%; Kansas [variable])

A previous study has shown that the IRI, faulting and percent slabs cracked (Coree et al. 2005) are sensitive to the variation in AADTT.

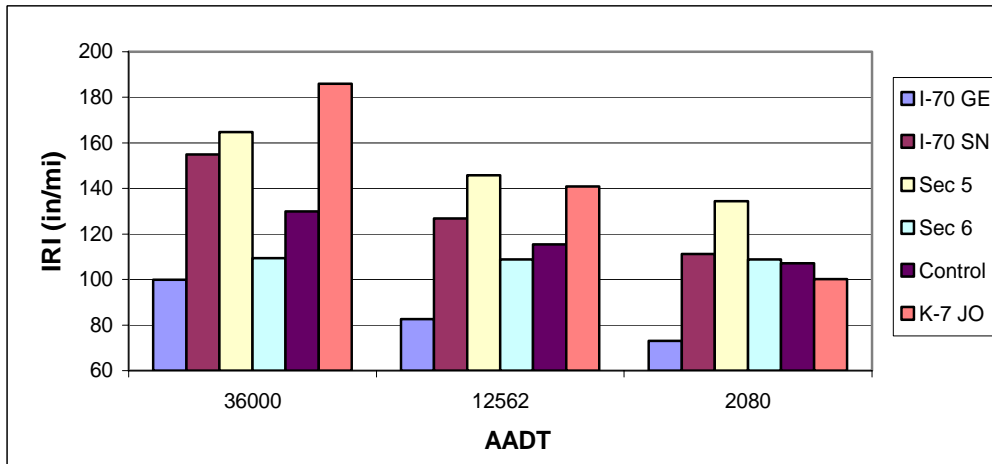
AADT

The Annual Average Daily Traffic (AADT) was varied at three levels with a constant truck percentage (23.2%), based on the range of AADT of the projects in this study. Table 4.3 lists the predicted IRI values. Figure 4.3(a) shows that with increasing AADT, IRI increases significantly. The increase is most significant for the I-70 Shawnee County and K-7 Johnson County projects. For the three levels of AADT chosen, the predicted IRI for the I-70 Shawnee County project increased from 111 in/mi to 155 in/mi. The effect on the K-7 Johnson County project is even more pronounced. The IRI increased from 100 in/mile to 186 in/mile. As mentioned earlier, these projects are different from other projects because the I-70 Shawnee County project has the lowest 28-day modulus of rupture (473 psi) and the K-7 Johnson County project has the lowest PCC slab thickness (9 inches). The effect of higher AADT is more pronounced on the PCC pavements with thinner slabs or lower strength.

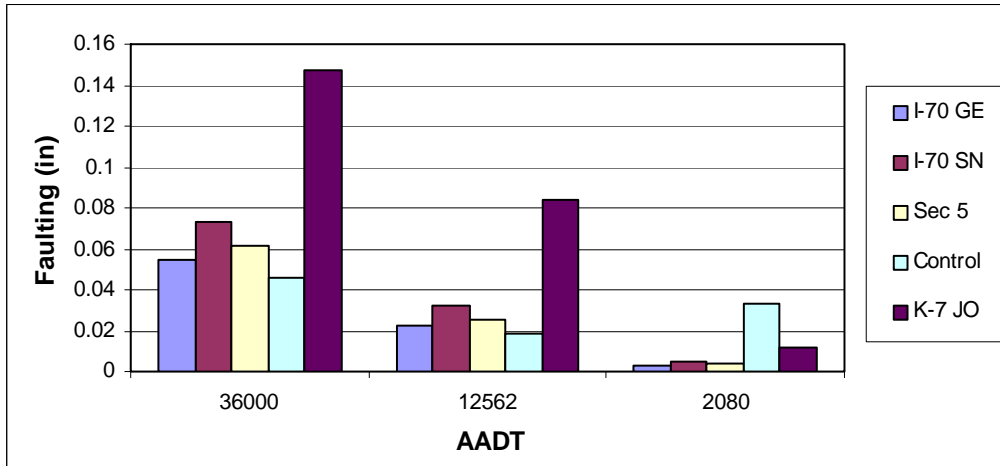
Figure 4.3(b) shows that the faulting on the K-7 Johnson County project is markedly affected by the increase in AADT. Faulting on any other sections is tolerable. Faulting on the I-70 Shawnee County project is slightly higher, though the values are negligible for all practical purposes. It appears that at higher AADT, faulting becomes a function of PCC slab thickness and strength.

Figure 4.3(c) shows that only two projects, I-70 Shawnee County and K-7 Johnson County, have predicted cracking. Cracking increases dramatically on both projects when AADT increases. In fact, the K-7 Johnson County project fails at the highest level of AADT. It appears that cracking is most sensitive to the increase in traffic level.

(a) IRI



(b) Faulting



(c) % Slabs Cracked

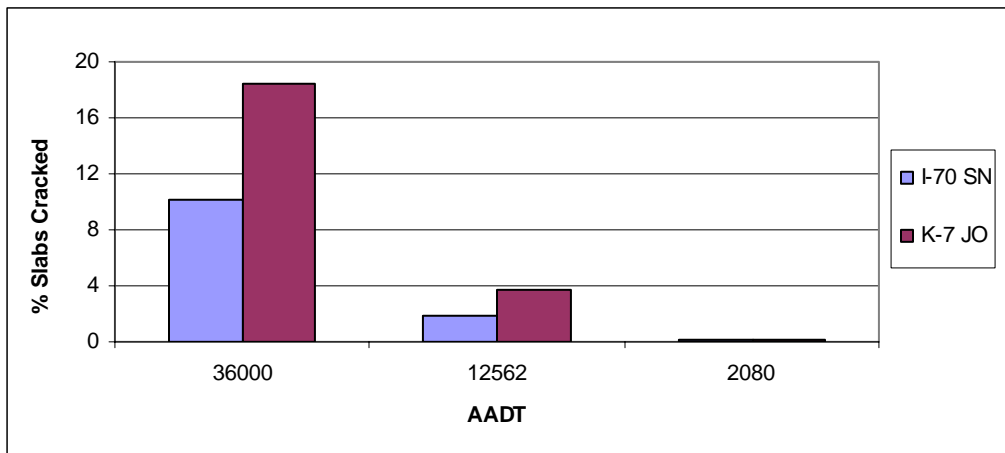


Figure 4.3 Predicted JPCP distresses at varying levels of AADT

Table 4.3 Effect of Traffic (AADT) on Predicted Responses

Project AADT	IRI (in/mi)			Faulting (in)			% Slabs Cracked		
	36000	12562	2080	36000	12562	2080	36000	12562	2080
I-70 GE	100	83	73	0.055	0.022	0.003	0	0	0
I-70 SN	155	127	111.2	0.073	0.032	0.005	10.1	1.9	0.1
Sec 5	165	146	134.4	0.061	0.025	0.004	0	0	0
Sec 6	109	109	108.9	0.001	0	0	0	0	0
Control	130	116	107.2	0.046	0.019	0.033	0	0	0
K-7 JO	186	141	100.1	0.147	0.084	0.012	18.5	3.7	0.1

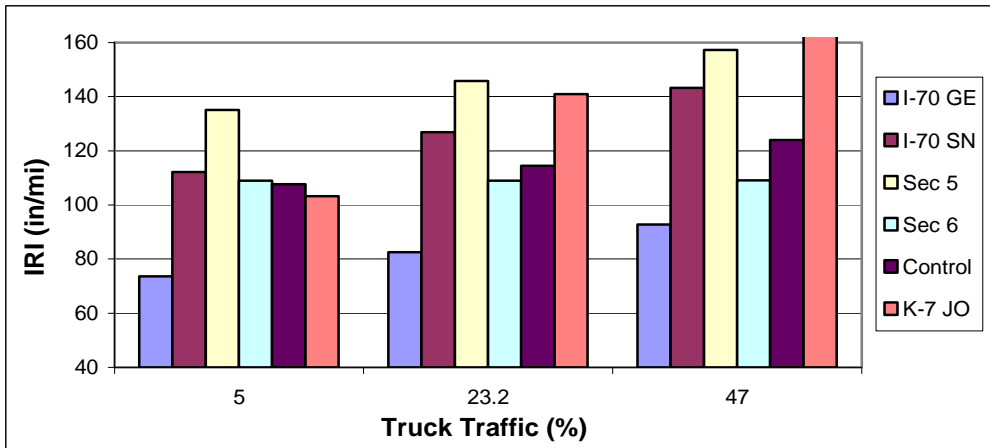
Truck Traffic

Figure 4.4 shows the variation of predicted distresses with different truck percentages at a constant AADT of 12,562, the average AADT level in this study. Figure 4.4(a) shows that with increasing percentage of trucks, IRI increases significantly for the SPS-2 Section 5, I-70 Shawnee County and K-7 Johnson County projects. SPS-2 Section 5 has a very high cement factor (862 lbs/cubic yd) and high modulus of rupture. Trend is similar for faulting as shown in Figures 4.4(b). Figure 4.4(c) shows that the I-70 Shawnee County and K-7 Johnson County projects show significant increase in cracking with higher truck percentages. No other section showed any cracking.

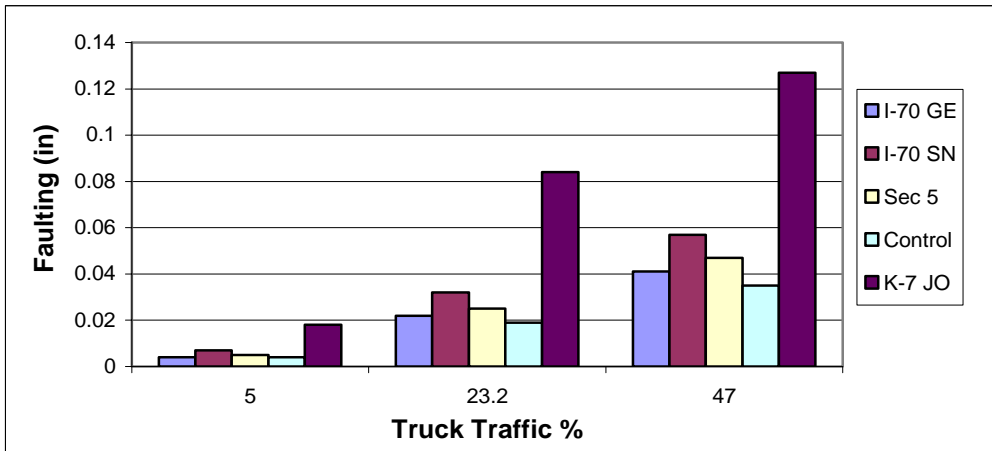
Truck Type

Since FHWA Class 9 trucks are the predominant truck type in Kansas, a sensitivity analysis was done with respect to varying percentages of this truck type. The MEPDG default percentage of Class 9 truck (74%), 50%, 40% and various percentages corresponding to different functional classes of routes in this study were used. The percentages varied from 75% for the I-70 projects (Interstate, Rural) to 25% for the K-7

(a) IRI



(b) Faulting



(c) % Slabs Cracked

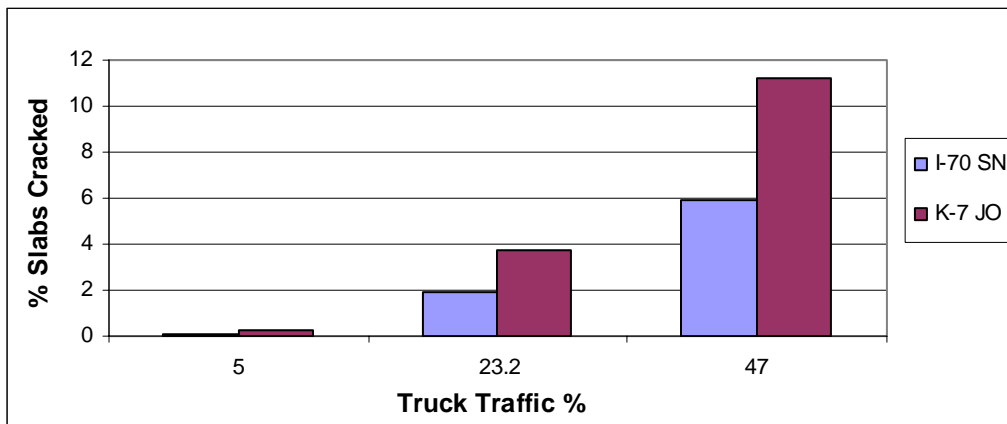
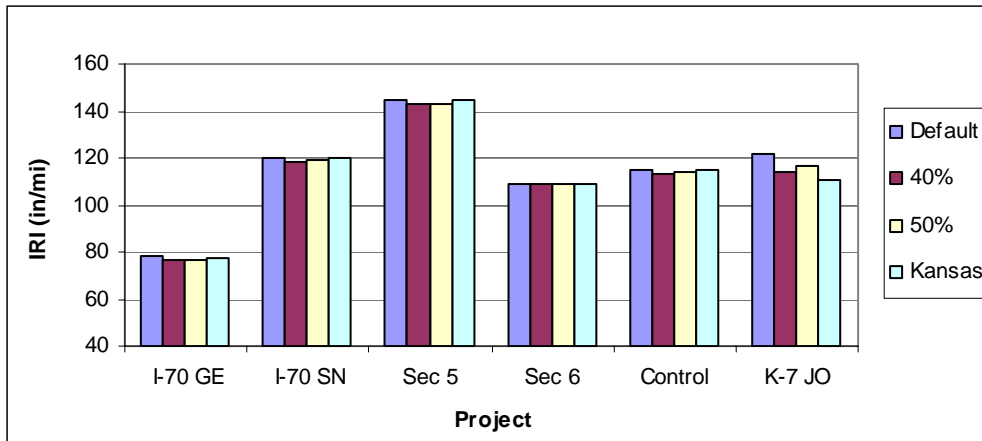
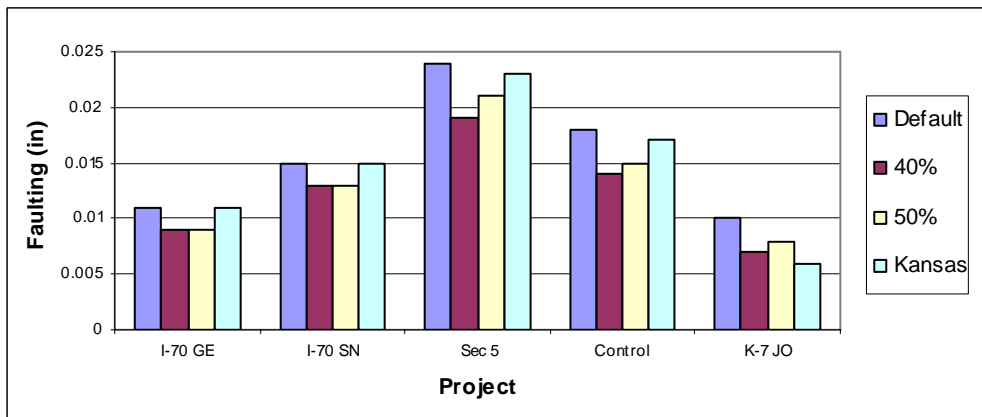


Figure 4.4 Predicted JPCP distresses at varying levels of truck traffic

(a) IRI



(b) Faulting



(c) % Slabs Cracked

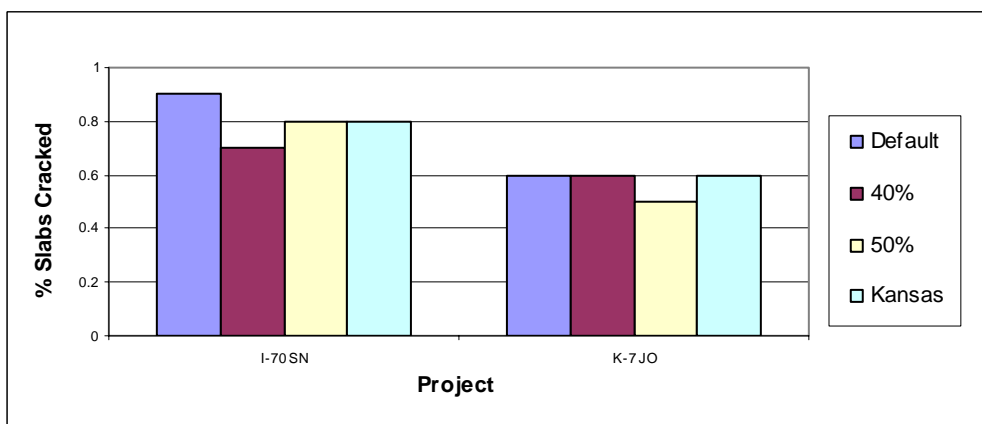


Figure 4.5 Predicted JPCP distresses at varying levels of class 9 truck type

Johnson County project (Urban Arterials, Others). The results show that the IRI values are fairly insensitive to the type of trucks. The faulting values and cracking values are relatively insensitive too.

4.2.2 *Material*

Compressive Strength

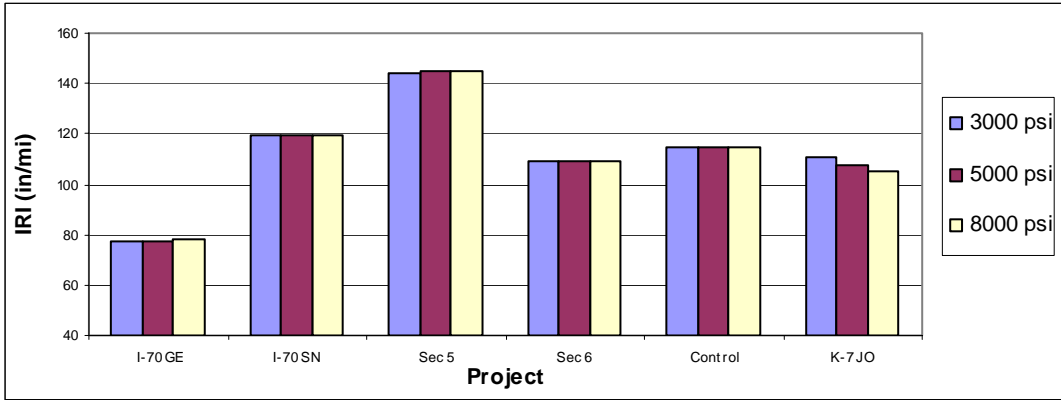
The MEPDG-predicted IRI values for the sections were compared at three levels of compressive strength- low (3,000 psi), average (5,000 psi), and high (8,000 psi). Figure 4.6 (a) shows the results. In general, the compressive strength does not affect predicted IRI. There is a slight effect for the K-7 Johnson County project. That section has the thinnest PCC slab among all sections. When the compressive strength was increased from 3,000 psi to 5,000 psi, IRI decreased from 111 in/mile to 108 in/mile. When the strength was increased to 8,000 psi, IRI was 105 in/mile. These decreases are negligible for all practical purposes.

Figure 4.6(b) shows the predicted faulting on all sections corresponding to three levels of compressive strength. Almost no changes in faulting values were observed for all projects. The predicted faulting values were also negligible for all practical purposes. It appears that faulting is fairly insensitive to strength.

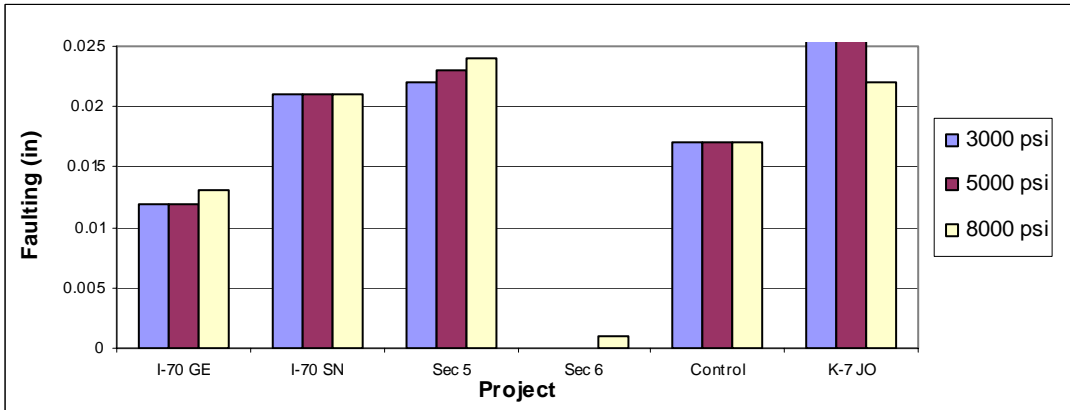
Figure 4.6(c) illustrates the effect of compressive strength on predicted percent slabs cracked. Although very small amounts of cracking were observed almost on all projects at the 3,000 psi level, no cracking was observed when the strength was increased

to 5,000 psi. The biggest change was observed for K-7, Johnson County- the project that had the lowest PCC slab thickness.

(a) IRI



(b) Faulting



(c) % Slabs Cracked

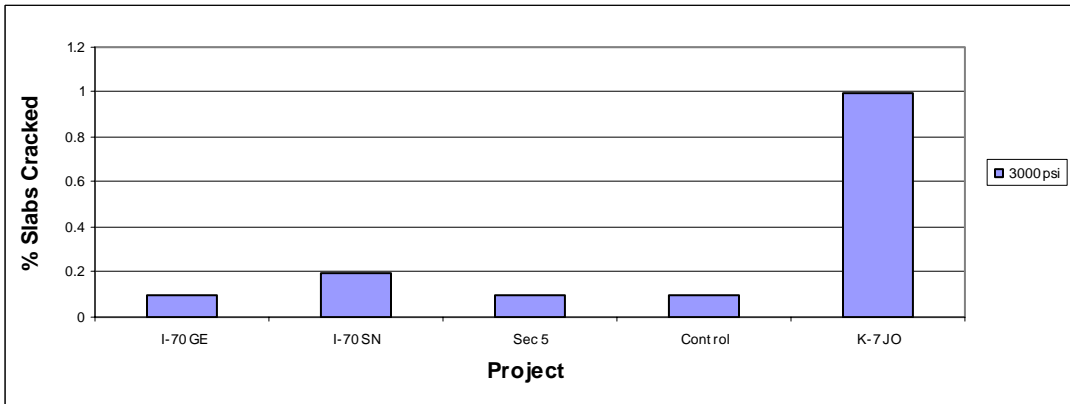


Figure 4.6 Predicted JPCP distresses for varying PCC strength

Coefficient of Thermal Expansion (CTE)

The MEPDG-predicted IRI for the sections were compared at three levels of PCC CTE input based on the TP-60 test results on the cores taken from the Kansas PCC pavements in the Long Term Pavement Performance (LTPP) program. Three levels of the PCC CTE input were, $4.3 \times 10^{-6}/^{\circ}\text{F}$ (average of the LTPP TP-60 highest 10% test results), $5.5 \times 10^{-6}/^{\circ}\text{F}$ (TP-60 test results from a recently built project), and $6.5 \times 10^{-6}/^{\circ}\text{F}$ (average of the LTPP TP-60 highest 10% test results).

Table 4.4 summarizes the results. Figure 4.7(a) shows the results. In general, higher PCC CTE would result in higher IRI. The effect is most pronounced on the I-70 Shawnee County and K-7 Johnson County projects. When the PCC CTE value increased from $4.33 \times 10^{-6}/^{\circ}\text{F}$ to $6.5 \times 10^{-6}/^{\circ}\text{F}$, the predicted IRI increased from 114 in/mile to 135 in/mile for the I-70 Shawnee County project. For the K-7 Johnson County project, the predicted IRI increase was similar (22 in/mile- from 101 to 123 in/mile). It is to be noted that these projects are different from others because the I-70 Shawnee County project has the lowest 28-day modulus of rupture (473 psi) and the K-7 Johnson County project has the lowest PCC slab thickness (9 inches). It appears the effect of PCC CTE input is more pronounced on JPCP with thinner slab or lower strength. It also is to be noted that PCC CTE value variation does not have any effect on the predicted IRI for the SPS-2 Section 6. That section has a widened lane of 14 ft with tied PCC shoulder. Thus, variation in the PCC CTE values studied in this project does not affect the predicted IRI for a JPCP with widened lane and tied PCC shoulder.

Figure 4.7(b) shows the predicted faulting on all sections corresponding to three levels of PCC CTE input value. No faulting was observed for the SPS-2 Section-6 which

has a widened lane of 14 ft. The effect of varying PCC CTE is most significant for the I-70 Shawnee County project, SPS-2 Section 5, and the K-7 Johnson County project. Section 5 has a very high cement factor (862 lbs/yd³). It appears that the combination of high cement factor and higher PCC CTE would result in higher faulting. However, the predicted faulting values are negligible for all practical purposes.

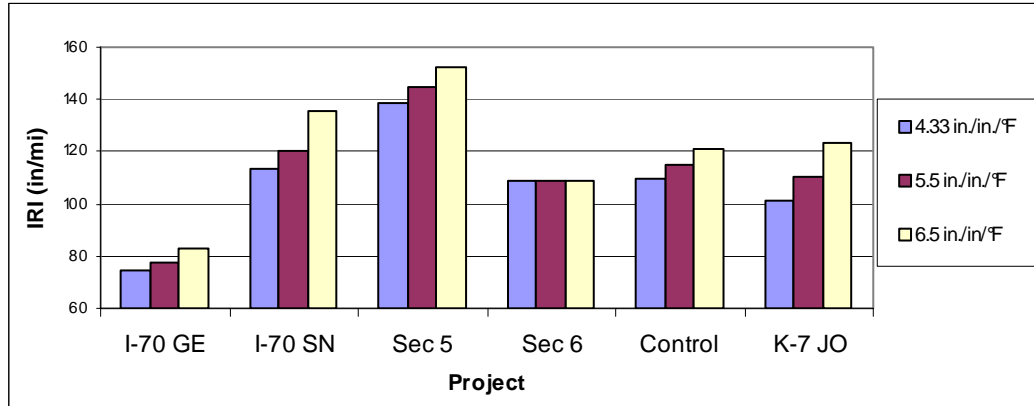
Table 4.4 Comparison of Predicted Response Corresponding to Different Coefficient of Thermal Expansion

Project	IRI (in/mi)			Faulting (in)			% Slabs Cracked		
	4.33 x10 ⁻⁶ /°F	5.5 x10 ⁻⁶ /°F	6.5 x10 ⁻⁶ /°F	4.33 x10 ⁻⁶ /°F	5.5 x10 ⁻⁶ /°F	6.5 x10 ⁻⁶ /°F	4.33 x10 ⁻⁶ /°F	5.5 x10 ⁻⁶ /°F	6.5 x10 ⁻⁶ /°F
I-70 GE	74	78	83	0.006	0.012	0.022	0	0	0
I-70 SN	114	120	135	0.01	0.021	0.035	0	0.8	10.3
Sec 5	138	145	152	0.011	0.023	0.038	0	0	0
Sec 6	109	109	109	0	0	0	0	0	0
Control	110	115	121	0.008	0.017	0.029	0	0	0
K-7 JO	101	110	123	0.014	0.031	0.053	0.2	0.6	1.9

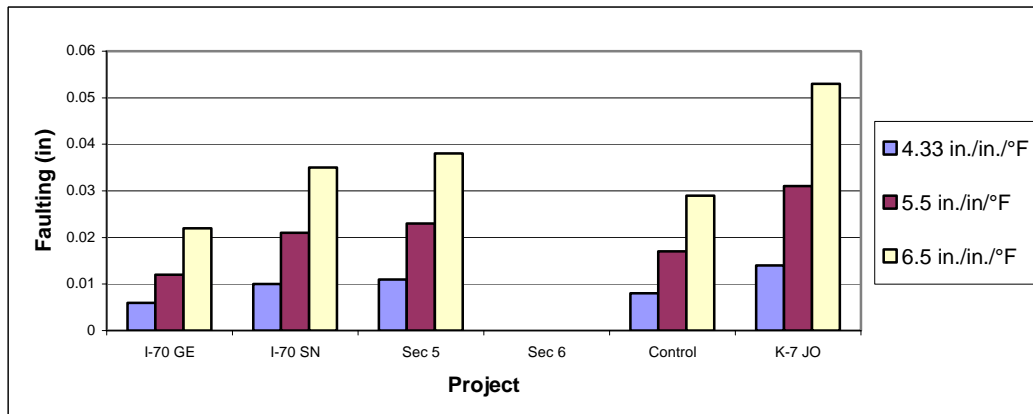
Figure 4.7(c) illustrates the effect of PCC CTE input on predicted percent slabs cracked. Only two projects, I-70 Shawnee County and K-7 Johnson County, appear to be affected by this input. The I-70 Shawnee County project is most severely affected although there was no cracking on this project at the lowest PCC CTE input (4.33 x10⁻⁶/°F). Fifty percent increase in this parameter resulted in 10% slabs cracked for this project. Also, as mentioned earlier, this project has the lowest concrete modulus of rupture among all projects studied. Although the amount of cracking is much lower for the K-7 Johnson County project, the increase is also pronounced. For the lowest PCC CTE value of 4.33 x10⁻⁶/°F, there was only 0.2% slabs cracked. For the highest PCC CTE input, 6.5 x10⁻⁶/°F, cracking increased to 2% – a tenfold increase due to 50%

increase in the PCC CTE value. This parameter was found to be extremely sensitive in others studies too (Beam 2003; Coree et al 2005; Nantung et al. 2005).

(a) IRI



(b) Faulting



(c) % Slabs Cracked

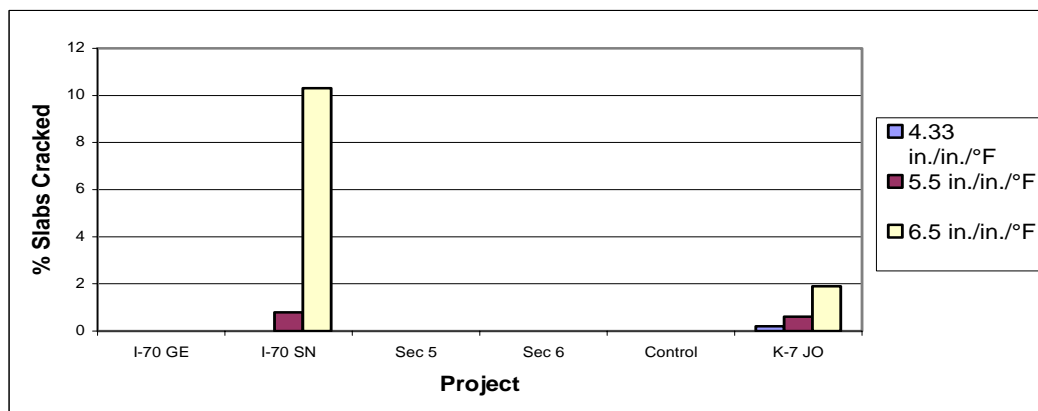


Figure 4.7 Predicted JPCP distresses for different CTE input

Shrinkage Strain

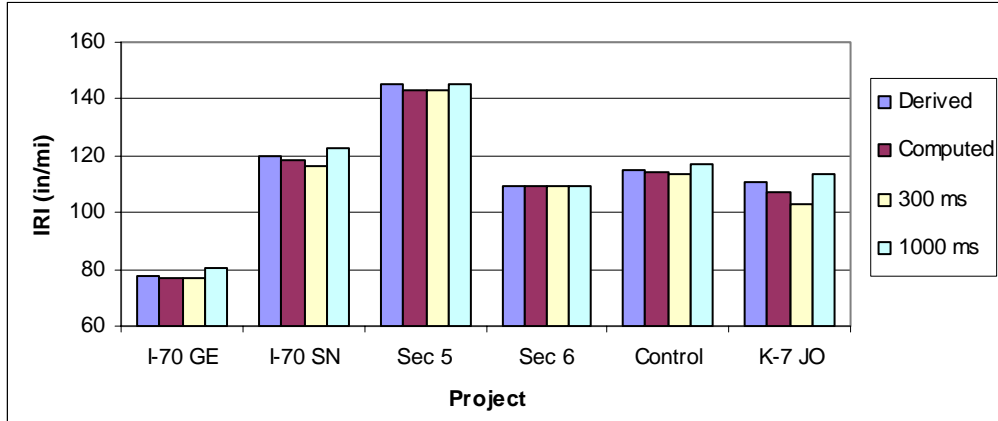
The MEPDG-predicted 20-year IRI values for the sections were compared at four levels of shrinkage strain – derived, computed, low (300 μm), and high (1,000 μm). Figure 4.8 (a) shows the results. In general, the shrinkage does not greatly affect IRI. The derived, computed, and lower shrinkage strain levels tend to predict similar IRI. There is a slight effect for the K-7 Johnson County project. When the shrinkage strain increased from 300 μm to 1,000 μm , IRI increased from 103 in/mile to 114 in/mile. According to the MEPDG algorithm, higher shrinkage strain results in higher faulting. That, in turn, is responsible for increased roughness.

Figure 4.8(b) shows the predicted faulting on all sections corresponding to four levels of shrinkage strain. Higher shrinkage strain results in higher faulting. The effect is most pronounced for the I-70 Shawnee and the K-7 Johnson County projects. When the shrinkage strain increased from 300 μm to 1,000 μm , faulting almost doubled though the faulting values are negligible for all practical purposes. Nevertheless, the faulting is very sensitive to the shrinkage strain.

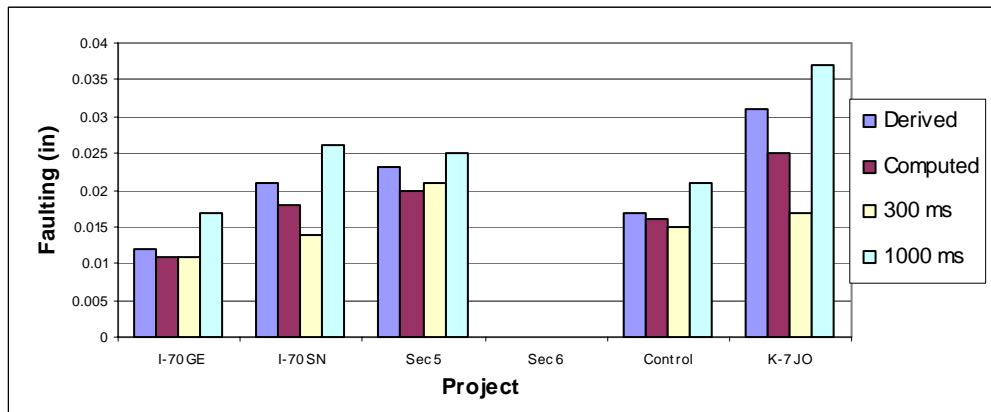
Figure 4.8(c) illustrates the effect of shrinkage strain on predicted percent slabs cracked for the JPCP projects in this study. Only two projects showed cracking, and the effect of shrinkage strain is almost negligible. The I-70 Shawnee County project showed a slight increase in cracking with higher strain. Cracking appears to be fairly insensitive to the shrinkage strain.

This parameter was found to be insensitive in previous studies (Beam 2003; Coree et al 2005; Nantung et al. 2005).

(a) IRI



(b) Faulting



(c) % Slabs Cracked

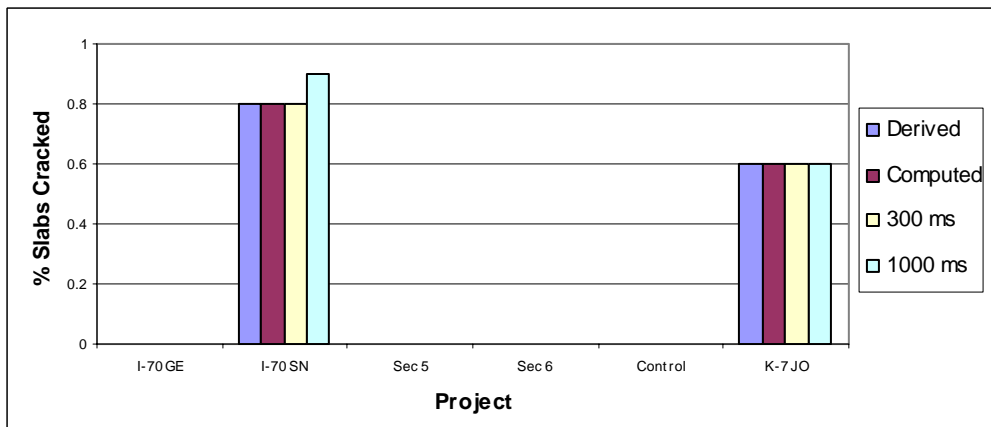


Figure 4.8 Predicted JPCP distresses for different shrinkage strain input

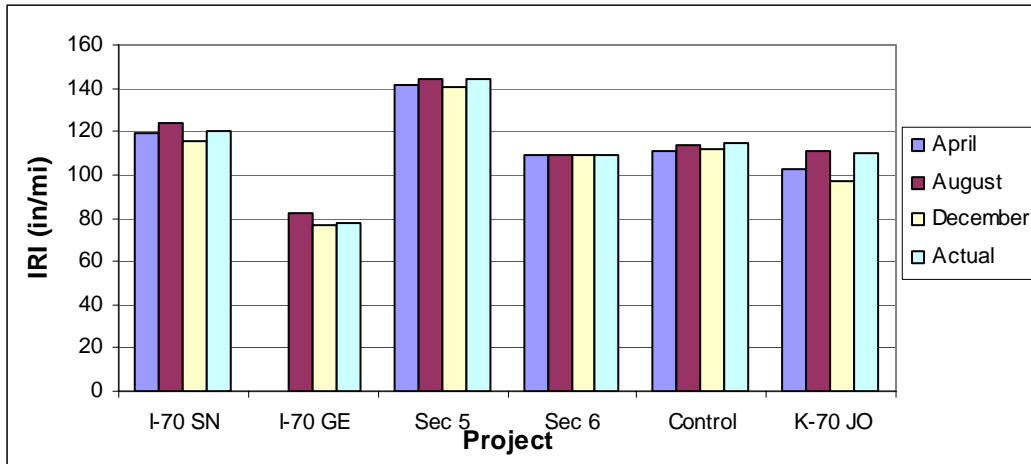
PCC Zero-Stress Temperature

Figure 4.9 shows the predicted JPCP distresses by NCHRP MEPDG corresponding to three probable and one actual construction months for the projects in this study. Three probable construction months were chosen based on an analysis of the mean monthly temperature (MMT) values obtained from the weather database for the years of construction of these projects. The months of April, August, and December were selected to represent high and low MMT or Tz values. October was also chosen but later disregarded since MMT values for this month are very similar to those in April. Actual construction months for the projects, shown in Table 3.1, are as follows: I-70 Geary County: November 1990; I-70 Shawnee County: October 1993; SPS-2's: July 1992; and K-7 Johnson County: September 1995.

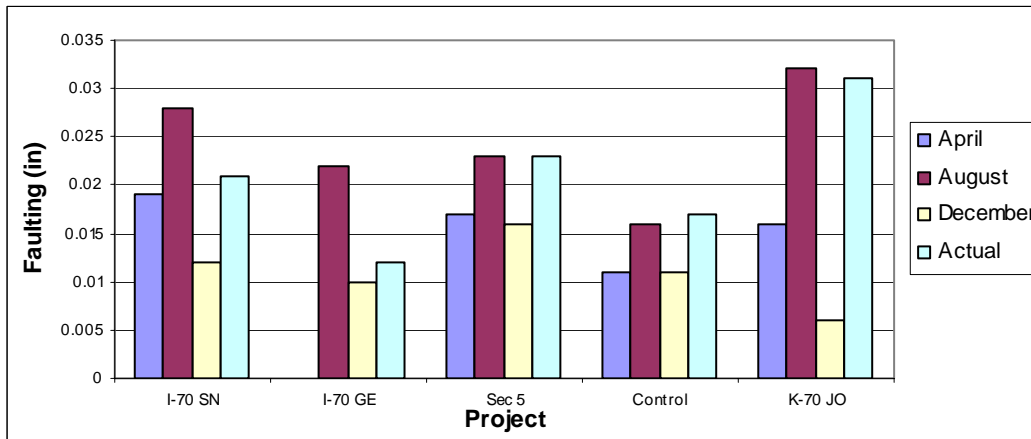
Figure 4.9(a) shows that construction month/Tz does not greatly affect the predicted IRI. For almost all projects, JPCP's constructed in April show slightly lower IRI. However, the initial IRI results in Table 3.1 show that the SPS sections, built in July 1992, have the highest initial or as-constructed IRI among all sections.

Construction months/Tz tends to make the biggest difference in predicted faulting as shown in Figure 4.9(b). It is clear that the pavements constructed in August (with highest MMT/Tz) will have much higher faulting than those constructed in temperate climate in April or even in colder time in December. The effect is very pronounced on I-70 Shawnee County and K-7 Johnson County - the projects with lower PCC strength and thinner PCC slab, respectively. The only project which is not affected by this parameter is SPS-2 Section 6. This pavement has a widened lane and that appears to address the higher faulting effect due to construction during the month with high MMT.

(a) IRI



(b) Faulting



(c) % Slabs Cracked

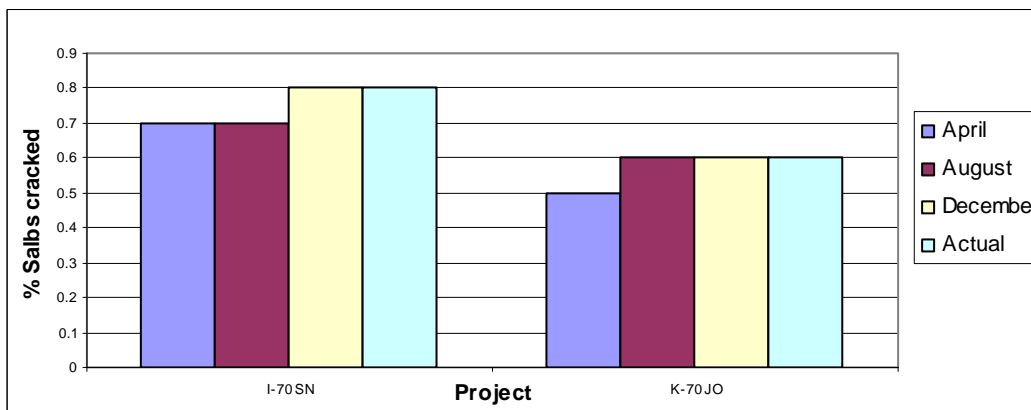


Figure 4.9 Predicted JPCP distresses for different pavement construction months

Figure 4.9(c) shows that predicted slab cracking is not highly affected by the construction month. However, both I-70 Shawnee County and K-7 Johnson County projects, where some cracking was observed, showed slightly less slab cracking for construction during April. Considering all results it appears that April and October are the two best months for JPCP construction (paving) in Kansas. However, previous studies (Beam 2003; Coree et al. 2005) found that the variation in distress corresponding to the changes in PCC zero stress temperature is not that significant.

Soil Class

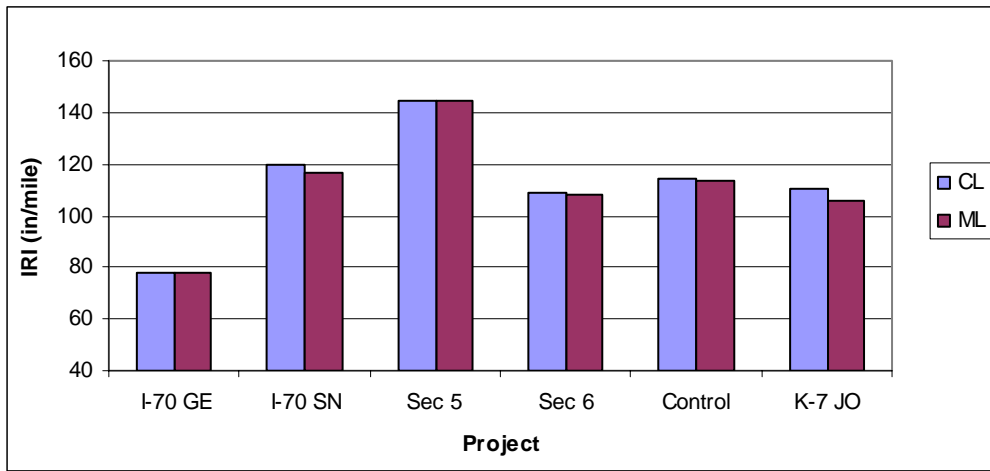
In this study, subgrade soil class was varied as: A-4 (Silt, ML) and A-7-6 or A-6 (Clay, CL). The properties used for these soils are summarized in Table 3.1.

No variation in IRI was observed for all projects except for the I-70 Shawnee and K-7 Johnson County projects as shown in Figure 4.10 (a). That variation was not significant. When the subgrade soil was changed from clay to silt, the predicted IRI decreased from 120 to 117 in/mile and 110 to 106 in/mi for the I-70 Shawnee and K-7 Johnson County projects, respectively. This variation is negligible for all practical purposes.

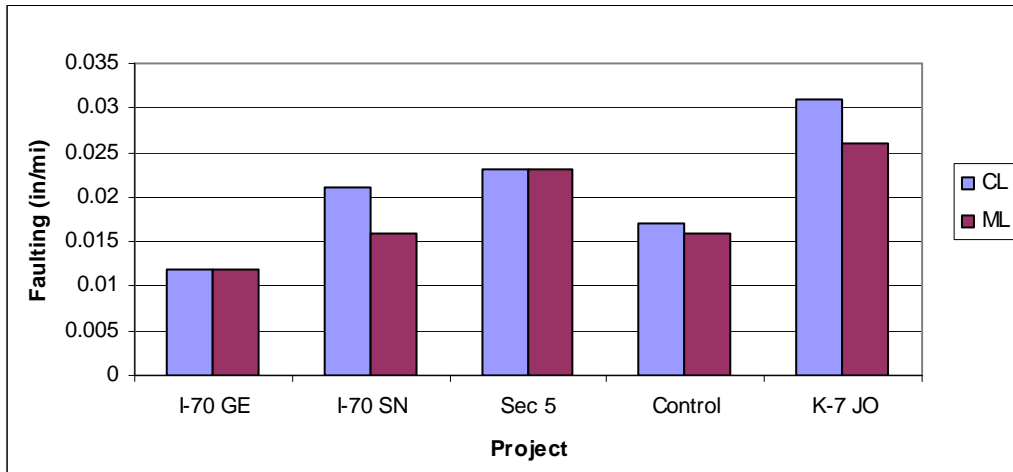
No significant variation in faulting was observed for all JPCP projects, except for the I-70 Shawnee County and K-7 Johnson County projects. Figure 4.10(b) shows that faulting increased by 0.005 in for both projects, when the soil type was changed from clay to silt. However, these faulting values are negligible for all practical purposes.

Figure 4.10(c) shows the predicted cracking on all sections. With the project-specific inputs, only I-70 Shawnee County and K-7 Johnson County sections showed some insignificant increase in slab cracking (around 1.2% and 0.3%, respectively) for

(a) IRI



(b) Faulting



(c) % Slabs Cracked

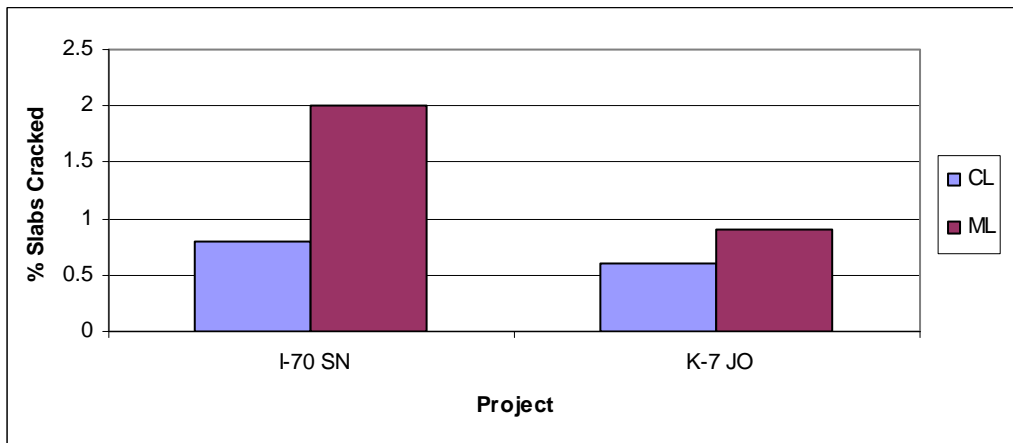


Figure 4.10 Predicted JPCP distresses for different subgrade soil type

different soil types. However, no variation in cracking was observed on all other projects. Therefore, cracking is not sensitive to the changes in soil type.

4.2.3 Design and Construction Features

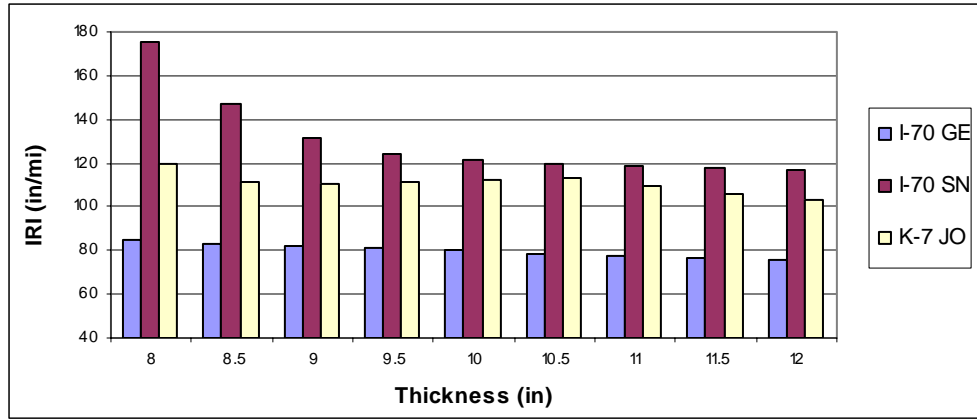
Thickness

The MEPDG-predicted IRI values for the KDOT sections were compared at nine levels of PCC slab thickness input- 8 inch to 12 inch with an increment of 0.5 inch. Figure 4.11(a) shows the results on non-SPS-2 sections. In general, higher slab thickness resulted in lower IRI. The effect is highly pronounced for the I-70 Shawnee County as well as for the Geary County project. When the PCC slab thickness was increased from 8 inch to 12 inch, the predicted IRI decreased from 176 in/mile to 117 in/mile for the I-70 Shawnee County project. For the I-70 Geary County project, the predicted IRI decrease was smaller (8.7 in/mile- from 84.5 to 75.8 in/mile). The effect on the K-7 Johnson County project was also very high. It is to be noted that the K-7 Johnson County project is different from the other projects because this project has the lowest PCC slab thickness (9 inch). The I-70 Shawnee County project has the lowest 28-day modulus of rupture (473 psi).

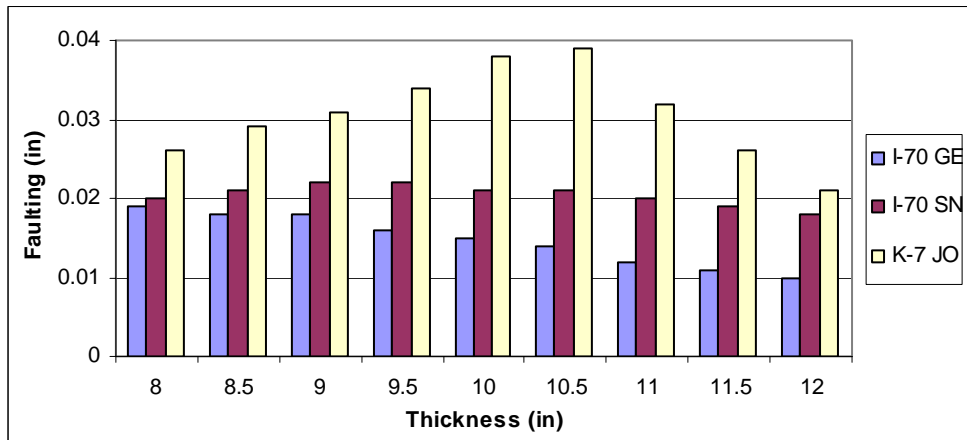
Figure 4.12(a) shows the change in predicted IRI with slab thickness for the three SPS-2 projects. For the SPS-2 Section 5 and Control Section, when the slab thickness was increased from 8 inch to 12 inch, the predicted IRI decreased from 151 in/mile to 145 in/mile and 124 in/mi to 115 in/mi, respectively. SPS-2 Section 5 has the highest modulus of rupture and the Control section has the highest thickness among all projects

studied. The effect of change in slab thickness on predicted IRI is not significant for the SPS-2 Section 6, which has a 14-ft widened lane.

(a) IRI



(b) Faulting



(c) % Slabs Cracked

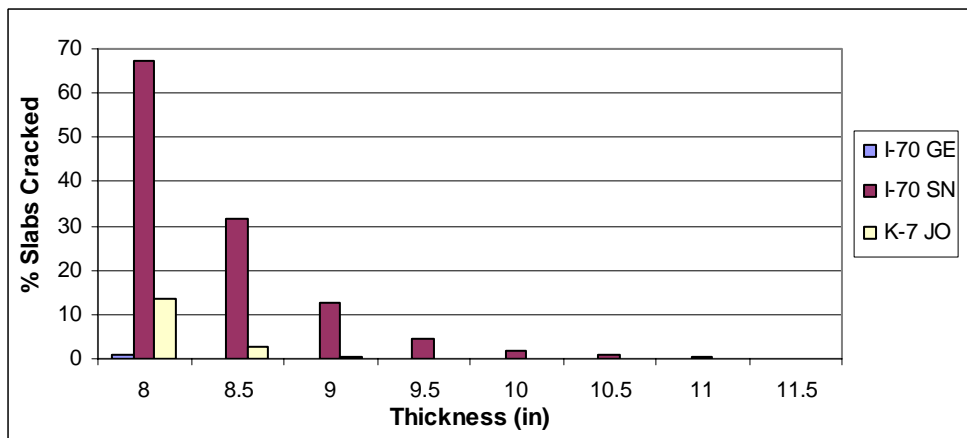


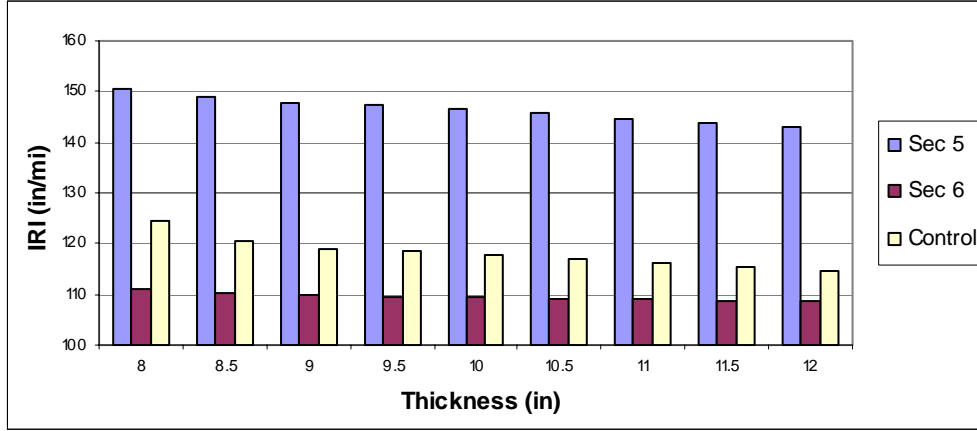
Figure 4.11 Predicted JPCP distresses on KDOT sections for varying thickness

It appears that the effect of thickness is more pronounced on the PCC pavements with thinner slab or low strength. However, this sensitivity was not observed for a JPCP with widened lane.

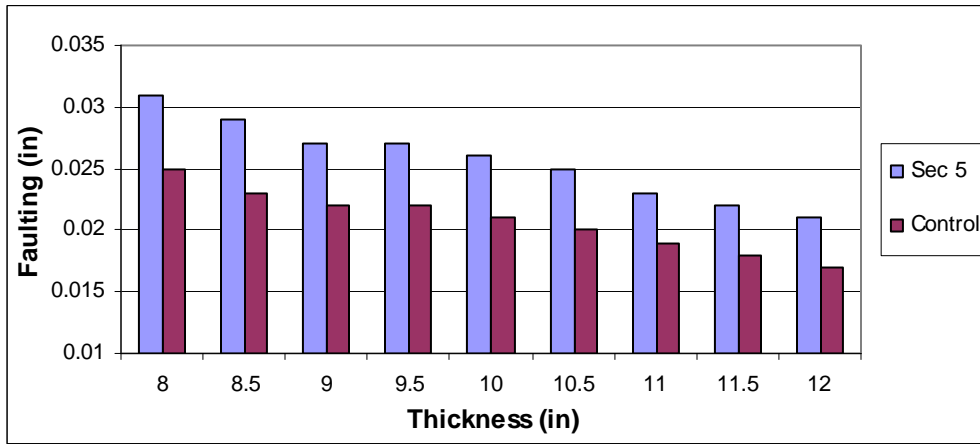
Figure 4.11(b) and 4.12(b) show the predicted faulting on all KDOT and SPS-2 sections. Significant changes in faulting values were observed for all projects except the SPS-2 Section 6. No faulting was observed for that particular project due to its widened lane effect. The effect of varying thickness is most significant for the I-70 Shawnee County and K-7 Johnson County projects. For the K-7 Johnson County project faulting increased with increasing thickness up to a certain point and then reduced with increasing thickness. Almost similar trend was also observed for the I-70 Shawnee County project. The highest faulting observed in the K-7 Johnson and I-70 Shawnee County projects were 0.039 inch at 10.5 inch PCC slab thickness and 0.022 in. at 9 inch thickness, respectively. The NCHRP MEPDG suggests that with increasing slab thickness (in order to reduce slab cracking for heavier traffic), dowel diameter be increased to control joint faulting. This may result in a small increase in predicted joint faulting due to a reduction in effective area of the dowel bar relative to the slab thickness (NCHRP 2004). Therefore, since the K-7 Johnson County project has the lowest dowel diameter (1.125 inch) compared to others, predicted faulting is greater at higher thickness. However, after a certain thickness level (nearly 11 in.), distresses get compensated for higher thickness as shown in Figure 4.11 (b). Though the dowel diameter for the I-70 Shawnee County project (1.375 inch) is not that low but the project has the lowest modulus of rupture compared to others. That may have resulted in a trend similar to the K-7 Johnson County project. For the I-70 Geary County project, as the thickness increased the predicted

faulting decreased. When the thickness was increased from 8 inch to 12 inch, faulting decreased from 0.02 inch to 0.01 inch.

(a) IRI



(b) Faulting



(c) % Slabs Cracked

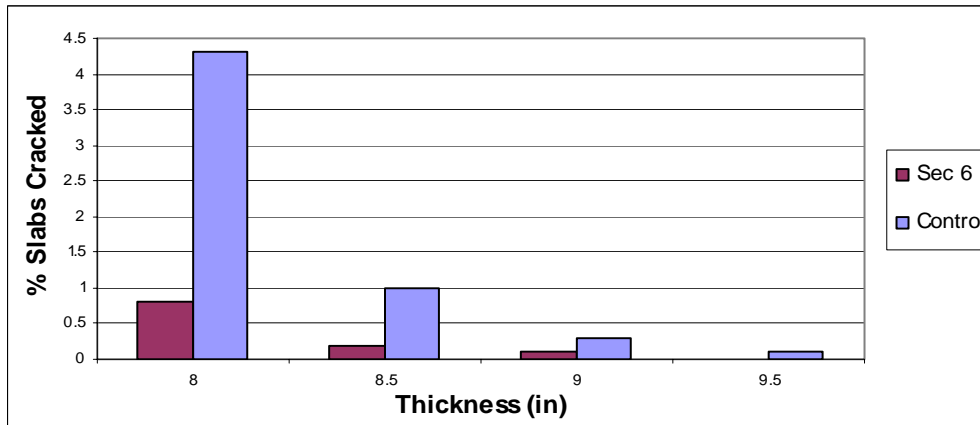


Figure 4.12 Predicted JPCP distresses on SPS-2 Sections for varying thickness

The SPS-2 Section 5 and SPS-2 Control section show similar trends of decreasing faulting with thickness, as illustrated in Figure 4.12(b). When the thickness increased from 8 inch to 12 inch, the predicted faulting decreased from 0.025 in. to 0.017 in. and 0.031 in. to 0.021 in. for the SPS-2 Control section and SPS-2 Section 5, respectively. No faulting was observed on Section 6, which has a 14 ft widened lane. However, all predicted faulting values are negligible for all practical purposes.

Figures 4.11(c) and 4.12(c) illustrate the effect of thickness on predicted percent slabs cracked for the JPCP projects in this study. Among the three KDOT sections, I-70 Shawnee County and K-7 Johnson County projects showed significant change in cracking with thickness. Figure 4.11(c) shows the when that thickness was increased from 8 inch to 12 inch, percent slabs cracked decreased from 67% to 0.1% for the I-70 Shawnee County project. For the K-7 Johnson County project, the predicted percent slabs cracked decreased from 14% to 0.1% when the slab thickness was increased from 8 inch to 9.5 inch. After that thickness level, no cracking was observed for that project. Among the three SPS-2 projects, SPS-2 Control section showed higher percentage of cracking (4.3%) at 8 inch thickness, and no cracking was observed at 10 inch as shown in Figure 4.12(c).

Cracking on SPS-2 Section 6 decreased almost similar to the SPS-2 Control Section (0.8% at 8 inch), and then reduced to none at 9.5 inch thickness. No cracking was observed on the SPS-2 Section 5 which has the highest modulus of rupture among all projects. Therefore, thickness significantly influences cracking on projects lower PCC strength.

Dowel Diameter

In this study, dowel diameter was varied at three levels of input: 1 in. (low), 1.25 in. (average) and 1.5 in (high). The predicted MEPDG distresses are tabulated in Table 4.5

Figure 4.13 (a) shows the predicted IRI results. In general, higher dowel diameter resulted in lower IRI. The effect is most pronounced for the I-70 Shawnee County and K-7 Johnson County projects as well as for the three SPS-2 projects. When the dowel diameter was increased from 1.0 to 1.5 inch, the predicted IRI decreased from 161 in/mile to 117 in/mile for the I-70 Shawnee County project. For the K-7 Johnson County project, predicted IRI decrease was almost similar (36 in/mile- from 133 to 97 in/mile). It is to be noted that these projects are different from the other projects because the I-70 Shawnee County project has the lowest 28-day modulus of rupture (473 psi) and the K-7 Johnson County project has the lowest PCC slab thickness (9 inches). Similar trends were also observed for the three SPS-2 projects. For the SPS-2 Section 5, when the dowel diameter was increased from 1.0 inch to 1.5 inch, the predicted IRI decreased from 194 in/mile to 145 in/mile. This section has the highest modulus of rupture among all projects studied. Dowel size effect is also significant for the SPS-2 Control section and Section 6, which has the highest slab thickness and 14-ft widened lane, respectively. With increasing dowel diameter from 1.0 inch to 1.5 inch, IRI decreased from 151 in/mile to 115 in/mile and 129 in/mile to 109 in/mile for these sections, respectively. It appears the effect of dowel diameter is more pronounced on the PCC pavements with thinner or thicker slab, and very high or low strength. It also is to be noted that that dowel diameter variation does not have any significant effect on the predicted IRI for the

I-70 Geary County project. That section has a slab thickness of 11 inch with a modulus of rupture of 690 psi.

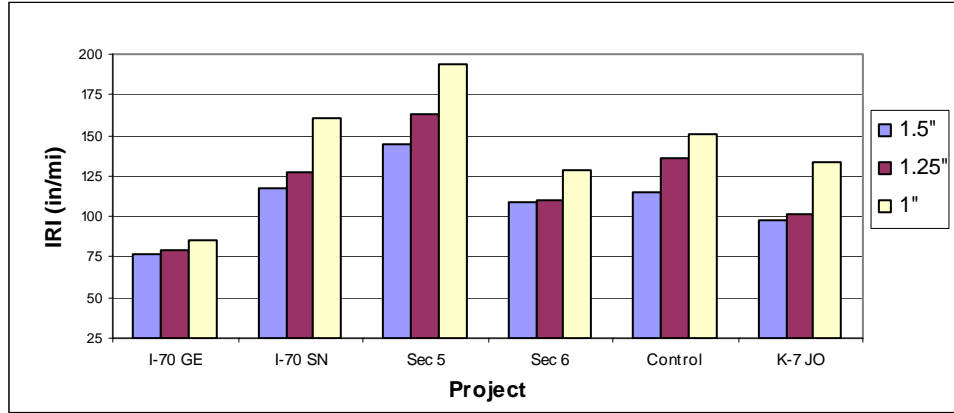
Table 4.5 Comparison of Predicted Response Corresponding to Varying Different Dowel Diameter

Project	IRI (in/mi)			Faulting (in)			% Slabs Cracked		
	1.5"	1.25"	1"	1.5"	1.25"	1"	1.5"	1.25"	1"
I-70	77	80	86	0.011	0.016	0.028	0	0	0
I-70	117	128	161	0.015	0.036	0.099	0.8	0.8	0.8
Sec 5	145	163	194	0.023	0.059	0.0117	0	0	0
Sec 6	109	111	129	0	0.003	0.038	0	0	0
Control	115	135	151	0.017	0.056	0.087	0	0	0
K-7 JO	97	101	133	0.006	0.014	0.075	0.6	0.6	0.6

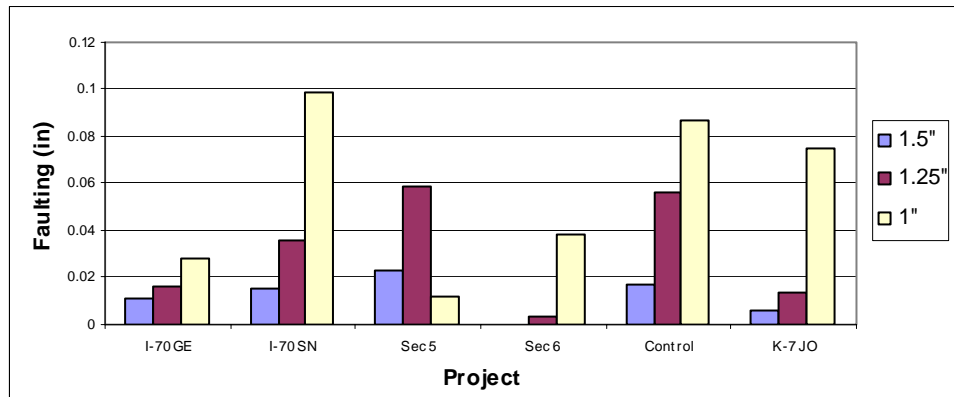
Figure 4.13(b) shows the predicted faulting on all sections corresponding to three levels of dowel diameter. Significant changes in faulting values were observed for all projects. The effect of varying dowel diameter is most significant for the I-70 Shawnee County project, SPS-2 Section 5, SPS-2 Control section and the K-7 Johnson County project. For the I-70 Shawnee County and K-7 Johnson County projects, when dowel diameter was increased from 1.0 in. to 1.5 in., the predicted faulting decreased from 0.10 to 0.015 in. and 0.08 to 0.006 in., respectively. For Section 5, which has a very high cement factor (862 lbs/yd³), the effect is even more significant. For that section faulting decreased from 0.12 to 0.02 in with an increase in dowel diameter from 1.0 to 1.5 inch. With increasing dowel diameter, the predicted faulting on the SPS-2 Control section decreased from 0.09 to 0.02 inch. It was also observed that with 1.5-inch dowels, no faulting was observed for the KDOT Section 6, which has a 14 ft widened lane.

However, faulting was present for lesser diameter dowels. The predicted faulting values are negligible for all practical purposes.

(a) IRI



(b) Faulting



(c) % Slabs Cracked

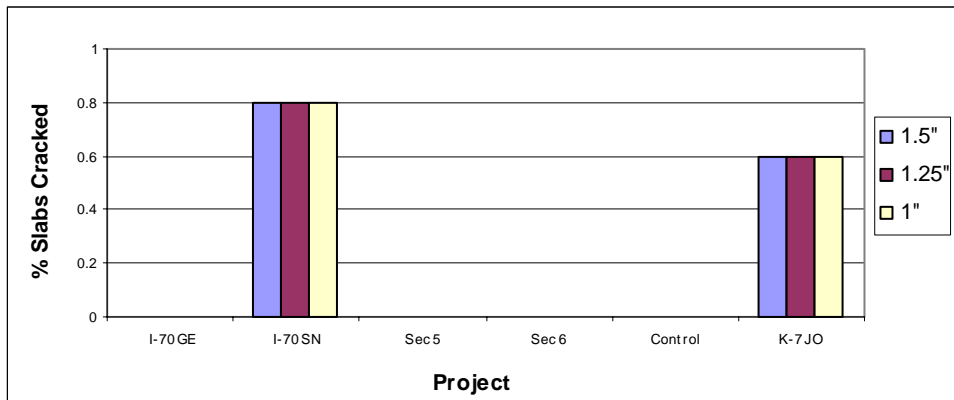


Figure 4.13 Predicted JPCP distresses for different dowel diameters

Figure 4.13(c) illustrates the effect of dowel diameter on predicted percent slabs cracked for the JPCP projects in this study. Only two projects, I-70 Shawnee County and K-7 Johnson County, appear to have this distress irrespective of dowel size. Very small amounts of cracking of 0.8% and 0.6 % were observed for the Shawnee County and Johnson County projects, respectively. Dowel size does not appear to affect slab cracking.

Dowel Spacing

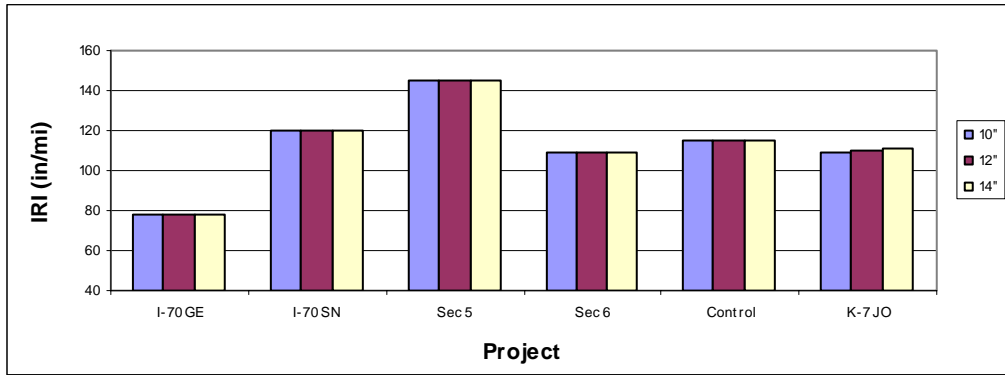
Figure 4.14(a) shows the predicted IRI on all sections corresponding to three levels of dowel spacing-10, 12, and 14 inches. No variation in IRI was observed for all projects except K-7 Johnson County. That variation was not significant. When the dowel spacing was increased from 10 in. to 14 in., the predicted IRI increased from 109 to 111 in/mile. This much variation is negligible for all practical purposes.

Figure 4.14(b) shows the predicted faulting on all sections corresponding to three levels of dowel spacing. However, no variation was observed almost for all projects. When the dowel spacing increased from 10 in. to 14 in., the predicted faulting increased from 0.029 in. to 0.032 in. for the K-7 Johnson County project. The predicted faulting values were negligible for all practical purposes.

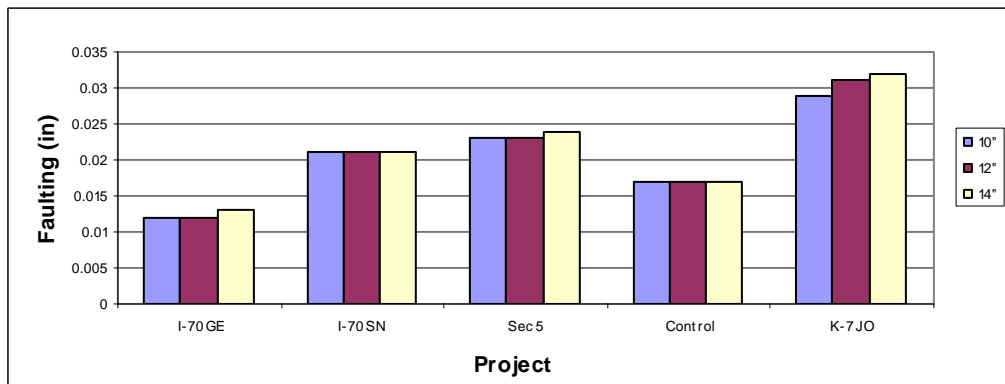
Figure 4.14(c) shows the predicted cracking on all sections. With the project-specific inputs, only I-70 Shawnee County and K-7 Johnson County sections showed some insignificant amounts of slab cracking. However, no variation in cracking amount was observed with varying dowel bar spacing. Therefore, cracking is not sensitive to the changes in dowel bar spacing.

Beam (2003) and Nantung et al. (2005) found that dowel diameter is a sensitive design input, whereas dowel spacing is insensitive. Coree et al. (2005) have shown that dowel diameter does not influence to the predicted percent slabs cracked.

(a) IRI



(b) Faulting



(c) % Slabs Cracked

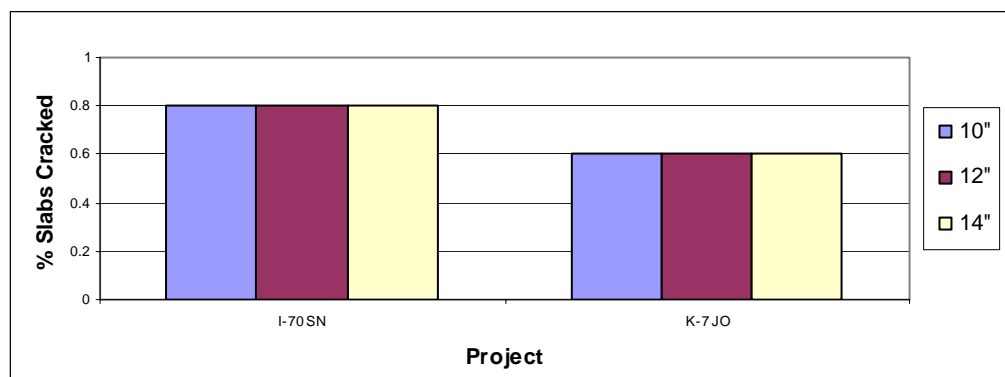


Figure 4.14 Predicted JPCP distresses for different dowel spacing

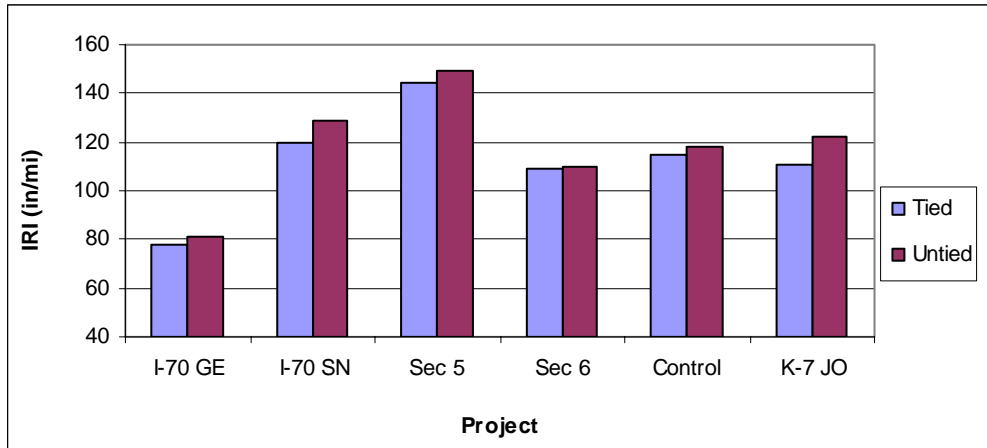
Shoulder Type

Tied PCC shoulders can significantly improve JPCP performance by reducing critical deflections and stresses (NCHRP 2004). For tied concrete shoulders, the long-term Load Transfer Efficiency (LTE) value between the lane and the tied shoulder must be provided. In this study, 60 percent LTE was considered for the projects with monolithically constructed, tied PCC shoulder. MEPDG-predicted IRI values, tabulated for all projects in Table 4.6, were compared for tied and untied shoulders. The effect was prominent for the same three sections (I-70 Shawnee, SPS-2 Section 5, and K-7 Johnson County) as was with the dowel size as shown in Figure 4.15 (a). When the PCC shoulder was untied on the K-7 Johnson County project, the predicted IRI increased from 110 in/mile to 122 in/mile. This project showed the greatest effect. The SPS-2 Section 6 did not show any change in IRI mainly due to the fact that this project has a widened lane of 14 ft.

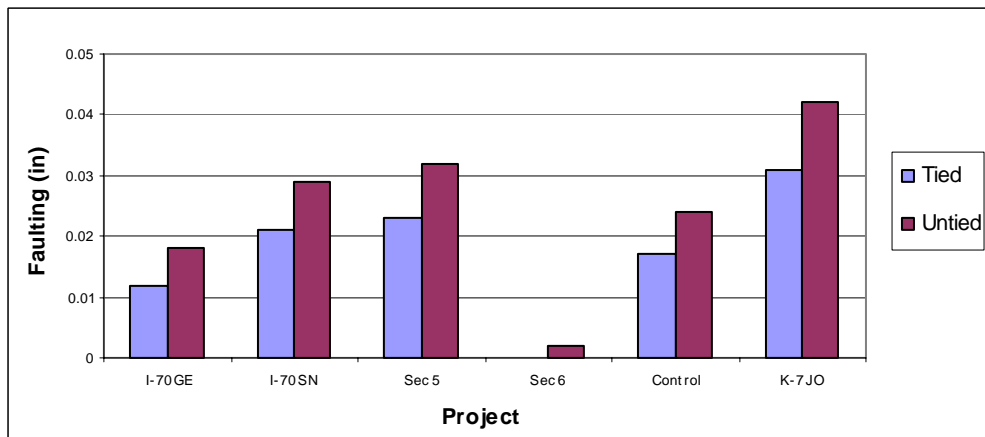
Table 4.6 Comparison of Predicted Responses Corresponding to Tied and Untied Shoulders

Project	IRI (in/mi)		Faulting (in)		% Slabs Cracked	
	Tied	Untied	Tied	Untied	Tied	Untied
I-70 GE	78	81	0.012	0.018	0	0
I-70 SN	120	128	0.021	0.029	0.8	5.6
Sec 5	145	149	0.023	0.032	0	0
Sec 6	109	110	0	0.002	0	0
Control	115	118	0.017	0.024	0	0
K-7 JO	110	122	0.031	0.042	0.6	7.9

(a) IRI



(b) Faulting



(c) % Slabs Cracked

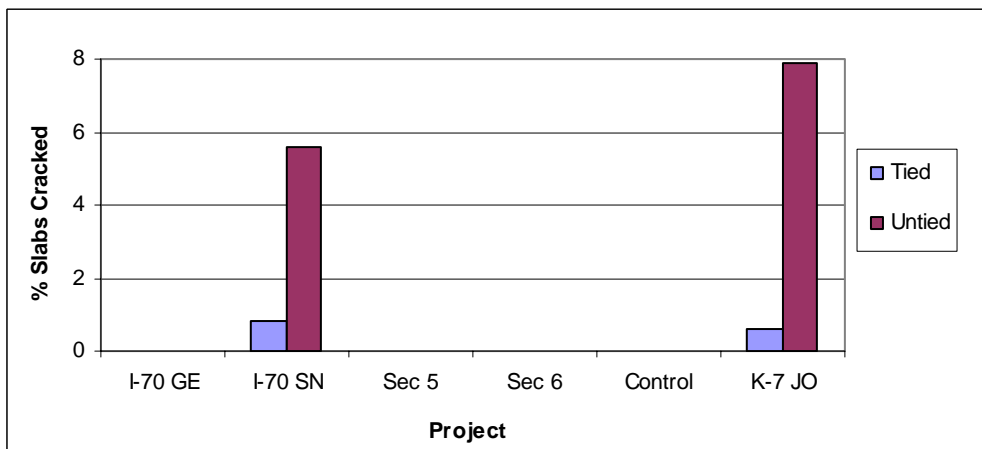


Figure 4.15 Predicted JPCP distresses for different shoulder type

Figure 4.15(b) illustrates the effect of untied shoulder on predicted faulting for the JPCP projects in this study. Effect was significant for all projects. When the shoulder was untied, the SPS-2 Section 6 also showed some faulting. However, with tied shoulder this project did not show any faulting. MEPDG-predicted faulting increased from 0.03 in. to 0.04 in when the shoulder was untied for the K-7 Johnson County project. Similar effect was also observed for all other projects.

The effect of tied shoulder was very pronounced on slab cracking as shown in Figure 4.15(c). For untied shoulder, percent slabs cracked increased from 0.8% to 5.6% and from 0.6% to 8% for the Shawnee and Johnson County projects, respectively.

Widen Lane

In this study, MEPDG-predicted IRI's for all sections were compared at two different lane widths- 12 and 14 ft. Table 4.7 tabulates and Figure 4.16 illustrates the results. In all projects, widened lane resulted in lower IRI as shown in Figure 4.16(a). On the I-70 Shawnee County project, when the lane width increased from 12 ft to 14 ft, the predicted IRI decreased from 120 in/mile to 109 in/mile. For the SPS-2 Section 5 and Section 6, decrease was almost similar (about 11 in/mile). The lowest decrease, about 7 in/mile, was observed for the I-70 Geary county project and the SPS-2 Control section. The effect is most pronounced for the K-7 Johnson County project. When the lane width was increased from 12 ft to 14 ft, the predicted IRI decreased from 111 in/mile to 94 in/mile. This project has the lowest PCC slab thickness (9 in.).

Widened lane also has significant effect on faulting. Figure 4.16(b) illustrates the predicted faulting on all sections corresponding to 12 ft lane width. When the lane width was increased to 14 ft, no faulting was observed for almost all sections except the

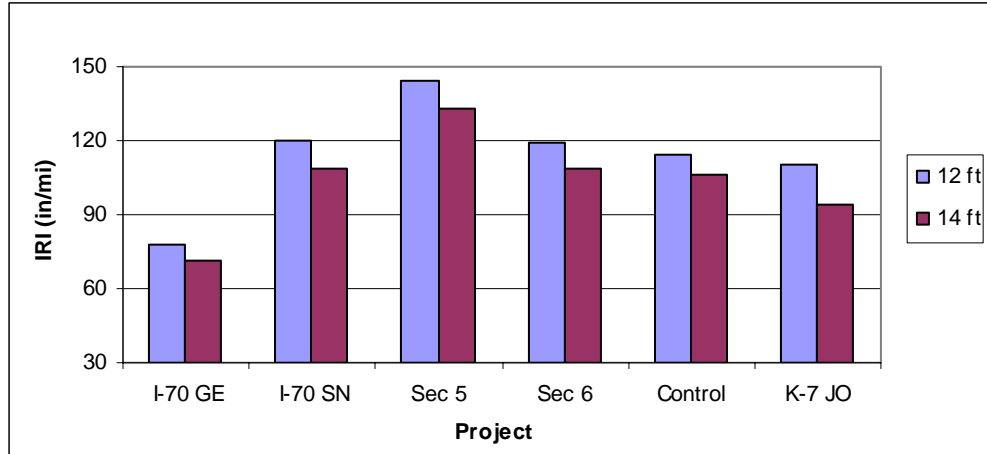
SPS-2 Section 5 and Control Sections. Insignificant amount of faulting was observed for those projects with 14 ft lane width too. The K-7 Johnson County project showed significant variation with the change in lane width. When the lane width increased from 12 ft to 14 ft, the predicted faulting decreased from 0.03 in. to none. Similar trend was observed for all other sections.

Table 4.7 Comparison of Predicted Response Corresponding to Varying Lane Width

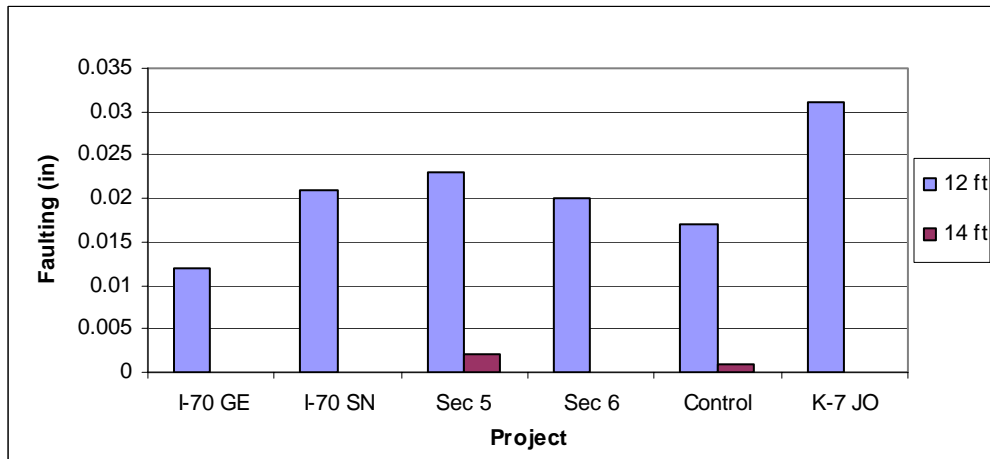
Project	IRI (in/mi)		Faulting (in)		% Slabs Cracked	
	12 ft	14 ft	12 ft	14 ft	12 ft	14 ft
I-70 GE	78	71	0.012	0	0	0
I-70 SN	120	109	0.021	0	0.8	0.5
Sec 5	145	133	0.023	0.002	0	0
Sec 6	120	109	0.02	0	0	0
Control	115	106	0.017	0.001	0	0
K-7 JO	110	94	0.031	0	0.6	0.2

Figure 4.16(c) shows the effect of lane width on predicted percent slabs cracked for the JPCP projects in this study. Only two projects, I-70 Shawnee County and K-7 Johnson County, appeared to be affected by this input though the predicted cracking values were negligible. When widened lane was used, percent slabs cracked decreased by about 0.3% to 0.4% for the Shawnee County and Johnson County projects, respectively. Widened lane appears to reduce cracking insignificantly for the projects with lower strength and thinner slabs.

(a) IRI



(b) Faulting



(c) % Slabs Cracked

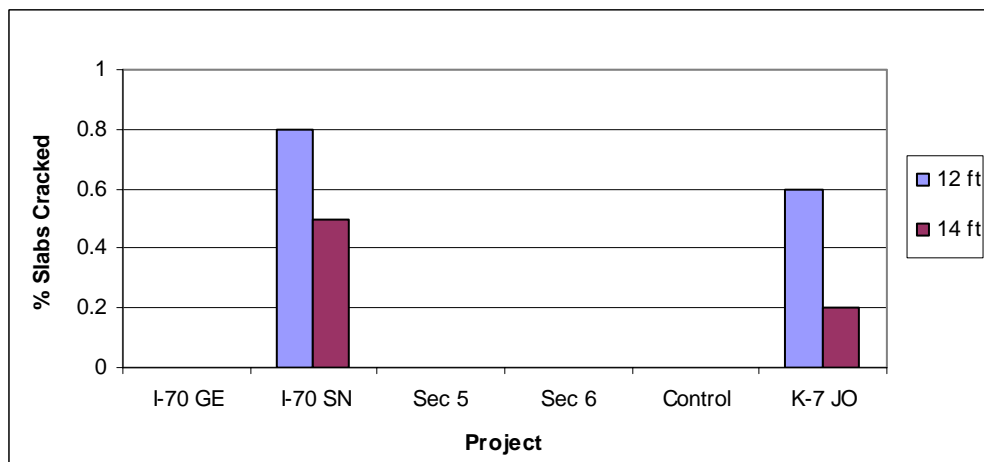
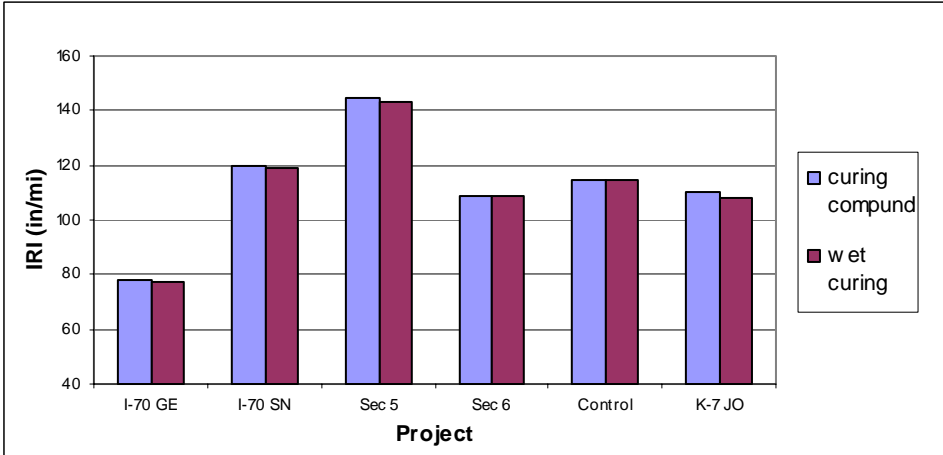
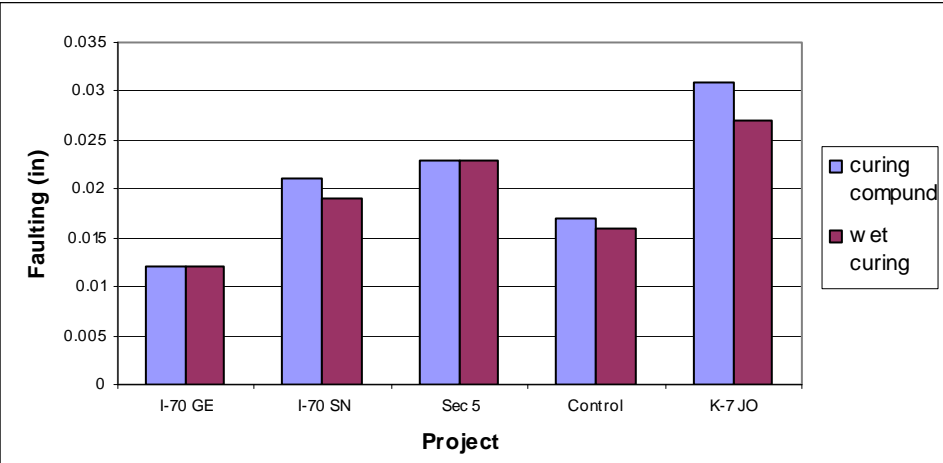


Figure 4.16 Predicted JPCP Distresses for Different Lane Widths

(a) IRI



(b) Faulting



(c) % Slabs Cracked

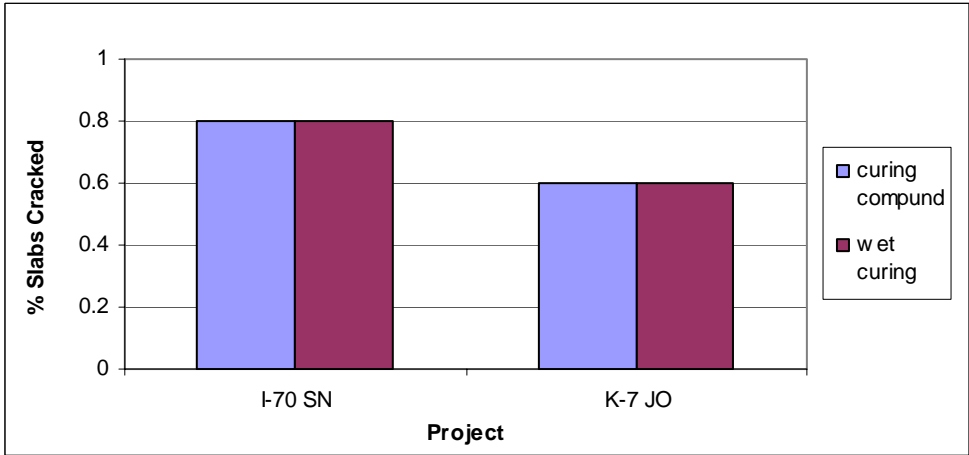


Figure 4.17 Predicted JPCP distresses for Curing type

Curing Method

Distresses were predicted using MEPDG for two different curing methods – sprayed curing compound and wet curing. No effect was observed for IRI, percent slabs cracked and faulting on most of the projects as shown in Figure 4.17. Only the K-7 Johnson County project showed slightly lower faulting with wet curing. Thus this factor did not appear to affect the MEPDG-predicted distresses on the study sections. This parameter was also found to be insensitive by Coree et al. (2005).

Base Type

Sensitivity analysis was done toward two types of base – stabilized and granular. Stabilized bases are asphalt-treated base (ATB), Portland cement-treated base (PCTB) and Bound drainable base (BDB). Dense graded aggregate base (DGAB), permeable base and semi-permeable base are under the granular base category.

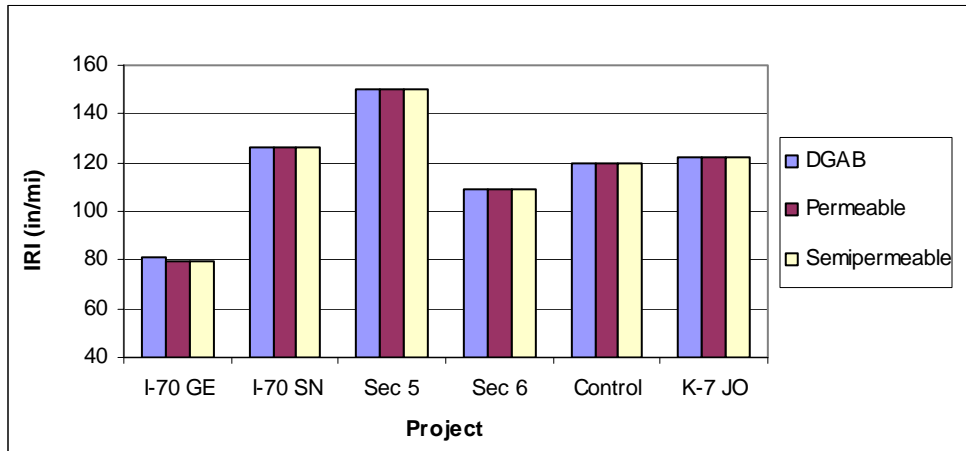
Asphalt treated bases (ATB) uses the same aggregates as in the granular bases, but mixed with an asphaltic binder. Typically two to three percent asphalt binder are added in Kansas. Granular base (DGAB) consists of untreated dense-graded aggregate, such as crushed stone. Unbound granular base properties such as, gradation and plasticity index are the required inputs in this category. BDB is similar to PCTB except for aggregate gradation and permeability requirements.

Granular Base

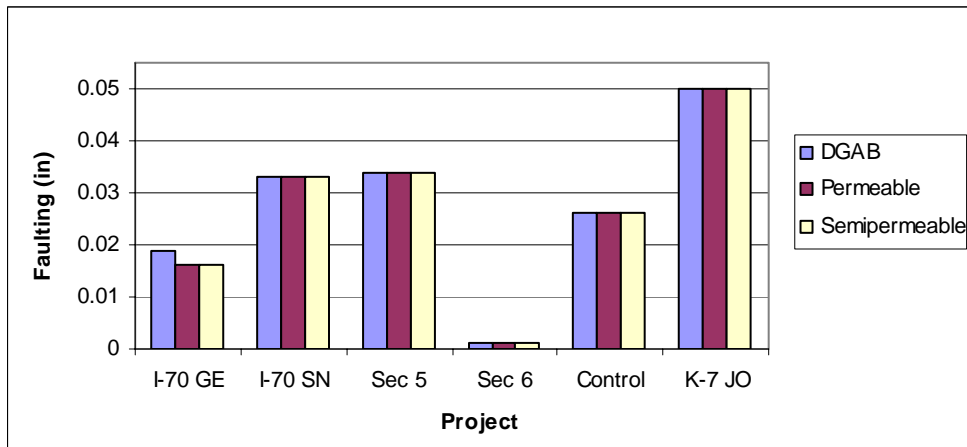
In this study, MEPDG-predicted IRI's for the sections were compared for two different granular base types- permeable and semi-permeable. Figure 4.18 (a) shows the predicted IRI values for granular bases. The predicted IRI remained unaffected by the

granular base type.

(a) IRI



(b) Faulting



(c) % Slabs Cracked

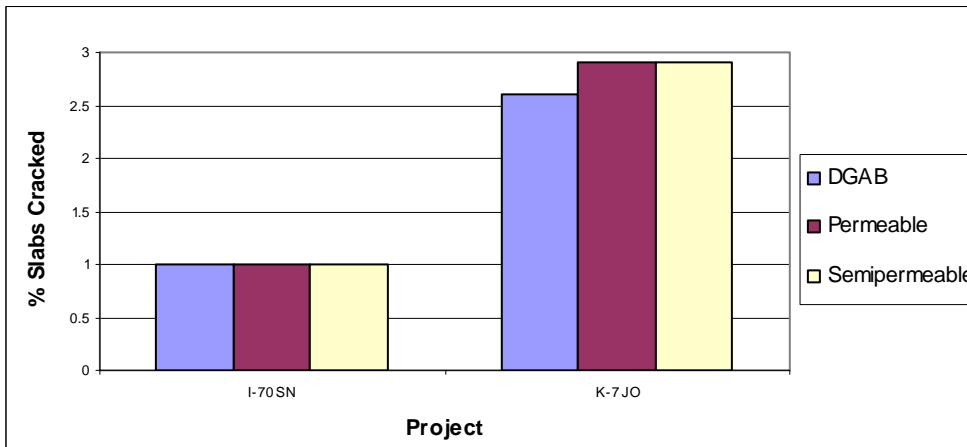


Figure 4.18 Predicted JPCP distresses for different granular bases

Figure 4.18 (b) illustrates the predicted faulting for all projects corresponding to different granular base type. Again, the predicted faulting is largely unaffected by granular base type. Cracking also remains somewhat unaffected by the granular base type as shown in Figure 4.18 (c).

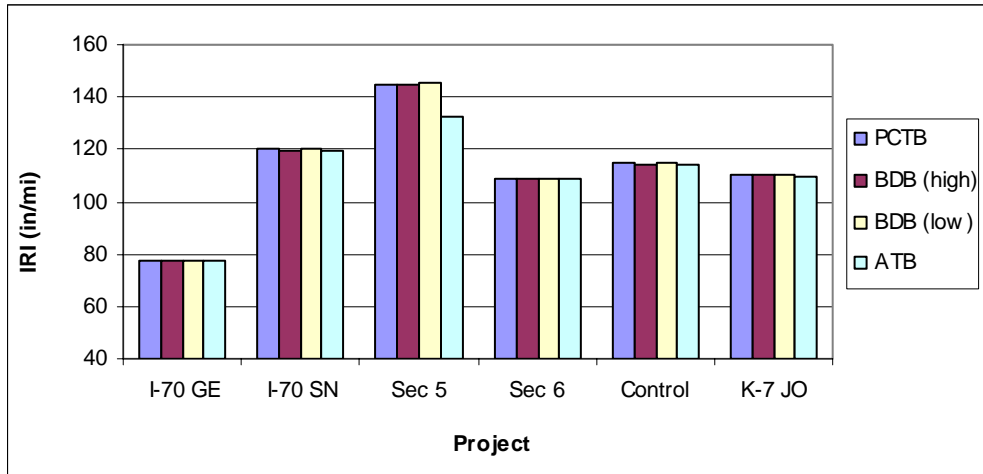
Stabilized Base

MEPDG-predicted IRI values for the sections were compared for three different stabilized base types- PCTB, BDB, and ATB. The BDB modulus was varied at two levels –low and high. Figure 4.19(a) shows the results. No significant variation was observed for all projects except SPS-2 Section 5 that has the highest 28-day modulus of rupture. The IRI decreased from 145 in/mile to 133 in/mile with ATB for this section.

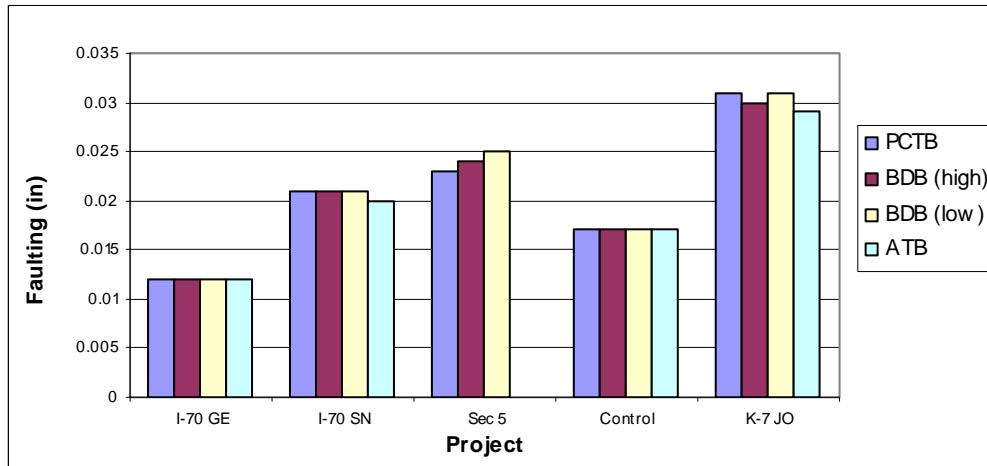
Figure 4.19(b) shows that the faulting on the SPS-2 Section 5 project was somewhat reduced by ATB. Reduced faulting with ATB was also observed for the K-7 Johnson County and I-70 Shawnee County projects. However, the predicted faulting values were negligible for all practical purposes.

MEPDG-predicted cracking was evaluated for all projects as shown in Figure 4.19(c). Negligible variation in cracking with respect to the treated base type was observed on the I-70 Shawnee County and the K-7 Johnson County projects. For K-7 Johnson County, ATB showed lower cracking compared to other bases, whereas completely reverse phenomenon was observed for the I-70 Shawnee County project. Also, high modulus BDB showed the lowest amount of cracking for the Shawnee County project.

(a) IRI



(b) Faulting



(c) % Slabs Cracked

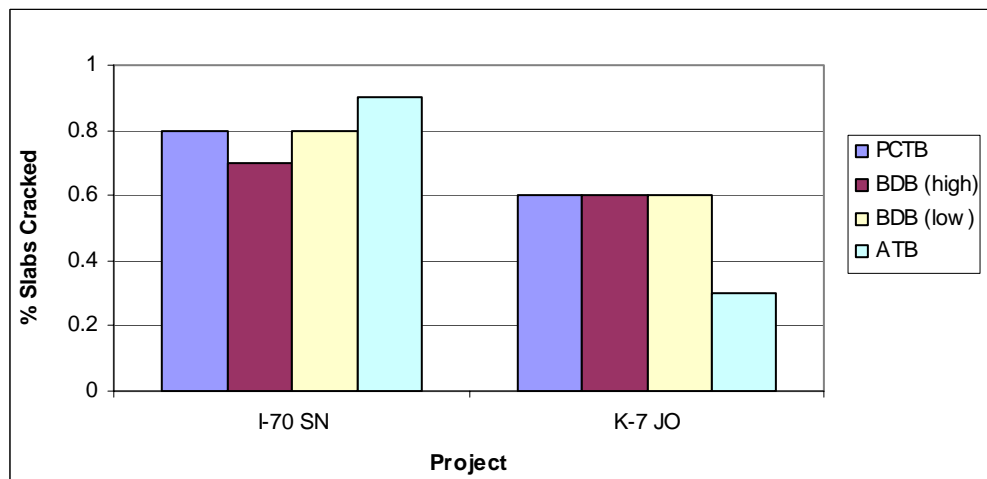


Figure 4.19 Predicted JPCP distresses for stabilized bases

4.2.4 Alternative Design

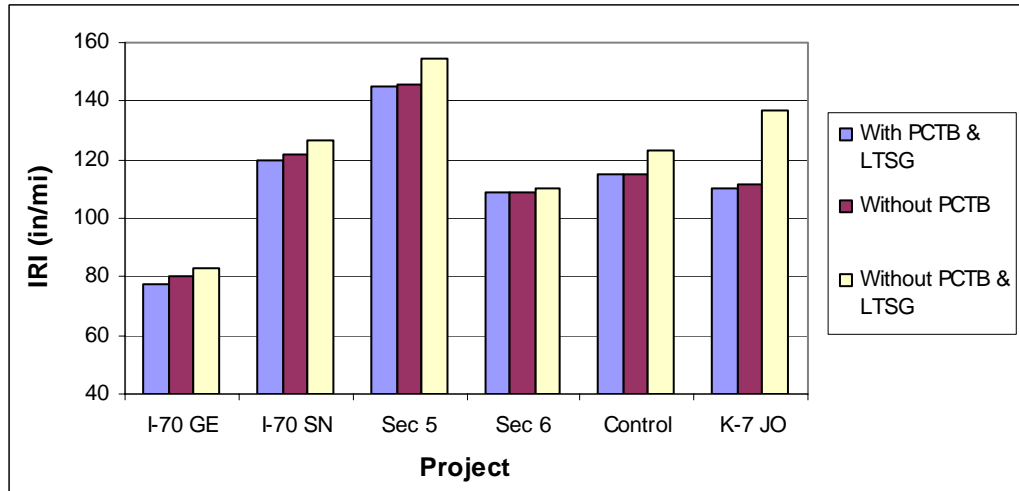
The 1993 AASHTO Design Guide was known to be fairly insensitive to the changes in the modulus of subgrade reaction of the foundation layer (AASHTO 1993). In this study, MEPDG sensitivity analysis was done for all KDOT and SPS-2 projects toward three alternate design strategies involving the JPCP foundation layer. First, the projects were analyzed with a Portland cement-treated base (PCTB) and a lime-treated subgrade (LTSG). Then the projects were analyzed without PCTB but with LTSG. Finally, the projects were assumed to be built directly on the compacted natural subgrade (no subgrade modification with lime). Typical JPCP distresses, IRI, faulting, and percent slabs cracked, were calculated and compared after 20 years. Table 4.8 tabulates the results.

Table 4.8 Comparison of Predicted Responses Corresponding to Different Design Strategy

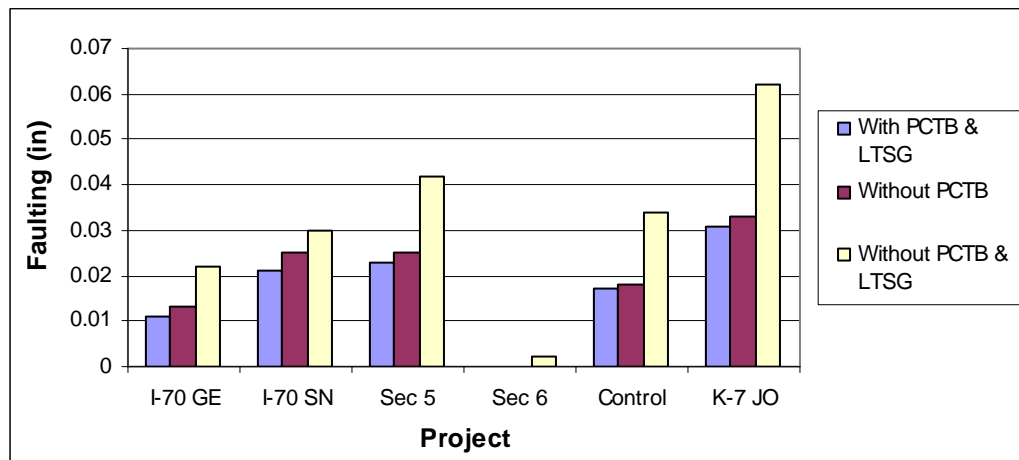
Project	IRI (in/mi)			Faulting (in)			% Slabs Cracked		
	With PCTB & LTSG	Without PCTB	Without PCTB & LTSG	With PCTB & LTSG	Without PCTB	Without PCTB & LTSG	With PCTB & LTSG	Without PCTB	Without PCTB & LTSG
I-70 GE	77	80	83	0.011	0.013	0.022	0	0	0
I-70 SN	120	122	127	0.021	0.025	0.03	0.8	0.8	3.2
Sec 5	145	146	155	0.023	0.025	0.042	0	0	0
Sec 6	109	109	110	0	0	0.002	0	0	0
Control	115	115	123	0.017	0.018	0.034	0	0	0
K-7 JO	110	111	137	0.031	0.033	0.062	0.6	0.7	13.5

The MEPDG-predicted IRI values for the sections were compared for different design alternatives. Figure 4.20(a) shows the results. In general, for pavements without

(a) IRI



(b) Faulting



(c) % Slabs Cracked

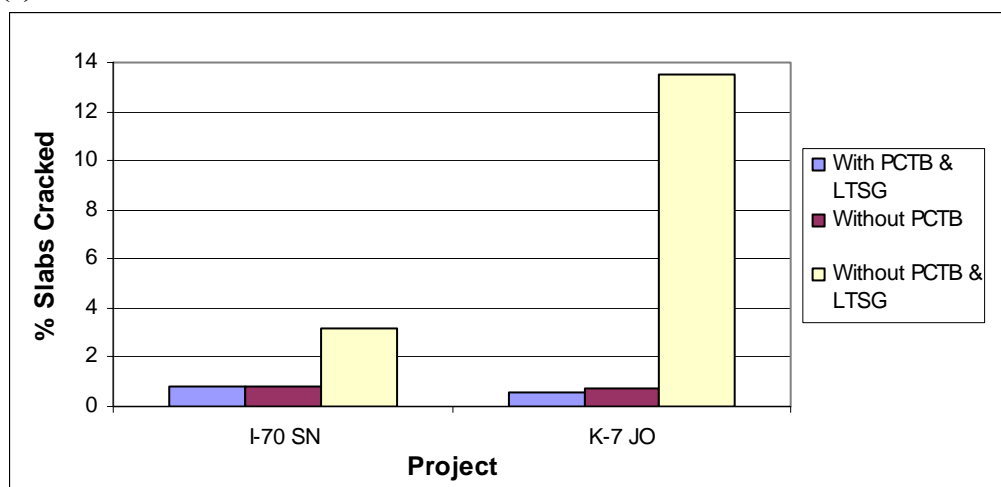


Figure 4.20 Predicted JPCP distresses for alternative designs

any treated base/subbase, the effect is not that pronounced on IRI. The projects without PCTB showed almost similar IRI compared to those with PCTB. However, IRI increased markedly for the projects built directly on the compacted subgrade. The effect is most pronounced for the K-7 Johnson County and SPS-2 Section 5 projects. On the K-7 Johnson County project, without any treated base and subgrade, predicted IRI would increase from 110 in/mile to 137 in/mile. It is to be noted that this project has the lowest PCC slab thickness (9 in.) among all projects. The effect is also significant for the SPS-2 Section 5. For the SPS-2 Section 5, without any treated base and subgrade, the predicted IRI increased from 145 in/mile to 155 in/mile. This section has the highest modulus of rupture among all projects studied. No effect on IRI was noticed for the SPS-2 Section 6 which has a widened lane.

Figure 4.20(b) shows that the faulting values on the K-7 Johnson County and SPS-2 Section 5 projects are markedly affected by the changes in design. Without PCTB and LTSG, faulting increased from 0.03 in to 0.06 in on the K-7 Johnson County project. This increasing trend is similar for all other projects. Although SPS-2 Section 6 with a widened lane and tied PCC shoulder did not have any faulting before, without PCTB and LTSG, faulting started to appear on this section. However, the amount is insignificant.

Figure 4.20(c) shows that only two projects, I-70 Shawnee County and K-7 Johnson County, had some cracking. Cracking increases dramatically on the K-7 Johnson County project when the projects were built without PCTB and LTSG. When the K-7 Johnson County project was designed to be built without any treated base and treated subgrade, the percent slabs cracked increased from 0.6% to 13.5%. In fact, the K-7 Johnson County project failed in reliability level for that design aspect.

It appears NCHRP MEPDG correctly predicts that the treated base and treated subgrade have far reaching effect on the performance of JPCP. Clayey and silty subgrades are subjected to erosion during “pumping.” Therefore, as shown in this analysis, JPCP’s should not be built in Kansas directly on compacted natural subgrade consisting of clayey and silty soils.

CHAPTER 5

EFFECT OF JPCP PERFORMANCE ON PCC QC/QA SPECIFICATIONS

5.1 Introduction

Over the last decade, there has been a growing interest in the Portland Cement Concrete pavement area for better quality control/quality assurance (QC/QA) specifications. The Federal Highway Administration (FHWA) sponsored research in the early nineties that resulted in prototype performance-related specifications (PRS) for jointed plain concrete pavements (Darter et al. 1993; Okamoto et al. 1993). Those specifications were refined in a more recent project (FHWA 1999). PRS are similar to the quality assurance specifications; however, the measured acceptance quality characteristics (or AQC's, which include concrete strength, slab thickness, initial smoothness and others) are directly related to pavement performance through mathematical relationships. Performance is defined by key distress types and smoothness, and is directly related to the future maintenance, rehabilitation, and user costs of the highway (FHWA 1999). This link between measured AQC's and future life-cycle costs (LCC's) provides the ability to develop rational and fair contractor pay adjustments that depend on the as-constructed quality delivered for the project.

The Kansas Department of Transportation (KDOT) has implemented QC/QA specifications for JPCP in the late nineties. KDOT intends to migrate towards performance-related specifications in the near future. Current KDOT PCC QC/QA specifications have been developed based largely on the performance of the PCC pavements designed using 1986 and 1993 AASHTO design guides. This chapter presents

the analysis results to evaluate the effect of predicted performance of typical Kansas JPCP pavements using NCHRP MEPDG on the current JPCP QC/QA specifications of KDOT and to identify the levels of PCC strength that will be acceptable for Kansas JPCP. Statistical analysis results to evaluate the effect of different levels of the PCC strength and slab thickness on predicted JPCP performance have also been presented.

5.2 KDOT QC/QA Specification for PCC

5.2.1 Overview

Current KDOT PCC pavement QC/QA specification is divided into the following parts: (1) Contractor quality control requirements; (2) Materials; (3) Construction requirements; and (4) Measurement and payment (KDOT 2005). For mainline pavement, pay adjustments are made for both thickness and compressive strength based on the measurements/tests on the cores. For acceleration lane pay adjustments are made only for thickness (unless otherwise specified).

Lots and Sublots

For mainline and other pavement subject to coring for pay adjustments for both thickness and strength, a lot is defined as the surface area of the mainline lane placed in a single day. Normally, a lot representing a day's production is divided into five sublots of approximately equal surface area. For high daily production rates, rates exceeding 6,000 square yards per day, the contractor may choose to divide the day's production into two approximately equal lots consisting of five sublots each. Normally one core is taken per subplot.

Pay Adjustment

A single combined pay adjustment for thickness and compressive strength is determined on a lot-by-lot basis based on the contractor quality control test results on all quality control (QC) samples from a lot provided the statistical check against the KDOT results is favorable. The combined pay factor (**P**) (positive or negative) is determined and used to compute the pay adjustment by multiplying **P** times the number of square yards included in the lot times the bid price per square yard. The combined pay factor (**P**) for a lot is calculated as:

$$P = \left(\frac{(PWL_T + PWL_S) * 0.60}{200} \right) - 0.54 \quad (5.1)$$

Where:

PWL_T = Thickness percent within limits value which is a function of thickness quality index (Q_T);

PWL_S = Strength percent within limits value which is a function of strength quality index (Q_S).

Q_T is calculated for a lot using Equation (5.2):

$$Q_T = \frac{\bar{X} - LSL}{S} \quad (5.2)$$

Where:

\bar{X} is the average measured core length of all QC samples representing a lot ;

LSL is the lower specification limit for thickness and is defined as 0.2 inch less than plan thickness; and

S is the sample standard deviation of the measured core lengths.

Q_s is calculated for a lot using Equation (5.3):

$$Q_s = \frac{\bar{X} - LSL}{S} \quad (5.3)$$

Where:

\bar{X} is the average measured compressive strength of all QC samples representing a lot;

LSL is the lower specification limit for compressive strength and is defined as 3,900 psi; and

S is the sample standard deviation of the measured compressive strengths.

5.3 KDOT PCCP PWL Pay Factor Computation Inputs

Calculation of thickness quality index using Equation (5.2) requires the average core length of all quality control cores, lower specification limit for thickness, and sample standard deviation of all core lengths. For the purpose of this study, the average core length was taken as the target plan thickness (8, 8.5 or 9 inches). The thickness standard deviation was selected based on the recommendation of Kher & Darter (1973).

For strength quality index calculation using Equation (5.3), the average measured compressive strength was taken as the target strength (3000, 5000 or 8000 psi). The target strength values represent the low, average and high 28-day PCC compressive available in MEPDG. For computing the standard deviation of compressive strength, a coefficient of variation of 10% was assumed following Kher & Darter (1973).

5.4 MEPDG-Predicted Performance and Corresponding PWL Results

Key rigid pavement distresses predicted for JPCP from the MEPDG analysis are IRI, faulting, and percent slabs cracked for a 20-year design period for three projects studied earlier- SPS-2 (KDOT Control), I-70 (Shawnee County), and K-7 (Johnson County). The projects were chosen based on the PCC slab thickness (Low, 9 in., K-7; medium, 10.5 in., I-70; and high, 12 in., KDOT Control). Table 5.1 shows the MEPDG-predicted distress quantities and the computed current KDOT PWL factors corresponding to different combinations of strength and thickness.

The results show that at the combination of the lowest levels of strength and thickness (3000 psi and 8 inches), the design failed due to lack of roughness reliability and/or for excessive percent slabs cracked for all three projects. Increasing the thickness to 8.5 inch caused the design to pass all criteria but the pay factor remained unchanged. This was true at any strength level. Increasing the strength to 5,000 psi caused the design to pass, and the pay factor increased. However, increasing the strength to 8,000 psi caused insignificant changes in predicted distresses, and the pay factor too remained unchanged. It appears that current KDOT PWL specifications for PCC pavement construction are more sensitive to the PCC strength than to the PCC slab thickness. Also, for each project, there would be an optimal combination of strength and thickness that would be the most economical design. This desired strength level for a given thickness can be found from the statistical analysis of a designed factorial involving strength and thickness.

Table 5.1 Predicted Distresses and PWL for the Projects

Strength	Factors	Shawnee County K-3344-01			SPS-2 KDOT Control Section SHRP 20-0259			Johnson County K-3382-01		
		8 in	8.5 in	9 in	8 in	8.5 in	9 in	8 in	8.5 in	9 in
3000 psi	Pay Factor (P)	-0.32	-0.32	-0.315	-0.32	-0.32	-0.315	-0.32	-0.32	-0.315
	IRI (in/mi)	130.5*	120.1	117.3	123.4	114.7	112.2	123.1*	110.7	108.3
	Faulting (in)	0.012	0.013	0.013	0.008	0.007	0.007	0.023	0.025	0.026
	% Slabs Cracked	16.8*	4.3	1.4	13.9*	3.9	1.4	20.1*	4.3	1.0
5000 psi	Pay Factor (P)	-0.02	-0.018	-0.015	-0.02	-0.018	-0.015	-0.02	-0.018	-0.015
	IRI (in/mi)	118.6	117.6	116.8	113.8	112.7	111.9	104.6	106.9	106.2
	Faulting (in)	0.015	0.015	0.014	0.01	0.009	0.009	0.024	0.024	0.024
	% Slabs Cracked	0.5	0.1	0	0.5	0.1	0	0.7	0.1	0
8000 psi	Pay Factor (P)	-0.02	-0.018	-0.015	-0.02	-0.018	-0.015	-0.02	-0.018	-0.015
	IRI (in/mi)	119.3	118.2	117.2	114.5	113.5	112.5	106.4	105.5	104.4
	Faulting (in)	0.017	0.016	0.015	0.013	0.011	0.01	0.023	0.022	0.02
	% Slabs Cracked	0	0	0	0	0	0	0	0	0

* Failed at 90% reliability level.

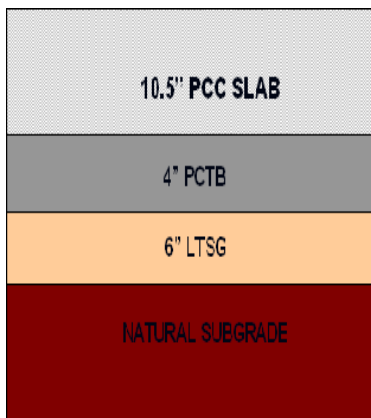
5.5 Statistical Analysis

As shown earlier, an optimum combination of strength and thickness exists for a JPCP project. It has also been shown that the truck traffic also needs to be considered since it has an overwhelming effect on the JPCP distresses predicted by the MEPDG analysis. In order to study the effect of these three factors (strength, thickness, and traffic) on the predicted JPCP distresses, a full factorial was designed. The projects chosen were the same as studied before - SPS-2 (KDOT Control), I-70 (Shawnee County), and K-7 (Johnson County).

Three levels of 28-day PCC compressive strength (3,000, 5,000, and 8,000 psi), nine levels of PCC slab thickness (8.0 to 12 in., at 0.5 inch intervals), and three levels of daily truck traffic (AADTT of 1,000, 5,000, and 10,000) were selected.

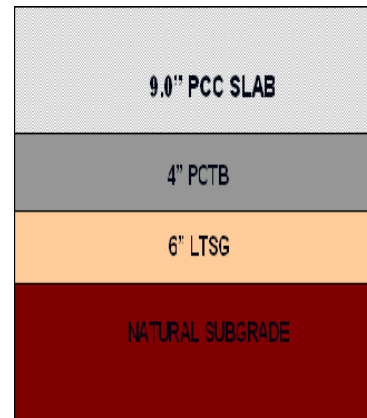
Figure 5.1 shows the cross section for each project selected. MEPDG JPCP analysis was done for each of the $3 * 9 * 3 = 81$ pavement sections for each project

(a) I-70 Shawnee County



t = 8 ~ 12 inch
fc' = 3000~8000 psi
AADTT = 1000~10,000

(b) K-7 Johnson County



(c) SPS-2 Control Section



t = 8 ~ 12 inch
fc' = 3000~8000 psi
AADTT = 1000~10,000

Figure 5.1 Cross section of the pavements studied

selected and IRI, faulting, and percent slabs cracked were calculated. All input parameters are shown in Tables 3.1 and 3.16.

Analysis of Variance (ANOVA) was used to describe the variation in predicted IRI, faulting, and percent slabs cracked for each project with the following factors:

Source of Variation	Definition	Type of Effect
S	Strength of PCC Slab	Fixed
T	Thickness of PCC Slab	Fixed
TR	Average Daily Truck Traffic (AADT)	Fixed

The following model was proposed:

$$\text{Distress}_{ijk} = S_i + T_j + TR_k + ST_{ij} + STR_{ik} + TTR_{jk} + \epsilon_{ijk} \quad (5.4)$$

$$i = 1, \dots, 3$$

$$j = 1, \dots, 9$$

$$k = 1, \dots, 3$$

where:

Distress_{ijk} = the predicted mean distress (IRI or faulting or percent slabs cracked) calculated at the i th level of Strength, the j th level of Thickness and at the k th level of Traffic = overall mean;

S_i = the effect of the i th level of (fixed) treatment Strength;

T_j = the effect of the j th level of (fixed) treatment Thickness;

TR_k = the effect of the k th level of (fixed) treatment Traffic;

ST_{ij} = the interaction effect between the i th level of Strength and the j th level of Thickness;

STR_{ik} = the interaction effect between the i th level of Strength and the j th level of Traffic;

TTR_{jk} = the interaction effect between the j th level of Thickness and the k th level of Traffic;

ε_{ijk} = the (random) error. The $\varepsilon(ijk)$ s are assumed to be normally and independently distributed with mean zero and variance Φ^2 .

It is important to note that in the model shown in Equation 5.4, the three way interaction was included. This is necessary because of absence of any replication. It was assumed that the STTR interaction is negligible, and hence MS_{STTR} will serve as MSE (Mean Square Error). Table 5.2 shows the ANOVA results for this factorial for all projects. From the ANOVA table, it is evident that almost all main factors of strength, thickness and traffic, and two factor interactions were significant at 5% and 10% level of significance. Only for predicted percent slabs cracked, interactions between thickness and truck traffic are insignificant for all projects at 5% level of significance. Strength-traffic interaction is also insignificant for predicted IRI on the Johnson county project. It appears that the interaction among all three factors, which was used as the error term, might be significant. Thus, the model described in Equation (5.4) may not be fully adequate to capture all the variation due to the factors studied and their interactions. It should be noted that in this analysis, replication of predicted distresses is not possible due to fixed nature of the inputs.

Statistical software SAS (SAS 1999) was used for the analysis and the Least-squares means (LS-means) were computed for each effect to determine the pair-wise comparison. The LSMEANS performs multiple comparisons on the interactions as well as on the main effects (Milliken and Johnson 1984).

Table 5.2 Analysis of Variance for the Effect of Strength, Thickness and Traffic

(a) Shawnee County, K-3344-01

Source of Variation	IRI (in/mi)				Faulting (in)				% Slabs Cracked			
	SS	DF	MS	P-value	SS	DF	MS	P-value	SS	DF	MS	P-value
Strength	1826.3	2	913.1	<0.0001	0.00038	2	0.00019	<0.0001	4081.3	2	2040.7	<0.0001
Thickness	9779.2	8	1222.4	<0.0001	0.00505	8	0.00063	<0.0001	5237.8	8	654.7	<0.0001
Traffic	29716	2	14858	<0.0001	0.07529	2	0.03764	<0.0001	1193.1	2	596.5	0.0024
S * TR	764.6	4	191.1	0.005	0.00015	4	0.00037	0.0005	1692.8	4	423.2	0.0024
S * T	3577.6	16	223.6	<0.0001	0.00056	16	0.00003	<0.0001	7293.1	16	455.8	<0.0001
TR * T	3111.4	16	194.5	0.0001	0.00231	16	0.00144	<0.0001	1934.0	16	120.9	0.165

(b) KDOT Control Section

Source of Variation	IRI (in/mi)				Faulting (in)				% Slabs Cracked			
	SS	DF	MS	P-value	SS	DF	MS	P-value	SS	DF	MS	P-value
Strength	1489.8	2	744.9	<0.0001	0.000701	2	0.00035	<0.0001	39023	2	1951.5	<0.0001
Thickness	6565.6	8	820.7	<0.0001	0.00151	8	0.00018	<0.0001	4685.1	8	585.6	<0.0001
Traffic	17492.5	2	8746	<0.0001	0.03934	2	0.01967	<0.0001	1212.2	2	606.1	0.0017
S * TR	708.3	4	177.1	0.0063	0.000241	4	0.00006	<0.0001	1744.7	4	436.2	0.0015
S * T	3285.8	16	205.4	<0.0001	0.000393	16	0.00002	<0.0001	6519.7	16	407.2	<0.0001
TR * T	2046.9	16	127.9	0.0028	0.000452	16	0.00002	<0.0001	1845.2	16	115.3	0.1626

Table 5.2 Analysis of Variance for the Effect of Strength, Thickness and Traffic (Continued)

(c) Johnson County, K-3382-01

Source of Variation	IRI (in/mi)				Faulting (in)				% Slabs Cracked			
	SS	DF	MS	P-value	SS	DF	MS	P-value	SS	DF	MS	P-value
Strength	1972.6	2	986.3	<0.0001	0.000036	2	0.000018	0.0506	2997.5	2	1498.8	<0.0001
Thickness	12187.3	8	1523.4	<0.0001	0.0185	8	0.0023	<0.0001	5494.6	8	686.8	<0.0001
Traffic	66923.4	2	33461.7	<0.0001	0.2019	2	0.101	<0.0001	804.8	2	402.4	0.0078
S * TR	222.6	4	55.6	0.2567	0.00059	4	0.00015	<0.0001	1061.1	4	265.3	0.0133
S * T	3276.1	16	204.8	<0.0001	0.00084	16	0.000053	<0.0001	7258.1	16	453.6	<0.0001
TR * T	8622.5	16	538.9	<0.0001	0.0233	16	0.00146	<0.0001	1806.8	16	112.9	0.1293

5.6 Effect of Thickness and Strength on Predicted Distresses

SPS-2, KDOT Control

Table 5.3 shows the results of the PCC slab thickness and strength interactions for the SPS-2, KDOT control section on I-70. The response variable is the predicted IRI after 20 years. All conclusions were made at 5% level of significance. According to the ANOVA results, the data are marginally normal with respect to the normality test. In addition, the diagnostic plot showed evidence of normality as shown in Appendix A. Thus, Bonferroni adjustment was also incorporated for the multiple comparison method and a conservative pair-wise comparison was also performed.

Table 5.3 Effect of Interaction of Thickness (T) and Strength (S) on Predicted IRI for SPS-2 Control Section

SxT	S1	S1	S1	S1	S1	S1	S1	S1	S1	S1	S2	S2	S2	S2	S2	S2	S2	S2	S2	S3	S3	S3	S3	S3	S3	S3	S3	S3	S3	S3	S3	S3	S3	S3			
	T1	T2	T3	T4	T5	T6	T7	T8	T9	T1	T2	T3	T4	T5	T6	T7	T8	T9	T1	T2	T3	T4	T5	T6	T7	T8	T9										
S1xT1		*	*	*	*	*	*	*	*	*	*	*	*	*	*	*	*	*	*	*	*	*	*	*	*	*	*	*	*	*	*	*	*	*	*		
S1xT2	*		*	*	*	*	*	*	*	*	*	*	*	*	*	*	*	*	*	*	*	*	*	*	*	*	*	*	*	*	*	*	*	*	*		
S1xT3	*	*			*	*	*	*	*		*	*	*	*	*	*	*	*	*			*	*	*	*	*	*	*	*	*	*	*	*	*	*		
S1xT4	*	*						*										*																*			
S1xT5	*	*	*							*																											
S1xT6	*	*	*							*																											
S1xT7	*	*	*							*											*																
S1xT8	*	*	*							*											*																
S1xT9	*	*	*	*						*											*	*															
S2xT1	*	*			*	*	*	*	*				*	*	*	*	*	*	*					*	*	*	*	*				*	*	*	*	*	
S2xT2	*	*	*							*																											
S2xT3	*	*	*																																		
S2xT4	*	*	*							*																											
S2xT5	*	*	*							*																											
S2xT6	*	*	*							*																											
S2xT7	*	*	*							*											*																
S2xT8	*	*	*							*											*																
S2xT9	*	*	*	*						*											*	*															
S3xT1	*	*					*	*	*							*	*	*	*							*	*	*			*	*	*	*	*	*	
S3xT2	*	*						*																												*	
S3xT3	*	*	*																																		
S3xT4	*	*	*																																		
S3xT5	*	*	*							*																											
S3xT6	*	*	*							*																											
S3xT7	*	*	*							*																											
S3xT8	*	*	*							*											*																
S3xT9	*	*	*							*											*	*															

* significant at 5% level of significance

The results show that within 3,000-psi strength level, for PCC slab thickness equal to or greater than 9.5 in., there are no significant differences in mean predicted IRI values. For 5,000-psi strength level, difference in mean predicted IRI becomes insignificant for thickness equal to or greater than 8.5 in. Within 8,000-psi strength level, IRI is almost insignificant at all thickness levels studied (8.5 inch to 12.0 inch), although significant difference was observed for 8.5 inch than other thickness levels. When the 3000-psi strength level is compared with the 5,000-strength level, IRI becomes insignificant at or beyond a PCC slab thickness of 9.5 in. Also, when the 5000-psi strength level is compared with the 8,000-strength level, IRI becomes insignificant at or beyond a PCC slab thickness of 8.5 in.

For faulting, at the 3,000-psi strength level, for PCC slab thickness up to 10.0 in., there are no significant differences in mean predicted values. The mean predicted faulting values after that become significant. Within 5000- and 8000-psi strength levels, faulting is significant at all levels. However, it is to be noted that the predicted faulting at all thickness and strength combination levels are negligible for all practical purposes.

For percent slabs cracked, at the 3,000-psi strength level, for PCC slab thickness up to 9.5 in., there are no significant differences in mean predicted values. Within 5000- and 8000-psi strength levels, cracking is not significant at any thickness level. Thus, strength has a very significant effect on predicted cracking by the NCHRP MEPDG. If the 3000-psi strength level is compared with the 5,000-strength level, cracking becomes insignificant at or beyond the PCC slab thickness of 9.5 in. When the 5000-psi strength level is compared with the 8,000-psi strength level, predicted cracking becomes insignificant at any level of thickness.

Considering all results for the SPS-2 Control Section, the optimum combination of thickness and strength appears to be 3,000 psi and 9.5 inch or 5000 psi and 8.5 inch. Any thickness or PCC strength beyond these levels would be conservative according to the NCHRP MEPDG.

I-70, Shawnee County

Table 5.4 shows the results of the PCC slab thickness and PCC strength interactions for the I-70 Shawnee County project. The response variable is the predicted IRI after 20 years. All conclusions were made at 5% level of significance.

The results show that within the 3,000-psi strength level, for the PCC slab thickness equal to or greater than 10 in., there are no significant differences in mean predicted IRI values. For the 5,000-psi strength level, difference in mean predicted IRI's becomes insignificant for thickness equal to or greater than 9.5 in. Within the 8,000-psi strength level, IRI is insignificant for a slab thickness level equal to or greater than 9.5. Although this is an anomaly, it was observed on this project as shown in Figure 5.2. At all three levels of strength, mean predicted IRI's corresponding to 8 in., 8.5 in. and 9 in. have significant differences with those corresponding to 11 in., 11.5 in. and 12 in. However, there are no differences in mean predicted IRI within these cluster thickness levels.

When the 3000-psi strength level is compared with the 5,000-strength level, IRI becomes insignificant at or beyond a PCC slab thickness of 9.5 in. When the 5000-psi strength level is compared with the 8,000-strength level, IRI becomes insignificant at or beyond a PCC slab thickness of 9.5 in.

Table 5.4 Effect of Interaction of Thickness (T) and Strength (S) on Predicted IRI for I-70, Shawnee County

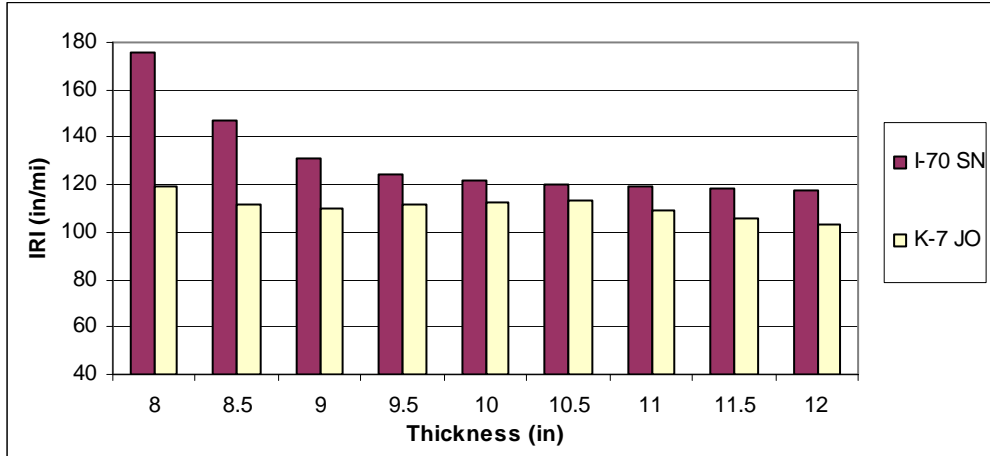
SxT	S1	S1	S1	S1	S1	S1	S1	S1	S1	S2	S2	S2	S2	S2	S2	S2	S2	S2	S3	S3	S3	S3	S3	S3	S3	S3	S3	S3
	x	x	x	x	x	x	x	x	x	x	x	x	x	x	x	x	x	x	x	x	x	x	x	x	x	x	x	x
SxT	T1	T2	T3	T4	T5	T6	T7	T8	T9	T1	T2	T3	T4	T5	T6	T7	T8	T9	T1	T2	T3	T4	T5	T6	T7	T8	T9	
S1xT1		*	*	*	*	*	*	*	*	*	*	*	*	*	*	*	*	*	*	*	*	*	*	*	*	*	*	*
S1xT2	*		*	*	*	*	*	*	*	*	*	*	*	*	*	*	*	*	*	*	*	*	*	*	*	*	*	*
S1xT3	*	*			*	*	*	*	*		*	*	*	*	*	*	*	*			*	*	*	*	*	*	*	*
S1xT4						*	*	*							*	*	*	*						*	*	*	*	
S1xT5	*	*	*							*																		
S1xT6	*	*	*	*						*	*	*								*	*	*						
S1xT7	*	*	*	*						*	*	*								*	*	*						
S1xT8	*	*	*	*						*	*									*	*							
S1xT9	*	*	*	*						*	*									*	*	*						
S2xT1	*	*			*	*	*	*	*				*	*	*	*	*	*					*	*	*	*	*	*
S2xT2	*	*	*												*	*	*	*						*	*	*	*	
S2xT3	*	*	*			*	*								*		*	*									*	
S2xT4	*	*	*							*																		
S2xT5	*	*	*							*																		
S2xT6	*	*	*	*						*	*									*	*	*						
S2xT7	*	*	*	*						*	*	*								*	*	*						
S2xT8	*	*	*	*						*	*									*	*	*						
S2xT9	*	*	*	*						*	*	*								*	*	*						
S3xT1	*	*				*	*	*	*						*	*	*	*						*	*	*	*	*
S3xT2	*	*				*	*	*	*						*	*	*	*						*	*	*	*	*
S3xT3	*	*	*			*	*		*						*	*	*	*						*	*	*	*	*
S3xT4	*	*	*																								*	
S3xT5	*	*	*								*																	
S3xT6	*	*	*	*						*	*									*	*	*						
S3xT7	*	*	*	*						*	*									*	*	*						
S3xT8	*	*	*	*						*	*									*	*	*						
S3xT9	*	*	*	*						*	*	*								*	*	*	*					

* significant at 5% level of significance

For faulting, at the 3,000-psi strength level, for PCC slab thickness at or less than 10 in., predicted faulting are insignificant. Beyond this thickness, there are significant differences in mean predicted faulting values. Within 5000 and 8000-psi strength levels, faulting is not significant until the thickness is 10 in. or higher. Again at these levels, mean predicted faulting at 8 in. thickness has no significant difference with those at 8.5, 9.0, 9.5 and 10 inch, but has significant differences with the mean predicted faulting at 10.5, 11.0, 11.5 and 12 in. This trend was also observed when comparing the 3000-psi versus 5000-psi, and the 5000-psi versus 8000-psi strength levels. However, it is to be noted that the predicted faulting at all thickness and strength combination levels is negligible for all practical purposes.

For percent slabs cracked, at the 3,000-psi strength level, for the PCC slab thickness equal to or greater than 9.5 in., there are no significant differences in mean predicted values. Within 5000- and 8000-psi strength levels, cracking is not significant at any thickness level. This reinforces the conclusion that strength has a very significant effect on predicted cracking by the NCHRP MEPDG. If the 3000-psi strength level is compared with the 5,000-strength level, cracking becomes insignificant at or beyond the PCC slab thickness of 9 in. When the 5000-psi strength level is compared with the 8,000-strength level, thickness does not affect cracking at all.

(a) IRI



(b) Faulting

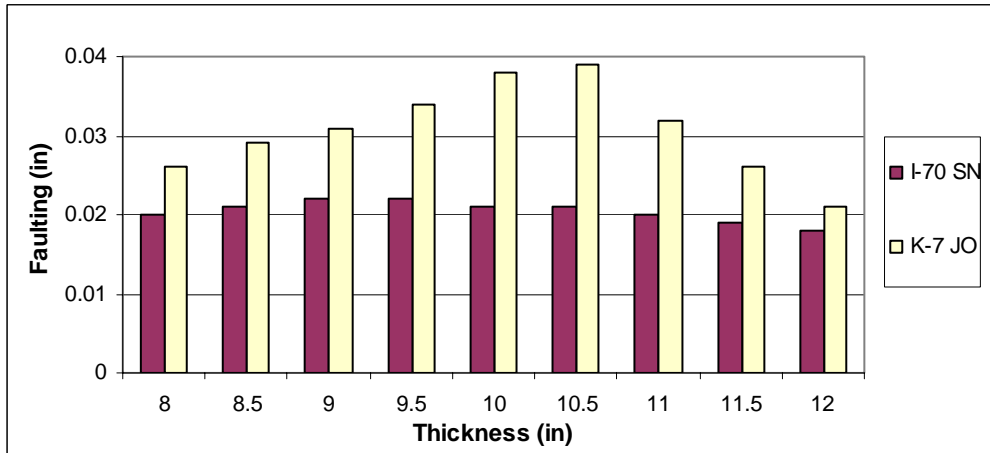


Figure 5.2 Variation of predicted distresses with thickness for I-70 Shawnee county and K-7 Johnson county projects

When all results are considered, it appears for the I-70 Shawnee County that, the optimum combination of thickness and strength for 3,000-psi strength is 10 inch or at 5000-psi strength is 9.5 inch. Any thickness or PCC strength beyond these levels would be conservative according to the NCHRP MEPDG.

K-7, Johnson County

Table 5.5 shows the results of the PCC slab thickness and PCC strength interactions for K-7, Johnson County. The response variable is the predicted IRI after 20 years. All conclusions were made at 5% level of significance.

The results at the 3,000-psi strength level for this project are quite fluctuating. The results indicate that mean predicted IRI's are similar at lower (8.0 and 8.5 in.) and higher (11.0, 11.5 and 12.0) thickness levels. This trend is also evident in Figure 5.2.

At 5000- and 8000-psi strength levels and at 10.5 in. or lower thickness levels, there are no significant differences in predicted IRI but for thickness equal to or greater than 11 in., significant differences exist. However, at 8000-psi strength level, predicted IRI at 8 in. thickness level is significantly different than other levels.

When the 3000-psi strength level is compared with the 5,000-strength level, mean predicted IRI's corresponding to a PCC slab thickness of 8 and 8.5 in. are significantly different from other thickness levels, but for thickness greater than 9 in., differences are not significant. At any thickness level greater than 11 in., the differences are significant. When the 5000-psi strength level is compared with the 8,000-strength level, differences in mean predicted IRI's are not significant at a PCC slab thickness of 10.5 in. or lower but become significant at or beyond a PCC slab thickness of 11 in.

Table 5.5 Effect of Interaction of Thickness (T) and Strength (S) on Predicted for K-7, Johnson County

SxT	S1	S1	S1	S1	S1	S1	S1	S1	S1	S2	S2	S2	S2	S2	S2	S2	S2	S2	S3	S3	S3	S3	S3	S3	S3	S3	S3
	x	x	x	x	x	x	x	x	x	x	x	x	x	x	x	x	x	x	x	x	x	x	x	x	x	x	x
SxT	T1	T2	T3	T4	T5	T6	T7	T8	T9	T1	T2	T3	T4	T5	T6	T7	T8	T9	T1	T2	T3	T4	T5	T6	T7	T8	T9
S1xT1		*	*	*	*	*	*	*	*	*	*	*	*	*	*	*	*	*	*	*	*	*	*	*	*	*	*
S1xT2			*	*	*	*	*	*	*	*	*	*	*	*	*	*	*	*	*	*	*	*	*	*	*	*	*
S1xT3	*	*					*	*	*			*					*	*	*			*			*	*	*
S1xT4	*	*					*		*							*	*	*							*	*	*
S1xT5	*	*					*	*	*							*	*	*							*	*	*
S1xT6	*	*					*	*	*							*	*	*							*	*	*
S1xT7	*	*	*	*	*	*		*		*	*	*	*	*	*		*		*	*	*	*	*	*	*		
S1xT8	*	*	*		*	*	*			*					*	*									*		
S1xT9	*	*	*	*	*	*				*	*	*	*	*	*				*	*	*	*	*	*	*		
S2xT1	*	*					*	*	*							*	*	*							*	*	*
S2xT2	*	*					*		*							*		*							*	*	*
S2xT3	*	*	*				*		*							*		*							*	*	*
S2xT4	*	*					*		*							*		*							*	*	*
S2xT5	*	*					*		*							*	*	*							*	*	*
S2xT6	*	*					*	*	*							*	*	*							*	*	*
S2xT7	*	*	*	*	*	*		*		*	*	*	*	*	*	*	*	*		*	*	*	*	*	*	*	
S2xT8	*	*	*	*	*	*	*			*				*	*	*			*	*				*	*		
S2xT9	*	*	*	*	*	*				*	*	*	*	*					*	*	*	*	*	*	*		
S3xT1	*	*					*		*						*	*	*	*	*	*	*	*	*	*			
S3xT2	*	*					*		*						*	*	*								*	*	*
S3xT3	*	*	*				*		*						*		*								*	*	*
S3xT4	*	*					*		*						*		*								*	*	*
S3xT5	*	*					*		*						*		*								*	*	*
S3xT6	*	*					*		*						*	*	*								*	*	*
S3xT7	*	*	*	*	*	*		*	*	*	*	*	*	*	*	*	*	*	*	*	*	*	*	*	*	*	
S3xT8	*	*	*	*	*	*				*	*	*	*	*	*	*	*	*	*	*	*	*	*	*	*	*	
S3xT9	*	*	*	*	*	*				*	*	*	*	*	*	*	*	*	*	*	*	*	*	*	*	*	

* significant at 5% level of significance

For faulting, at the 3,000-psi strength level, there are significant differences at all levels of thickness studied. For 5,000-psi strength level, there are insignificant differences in mean predicted faulting values corresponding to the thickness levels with 0.5 to 1.0 in. difference. For 5,000-psi strength level, there are insignificant differences in mean predicted faulting values corresponding to the thickness levels with 0.5 to 1.0 in. difference. For 8,000-psi strength level, there are insignificant differences in mean predicted faulting values corresponding to the thickness levels less than or equal to 11 in. For 3000-psi versus 5000-psi strength levels, mean predicted faulting are significant at all thickness levels. For 5000-psi versus 8000-psi strength level, no significant differences in mean predicted faulting was observed for thickness less than or equal to 10 in. However, it is to be noted that the predicted faulting at all thickness and strength combination levels are negligible for all practical purposes.

The NCHRP MEPDG suggests that with increasing slab thickness (in order to reduce slab cracking for heavier traffic), dowel diameter be increased to control joint faulting. This may result in a small increase in predicted joint faulting due to a reduction in effective area of the bar relative to the slab thickness (NCHRP 2004). Therefore, since this project has the lowest dowel diameter compared to others, predicted faulting is greater at higher thickness though after a certain thickness level (nearly 11 in.), distresses got compensated for high thickness as shown in Figure 5.2. This explains why very high and low levels of thickness have significant interactions with one another at different levels of strength.

For percent slabs cracked, at the 3,000-psi strength level, for PCC slab thickness equal to or greater than 9.5 in., there are no significant differences in mean predicted

values. Within 5000- and 8000-psi strength levels, cracking is not significant at any thickness level. If the 3000-psi strength level is compared with the 5,000-strength level, cracking becomes insignificant at or beyond a PCC slab thickness of 9.5 in. When the 5000-psi strength level is compared with the 8,000-psi strength level, thickness does not affect cracking at all.

When all results are compiled, it appears that for K-7, Johnson County, the optimum combination of thickness and strength would be 9.5 in. and 3,000 psi or 9 in. and 5000 psi. Any thickness or strength beyond these levels would be conservative according to the NCHRP MEPDG prediction.

5.7 Interaction of Thickness and Strength on Predicted Distresses Based on Bonferroni Adjustment

A large amount of information in ANOVA is obtained by examining the contrasts. In ANOVA, with a moderate number of treatments there are many contrasts to consider. The purpose of multiple comparison methods is to control the probability of making a specific type of error. In particular such methods control the probability of rejecting at least one contrast, when all contrasts are true. For a given level α , the probability statement in 5.5 holds,

$$P(\text{Reject} \geq 1 \text{ contrast} / \text{all contrasts true}) \leq \alpha \quad (5.5)$$

The Bonferroni correction is a multiple-comparison correction used when several dependent or independent statistical tests are being performed simultaneously (while a

given level of significance (α) may be appropriate for each individual comparison, it may not be applicable to the set of *all* comparisons). In order to avoid spurious positives, the alpha value can be lowered to account for the number k of comparisons being performed (Bonferroni 2005). A conservative method (for moderate to large values of k) divides the desired overall test-wise significance level by the number of contrasts to ensure that 5.5 holds.

In spite of this simplicity, a difficulty with this procedure is that it can be very conservative. Due to this correction, each individual test is held to an unreasonably high standard by controlling the group-wise error. Another criticism of this method is that this correction also makes it likely that legitimately significant results will fail to be detected (Bonferroni 2005).

In this study, *Bonferroni* correction was introduced in order to have conservative comparisons of the interactions between strength and thickness.

SPS-2 KDOT Control Section

For the SPS-2 KDOT Control section, the results, summarized in Table 5.6, show that within 3,000-psi strength level, for a PCC slab thickness greater than or equal to 9 in., there are no significant differences in mean predicted IRI values. For 5,000-psi and 8,000-psi strength levels, difference in mean predicted IRI becomes insignificant at all levels of thickness (8.5 inch to 12.0 inch). When the 3,000-psi strength level is compared with the 5,000-strength level, IRI becomes insignificant at or beyond a PCC slab thickness of 9 in. IRI became insignificant for the 8000-psi strength level.

For faulting, at the 3,000-psi strength level, for a PCC slab thickness up to 11 in., there are no significant differences in mean predicted values. The mean predicted faulting values after that become significant. For 5000-psi and 8000-psi strength levels predicted IRI became insignificant at or beyond 10 in. and 10.5 in., respectively. When the strength level is changed from the 3,000-psi level to the 5,000-psi level, no significant effect was observed at or beyond 9.5 in. and similar effect was noted (at or beyond 9 in.) for the 8,000- psi strength level.

Effect on the percent slabs cracked is almost similar to the previously described interactions. For 3,000-psi strength level, no significant difference was observed at or beyond the 9- in. thickness. When the 3,000-psi level is compared with the 5,000-psi level, percent slabs cracked becomes insignificant at or beyond 9.5 in.

Shawnee County, I-70

For the I-70 Shawnee county project, the interactions are summarized in Table 5.7. The results show that within 3,000-psi strength level, for a PCC slab thickness equal to or greater than 9.5 in., there are no significant differences in mean predicted IRI values. For 5,000-psi and 8,000-psi strength levels, difference in mean predicted IRI becomes insignificant at all level of thickness (8.5 in. to 12 in.). When the 3000-psi strength level is compared with the 5,000-strength level, IRI becomes insignificant at or beyond a PCC slab thickness of 9.5 in. IRI became insignificant at all levels of thickness for 8,000-psi strength.

Table 5.6 Effect of Interaction of Thickness and Strength on Predicted IRI for SPS-2 Control Section (with Bonferroni adjustment)

SxT	S1	S1	S1	S1	S1	S1	S1	S1	S1	S2	S2	S2	S2	S2	S2	S2	S2	S2	S3	S3	S3	S3	S3	S3	S3	S3	S3
	X	X	X	X	X	X	X	X	X	X	X	X	X	X	X	X	X	X	X	X	X	X	X	X	X	X	X
SxT	T1	T2	T3	T4	T5	T6	T7	T8	T9	T1	T2	T3	T4	T5	T6	T7	T8	T9	T1	T2	T3	T4	T5	T6	T7	T8	T9
S1xT1			*	*	*	*	*	*	*	*	*	*	*	*	*	*	*	*	*	*	*	*	*	*	*	*	*
S1xT2				*	*	*	*	*	*		*	*	*	*	*	*	*	*		*	*	*	*	*	*	*	*
S1xT3	*																										
S1xT4	*	*																									
S1xT5	*	*																									
S1xT6	*	*																									
S1xT7	*	*																									
S1xT8	*	*																									
S1xT9	*	*																									
S2xT1	*																										
S2xT2	*	*																									
S2xT3	*	*																									
S2xT4	*	*																									
S2xT5	*	*																									
S2xT6	*	*																									
S2xT7	*	*																									
S2xT8	*	*																									
S2xT9	*	*																									
S3xT1	*																										
S3xT2	*	*																									
S3xT3	*	*																									
S3xT4	*	*																									
S3xT5	*	*																									
S3xT6	*	*																									
S3xT7	*	*																									
S3xT8	*	*																									
S3xT9	*	*																									

* significant at 5% level of significance

For faulting, at the 3,000-psi strength level, for a PCC slab thickness up to 10.5 in., there are no significant differences in mean predicted values. The mean predicted faulting values after that become significant. When the strength is changed from the 3,000-psi level to the 5,000-psi level, no significant effect was observed at or beyond 10.5 in. within that strength level and similar effect was noticed for the 8,000-psi strength

level. Observed effect for comparisons at different levels of strength was similar to the previous interaction.

Table 5.7 Effect of Interaction of Thickness (T) and Strength (S) on Predicted IRI for I-70, Shawnee County (With Bonferroni adjustment)

SxT	S1	S1	S1	S1	S1	S1	S1	S1	S1	S2	S2	S2	S2	S2	S2	S2	S2	S2	S3	S3	S3	S3	S3	S3	S3	S3	S3	S3
	X	X	X	X	X	X	X	X	X	X	X	X	X	X	X	X	X	X	X	X	X	X	X	X	X	X	X	X
SxT	T1	T2	T3	T4	T5	T6	T7	T8	T9	T1	T2	T3	T4	T5	T6	T7	T8	T9	T1	T2	T3	T4	T5	T6	T7	T8	T9	
S1xT1		*	*	*	*	*	*	*	*	*	*	*	*	*	*	*	*	*	*	*	*	*	*	*	*	*	*	*
S1xT2	*		*	*	*	*	*	*	*	*	*	*	*	*	*	*	*	*	*	*	*	*	*	*	*	*	*	*
S1xT3	*	*			*	*	*	*	*		*	*	*	*	*	*	*	*			*	*	*	*	*	*	*	*
S1xT4						*	*	*							*	*	*	*						*	*	*	*	*
S1xT5	*	*	*							*																		
S1xT6	*	*	*	*						*	*	*							*	*	*							
S1xT7	*	*	*	*						*	*	*							*	*	*							
S1xT8	*	*	*	*						*	*								*	*								
S1xT9	*	*	*	*						*	*								*	*	*							
S2xT1	*	*			*	*	*	*	*				*	*	*	*	*	*					*	*	*	*	*	*
S2xT2	*	*	*												*	*	*	*						*	*	*	*	*
S2xT3	*	*	*			*	*									*		*										*
S2xT4	*	*	*							*																		
S2xT5	*	*	*							*																		
S2xT6	*	*	*	*						*	*								*	*	*							
S2xT7	*	*	*	*						*	*	*							*	*	*							
S2xT8	*	*	*	*						*	*								*	*	*							
S2xT9	*	*	*	*						*	*	*							*	*	*							
S3xT1	*	*				*	*	*	*					*	*	*	*	*						*	*	*	*	*
S3xT2	*	*				*	*	*	*					*	*	*	*	*						*	*	*	*	*
S3xT3	*	*	*			*	*		*					*	*	*	*	*						*	*	*	*	*
S3xT4	*	*	*																									*
S3xT5	*	*	*							*																		
S3xT6	*	*	*	*						*	*								*	*	*							
S3xT7	*	*	*	*						*	*								*	*	*							
S3xT8	*	*	*	*						*	*								*	*	*							
S3xT9	*	*	*	*						*	*	*							*	*	*	*						

* significant at 5% level of significance

Effect on the percent slabs cracked is almost similar to the previously described interactions. For the 3,000-psi strength level, no significant difference was observed at or

beyond 9.0-inch thickness. Within 5,000- and 8,000-psi strength levels, cracking is not significant at any thickness level.

Johnson County, K-7

Table 5.8 shows the results of the PCC slab thickness and strength interactions with Bonferroni adjustment for the Johnson County project on K-7. For 3000-psi strength, significant effect was observed for 8 in., 8.5 in. and 11 in. thickness levels. For 5,000 and 8,000-psi strength levels, significant effect was noticed on predicted IRI only at 11 in. thickness. Beyond that thickness, no significant interaction was observed.

For faulting, at the 3,000-psi strength level, for PCC slab thickness at or beyond 9.5 in., there are significant differences in mean predicted values. At the 5000-psi strength level, at or beyond 10.5 in., significant difference exists in predicted faulting. For the 8,000-psi level, at or beyond 11.0 inch, thickness effect was significant. The reason for it, based on dowel diameter, has been explained earlier. When the strength is changed from the 5,000-psi level to the 8,000-psi level, no significant effect was observed at or beyond 11 in.

Effect on the percent slabs cracked is almost similar to the previously described interactions. For the 3000-psi strength level, no significant difference observed at or beyond 9 in. Within 5000- and 8000-psi strength levels, cracking is not significant at any thickness level. For 5000-psi strength level, predicted percent slabs cracked became insignificant at or beyond 9 in.

Table 5.8 Effect of Interaction of Thickness (T) and Strength (S) on Predicted IRI for K-7, Johnson County (with Bonferroni adjustment)

SxT	S1	S1	S1	S1	S1	S1	S1	S1	S1	S2	S2	S2	S2	S2	S2	S2	S2	S2	S3	S3	S3	S3	S3	S3	S3	S3	S3	S3
	X	X	X	X	X	X	X	X	X	X	X	X	X	X	X	X	X	X	X	X	X	X	X	X	X	X	X	X
SxT	T1	T2	T3	T4	T5	T6	T7	T8	T9	T1	T2	T3	T4	T5	T6	T7	T8	T9	T1	T2	T3	T4	T5	T6	T7	T8	T9	
S1xT1			*	*	*	*	*	*	*	*	*	*	*	*	*	*	*	*	*	*	*	*	*	*	*	*	*	*
S1xT2	*			*	*	*	*	*	*		*	*	*	*	*	*	*	*	*	*	*	*	*	*	*	*	*	*
S1xT3	*	*					*		*							*		*							*	*	*	
S1xT4	*	*					*									*									*			
S1xT5	*	*					*									*									*			
S1xT6	*	*					*									*									*		*	
S1xT7	*	*	*	*	*	*				*	*			*	*				*	*				*				
S1xT8	*	*																										
S1xT9	*	*	*																									
S2xT1	*						*									*		*						*		*		
S2xT2	*	*					*									*									*			
S2xT3	*	*														*									*			
S2xT4	*	*														*									*			
S2xT5	*	*					*									*									*			
S2xT6	*	*					*									*									*			
S2xT7	*	*	*	*	*	*				*	*	*	*	*	*				*	*	*	*	*	*	*			
S2xT8	*	*																										
S2xT9	*	*	*						*																			
S3xT1	*	*					*									*									*			
S3xT2	*	*					*									*									*			
S3xT3	*	*														*									*			
S3xT4	*	*														*									*			
S3xT5	*	*														*									*			
S3xT6	*	*					*									*									*			
S3xT7	*	*	*	*	*	*				*	*	*	*	*	*				*	*	*	*	*	*	*			
S3xT8	*	*	*																									
S3xT9	*	*	*			*				*																		

* significant at 5% level of significance

5.8 Interaction of Strength-Traffic Based on With and Without Bonferroni Adjustment

I-70, Shawnee County and SPS-2 KDOT Control Section

Strength-traffic interaction was significant for the I-70 Shawnee County project for all levels of strength and traffic for predicted IRI and faulting. Within the same strength level (3000, 5000 or 8000 psi), significant interactions exist for all three levels of traffic (1000, 5000 and 10,000 AADTT). When the strength level was changed from 3000 psi to 5000 psi or 5000 psi to 8000 psi, significant interaction was also observed at all three traffic levels.

For percent slabs cracked, strength-traffic interaction was significant within the 3000-psi strength level. For the 5000-psi and 8000-psi strength levels, no interaction was observed. Again when the 3000-psi strength level was compared with the 5000-psi strength level, and the 5000-psi strength level was compared with the 8000-psi strength level, the 1000-AADTT traffic level had no interaction with other levels. After that significant interaction exists for each level of traffic.

It can be concluded that when the truck traffic is higher, strength becomes irrelevant because of the overwhelming effect of traffic.

K-7 Johnson County

As mentioned earlier, this project has the lowest thickness compared to all other projects, and there is an inconsistency in the predicted faulting values. The predicted percent slabs cracked results for this particular project illustrate that no significant

strength-traffic interaction exists within the 3000-psi strength level except for the 1,000-AADTT and 10,000- AADTT traffic levels.

5.9 Thickness-Traffic Interaction Based on With and Without Bonferroni Adjustment

For all projects, thickness-traffic interaction effect on predicted IRI was significant at every level of traffic studied. Within the same traffic level, after a certain thickness level, no significant interaction was observed for this combination. With the multiple comparison adjustment (Bonferroni), the observation was even more conservative.

For faulting, both I-70 Shawnee County and SPS-2 KDOT control section showed similar results. Within the low traffic level (1,000 AADTT), the effect of increasing thickness became insignificant after a certain level of thickness. Higher thickness also had significant effect compared to the lower thickness level. For the K-7 Johnson County project, significant interaction was observed for each thickness level within the same traffic level and also for different traffic levels. This also signifies the overwhelming impact of traffic on predicted performance.

For percent slabs cracked, within the low traffic level, no significant difference exists. When the traffic level was changed from the mid (5,000 AADTT) to the high level (10,000 AADTT), interaction exists only for the lowest level (8 inch) of thickness. After that no interaction was observed.

With Bonferroni adjustment, the thickness-traffic interaction was found to be not significant at all thickness levels.

CHAPTER 6

CONCLUSIONS AND RECOMMENDATIONS

6.1 Conclusions

Kansas rigid pavement analysis results following the Mechanistic-Empirical Pavement Design Guide (MEPDG) have been presented in this thesis. Design analysis following MEPDG was done for eight in-service concrete pavement projects in Kansas. The predicted distresses were compared with the measured values. A sensitivity analysis of JPCP design following MEPDG was also done with respect to key input parameters used in the design process. Some alternative JPCP designs were also evaluated with the MEPDG analysis. The interaction of selected significant factors through statistical analysis was identified to find the effect on current KDOT specifications for rigid pavement construction. Based on the results of this study the following conclusions may be drawn:

1. For most projects in this study, the predicted IRI was similar to the measured values. MEPDG analysis showed minimal or no faulting and it was confirmed by visual observation. Cracking was predicted only on projects with lower flexural strength or lower slab thickness.
2. Predicted JPCP roughness (IRI) by MEPDG is very sensitive to varying thickness. Lower PCC slab thickness results in higher JPCP faulting. Variation in thickness also affects the predicted cracking.
3. Predicted JPCP roughness (IRI) and faulting by MEPDG are not very sensitive to the PCC compressive strength. However, slab cracking is affected by strength, and cracking decreases with increasing strength.

4. Predicted JPCP roughness (IRI) by MEPDG is very sensitive to varying dowel diameter. Lower dowel diameter results in higher JPCP faulting. However, variation in dowel diameter does not affect predicted cracking. No significant effect on IRI, faulting and slab cracking was observed for dowels spaced from 10 to 14 inches.
5. Effect of tied shoulder on predicted JPCP roughness, faulting, and percent slabs cracked is very pronounced. The distresses are markedly reduced by tied PCC shoulder. No faulting was observed for a JPCP with widened lane that also had tied PCC shoulder. Reduced roughness and lower cracking amount were also obtained for the project with a widened lane.
6. According to the MEPDG analysis, JPCP designs without treated base and subgrade show significant increase in predicted distresses. There are no marked differences in performance with respect to treated base type, although asphalt treated base (ATB) appeared to be beneficial in a few cases.
7. No significant variation on predicted distresses was observed for different soil type. However, clay soil predicts slightly higher distresses compare to the silty soil.
8. Effect of curing method on the predicted distresses is not very prominent though there are indications that wet curing may reduce faulting.
9. The effect of PCC CTE input on predicted roughness is more pronounced on JPCP's with thinner slabs or lower strength; however the level of input is not defined in the software. A combination of high cement factor and higher PCC CTE would result in higher JPCP faulting. In general, faulting is sensitive to the

PCC CTE values. However, no faulting was observed for a JPCP with widened lane that also had tied PCC shoulder. PCC CTE has a very significant effect on percent slabs cracked. PCC CTE does not affect the predicted IRI for a JPCP with widened lane and tied PCC shoulder.

10. In general, the shrinkage does not greatly affect predicted IRI. The higher shrinkage strain results in higher faulting. Cracking appears to be fairly insensitive to the shrinkage strain.
11. MEPDG predicted IRI and percent slabs cracked are fairly insensitive to the zero-stress temperature but the faulting is severely affected. However, a JPCP section (SPS-2 Section 6) with widened lane and tied PCC shoulder did not show any faulting even for the highest zero-stress temperature. April and October are the best months for JPCP construction (paving) in Kansas.
12. Lower PCC slab thickness would result in higher JPCP faulting for a given traffic input. However, the predicted faulting values in this project were negligible for all practical purposes.
13. Monthly adjustment factors for the truck traffic are necessary in Kansas since traffic is heavier during the winter and spring months (December through April). Truck traffic type distributions for some functional classes in Kansas are dissimilar to those in MEPDG default. In contrast to the MEPDG default axle load spectra, Kansas has a higher percentages of trucks distributed in the lower axle load categories. Predicted JPCP roughness (IRI) by MEPDG is very sensitive to thickness at varying traffic level. However, traffic inputs studied in this project did not affect the predicted IRI for a JPCP with widened lane and tied PCC

shoulder. MEPDG traffic input causes more JPCP slab cracking than the Kansas input. Effects of higher AADT and truck traffic on predicted roughness, faulting and percent slabs cracked is more pronounced on the JPCP pavements with thinner slabs or lower strength. Variations in truck type do not affect predicted distresses on JPCP.

14. Current KDOT Percent within Limits (PWL) specifications for PCC pavement construction are more sensitive to the PCC strength than to the PCC slab thickness. For the current KDOT PCCP PWL specifications, the pay factor remains relatively unchanged for varying thickness. PCC slab thickness, PCC strength and truck traffic significantly influence the distresses predicted by the NCHRP MEPDG in most cases. The interactions among these factors are almost always significant.

15. For each JPCP project, there would be an optimal combination of PCC strength and slab thickness that is the most economical design. The optimum PCC slab thickness appears to be 9.5 to 10 in. for 3,000-psi concrete and 8.5 to 9.0 in. for 5,000-psi concrete for the traffic levels studied. Any thickness or strength increase beyond these levels may become conservative according to the NCHRP MEPDG analysis.

6.2 Recommendations

The following recommendations are made for further studies:

1. The AASHTO TP-60 tests can produce very valuable inputs in the MEPDG JPCP design process. This test should be implemented. A precision and bias statement should be developed.
2. Traffic data analysis needs to be extensive.
3. Based on the statistical analysis, each MEPDG JPCP design analysis should be studied for sensitivity toward PCC strength. An Upper Specification Limit (USL) also should be considered for strength in KDOT PWL specifications.
4. Interactions of several other key input parameters such as, dowel diameter, coefficient of thermal expansion, etc. with the PCC thickness and strength need to be studied in future research.

REFERENCES

- AASHTO Provisional Standards. Interim Edition, April 2001.
- American Association of State Highways and Transportation Officials (AASHTO). *A Policy on Geometric Design of Highways and Streets*, Washington, D.C., 2004.
- American Association of State Highways and Transportation Officials (AASHTO). *A Policy on Geometric Design of Highways and Streets*, Washington, D.C.1984.
- American Association of State Highways and Transportation Officials (AASHTO). *AASHTO Guide for Design of Pavement Structures*, Washington, D.C., 1993.
- American Association of State Highways and Transportation Officials (AASHTO). *AASHTO Guide for Design of Pavement Structures*, Washington, D.C., 1986.
- American Concrete Pavement Association (ACPA). *Concrete Pavement Fundamentals*, URL: <http://www.pavement.com/pavtech/tech/fundamentals/main.html>, Accessed June, 2005.
- Baladi, Y. G. and M.B. Snyder. *Highway Pavements Volume II & III*. Report No. FHWA HI-90-027 & FHWA HI-90-028. National Highway Institute, Federal Highway Administration, Washington, D.C., September 1992.
- Barry, C. R. and C. Schwartz. *Geotechnical Aspects of Pavements*. Report No. FHWA NHI-05-037. National Highway Institute, Federal Highway Administration, Washington, D.C., January 2005.
- Beam, S. *2002 Pavement Design Guide Design Input Evaluation: JPCP Pavements*, Master's Thesis, University of Arkansas, Fayetteville, December 2003.
- Bonferroni correction. Available at <http://mathworld.wolfram.com/BonferroniCorrection.html>. Accessed July 26, 2005.
- Bonferroni correction. Available at <http://www.umanitoba.ca/centres/mchp/concept/dict/Statistics/bonferroni.html>. Accessed July 5, 2005.
- Coree, B., Ceylan, H., and Harrington, D., *Implementing the Mechanistic-Empirical Pavement Design Guide*-Technical Report, Iowa Highway Research Board and Iowa Department of Transportation, Ames, Iowa, May 2005.
- Croney, D., and P. Croney. *The Design and Performance of Road Pavements*, McGraw-Hill Book Company, London, U.K., 1991.

Darter, M.I., Abdelrahman, M., Okamoto, P.A. and K.D. Smith. *Performance-Related Specifications for Concrete Pavements: Volume I—Development of a Prototype Performance-Related Specification*. FHWA-RD-93-042. Washington, DC: Federal Highway Administration, 1993.

Darter, M.I., Abdelrahman, M., Hoerner, T., Phillips, M., K.D. Smith, and Okamoto, P.A. *Performance-Related Specifications for Concrete Pavements: Volume II—Appendix A, B, and C*. FHWA-RD-93-043. Washington, DC: Federal Highway Administration, 1993.

FHWA. Guide to Developing Performance-Related Specifications for PCC Pavements. Publication No. FHWA-RD-98-155, February 1999. Available at <http://www.tfhrc.gov/pavement/pccp/pavespec/vol1/foreword/>. Accessed July 24, 2005.

Milliken, G. A. and Johnson, D. E. *Analysis of Messy Data*. Lifetime Learning Publications, Belmont, Calif., 1984, pp. 150-158.

Huang, Y.H. *Pavement Analysis and Design*. Prentice Hall, Inc., New Jersey, 2003.

Ingles, O.G., and J. B. Metcalf. *Soil Stabilization: Principles and Practice*, Butterworths Pty. Limited, 1972.

KDOT. *Kansas Department of Transportation Special Provisions*. Topeka, KS, Kansas Department of Transportation, Topeka, 1990

KDOT. *Kansas Traffic Monitoring System for Highways*. Bureau of Transportation Planning, Kansas Department of Transportation, Topeka, December 2003.

KDOT. *Pavement Management System*. NOS Condition Survey Report, Kansas Department of Transportation, Topeka, 2004.

KDOT. *Special Provision to the Standard Specifications of 1990; No. 90P-244, PCC Quality Control/Quality Assurance (QC/QA)*. Kansas Department of Transportation, Topeka, 2005.

Khazanovich, L., Darter, M. Bartlett, R., and McPeak, T. *Common Characteristics of Good and Poorly Performing PCC Pavements*. Report No. FHWA-RD97-131, Federal Highway Administration, McLean, Virginia, January 1998.

Kher, R.K. and M.I. Darter. Probabilistic concepts and their applications to AASHTO interim guide for rigid pavements. In HRR 466, Highway Research Board, Washington, D.C., 1973, pp. 20-36.

Kulkarni, R., F. Finn, E. Alviti, J. Chuang, and J. Rubinstein. Development of a Pavement Management System. Report to the Kansas Department of Transportation, Woodward-Clyde Consultants, 1983.

Little, D. N. *Handbook for Stabilization of Pavement Subgrades and Base Courses with Lime*, Kendal/Hunt Publishing Company, Iowa, 1995.

Melhem, H. G., Roger, S. and S. Walker. *Accelerated Testing for Studying Pavement Design and Performance*. Publication FHWA KS-02-7, Kansas Department of Transportation, Topeka, November 2003.

Milestones 2002. *Moving Towards the 2002 Pavement Design Guide*. A summary prepared for NCHRP Project 1-37A, ERES Consultants, Champaign, Illinois, 2001

Miller, R.W., Vedula, K., Hossain, M., and Cumberledge, G. Assessment of AASHTO Provisional Standards for Profile Data Collection and Interpretation. In *Transportation Research Record No. 1889*, Journal of the Transportation Research Board, National Research Council, 2004, pp. 134-143.

Nautung, T., Chehab, G., Newbolds, S., Galal, K., Li S. and Kim, H. Dae. Implementation Initiatives of the Mechanistic-Empirical Pavement Design Guides in Indiana. Preprint CD-ROM, 84th Annual Meeting of the Transportation Research Board, National Research Council, Washington, D.C., January 2005.

NCHRP. *Calibrated Mechanistic Structural Analysis Procedures for Pavements*. Final Report for Project 1-26. University of Illinois Construction Technology Laboratories, March 1990.

NCHRP. *Guide for Mechanistic-Empirical Design of New and Rehabilitated Pavement Structures*. Final Report for Project 1-37A, Part 1, 2 & 3, Chapter 4. National Cooperative Highway Research Program, Transportation Research Board, National Research Council, Washington, D.C., March 2004.

NCHRP. *Traffic Data Collection, Analysis and Forecasting for Mechanistic Pavement Design*. NCHRP Report No. 538, National Cooperative Highway Research Program, Transportation Research Board, National Research Council, Washington, D.C., 2005.

NHI. *Introduction to Mechanistic-Empirical Pavement Design of New and Rehabilitated Pavements*. Course No. 131064. National Highway Institute, Federal Highway Administration, Washington, D.C., April 2002.

NHI. *Pavement Subsurface Drainage Design*. National Highway Institute, Washington, D.C., April 1998.

Okamoto, P.A., C.L. Wu, S.M. Tarr, Darter, M.I. and K.D. Smith. *Performance-Related Specifications for Concrete Pavements: Volume III—Appendix D and E*. FHWA-RD-93-044. Federal Highway Administration, Washington, D.C., 1993.

Owusu-Antwi, E.B., Titus-Glover, L. and M.I. Darter. *Design and Construction of PCC Pavements. Volume I: Summary of Design Features and Construction Practices that*

Influence Performance of Pavements. Report No. FHWA-RD-98-052, Federal Highway Administration, McLean, Virginia, April 1998.

Portland Cement Association (PCA). *Design and Control of Concrete Mixtures*, Chapter 9, Skokie, Illinois, 2002.

Portland Cement Association (PCA). *Thickness Design for Concrete Highways and Street Pavements*, Chicago, Illinois, 1984.

“Implementation of the 2002 AASHTO Design Guide for Pavement Structures in KDOT.” Proposal submitted to the Kansas Department of Transportation, Topeka, Kansas, July 2003.

SAS. Statistical Analysis System, The SAS Institute, Cary, North Carolina, 1999.

Sayers, M.W. Development, Implementation, and Application of the Reference Quarter-Car Simulation. *ASTM Special Technical Publication No. 884*, American Society for Testing and Materials, Philadelphia, Penna., 1985.

Sharp, D.R. *Concrete in Highway Engineering*, Pergamon Press, Oxford, UK, 1970.

Smith, D. K. and K.T. Hall. *Concrete Pavement Design Details and Construction Practices*. Report No. FHWA NHI-02-015. National Highway Institute, Federal Highway Administration, Washington, D.C., December 2001.

Tam, W. O., and Quintus, H. V. Use of Long Term Pavement Performance data to develop traffic defaults in support of mechanistic-empirical pavement design procedures. Preprint CD-ROM, 83rd Annual Meeting of the Transportation Research Board, National Research Council, Washington, D.C., March 2004.

Timm, D., Birgisson, B., and D. Newcomb. Development of mechanistic-empirical pavement design in Minnesota. In *Transportation Research Record No. 1626*. Transportation Research Board, National Research Council, Washington, D.C., pp. 181-188, 1998

Vedula, K., Hossain, M., Siddique, Z.Q., and Miller, R.W., *Pavement Condition Measurement (Test Implementation of Distress Identification Protocols)- Final Report Vol. II: Profile Information*, Final Report, FHWA Project No.: TE21, Kansas State University, June 2004 (unpublished).

Wright, P. H., and R. J. Paquette. *Highway Engineering*, John Wiley & Sons, New York, 1987.

WSDOT. *WSDOT Pavement Guide*, Washington State Department of Transportation, URL: http://hotmix.ce.washington.edu/wsdot_web/, Accessed August 2003.

Yoder, E. J. and M. W. Witzak. *Principles of Pavement Design*, John Wiley and Sons, Inc, New York, N.Y., 1975.

APPENDIX A
Typical SAS Input and Output File

INPUT FILE

Data JPCP;
Input Strength Traffic Thickness IRI;
Cards;
3000 1000 8.0 130.5
3000 1000 8.5 120.1
3000 1000 9.0 117.3
3000 1000 9.5 116.1
3000 1000 10.0 115.3
3000 1000 10.5 112.5
3000 1000 11.0 111.8
3000 1000 11.5 113.3
3000 1000 12.0 112.7
3000 5000 8.0 203.4
3000 5000 8.5 174.1
3000 5000 9.0 153.4
3000 5000 9.5 143.5
3000 5000 10.0 138.9
3000 5000 10.5 136.3
3000 5000 11.0 124.3
3000 5000 11.5 132.7
3000 5000 12.0 131.2
3000 10000 8.0 234.1
3000 10000 8.5 219.2
3000 10000 9.0 193.0
3000 10000 9.5 172.2
3000 10000 10.0 161.3
3000 10000 10.5 138.9
3000 10000 11.0 152.0
3000 10000 11.5 148.9
3000 10000 12.0 146.6
5000 1000 8.0 118.6
5000 1000 8.5 117.6
5000 1000 9.0 116.8
5000 1000 9.5 116.0
5000 1000 10.0 115.2
5000 1000 10.5 112.9
5000 1000 11.0 112.1
5000 1000 11.5 112.9
5000 1000 12.0 112.2
5000 5000 8.0 149.7
5000 5000 8.5 144.1
5000 5000 9.0 141.8
5000 5000 9.5 139.9
5000 5000 10.0 137.9
5000 5000 10.5 135.9
5000 5000 11.0 125.7
5000 5000 11.5 131.8
5000 5000 12.0 129.9
5000 10000 8.0 181.5
5000 10000 8.5 167.1
5000 10000 9.0 162.5
5000 10000 9.5 159.5
5000 10000 10.0 156.4

```

5000 10000 10.5 141.8
5000 10000 11.0 150.6
5000 10000 11.5 147.7
5000 10000 12.0 145.1
8000 1000 8.0 119.3
8000 1000 8.5 118.2
8000 1000 9.0 117.2
8000 1000 9.5 116.2
8000 1000 10.0 115.2
8000 1000 10.5 113.2
8000 1000 11.0 112.3
8000 1000 11.5 112.4
8000 1000 12.0 111.7
8000 5000 8.0 148.2
8000 5000 8.5 145.8
8000 5000 9.0 143.5
8000 5000 9.5 141.0
8000 5000 10.0 138.3
8000 5000 10.5 135.6
8000 5000 11.0 126.5
8000 5000 11.5 130.8
8000 5000 12.0 128.7
8000 10000 8.0 171.1
8000 10000 8.5 167.8
8000 10000 9.0 164.5
8000 10000 9.5 161.0
8000 10000 10.0 157.3
8000 10000 10.5 143.7
8000 10000 11.0 150.1
8000 10000 11.5 146.8
8000 10000 12.0 143.7
;
proc print;Title '3-way Factorial Design for KDOT Control section';
proc glm data=JPCP;
Class Strength Traffic Thickness;
Model IRI=Strength Traffic Thickness Strength*Traffic Strength*Thickness Traffic*Thickness;
lsmeans Strength Traffic Thickness Strength*Traffic Strength*Thickness Traffic*Thickness / pdiff stderr;
output out=new p=dpred student=sres r=res;
proc print data=new;
run;

proc plot data=new;
plot sres*dpred;
plot sres*strength;
plot sres*Traffic;
plot sres*Thickness;

proc univariate data=new normal plot;
var sres;
run;
proc glm data=new;
class strength;
model res=strength;
means strength / Hovtest = Levene (type = abs);
run ;

```

OUTPUT FILES

The GLM Procedure

Class	Class Level Information
Levels	Values
Strength	3 3000 5000 8000
Traffic	3 1000 5000 10000
Thickness	9 8 8.5 9 9.5 10 10.5 11 11.5 12
Number of observations 81	

15:05 Friday, July 8, 2005

The GLM Procedure

Dependent Variable: IRI

Source	DF	Sum of Squares	Mean Square	F Value	Pr > F
Model	48	48775.04148	1016.14670	24.20	<.0001
Error	32	1343.76074	41.99252		
Corrected Total	80	50118.80222			

R-Square	Coeff Var	Root MSE	IRI Mean
0.973188	4.638136	6.480164	139.7148

Source	DF	Type I SS	Mean Square	F Value	Pr > F
Strength	2	1826.27185	913.13593	21.75	<.0001
Traffic	2	29716.00222	14858.00111	353.82	<.0001
Thickness	8	9779.20000	1222.40000	29.11	<.0001
Strength*Traffic	4	764.55037	191.13759	4.55	0.0050
Strength*Thickness	16	3577.57704	223.59856	5.32	<.0001
Traffic*Thickness	16	3111.44000	194.46500	4.63	0.0001

Source	DF	Type III SS	Mean Square	F Value	Pr > F
Strength	2	1826.27185	913.13593	21.75	<.0001
Traffic	2	29716.00222	14858.00111	353.82	<.0001
Source	DF	Type III SS	Mean Square	F Value	Pr > F

Thickness	8	9779.20000	1222.40000	29.11	<.0001
Strength*Traffic	4	764.55037	191.13759	4.55	0.0050
Strength*Thickness	16	3577.57704	223.59856	5.32	<.0001
Traffic*Thickness	16	3111.44000	194.46500	4.63	0.0001

15:05 Friday, July 8, 2005

The GLM Procedure
Least Squares Means

Strength	IRI LSMEAN	Standard Error	Pr > t	LSMEAN Number
3000	146.429630	1.247108	<.0001	1
5000	136.414815	1.247108	<.0001	2
8000	136.300000	1.247108	<.0001	3

Least Squares Means for effect Strength
Pr > |t| for H0: LSMean(i)=LSMean(j)
Dependent Variable: IRI

i/j	1	2	3
1		<.0001	<.0001
2	<.0001		0.9485
3	<.0001	0.9485	

NOTE: To ensure overall protection level, only probabilities associated with pre-planned comparisons should be used.

Traffic	IRI LSMEAN	Standard Error	Pr > t	LSMEAN Number
1000	115.540741	1.247108	<.0001	1
5000	141.218519	1.247108	<.0001	2
10000	162.385185	1.247108	<.0001	3

15:05 Friday, July 8, 2005

The GLM Procedure
Least Squares Means

Least Squares Means for effect Traffic
Pr > |t| for H0: LSMean(i)=LSMean(j)

Dependent Variable: IRI			
i/j	1	2	3
1		<.0001	<.0001
2	<.0001		<.0001
3	<.0001	<.0001	

NOTE: To ensure overall protection level, only probabilities associated with pre-planned comparisons should be used.

Thickness	IRI LSMEAN	Standard Error	Pr > t	LSMEAN Number
8	161.822222	2.160055	<.0001	1
8.5	152.666667	2.160055	<.0001	2
9	145.555556	2.160055	<.0001	3
9.5	140.600000	2.160055	<.0001	4
10	137.311111	2.160055	<.0001	5
10.5	130.088889	2.160055	<.0001	6
11	129.488889	2.160055	<.0001	7
11.5	130.811111	2.160055	<.0001	8
12	129.088889	2.160055	<.0001	9

15:05 Friday, July 8, 2005

The GLM Procedure
Least Squares Means
Least Squares Means for effect Thickness
Pr > |t| for H0: LSMean(i)=LSMean(j)
Dependent Variable: IRI

i/j	1	2	3	4	5	6	7	8	9
1		0.0052	<.0001	<.0001	<.0001	<.0001	<.0001	<.0001	<.0001
2	0.0052		0.0264	0.0004	<.0001	<.0001	<.0001	<.0001	<.0001
3	<.0001	0.0264		0.1146	0.0110	<.0001	<.0001	<.0001	<.0001
4	<.0001	0.0004	0.1146		0.2897	0.0016	0.0010	0.0031	0.0007
5	<.0001	<.0001	0.0110	0.2897		0.0243	0.0154	0.0412	0.0112
6	<.0001	<.0001	<.0001	0.0016	0.0243		0.8455	0.8146	0.7455
7	<.0001	<.0001	<.0001	0.0010	0.0154	0.8455		0.6680	0.8966
8	<.0001	<.0001	<.0001	0.0031	0.0412	0.8146	0.6680		0.5768
9	<.0001	<.0001	<.0001	0.0007	0.0112	0.7455	0.8966	0.5768	

NOTE: To ensure overall protection level, only probabilities associated with pre-planned comparisons should be used.

Strength	Traffic	IRI LSMEAN	Standard Error	Pr > t	LSMEAN Number
3000	1000	116.622222	2.160055	<.0001	1
3000	5000	148.644444	2.160055	<.0001	2
3000	10000	174.022222	2.160055	<.0001	3
5000	1000	114.922222	2.160055	<.0001	4
5000	5000	137.411111	2.160055	<.0001	5

15:05 Friday, July 8, 2005

The GLM Procedure
Least Squares Means

Strength	Traffic	IRI LSMEAN	Standard Error	Pr > t	LSMEAN Number
5000	10000	156.911111	2.160055	<.0001	6
8000	1000	115.077778	2.160055	<.0001	7
8000	5000	137.600000	2.160055	<.0001	8
8000	10000	156.222222	2.160055	<.0001	9

Least Squares Means for effect Strength*Traffic
Pr > |t| for H0: LSMean(i)=LSMean(j)

Dependent Variable: IRI

i/j	1	2	3	4	5	6	7	8	9
1		<.0001	<.0001	0.5817	<.0001	<.0001	0.6166	<.0001	<.0001
2	<.0001		<.0001	<.0001	0.0009	0.0108	<.0001	0.0010	0.0186
3	<.0001	<.0001		<.0001	<.0001	<.0001	<.0001	<.0001	<.0001
4	0.5817	<.0001	<.0001		<.0001	<.0001	0.9597	<.0001	<.0001
5	<.0001	0.0009	<.0001	<.0001		<.0001	<.0001	0.9511	<.0001
6	<.0001	0.0108	<.0001	<.0001	<.0001		<.0001	<.0001	0.8230
7	0.6166	<.0001	<.0001	0.9597	<.0001	<.0001		<.0001	<.0001
8	<.0001	0.0010	<.0001	<.0001	0.9511	<.0001	<.0001		<.0001
9	<.0001	0.0186	<.0001	<.0001	<.0001	0.8230	<.0001	<.0001	

NOTE: To ensure overall protection level, only probabilities associated with pre-planned comparisons should be used.

15:05 Friday, July 8, 2005

The GLM Procedure					
Least Squares Means					
Strength	Thickness	IRI LSMEAN	Standard Error	Pr > t	LSMEAN Number
3000	8	189.333333	3.741324	<.0001	1
3000	8.5	171.133333	3.741324	<.0001	2
3000	9	154.566667	3.741324	<.0001	3
3000	9.5	143.933333	3.741324	<.0001	4
3000	10	138.500000	3.741324	<.0001	5
3000	10.5	129.233333	3.741324	<.0001	6
3000	11	129.366667	3.741324	<.0001	7
3000	11.5	131.633333	3.741324	<.0001	8
3000	12	130.166667	3.741324	<.0001	9
5000	8	149.933333	3.741324	<.0001	10
5000	8.5	142.933333	3.741324	<.0001	11
5000	9	140.366667	3.741324	<.0001	12
5000	9.5	138.466667	3.741324	<.0001	13
5000	10	136.500000	3.741324	<.0001	14
5000	10.5	130.200000	3.741324	<.0001	15
5000	11	129.466667	3.741324	<.0001	16
5000	11.5	130.800000	3.741324	<.0001	17
5000	12	129.066667	3.741324	<.0001	18
8000	8	146.200000	3.741324	<.0001	19
8000	8.5	143.933333	3.741324	<.0001	20
8000	9	141.733333	3.741324	<.0001	21
8000	9.5	139.400000	3.741324	<.0001	22
8000	10	136.933333	3.741324	<.0001	23
8000	10.5	130.833333	3.741324	<.0001	24
8000	11	129.633333	3.741324	<.0001	25
8000	11.5	130.000000	3.741324	<.0001	26
8000	12	128.033333	3.741324	<.0001	27

15:05 Friday, July 8, 2005

The GLM Procedure
Least Squares Means

Least Squares Means for effect Strength*Thickness
Pr > |t| for H0: LSMean(i)=LSMean(j)

Dependent Variable: IRI

i/j	1	2	3	4	5	6	7	8	9
1		0.0016	<.0001	<.0001	<.0001	<.0001	<.0001	<.0001	<.0001
2	0.0016		0.0037	<.0001	<.0001	<.0001	<.0001	<.0001	<.0001
3	<.0001	0.0037		0.0530	0.0047	<.0001	<.0001	0.0001	<.0001
4	<.0001	<.0001	0.0530		0.3122	0.0091	0.0096	0.0266	0.0139
5	<.0001	<.0001	0.0047	0.3122		0.0895	0.0940	0.2036	0.1251
6	<.0001	<.0001	<.0001	0.0091	0.0895		0.9801	0.6532	0.8611
7	<.0001	<.0001	<.0001	0.0096	0.0940	0.9801		0.6712	0.8808
8	<.0001	<.0001	0.0001	0.0266	0.2036	0.6532	0.6712		0.7834
9	<.0001	<.0001	<.0001	0.0139	0.1251	0.8611	0.8808	0.7834	
10	<.0001	0.0003	0.3877	0.2652	0.0383	0.0004	0.0005	0.0016	0.0007
11	<.0001	<.0001	0.0352	0.8513	0.4083	0.0144	0.0152	0.0405	0.0217
12	<.0001	<.0001	0.0114	0.5051	0.7266	0.0433	0.0457	0.1086	0.0628
13	<.0001	<.0001	0.0047	0.3093	0.9950	0.0906	0.0951	0.2058	0.1266
14	<.0001	<.0001	0.0018	0.1697	0.7079	0.1792	0.1871	0.3646	0.2401
15	<.0001	<.0001	<.0001	0.0141	0.1266	0.8562	0.8758	0.7882	0.9950
16	<.0001	<.0001	<.0001	0.0101	0.0975	0.9651	0.9850	0.6849	0.8956
17	<.0001	<.0001	<.0001	0.0185	0.1553	0.7691	0.7882	0.8758	0.9055
18	<.0001	<.0001	<.0001	0.0084	0.0841	0.9751	0.9551	0.6309	0.8366
19	<.0001	<.0001	0.1236	0.6712	0.1553	0.0030	0.0033	0.0096	0.0048
20	<.0001	<.0001	0.0530	1.0000	0.3122	0.0091	0.0096	0.0266	0.0139
21	<.0001	<.0001	0.0211	0.6803	0.5455	0.0244	0.0258	0.0653	0.0362
22	<.0001	<.0001	0.0073	0.3979	0.8660	0.0636	0.0670	0.1519	0.0906
23	<.0001	<.0001	0.0022	0.1952	0.7691	0.1553	0.1624	0.3240	0.2101

15:05 Friday, July 8, 2005

The GLM Procedure
Least Squares Means

Least Squares Means for effect Strength*Thickness
Pr > |t| for H0: LSMean(i)=LSMean(j)

i/j	Dependent Variable: IRI								
	10	11	12	13	14	15	16	17	18
1	<.0001	<.0001	<.0001	<.0001	<.0001	<.0001	<.0001	<.0001	<.0001
2	0.0003	<.0001	<.0001	<.0001	<.0001	<.0001	<.0001	<.0001	<.0001
3	0.3877	0.0352	0.0114	0.0047	0.0018	<.0001	<.0001	<.0001	<.0001
4	0.2652	0.8513	0.5051	0.3093	0.1697	0.0141	0.0101	0.0185	0.0084
5	0.0383	0.4083	0.7266	0.9950	0.7079	0.1266	0.0975	0.1553	0.0841
6	0.0004	0.0144	0.0433	0.0906	0.1792	0.8562	0.9651	0.7691	0.9751
7	0.0005	0.0152	0.0457	0.0951	0.1871	0.8758	0.9850	0.7882	0.9551
8	0.0016	0.0405	0.1086	0.2058	0.3646	0.7882	0.6849	0.8758	0.6309
9	0.0007	0.0217	0.0628	0.1266	0.2401	0.9950	0.8956	0.9055	0.8366
10		0.1952	0.0800	0.0378	0.0162	0.0007	0.0005	0.0010	0.0004
11	0.1952		0.6309	0.4048	0.2329	0.0220	0.0159	0.0286	0.0133

12	0.0800	0.6309		0.7219	0.4702	0.0636	0.0476	0.0800	0.0405
13	0.0378	0.4048	0.7219		0.7126	0.1280	0.0986	0.1571	0.0851
14	0.0162	0.2329	0.4702	0.7126		0.2425	0.1932	0.2894	0.1697
15	0.0007	0.0220	0.0636	0.1280	0.2425		0.8906	0.9104	0.8318
16	0.0005	0.0159	0.0476	0.0986	0.1932	0.8906		0.8027	0.9402
17	0.0010	0.0286	0.0800	0.1571	0.2894	0.9104	0.8027		0.7453
18	0.0004	0.0133	0.0405	0.0851	0.1697	0.8318	0.9402	0.7453	
19	0.4855	0.5413	0.2785	0.1536	0.0761	0.0049	0.0034	0.0065	0.0028
20	0.2652	0.8513	0.5051	0.3093	0.1697	0.0141	0.0101	0.0185	0.0084
21	0.1310	0.8220	0.7978	0.5413	0.3300	0.0367	0.0270	0.0470	0.0227
22	0.0551	0.5091	0.8562	0.8611	0.5874	0.0917	0.0696	0.1139	0.0596
23	0.0196	0.2652	0.5210	0.7738	0.9352	0.2123	0.1678	0.2550	0.1469

15:05 Friday, July 8, 2005

The GLM Procedure
Least Squares Means
Least Squares Means for effect Strength*Thickness
Pr > |t| for H0: LSMean(i)=LSMean(j)

Dependent Variable: IRI

i/j	19	20	21	22	23	24	25	26	27
1	<.0001	<.0001	<.0001	<.0001	<.0001	<.0001	<.0001	<.0001	<.0001
2	<.0001	<.0001	<.0001	<.0001	<.0001	<.0001	<.0001	<.0001	<.0001
3	0.1236	0.0530	0.0211	0.0073	0.0022	<.0001	<.0001	<.0001	<.0001
4	0.6712	1.0000	0.6803	0.3979	0.1952	0.0188	0.0109	0.0129	0.0051
5	0.1553	0.3122	0.5455	0.8660	0.7691	0.1571	0.1035	0.1180	0.0566
6	0.0030	0.0091	0.0244	0.0636	0.1553	0.7643	0.9402	0.8857	0.8220
7	0.0033	0.0096	0.0258	0.0670	0.1624	0.7834	0.9601	0.9055	0.8027
8	0.0096	0.0266	0.0653	0.1519	0.3240	0.8808	0.7079	0.7596	0.5011
9	0.0048	0.0139	0.0362	0.0906	0.2101	0.9005	0.9203	0.9751	0.6895
10	0.4855	0.2652	0.1310	0.0551	0.0196	0.0010	0.0006	0.0007	0.0002
11	0.5413	0.8513	0.8220	0.5091	0.2652	0.0290	0.0172	0.0202	0.0083
12	0.2785	0.5051	0.7978	0.8562	0.5210	0.0810	0.0509	0.0588	0.0262
13	0.1536	0.3093	0.5413	0.8611	0.7738	0.1588	0.1048	0.1194	0.0573
14	0.0761	0.1697	0.3300	0.5874	0.9352	0.2922	0.2036	0.2282	0.1194
15	0.0049	0.0141	0.0367	0.0917	0.2123	0.9055	0.9154	0.9701	0.6849
16	0.0034	0.0101	0.0270	0.0696	0.1678	0.7978	0.9751	0.9203	0.7882
17	0.0065	0.0185	0.0470	0.1139	0.2550	0.9950	0.8269	0.8808	0.6046
18	0.0028	0.0084	0.0227	0.0596	0.1469	0.7406	0.9154	0.8611	0.8464
19		0.6712	0.4048	0.2079	0.0895	0.0066	0.0037	0.0044	0.0017
20	0.6712		0.6803	0.3979	0.1952	0.0188	0.0109	0.0129	0.0051
21	0.4048	0.6803		0.6622	0.3711	0.0476	0.0290	0.0338	0.0144
22	0.2079	0.3979	0.6622		0.6442	0.1152	0.0742	0.0851	0.0394
23	0.0895	0.1952	0.3711	0.6442		0.2575	0.1772	0.1994	0.1023

15:05 Friday, July 8, 2005

The GLM Procedure
Least Squares Means

Least Squares Means for effect Strength*Thickness
Pr > |t| for H0: LSMean(i)=LSMean(j)
Dependent Variable: IRI

i/j	1	2	3	4	5	6	7	8	9
24	<.0001	<.0001	<.0001	0.0188	0.1571	0.7643	0.7834	0.8808	0.9005
25	<.0001	<.0001	<.0001	0.0109	0.1035	0.9402	0.9601	0.7079	0.9203
26	<.0001	<.0001	<.0001	0.0129	0.1180	0.8857	0.9055	0.7596	0.9751
27	<.0001	<.0001	<.0001	0.0051	0.0566	0.8220	0.8027	0.5011	0.6895

Least Squares Means for effect Strength*Thickness
Pr > |t| for H0: LSMean(i)=LSMean(j)
Dependent Variable: IRI

i/j	10	11	12	13	14	15	16	17	18
24	0.0010	0.0290	0.0810	0.1588	0.2922	0.9055	0.7978	0.9950	0.7406
25	0.0006	0.0172	0.0509	0.1048	0.2036	0.9154	0.9751	0.8269	0.9154
26	0.0007	0.0202	0.0588	0.1194	0.2282	0.9701	0.9203	0.8808	0.8611
27	0.0002	0.0083	0.0262	0.0573	0.1194	0.6849	0.7882	0.6046	0.8464

15:05 Friday, July 8, 2005

The GLM Procedure
Least Squares Means

Least Squares Means for effect Strength*Thickness
Pr > |t| for H0: LSMean(i)=LSMean(j)
Dependent Variable: IRI

i/j	19	20	21	22	23	24	25	26	27
24	0.0066	0.0188	0.0476	0.1152	0.2575		0.8220	0.8758	0.6003
25	0.0037	0.0109	0.0290	0.0742	0.1772	0.8220		0.9452	0.7643
26	0.0044	0.0129	0.0338	0.0851	0.1994	0.8758	0.9452		0.7126
27	0.0017	0.0051	0.0144	0.0394	0.1023	0.6003	0.7643	0.7126	

NOTE: To ensure overall protection level, only probabilities associated with pre-planned comparisons should be used.

Traffic	Thickness	IRI LSMEAN	Standard Error	Pr > t	LSMEAN Number
1000	8	122.800000	3.741324	<.0001	1
1000	8.5	118.633333	3.741324	<.0001	2
1000	9	117.100000	3.741324	<.0001	3
1000	9.5	116.100000	3.741324	<.0001	4
1000	10	115.233333	3.741324	<.0001	5
1000	10.5	112.866667	3.741324	<.0001	6
1000	11	112.066667	3.741324	<.0001	7
1000	11.5	112.866667	3.741324	<.0001	8
1000	12	112.200000	3.741324	<.0001	9
5000	8	167.100000	3.741324	<.0001	10

15:05 Friday, July 8, 2005

The GLM Procedure
Least Squares Means

Traffic	Thickness	IRI LSMEAN	Standard Error	Pr > t	LSMEAN Number
5000	8.5	154.666667	3.741324	<.0001	11
5000	9	146.233333	3.741324	<.0001	12
5000	9.5	141.466667	3.741324	<.0001	13
5000	10	138.366667	3.741324	<.0001	14
5000	10.5	135.933333	3.741324	<.0001	15
5000	11	125.500000	3.741324	<.0001	16
5000	11.5	131.766667	3.741324	<.0001	17
5000	12	129.933333	3.741324	<.0001	18
10000	8	195.566667	3.741324	<.0001	19
10000	8.5	184.700000	3.741324	<.0001	20
10000	9	173.333333	3.741324	<.0001	21
10000	9.5	164.233333	3.741324	<.0001	22
10000	10	158.333333	3.741324	<.0001	23
10000	10.5	141.466667	3.741324	<.0001	24
10000	11	150.900000	3.741324	<.0001	25
10000	11.5	147.800000	3.741324	<.0001	26
10000	12	145.133333	3.741324	<.0001	27

15:05 Friday, July 8, 2005

The GLM Procedure
Least Squares Means

Least Squares Means for effect Traffic*Thickness
Pr > |t| for H0: LSMean(i)=LSMean(j)

Dependent Variable: IRI

i/j	1	2	3	4	5	6	7	8	9
1		0.4368	0.2894	0.2145	0.1624	0.0696	0.0509	0.0696	0.0537
2	0.4368		0.7738	0.6353	0.5251	0.2839	0.2236	0.2839	0.2329
3	0.2894	0.7738		0.8513	0.7266	0.4296	0.3486	0.4296	0.3613
4	0.2145	0.6353	0.8513		0.8709	0.5455	0.4515	0.5455	0.4664
5	0.1624	0.5251	0.7266	0.8709		0.6577	0.5537	0.6577	0.5705
6	0.0696	0.2839	0.4296	0.5455	0.6577		0.8808	1.0000	0.9005
7	0.0509	0.2236	0.3486	0.4515	0.5537	0.8808		0.8808	0.9801
8	0.0696	0.2839	0.4296	0.5455	0.6577	1.0000	0.8808		0.9005
9	0.0537	0.2329	0.3613	0.4664	0.5705	0.9005	0.9801	0.9005	
10	<.0001	<.0001	<.0001	<.0001	<.0001	<.0001	<.0001	<.0001	<.0001
11	<.0001	<.0001	<.0001	<.0001	<.0001	<.0001	<.0001	<.0001	<.0001
12	<.0001	<.0001	<.0001	<.0001	<.0001	<.0001	<.0001	<.0001	<.0001
13	0.0013	0.0001	<.0001	<.0001	<.0001	<.0001	<.0001	<.0001	<.0001
14	0.0060	0.0007	0.0003	0.0002	0.0001	<.0001	<.0001	<.0001	<.0001
15	0.0185	0.0026	0.0012	0.0007	0.0004	0.0001	<.0001	0.0001	<.0001
16	0.6133	0.2036	0.1222	0.0851	0.0612	0.0230	0.0162	0.0230	0.0172
17	0.0998	0.0185	0.0092	0.0057	0.0038	0.0011	0.0008	0.0011	0.0008
18	0.1871	0.0405	0.0211	0.0135	0.0091	0.0029	0.0019	0.0029	0.0021
19	<.0001	<.0001	<.0001	<.0001	<.0001	<.0001	<.0001	<.0001	<.0001
20	<.0001	<.0001	<.0001	<.0001	<.0001	<.0001	<.0001	<.0001	<.0001
21	<.0001	<.0001	<.0001	<.0001	<.0001	<.0001	<.0001	<.0001	<.0001
22	<.0001	<.0001	<.0001	<.0001	<.0001	<.0001	<.0001	<.0001	<.0001
23	<.0001	<.0001	<.0001	<.0001	<.0001	<.0001	<.0001	<.0001	<.0001

15:05 Friday, July 8, 2005

The GLM Procedure
Least Squares Means
Least Squares Means for effect Traffic*Thickness
Pr > |t| for H0: LSMean(i)=LSMean(j)

Dependent Variable: IRI

i/j	10	11	12	13	14	15	16	17	18
1	<.0001	<.0001	0.0001	0.0013	0.0060	0.0185	0.6133	0.0998	0.1871
2	<.0001	<.0001	<.0001	0.0001	0.0007	0.0026	0.2036	0.0185	0.0405
3	<.0001	<.0001	<.0001	<.0001	0.0003	0.0012	0.1222	0.0092	0.0211
4	<.0001	<.0001	<.0001	<.0001	0.0002	0.0007	0.0851	0.0057	0.0135

5	<.0001	<.0001	<.0001	<.0001	0.0001	0.0004	0.0612	0.0038	0.0091
6	<.0001	<.0001	<.0001	<.0001	<.0001	0.0001	0.0230	0.0011	0.0029
7	<.0001	<.0001	<.0001	<.0001	<.0001	<.0001	0.0162	0.0008	0.0019
8	<.0001	<.0001	<.0001	<.0001	<.0001	0.0001	0.0230	0.0011	0.0029
9	<.0001	<.0001	<.0001	<.0001	<.0001	<.0001	0.0172	0.0008	0.0021
10		0.0251	0.0004	<.0001	<.0001	<.0001	<.0001	<.0001	<.0001
11	0.0251		0.1208	0.0180	0.0042	0.0012	<.0001	0.0001	<.0001
12	0.0004	0.1208		0.3744	0.1469	0.0604	0.0004	0.0101	0.0042
13	<.0001	0.0180	0.3744		0.5621	0.3035	0.0050	0.0761	0.0367
14	<.0001	0.0042	0.1469	0.5621		0.6487	0.0208	0.2213	0.1208
15	<.0001	0.0012	0.0604	0.3035	0.6487		0.0573	0.4368	0.2652
16	<.0001	<.0001	0.0004	0.0050	0.0208	0.0573		0.2450	0.4083
17	<.0001	0.0001	0.0101	0.0761	0.2213	0.4368	0.2450		0.7312
18	<.0001	<.0001	0.0042	0.0367	0.1208	0.2652	0.4083	0.7312	
19	<.0001	<.0001	<.0001	<.0001	<.0001	<.0001	<.0001	<.0001	<.0001
20	0.0022	<.0001	<.0001	<.0001	<.0001	<.0001	<.0001	<.0001	<.0001
21	0.2474	0.0013	<.0001	<.0001	<.0001	<.0001	<.0001	<.0001	<.0001
22	0.5917	0.0800	0.0018	0.0001	<.0001	<.0001	<.0001	<.0001	<.0001
23	0.1073	0.4933	0.0290	0.0032	0.0007	0.0002	<.0001	<.0001	<.0001

15:05 Friday, July 8, 2005

The GLM Procedure
Least Squares Means

Least Squares Means for effect Traffic*Thickness
Pr > |t| for H0: LSMean(i)=LSMean(j)

Dependent Variable: IRI

i/j	19	20	21	22	23	24	25	26	27
1	<.0001	<.0001	<.0001	<.0001	<.0001	0.0013	<.0001	<.0001	0.0002
2	<.0001	<.0001	<.0001	<.0001	<.0001	0.0001	<.0001	<.0001	<.0001
3	<.0001	<.0001	<.0001	<.0001	<.0001	<.0001	<.0001	<.0001	<.0001
4	<.0001	<.0001	<.0001	<.0001	<.0001	<.0001	<.0001	<.0001	<.0001
5	<.0001	<.0001	<.0001	<.0001	<.0001	<.0001	<.0001	<.0001	<.0001
6	<.0001	<.0001	<.0001	<.0001	<.0001	<.0001	<.0001	<.0001	<.0001
7	<.0001	<.0001	<.0001	<.0001	<.0001	<.0001	<.0001	<.0001	<.0001
8	<.0001	<.0001	<.0001	<.0001	<.0001	<.0001	<.0001	<.0001	<.0001
9	<.0001	<.0001	<.0001	<.0001	<.0001	<.0001	<.0001	<.0001	<.0001
10	<.0001	0.0022	0.2474	0.5917	0.1073	<.0001	0.0044	0.0009	0.0002
11	<.0001	<.0001	0.0013	0.0800	0.4933	0.0180	0.4817	0.2036	0.0810
12	<.0001	<.0001	<.0001	0.0018	0.0290	0.3744	0.3844	0.7691	0.8366
13	<.0001	<.0001	<.0001	0.0001	0.0032	1.0000	0.0841	0.2401	0.4933
14	<.0001	<.0001	<.0001	<.0001	0.0007	0.5621	0.0241	0.0841	0.2101
15	<.0001	<.0001	<.0001	<.0001	0.0002	0.3035	0.0080	0.0320	0.0917
16	<.0001	<.0001	<.0001	<.0001	<.0001	0.0050	<.0001	0.0002	0.0008
17	<.0001	<.0001	<.0001	<.0001	<.0001	0.0761	0.0010	0.0048	0.0167

18	<.0001	<.0001	<.0001	<.0001	<.0001	0.0367	0.0004	0.0019	0.0072
19		0.0482	0.0002	<.0001	<.0001	<.0001	<.0001	<.0001	<.0001
20	0.0482		0.0394	0.0005	<.0001	<.0001	<.0001	<.0001	<.0001
21	0.0002	0.0394		0.0951	0.0079	<.0001	0.0002	<.0001	<.0001
22	<.0001	0.0005	0.0951		0.2731	0.0001	0.0169	0.0040	0.0010
23	<.0001	<.0001	0.0079	0.2731		0.0032	0.1697	0.0551	0.0180

15:05 Friday, July 8, 2005

The GLM Procedure
Least Squares Means
Least Squares Means for effect Traffic*Thickness
Pr > |t| for H0: LSMean(i)=LSMean(j)

Dependent Variable: IRI									
i/j	1	2	3	4	5	6	7	8	9
24	0.0013	0.0001	<.0001	<.0001	<.0001	<.0001	<.0001	<.0001	<.0001
25	<.0001	<.0001	<.0001	<.0001	<.0001	<.0001	<.0001	<.0001	<.0001
26	<.0001	<.0001	<.0001	<.0001	<.0001	<.0001	<.0001	<.0001	<.0001
27	0.0002	<.0001	<.0001	<.0001	<.0001	<.0001	<.0001	<.0001	<.0001

Least Squares Means for effect Traffic*Thickness
Pr > |t| for H0: LSMean(i)=LSMean(j)
Dependent Variable: IRI

i/j	10	11	12	13	14	15	16	17	18
24	<.0001	0.0180	0.3744	1.0000	0.5621	0.3035	0.0050	0.0761	0.0367
25	0.0044	0.4817	0.3844	0.0841	0.0241	0.0080	<.0001	0.0010	0.0004
26	0.0009	0.2036	0.7691	0.2401	0.0841	0.0320	0.0002	0.0048	0.0019
27	0.0002	0.0810	0.8366	0.4933	0.2101	0.0917	0.0008	0.0167	0.0072

15:05 Friday, July 8, 2005

The GLM Procedure
Least Squares Means
Least Squares Means for effect Traffic*Thickness
Pr > |t| for H0: LSMean(i)=LSMean(j)

Dependent Variable: IRI

i/j	19	20	21	22	23	24	25	26	27
24	<.0001	<.0001	<.0001	0.0001	0.0032		0.0841	0.2401	0.4933
25	<.0001	<.0001	0.0002	0.0169	0.1697	0.0841		0.5621	0.2839
26	<.0001	<.0001	<.0001	0.0040	0.0551	0.2401	0.5621		0.6177
27	<.0001	<.0001	<.0001	0.0010	0.0180	0.4933	0.2839	0.6177	

NOTE: To ensure overall protection level, only probabilities associated with pre-planned comparisons should be used.

15:05 Friday, July 8, 2005

Obs	Strength	Traffic	Thickness	IRI	dpred	sres	res
1	3000	1000	8.0	130.5	144.678	-3.48089	-14.1778
2	3000	1000	8.5	120.1	131.467	-2.79071	-11.3667
3	3000	1000	9.0	117.3	120.478	-0.78020	-3.1778
4	3000	1000	9.5	116.1	113.800	0.56469	2.3000
5	3000	1000	10.0	115.3	110.789	1.10755	4.5111
6	3000	1000	10.5	112.5	106.378	1.50311	6.1222
7	3000	1000	11.0	111.8	106.311	1.34762	5.4889
8	3000	1000	11.5	113.3	108.056	1.28760	5.2444
9	3000	1000	12.0	112.7	107.644	1.24122	5.0556
10	3000	5000	8.0	203.4	195.322	1.98323	8.0778
11	3000	5000	8.5	174.1	173.844	0.06274	0.2556
12	3000	5000	9.0	153.4	155.956	-0.62743	-2.5556
13	3000	5000	9.5	143.5	145.511	-0.49376	-2.0111
14	3000	5000	10.0	138.9	140.267	-0.33554	-1.3667
15	3000	5000	10.5	136.3	135.789	0.12549	0.5111
16	3000	5000	11.0	124.3	126.089	-0.43920	-1.7889
17	3000	5000	11.5	132.7	133.300	-0.14731	-0.6000
18	3000	5000	12.0	131.2	131.722	-0.12821	-0.5222
19	3000	10000	8.0	234.1	228.000	1.49765	6.1000
20	3000	10000	8.5	219.2	208.089	2.72797	11.1111
21	3000	10000	9.0	193.0	187.267	1.40763	5.7333
22	3000	10000	9.5	172.2	172.489	-0.07093	-0.2889
23	3000	10000	10.0	161.3	164.444	-0.77201	-3.1444
24	3000	10000	10.5	138.9	145.533	-1.62860	-6.6333
25	3000	10000	11.0	152.0	155.700	-0.90841	-3.7000
26	3000	10000	11.5	148.9	153.544	-1.14029	-4.6444
27	3000	10000	12.0	146.6	151.133	-1.11301	-4.5333
28	5000	1000	8.0	118.6	113.593	1.22940	5.0074
29	5000	1000	8.5	111.6	111.581	1.47765	6.0185
30	5000	1000	9.0	116.8	114.593	0.54196	2.2074
31	5000	1000	9.5	116.0	116.648	-0.15913	-0.6481

15:05 Friday, July 8, 2005

Obs	Strength	Traffic	Thickness	IRI	dpred	sres	res
32	5000	1000	10.0	115.2	117.104	-0.46739	-1.90370
33	5000	1000	10.5	112.9	115.659	-0.67745	-2.75926
34	5000	1000	11.0	112.1	114.726	-0.64471	-2.62593
35	5000	1000	11.5	112.9	115.537	-0.64744	-2.63704
36	5000	1000	12.0	112.2	114.859	-0.65289	-2.65926
37	5000	5000	8.0	149.7	154.704	-1.22849	-5.00370
38	5000	5000	8.5	144.1	144.426	-0.08002	-0.32593
39	5000	5000	9.0	141.8	140.537	0.31008	1.26296
40	5000	5000	9.5	139.9	138.826	0.26370	1.07407
41	5000	5000	10.0	137.9	137.048	0.20914	0.85185
42	5000	5000	10.5	135.9	135.537	0.08911	0.36296
43	5000	5000	11.0	125.7	124.970	0.17914	0.72963
44	5000	5000	11.5	131.8	131.248	0.13549	0.55185
45	5000	5000	12.0	129.9	129.404	0.12185	0.49630
46	5000	10000	8.0	181.5	181.504	-0.00091	-0.00370
47	5000	10000	8.5	167.1	172.793	-1.39763	-5.69259
48	5000	10000	9.0	162.5	165.970	-0.85203	-3.47037
49	5000	10000	9.5	159.5	159.926	-0.10457	-0.42593
50	5000	10000	10.0	156.4	155.348	0.25825	1.05185
51	5000	10000	10.5	141.8	139.404	0.58833	2.39630
52	5000	10000	11.0	150.6	148.704	0.46557	1.89630
53	5000	10000	11.5	147.7	145.615	0.51195	2.08519
54	5000	10000	12.0	145.1	142.937	0.53104	2.16296
55	8000	1000	8.0	119.3	110.130	2.25148	9.17037
56	8000	1000	8.5	118.2	112.852	1.31306	5.34815
57	8000	1000	9.0	117.2	116.230	0.23824	0.97037
58	8000	1000	9.5	116.2	117.852	-0.40556	-1.65185
59	8000	1000	10.0	115.2	117.807	-0.64016	-2.60741
60	8000	1000	10.5	113.2	116.563	-0.82566	-3.36296
61	8000	1000	11.0	112.3	115.163	-0.70291	-2.86296
62	8000	1000	11.5	112.4	115.007	-0.64016	-2.60741

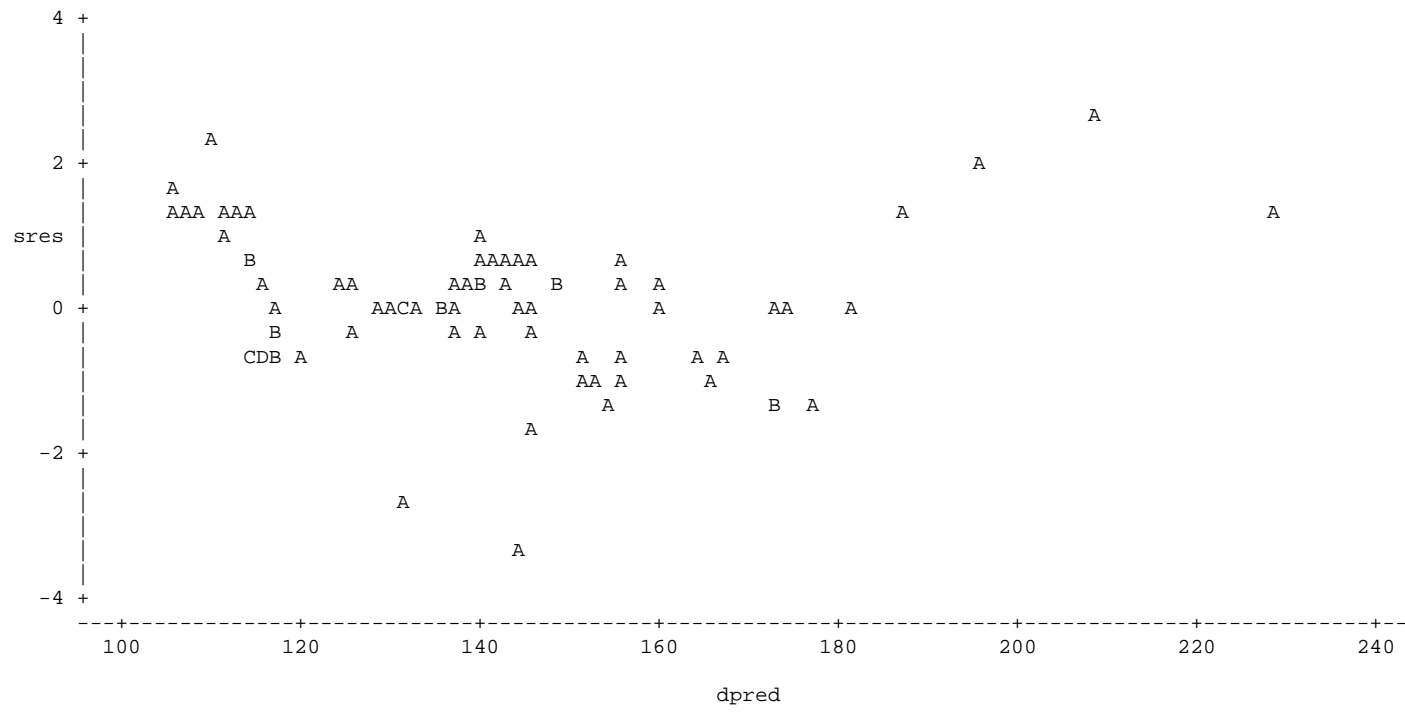
15:05 Friday, July 8, 2005

Obs	Strength	Traffic	Thickness	IRI	dpred	sres	res
63	8000	1000	12.0	111.7	114.096	-0.58833	-2.39630
64	8000	5000	8.0	148.2	151.274	-0.75474	-3.07407
65	8000	5000	8.5	145.8	145.730	0.01728	0.07037
66	8000	5000	9.0	143.5	142.207	0.31735	1.29259
67	8000	5000	9.5	141.0	140.063	0.23006	0.93704
68	8000	5000	10.0	138.3	137.785	0.12640	0.51481
69	8000	5000	10.5	135.6	136.474	-0.21460	-0.87407

70	8000	5000	11.0	126.5	125.441	0.26007	1.05926
71	8000	5000	11.5	130.8	130.752	0.01182	0.04815
72	8000	5000	12.0	128.7	128.674	0.00637	0.02593
73	8000	10000	8.0	171.1	177.196	-1.49674	-6.09630
74	8000	10000	8.5	167.8	173.219	-1.33034	-5.41852
75	8000	10000	9.0	164.5	166.763	-0.55560	-2.26296
76	8000	10000	9.5	161.0	160.285	0.17550	0.71481
77	8000	10000	10.0	157.3	155.207	0.51377	2.09259
78	8000	10000	10.5	143.7	139.463	1.04026	4.23704
79	8000	10000	11.0	150.1	148.296	0.44284	1.80370
80	8000	10000	11.5	146.8	144.241	0.62834	2.55926
81	8000	10000	12.0	143.7	141.330	0.58197	2.37037

15:05 Friday, July 8, 2005

Plot of sres*dpred. Legend: A = 1 obs, B = 2 obs, etc.



15:05 Friday, July 8, 2005

The UNIVARIATE Procedure
Variable: sres
Moments

N	81	Sum Weights	81
Mean	0	Sum Observations	0
Std Deviation	1.00623059	Variance	1.0125
Skewness	-0.2589343	Kurtosis	1.73689566
Uncorrected SS	81	Corrected SS	81
Coeff Variation	.	Std Error Mean	0.1118034

Basic Statistical Measures

Location		Variability	
Mean	0.000000	Std Deviation	1.00623
Median	0.017277	Variance	1.01250
Mode	.	Range	6.20885
		Interquartile Range	1.15393

Tests for Location: Mu0=0

Test	-Statistic-	-----p Value-----		
Student's t	t	0	Pr > t	1.0000
Sign	M	2.5	Pr >= M	0.6570
Signed Rank	S	-16	Pr >= S	0.9405

15:05 Friday, July 8, 2005

The UNIVARIATE Procedure
Variable: sres
Tests for Normality

Test	--Statistic--	-----p Value-----		
Shapiro-Wilk	W	0.967457	Pr < W	0.0372
Kolmogorov-Smirnov	D	0.094193	Pr > D	0.0759
Cramer-von Mises	W-Sq	0.120931	Pr > W-Sq	0.0598
Anderson-Darling	A-Sq	0.769522	Pr > A-Sq	0.0449

Quantiles (Definition 5)

Quantile	Estimate
100% Max	2.7279665

```

99%          2.7279665
95%          1.4976536
90%          1.3130612
75% Q3      0.5137670
50% Median  0.0172771
25% Q1     -0.6401628
10%        -1.1130103
5%         -1.3976281
1%         -3.4808852
0% Min     -3.4808852

```

15:05 Friday, July 8, 2005

The UNIVARIATE Procedure
Variable: sres
Extreme Observations

-----Lowest-----		-----Highest-----	
Value	Obs	Value	Obs
-3.48089	1	1.49765	19
-2.79071	2	1.50311	6
-1.62860	24	1.98323	10
-1.49674	73	2.25148	55
-1.39763	47	2.72797	20

```

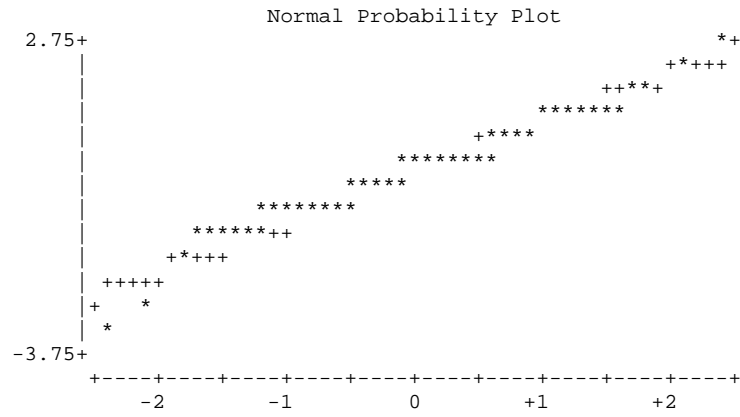
Stem Leaf          #
 2 7                1
 2 03               2
 1 555              3
 1 01223334        8
 0 555556666       9
 0 00011111122222333334 20
-0 44322111110    11
-0 99888877766666655 18
-1 43211           5
-1 65              2
-2                 1
-2 8               1
-3                 1
-3 5               1
-----+-----+-----+

```

```

#   Boxplot
1   0
2   0
3   |
8   |
9   +-----+
20  *---+---*
11  |         |
18  +-----+
5   |
2   |
1   0
1   0

```



APPENDIX B
MEPDG Software Output File

Project: K-3344-

General Information

Design Life 20 years
Pavement construction: October,
Traffic open: December,

Type of design JPCP

Description:

Analysis Parameters

Analysis type Probabilistic

Performance Criteria

	Limit	ity
Initial IRI (in/mi)	96	
Terminal IRI (in/mi)	164	90
Transverse Cracking (% slabs cracked)	15	90
Mean Joint Faulting (in)	0.12	90

Location: Shawne county,I-70
Project ID: K-3344-01
Section ID: Rural Interstate
Principal Arterials - Interstate and Defense Routes
Date: 5/28/2004

Station/milepost format: Miles: 0.000
Station/milepost begin: 9
Station/milepost end: 10
Traffic direction: West bound

Default Input Level

Default input level Level 3, Default and historical agency values.

Traffic

Initial two-way aadtt: 1800
Number of lanes in design direction: 2
Percent of trucks in design direction (%): 50
Percent of trucks in design lane (%): 95
Operational speed (mph): 70

Traffic -- Volume Adjustment

Monthly Adjustment Factors (Level 1, Site Specific - MAF)

Month	Vehicle Class									
	Class 4	Class 5	Class 6	Class 7	Class 8	Class 9	Class 10	Class 11	Class 12	Class 13
January	1.16	1.16	1.16	1.16	1.16	1.16	1.16	1.16	1.16	1.16
February	1.15	1.15	1.15	1.15	1.15	1.15	1.15	1.15	1.15	1.15
March	1.03	1.03	1.03	1.03	1.03	1.03	1.03	1.03	1.03	1.03
April	1.03	1.03	1.03	1.03	1.03	1.03	1.03	1.03	1.03	1.03
May	0.97	0.97	0.97	0.97	1.00	0.97	0.97	0.97	0.97	0.97
June	0.95	0.95	0.95	0.95	1.00	0.95	0.95	0.95	0.95	0.95
July	0.93	0.93	0.93	0.93	1.00	0.93	0.93	0.93	0.93	0.93
August	0.96	0.96	0.96	0.96	1.00	0.96	0.96	0.96	0.96	0.96
September	1.01	1.01	1.01	1.01	1.00	1.01	1.01	1.01	1.01	1.01
October	1.02	1.02	1.02	1.02	1.00	1.02	1.02	1.02	1.02	1.02
November	1.01	1.01	1.01	1.01	1.00	1.01	1.01	1.01	1.01	1.01
December	1.05	1.05	1.05	1.05	1.00	1.05	1.05	1.05	1.05	1.05

Vehicle Class Distribution

(Level 1, Site Specific Distribution)

AADTT distribution by vehicle

Class 4	2.4%
Class 5	9.0%
Class 6	2.5%
Class 7	0.9%
Class 8	6.7%
Class 9	69.0%
Class 10	1.1%
Class 11	4.6%
Class 12	1.7%
Class 13	2.1%

Hourly truck traffic

by period beginning:

ht	2.1%	Noon	5.5%
1:00	2.0%	1:00	6.7%
2:00	2.1%	2:00	6.1%
3:00	1.7%	3:00	6.9%
4:00	1.9%	4:00	6.4%
5:00	2.3%	5:00	6.0%
6:00	2.1%	6:00	5.6%
7:00	3.4%	7:00	5.1%
8:00	4.1%	8:00	4.3%
9:00	4.8%	9:00	4.4%
10:00	4.6%	10:00	3.5%
11:00 am	5.7%	11:00 pm	2.7%

Traffic Growth Factor

Vehicle Class	Growth Rate	Growth Function
Class 4	3.0%	Linear
Class 5	3.0%	Linear
Class 6	3.0%	Linear
Class 7	3.0%	Linear
Class 8	3.0%	Linear
Class 9	3.0%	Linear
Class 10	3.0%	Linear
Class 11	3.0%	Linear
Class 12	3.0%	Linear
Class 13	3.0%	Linear

Traffic -- Axle Load Distribution

Level 1: Site Specific

Traffic -- General Traffic Inputs

Mean wheel location (inches from the lane marking): 18
 Traffic wander standard deviation: 10
 Design lane width (ft): 12

Number of Axles per Truck

Vehicle Class	Single Axle	Tandem	Tridem	Quad Axle
Class 4	1.62	0.39	0.00	0.00
Class 5	2.00	0.00	0.00	0.00
Class 6	1.02	0.99	0.00	0.00
Class 7	1.00	0.26	0.83	0.00
Class 8	2.38	0.67	0.00	0.00
Class 9	1.13	1.93	0.00	0.00
Class 10	1.19	1.09	0.89	0.00
Class 11	4.29	0.26	0.06	0.00
Class 12	3.52	1.14	0.06	0.00
Class 13	2.15	2.13	0.35	0.00

Axle Configuration

Average axle width (edge-to-edge) outside dimensions,ft): 8.5
 Dual tire spacing (in): 12

Axle Configuration

Single Tire (psi): 120
 Dual Tire (psi): 120

Average Axle Spacing

Tandem axle(psi): 51.6
 Tridem axle(psi): 49.2
 Quad axle(psi): 49.2

Wheelbase Truck Tractor

	Short	Medium	Long
Average Axle Spacing	12	15	18
Percent of trucks	33%	33%	34%

Climate

icm file:

C:\DG2002\Projects\Shawnee county,KS.icm

Latitude (degrees.minutes) 39.04
 Longitude (degrees.minutes) -95.4
 Elevation (ft) 880
 Depth of water table (ft) 10

Structure--Design Features

Permanent curl/warp effective temperature difference (°F): -10

Joint Design

Joint spacing (ft): 15
Sealant type: Liquid
Dowel diameter (in): 1.375
Dowel bar spacing (in): 12

Edge Support

Tied PCC shoulder
Long-term LTE(%): 60
Widened Slab (ft): n/a

Base Properties

Base type: Cement treated
Erodibility index: Erosion Resistant (3)
Base/slab friction coefficient: 0.65
PCC-Base Interface: Bonded
Loss of bond age (months): 60

Structure--ICM Properties

Surface shortwave absorptivity: 0.85

Drainage Parameters

Infiltration: Moderate (50%)
Drainage path length (ft): 12
Pavement cross slope (%): 1.6

Structure--Layers

Layer 1 -- JPCP

General Properties

PCC material: JPCP
Layer thickness (in): 10.5
Unit weight (pcf): 142
Poisson's ratio: 0.2

Thermal Properties

Coefficient of thermal expansion (per F° x 10⁻⁵): 5.5
Thermal conductivity (BTU/hr-ft-F°): 1.25
Heat capacity (BTU/lb-F°): 0.28

Mix Properties

Cement type: Type I
Cementitious material content (lb/yd³): 630
Water/cement ratio: 0.411
Aggregate type: Limestone
PCC zero-stress temperature (F°): Derived
Ultimate shrinkage at 40% R.H (microstrain): Derived
Reversible shrinkage (% of ultimate): 50
Time to develop 50% of ultimate shrinkage: 35
Curing method: Curing compound

Strength Properties

Input level:	Level 3
28-day PCC modulus of rupture (psi):	473
28-day PCC compressive strength	n/a

Layer 2 -- Cement Stabilized**General Properties**

Material type:	Cement Stabilized
Layer thickness (in):	4
Unit weight (pcf):	135
Poisson's ratio:	0.15

Strength Properties

Elastic/resilient modulus (psi):	500000
----------------------------------	--------

Thermal Properties

Thermal conductivity (BTU/hr-ft-F°) :	1.25
Heat capacity (BTU/lb-F°):	0.28

Layer 3 -- Lime Stabilized**General Properties**

Material type:	Lime Stabilized
Layer thickness (in):	6
Unit weight (pcf):	125
Poisson's ratio:	0.2

Strength Properties

Elastic/resilient modulus (psi):	50000
----------------------------------	-------

Thermal Properties

Thermal conductivity (BTU/hr-ft-F°) :	1.25
Heat capacity (BTU/lb-F°):	0.28

Layer 4 -- A-7-6

Unbound Material:	A-7-6
Thickness(in):	12

Strength Properties

Input Level:	Level 2
Analysis Type:	ICM inputs (ICM Calculated)
Poisson's ratio:	0.35
Coefficient of lateral	0.5
Based upon PI and Gradation:	-9999
Modulus (calculated) (psi):	6268

ICM InputsGradation and Plasticity Index

Plasticity Index, PI: 25.7
 Passing #200 sieve (%): 93.3
 Passing #4 sieve (%): 100
 D60 (mm): 0.001

Calculated/Derived Parameters

Maximum dry unit weight (pcf): 98.1 (derived)
 Specific gravity of solids, Gs: 2.75 (derived)
 Saturated hydraulic conductivity (ft/hr): 3.25e-005 (derived)
 Optimum gravimetric water content: 24.2 (derived)
 Calculated degree of saturation (%): 88.8 (calculated)

Soil water characteristic curve: Default values

Parameters	Value
a	259
b	1.01
c	0.725
Hr.	13100

Layer 5 -- A-7-6

Unbound Material: A-7-6
 Thickness(in): Semi-infinite

Strength Properties

Input Level: Level 2
 Analysis Type: ICM inputs (ICM Calculated)
 Poisson's ratio: 0.35
 Coefficient of lateral: 0.5
 Based upon PI and Gradation: -9999
 Modulus (calculated) (psi): 6268

ICM InputsGradation and Plasticity Index

Plasticity Index, PI: 25.7
 Passing #200 sieve (%): 93.3
 Passing #4 sieve (%): 100
 D60 (mm): 0.001

Calculated/Derived Parameters

Maximum dry unit weight (pcf): 88.3 (derived)
 Specific gravity of solids, Gs: 2.75 (derived)
 Saturated hydraulic conductivity (ft/hr): 3.25e-005 (derived)
 Optimum gravimetric water content: 24.2 (derived)
 Calculated degree of saturation (%): 88.8 (calculated)

Soil water characteristic curve

Default values

Parameters	Value
a	259
b	1.01
c	0.725
Hr.	13100

Distress Model Calibration Settings - Rigid

Faulting

Faulting Coefficients

C1	1.29
C2	1.1
C3	0
C4	0
C5	250
C6	0.4
C7	1.2
C8	400

Reliability (FAULT)

Std. Dev.

$\text{POWER}((0.03261 \cdot \text{FAULT} + 0.00009799), 0.5)$

Cracking

Fatigue Coefficients

C1	2
C2	1.22

Cracking Coefficients

C4	1
C5	-1.68

Reliability (CRACK)

Std. Dev.

$-0.00172 \cdot \text{POWER}(\text{CRACK}, 2) + 0.3447 \cdot \text{CRACK} + 4.6772$

IRI(jpcp)

C1	0.82
C2	0.44
C3	20.4
C4	1.49
C5	25.2
Standard deviation in initial IRI	5.4

**Project: K-3344-
01.dgp
Reliability Summary**

Performance Criteria	Distress Target	Reliability Target	Distress Predicted	Reliability Predicted	Accept- able
Terminal IRI (in/mi)	164	90	120	91.88	Pass
Transverse Cracking (% slabs cracked)	15	90	0.8	99.79	Pass
Mean Joint Faulting (in)	0.12	90	0.021	99.98	Pass

Predicted distress: Project K-3344-01.dgp

Pavement age		Month	Epcc Mpsi	Ebase ksi	Dyn. k psi/in	Faultin g	Percent slabs cracked	IRI in/mile	Heavy Trucks (cumulative)	IRI at specified reliability
mo	yr									
1	0.08	December	2.92	500	121	0	0	96	27237	132.3
2	0.17	January	2.96	500	121	0	0	96.2	57427	132.5
3	0.25	February	3	500	121	0	0	96.3	87356	132.6
4	0.33	March	3.02	500	121	0	0	96.4	114163	132.7
5	0.42	April	3.04	500	121	0	0	96.4	140970	132.8
6	0.5	May	3.06	500	121	0	0	96.5	166267	132.8
7	0.58	June	3.07	500	121	0	0	96.5	191076	132.9
8	0.67	July	3.09	500	121	0	0	96.6	215400	133
9	0.75	August	3.1	500	121	0	0	96.7	240451	133
10	0.83	September	3.11	500	121	0	0	96.8	266719	133.1
11	0.92	October	3.12	500	121	0.001	0	96.8	293230	133.2
12	1	November	3.12	500	121	0.001	0	96.9	319497	133.3
13	1.08	December	3.13	500	121	0.001	0	96.9	347551	133.3
14	1.17	January	3.14	500	121	0.001	0	97	378647	133.4
15	1.25	February	3.14	500	121	0.001	0	97.1	409474	133.6
16	1.33	March	3.15	500	121	0.001	0	97.2	437085	133.6
17	1.42	April	3.16	500	121	0.001	0	97.3	464696	133.7
18	1.5	May	3.16	500	121	0.001	0	97.4	490752	133.8
19	1.58	June	3.17	500	121	0.001	0	97.4	516306	133.9
20	1.67	July	3.17	500	121	0.001	0	97.4	541360	133.9
21	1.75	August	3.18	500	121	0.001	0	97.5	567162	134
22	1.83	September	3.18	500	121	0.001	0	97.6	594218	134.1
23	1.92	October	3.18	500	121	0.001	0	97.6	621524	134.1
24	2	November	3.19	500	121	0.001	0	97.7	648579	134.2
25	2.08	December	3.19	500	121	0.001	0	97.8	677451	134.3
26	2.17	January	3.19	500	121	0.001	0	97.9	709452	134.5
27	2.25	February	3.2	500	121	0.001	0	98	741177	134.5
28	2.33	March	3.2	500	121	0.002	0	98	769592	134.6
29	2.42	April	3.2	500	121	0.002	0	98.1	798007	134.7
30	2.5	May	3.21	500	121	0.002	0	98.2	824823	134.9
31	2.58	June	3.21	500	121	0.002	0	98.3	851120	134.9
32	2.67	July	3.21	500	121	0.002	0	98.4	876904	135
33	2.75	August	3.22	500	121	0.002	0	98.4	903458	135.1
34	2.83	September	3.22	500	121	0.002	0	98.5	931302	135.1
35	2.92	October	3.22	500	121	0.002	0	98.6	959403	135.2
36	3	November	3.22	500	121	0.002	0	98.6	987247	135.3
37	3.08	December	3.23	500	121	0.002	0	98.7	1016930	135.4
38	3.17	January	3.23	500	121	0.002	0	98.8	1049840	135.6
39	3.25	February	3.23	500	121	0.002	0	98.9	1082460	135.6
40	3.33	March	3.23	500	121	0.002	0	99	1111680	135.8
41	3.42	April	3.23	500	121	0.002	0	99.1	1140900	135.8
42	3.5	May	3.24	500	121	0.002	0	99.2	1168480	135.9
43	3.58	June	3.24	500	121	0.003	0	99.2	1195520	136
44	3.67	July	3.24	500	121	0.003	0	99.3	1222030	136.1
45	3.75	August	3.24	500	121	0.003	0	99.3	1249340	136.1
46	3.83	September	3.24	500	121	0.003	0	99.4	1277970	136.3
47	3.92	October	3.24	500	121	0.003	0	99.5	1306870	136.3
48	4	November	3.25	500	121	0.003	0	99.6	1335500	136.4
49	4.08	December	3.25	500	121	0.003	0	99.7	1366000	136.5
50	4.17	January	3.25	500	121	0.003	0	99.8	1399820	136.7

51	4.25	February	3.25	500	121	0.003	0	99.9	1433340	136.8
52	4.33	March	3.25	500	121	0.003	0	100	1463360	137
53	4.42	April	3.25	500	121	0.003	0.1	100.2	1493380	137.2
54	4.5	May	3.26	500	121	0.003	0.1	100.3	1521720	137.3
55	4.58	June	3.26	500	121	0.003	0.1	100.3	1549500	137.3
56	4.67	July	3.26	500	121	0.004	0.1	100.4	1576750	137.4
57	4.75	August	3.26	500	121	0.004	0.1	100.5	1604800	137.5
58	4.83	September	3.26	500	121	0.004	0.1	100.5	1634220	137.5
59	4.92	October	3.26	500	121	0.004	0.1	100.6	1663920	137.6
60	5	November	3.26	500	121	0.004	0.1	100.7	1693340	137.8
61	5.08	December	3.27	500	121	0.004	0.1	100.8	1724660	137.9
62	5.17	January	3.27	500	121	0.004	0.1	100.9	1759380	138
63	5.25	February	3.27	500	121	0.004	0.1	101	1793790	138.1
64	5.33	March	3.27	500	121	0.004	0.1	101.1	1824620	138.2
65	5.42	April	3.27	500	121	0.004	0.1	101.2	1855450	138.3
66	5.5	May	3.27	500	121	0.004	0.1	101.3	1884540	138.5
67	5.58	June	3.27	500	121	0.004	0.1	101.4	1913070	138.6
68	5.67	July	3.27	500	121	0.004	0.1	101.4	1941050	138.6
69	5.75	August	3.28	500	121	0.004	0.1	101.5	1969850	138.7
70	5.83	September	3.28	500	121	0.005	0.1	101.6	2000060	138.8
71	5.92	October	3.28	500	121	0.005	0.1	101.7	2030550	138.9
72	6	November	3.28	500	121	0.005	0.1	101.8	2060760	139
73	6.08	December	3.28	500	121	0.005	0.1	101.9	2092900	139.1
74	6.17	January	3.28	500	121	0.005	0.1	102	2128520	139.2
75	6.25	February	3.28	500	121	0.005	0.1	102.1	2163840	139.4
76	6.33	March	3.28	500	121	0.005	0.1	102.2	2195470	139.5
77	6.42	April	3.28	500	121	0.005	0.1	102.3	2227100	139.7
78	6.5	May	3.29	500	121	0.005	0.1	102.4	2256950	139.8
79	6.58	June	3.29	500	121	0.005	0.1	102.4	2286230	139.8
80	6.67	July	3.29	500	121	0.005	0.1	102.5	2314930	139.9
81	6.75	August	3.29	500	121	0.005	0.1	102.6	2344490	140
82	6.83	September	3.29	500	121	0.006	0.1	102.6	2375490	140
83	6.92	October	3.29	500	121	0.006	0.1	102.7	2406770	140.2
84	7	November	3.29	500	121	0.006	0.1	102.8	2437760	140.3
85	7.08	December	3.29	500	121	0.006	0.1	102.9	2470720	140.4
86	7.17	January	3.29	500	121	0.006	0.1	103	2507250	140.5
87	7.25	February	3.29	500	121	0.006	0.1	103.1	2543460	140.6
88	7.33	March	3.3	500	121	0.006	0.1	103.3	2575900	140.8
89	7.42	April	3.3	500	121	0.006	0.1	103.4	2608340	140.9
90	7.5	May	3.3	500	121	0.006	0.1	103.5	2638950	141
91	7.58	June	3.3	500	121	0.006	0.1	103.5	2668970	141.1
92	7.67	July	3.3	500	121	0.006	0.1	103.6	2698400	141.2
93	7.75	August	3.3	500	121	0.007	0.2	103.7	2728710	141.3
94	7.83	September	3.3	500	121	0.007	0.2	103.8	2760490	141.5
95	7.92	October	3.3	500	121	0.007	0.2	103.9	2792570	141.5
96	8	November	3.3	500	121	0.007	0.2	104	2824360	141.7
97	8.08	December	3.3	500	121	0.007	0.2	104.1	2858130	141.8
98	8.17	January	3.3	500	121	0.007	0.2	104.2	2895570	141.9
99	8.25	February	3.3	500	121	0.007	0.2	104.3	2932680	142.1
100	8.33	March	3.3	500	121	0.007	0.2	104.5	2965920	142.2
101	8.42	April	3.31	500	121	0.007	0.2	104.6	2999160	142.4
102	8.5	May	3.31	500	121	0.007	0.2	104.7	3030530	142.5
103	8.58	June	3.31	500	121	0.008	0.2	104.7	3061290	142.5
104	8.67	July	3.31	500	121	0.008	0.2	104.8	3091450	142.6
105	8.75	August	3.31	500	121	0.008	0.2	104.9	3122520	142.7

106	8.83	September	3.31	500	121	0.008	0.2	105	3155090	142.8
107	8.92	October	3.31	500	121	0.008	0.2	105	3187960	142.9
108	9	November	3.31	500	121	0.008	0.2	105.2	3220530	143
109	9.08	December	3.31	500	121	0.008	0.2	105.3	3255120	143.2
110	9.17	January	3.31	500	121	0.008	0.2	105.4	3293460	143.3
111	9.25	February	3.31	500	121	0.008	0.2	105.5	3331470	143.4
112	9.33	March	3.31	500	121	0.009	0.2	105.6	3365520	143.6
113	9.42	April	3.31	500	121	0.009	0.2	105.7	3399560	143.7
114	9.5	May	3.31	500	121	0.009	0.2	105.8	3431690	143.8
115	9.58	June	3.31	500	121	0.009	0.2	105.9	3463200	143.9
116	9.67	July	3.31	500	121	0.009	0.2	106	3494090	144
117	9.75	August	3.31	500	121	0.009	0.2	106	3525910	144.1
118	9.83	September	3.31	500	121	0.009	0.2	106.1	3559270	144.2
119	9.92	October	3.32	500	121	0.009	0.2	106.2	3592930	144.2
120	10	November	3.32	500	121	0.009	0.3	106.4	3626290	144.5
121	10.1	December	3.32	500	121	0.009	0.3	106.5	3661700	144.6
122	10.2	January	3.32	500	121	0.009	0.3	106.6	3700950	144.7
123	10.3	February	3.32	500	121	0.009	0.3	106.7	3739860	144.9
124	10.3	March	3.32	500	121	0.01	0.3	106.9	3774710	145.1
125	10.4	April	3.32	500	121	0.01	0.3	107	3809550	145.2
126	10.5	May	3.32	500	121	0.01	0.3	107.1	3842440	145.3
127	10.6	June	3.32	500	121	0.01	0.3	107.1	3874690	145.3
128	10.7	July	3.32	500	121	0.01	0.3	107.2	3906310	145.5
129	10.8	August	3.32	500	121	0.01	0.3	107.3	3938880	145.5
130	10.8	September	3.32	500	121	0.01	0.3	107.4	3973030	145.6
131	10.9	October	3.32	500	121	0.01	0.3	107.5	4007490	145.8
132	11	November	3.32	500	121	0.01	0.3	107.6	4041640	145.9
133	11.1	December	3.32	500	121	0.01	0.3	107.7	4077870	146
134	11.2	January	3.32	500	121	0.01	0.3	107.8	4118020	146.1
135	11.3	February	3.32	500	121	0.011	0.3	107.9	4157820	146.2
136	11.3	March	3.32	500	121	0.011	0.3	108	4193480	146.4
137	11.4	April	3.32	500	121	0.011	0.3	108.1	4229130	146.6
138	11.5	May	3.32	500	121	0.011	0.3	108.3	4262780	146.8
139	11.6	June	3.32	500	121	0.011	0.3	108.3	4295770	146.8
140	11.7	July	3.32	500	121	0.011	0.3	108.4	4328120	146.9
141	11.8	August	3.32	500	121	0.011	0.3	108.5	4361440	147
142	11.8	September	3.32	500	121	0.011	0.3	108.5	4396380	147
143	11.9	October	3.32	500	121	0.011	0.3	108.6	4431640	147.1
144	12	November	3.32	500	121	0.011	0.3	108.8	4466570	147.3
145	12.1	December	3.32	500	121	0.012	0.3	108.9	4503610	147.4
146	12.2	January	3.32	500	121	0.012	0.3	109	4544670	147.6
147	12.3	February	3.33	500	121	0.012	0.3	109.1	4585380	147.7
148	12.3	March	3.33	500	121	0.012	0.3	109.3	4621830	147.9
149	12.4	April	3.33	500	121	0.012	0.4	109.5	4658290	148.1
150	12.5	May	3.33	500	121	0.012	0.4	109.6	4692690	148.2
151	12.6	June	3.33	500	121	0.012	0.4	109.6	4726440	148.3
152	12.7	July	3.33	500	121	0.012	0.4	109.7	4759520	148.4
153	12.8	August	3.33	500	121	0.012	0.4	109.8	4793590	148.5
154	12.8	September	3.33	500	121	0.012	0.4	109.9	4829310	148.6
155	12.9	October	3.33	500	121	0.012	0.4	109.9	4865360	148.6
156	13	November	3.33	500	121	0.013	0.4	110.1	4901090	148.8
157	13.1	December	3.33	500	121	0.013	0.4	110.2	4938950	149
158	13.2	January	3.33	500	121	0.013	0.4	110.3	4980910	149.1
159	13.3	February	3.33	500	121	0.013	0.4	110.4	5022510	149.2
160	13.3	March	3.33	500	121	0.013	0.4	110.6	5059770	149.4

161	13.4	April	3.33	500	121	0.013	0.4	110.7	5097040	149.5
162	13.5	May	3.33	500	121	0.013	0.4	110.8	5132200	149.7
163	13.6	June	3.33	500	121	0.013	0.4	110.9	5166680	149.8
164	13.7	July	3.33	500	121	0.013	0.4	111	5200490	149.9
165	13.8	August	3.33	500	121	0.013	0.4	111	5235320	150
166	13.8	September	3.33	500	121	0.013	0.4	111.1	5271830	150
167	13.9	October	3.33	500	121	0.014	0.4	111.2	5308680	150.1
168	14	November	3.33	500	121	0.014	0.4	111.3	5345190	150.3
169	14.1	December	3.33	500	121	0.014	0.5	111.6	5383870	150.6
170	14.2	January	3.33	500	121	0.014	0.5	111.7	5426740	150.7
171	14.3	February	3.33	500	121	0.014	0.5	111.8	5469230	150.8
172	14.3	March	3.33	500	121	0.014	0.5	111.9	5507300	151
173	14.4	April	3.33	500	121	0.014	0.5	112	5545370	151.1
174	14.5	May	3.33	500	121	0.014	0.5	112.1	5581290	151.3
175	14.6	June	3.33	500	121	0.014	0.5	112.3	5616520	151.4
176	14.7	July	3.33	500	121	0.015	0.5	112.3	5651060	151.4
177	14.8	August	3.33	500	121	0.015	0.5	112.4	5686630	151.6
178	14.8	September	3.33	500	121	0.015	0.5	112.5	5723930	151.6
179	14.9	October	3.33	500	121	0.015	0.5	112.6	5761580	151.8
180	15	November	3.33	500	121	0.015	0.5	112.7	5798880	151.9
181	15.1	December	3.33	500	121	0.015	0.5	112.8	5838370	152
182	15.2	January	3.33	500	121	0.015	0.5	113	5882140	152.2
183	15.3	February	3.33	500	121	0.015	0.5	113.1	5925540	152.3
184	15.3	March	3.33	500	121	0.015	0.5	113.2	5964410	152.5
185	15.4	April	3.33	500	121	0.016	0.5	113.3	6003280	152.7
186	15.5	May	3.33	500	121	0.016	0.5	113.5	6039960	152.8
187	15.6	June	3.34	500	121	0.016	0.5	113.5	6075940	152.9
188	15.7	July	3.34	500	121	0.016	0.5	113.6	6111210	153
189	15.8	August	3.34	500	121	0.016	0.5	113.7	6147530	153.1
190	15.8	September	3.34	500	121	0.016	0.6	113.9	6185620	153.3
191	15.9	October	3.34	500	121	0.016	0.6	114	6224060	153.4
192	16	November	3.34	500	121	0.016	0.6	114.1	6262150	153.5
193	16.1	December	3.34	500	121	0.016	0.6	114.2	6302460	153.7
194	16.2	January	3.34	500	121	0.016	0.6	114.4	6347140	153.9
195	16.3	February	3.34	500	121	0.017	0.6	114.5	6391430	154
196	16.3	March	3.34	500	121	0.017	0.6	114.7	6431110	154.2
197	16.4	April	3.34	500	121	0.017	0.6	114.8	6470780	154.3
198	16.5	May	3.34	500	121	0.017	0.6	114.9	6508220	154.5
199	16.6	June	3.34	500	121	0.017	0.6	114.9	6544940	154.5
200	16.7	July	3.34	500	121	0.017	0.6	115.1	6580940	154.7
201	16.8	August	3.34	500	121	0.017	0.6	115.1	6618010	154.7
202	16.8	September	3.34	500	121	0.017	0.6	115.2	6656890	154.9
203	16.9	October	3.34	500	121	0.017	0.6	115.4	6696130	155
204	17	November	3.34	500	121	0.017	0.6	115.5	6735000	155.1
205	17.1	December	3.34	500	121	0.017	0.6	115.6	6776130	155.3
206	17.2	January	3.34	500	121	0.018	0.6	115.8	6821720	155.5
207	17.3	February	3.34	500	121	0.018	0.6	115.9	6866910	155.6
208	17.3	March	3.34	500	121	0.018	0.6	116	6907390	155.8
209	17.4	April	3.34	500	121	0.018	0.6	116.2	6947870	155.9
210	17.5	May	3.34	500	121	0.018	0.6	116.3	6986070	156.1
211	17.6	June	3.34	500	121	0.018	0.6	116.3	7023530	156.1
212	17.7	July	3.34	500	121	0.018	0.7	116.5	7060260	156.4
213	17.8	August	3.34	500	121	0.018	0.7	116.6	7098080	156.4
214	17.8	September	3.34	500	121	0.018	0.7	116.7	7137750	156.6
215	17.9	October	3.34	500	121	0.018	0.7	116.8	7177780	156.7

216	18	November	3.35	500	121	0.018	0.7	117	7217440	156.8
217	18.1	December	3.35	500	121	0.019	0.7	117.1	7259390	157
218	18.2	January	3.35	500	121	0.019	0.7	117.2	7305880	157.2
219	18.3	February	3.35	500	121	0.019	0.7	117.4	7351970	157.3
220	18.3	March	3.35	500	121	0.019	0.7	117.5	7393250	157.5
221	18.4	April	3.35	500	121	0.019	0.7	117.7	7434540	157.7
222	18.5	May	3.35	500	121	0.019	0.7	117.8	7473490	157.8
223	18.6	June	3.35	500	121	0.019	0.7	117.9	7511700	157.9
224	18.7	July	3.35	500	121	0.019	0.7	118	7549160	158
225	18.8	August	3.35	500	121	0.019	0.7	118.1	7587740	158.1
226	18.8	September	3.35	500	121	0.019	0.8	118.2	7628190	158.3
227	18.9	October	3.35	500	121	0.02	0.8	118.4	7669020	158.4
228	19	November	3.35	500	121	0.02	0.8	118.5	7709470	158.6
229	19.1	December	3.35	500	121	0.02	0.8	118.6	7752230	158.7
230	19.2	January	3.35	500	121	0.02	0.8	118.8	7799630	158.9
231	19.3	February	3.35	500	121	0.02	0.8	118.9	7846620	159.1
232	19.3	March	3.35	500	121	0.02	0.8	119.1	7888700	159.3
233	19.4	April	3.35	500	121	0.02	0.8	119.2	7930790	159.4
234	19.5	May	3.36	500	121	0.02	0.8	119.4	7970510	159.6
235	19.6	June	3.36	500	121	0.02	0.8	119.4	8009460	159.7
236	19.7	July	3.36	500	121	0.021	0.8	119.5	8047650	159.8
237	19.8	August	3.36	500	121	0.021	0.8	119.6	8086980	159.9
238	19.8	September	3.36	500	121	0.021	0.8	119.7	8128220	160
239	19.9	October	3.36	500	121	0.021	0.8	119.8	8169840	160.1
240	20	November	3.36	500	121	0.021	0.8	120	8211080	160.4

Predicted faulting: Project K-3344-01(traffic).dgp

Pavement		Month	Epc Mpsi	Ebase ksi	Dyn. k psi/in	Ave. R.H. %	Ave. ΔT °F	Joint open. in	L T E %	18-kip single		36-kip tandem		D.E. in-lb	Faulting in	Faulting at specified reliability
mo	yr									Loa ded	Unlo aded	Loa ded	Unlo aded			
1	0	December	2.9	500	121	74	-21	0.053	95	0	0.03	0	0.03	0.5	0	0.013
2	0	January	3	500	121	75.8	-18	0.057	95	0	0.03	0	0.03	0.4	0	0.013
3	0	February	3	500	121	72.7	-17	0.054	95	0	0.02	0	0.03	0.7	0	0.013
4	0	March	3	500	121	68.2	-17	0.05	95	0	0.03	0	0.03	0.5	0	0.013
5	0	April	3	500	121	66.5	-16	0.043	95	0	0.02	0	0.03	0.7	0	0.013
6	1	May	3.1	500	121	70.4	-17	0.035	95	0	0.02	0	0.03	0.1	0	0.013
7	1	June	3.1	500	121	73.6	-18	0.031	95	0	0.03	0	0.03	0.6	0	0.014
8	1	July	3.1	500	121	71.8	-19	0.025	95	0	0.03	0	0.03	0.3	0	0.014
9	1	August	3.1	500	121	67.8	-20	0.025	95	0	0.03	0	0.03	0.6	0	0.014
10	1	September	3.1	500	121	68.7	-22	0.034	95	0	0.03	0	0.03	0.7	0	0.014
11	1	October	3.1	500	121	69.2	-20	0.042	95	0	0.03	0	0.03	0.8	0.001	0.014
12	1	November	3.1	500	121	69.6	-21	0.051	95	0	0.03	0	0.03	0.5	0.001	0.014
13	1	December	3.1	500	121	74	-21	0.06	94	0	0.03	0	0.03	0.8	0.001	0.014
14	1	January	3.1	500	121	75.8	-19	0.062	94	0	0.03	0	0.03	0.6	0.001	0.015
15	1	February	3.1	500	121	72.7	-17	0.058	94	0	0.02	0	0.03	1	0.001	0.015
16	1	March	3.2	500	121	68.2	-17	0.053	94	0	0.02	0	0.03	0.7	0.001	0.015
17	1	April	3.2	500	121	66.5	-16	0.046	95	0	0.02	0	0.03	0.7	0.001	0.015
18	2	May	3.2	500	121	70.4	-17	0.038	95	0	0.02	0	0.03	0.1	0.001	0.015
19	2	June	3.2	500	121	73.6	-18	0.033	95	0	0.03	0	0.03	0.6	0.001	0.015
20	2	July	3.2	500	121	71.8	-19	0.027	95	0	0.03	0	0.03	0.3	0.001	0.015
21	2	August	3.2	500	121	67.8	-20	0.027	95	0	0.03	0	0.03	0.6	0.001	0.016
22	2	September	3.2	500	121	68.7	-22	0.035	95	0	0.03	0	0.03	0.7	0.001	0.016
23	2	October	3.2	500	121	69.2	-20	0.043	95	0	0.03	0	0.03	0.9	0.001	0.016
24	2	November	3.2	500	121	69.6	-21	0.052	94	0	0.03	0	0.03	0.7	0.001	0.016
25	2	December	3.2	500	121	74	-21	0.061	93	0	0.03	0	0.03	1.1	0.001	0.016
26	2	January	3.2	500	121	75.8	-19	0.063	93	0	0.03	0	0.03	0.8	0.001	0.016
27	2	February	3.2	500	121	72.7	-17	0.059	93	0	0.02	0	0.03	1.3	0.001	0.017
28	2	March	3.2	500	121	68.2	-17	0.054	93	0	0.02	0	0.03	0.9	0.002	0.017
29	2	April	3.2	500	121	66.5	-16	0.046	94	0	0.02	0	0.03	0.9	0.002	0.017
30	3	May	3.2	500	121	70.4	-17	0.038	95	0	0.02	0	0.03	0.1	0.002	0.017
31	3	June	3.2	500	121	73.6	-18	0.033	95	0	0.02	0	0.03	0.6	0.002	0.018
32	3	July	3.2	500	121	71.8	-19	0.028	95	0	0.03	0	0.03	0.4	0.002	0.018
33	3	August	3.2	500	121	67.8	-20	0.028	95	0	0.03	0	0.03	0.6	0.002	0.018
34	3	September	3.2	500	121	68.7	-22	0.035	95	0	0.03	0	0.03	0.7	0.002	0.018
35	3	October	3.2	500	121	69.2	-20	0.043	95	0	0.03	0	0.03	1	0.002	0.018
36	3	November	3.2	500	121	69.6	-21	0.052	93	0	0.03	0	0.03	0.9	0.002	0.018
37	3	December	3.2	500	121	74	-21	0.061	92	0	0.03	0	0.03	1.3	0.002	0.019
38	3	January	3.2	500	121	75.8	-19	0.063	92	0	0.03	0	0.03	1	0.002	0.019

39	3	February	3.2	500	121	72.7	-17	0.059	92	0	0.02	0	0.03	1.6	0.002	0.019
40	3	March	3.2	500	121	68.2	-17	0.054	93	0	0.02	0	0.03	1.1	0.002	0.019
41	3	April	3.2	500	121	66.5	-16	0.047	94	0	0.02	0	0.03	1.1	0.002	0.019
42	4	May	3.2	500	121	70.4	-17	0.039	95	0	0.02	0	0.03	0.2	0.002	0.019
43	4	June	3.2	500	121	73.6	-18	0.034	95	0	0.02	0	0.03	0.7	0.003	0.02
44	4	July	3.2	500	121	71.8	-19	0.028	95	0	0.03	0	0.03	0.4	0.003	0.02
45	4	August	3.2	500	121	67.8	-20	0.028	95	0	0.03	0	0.03	0.6	0.003	0.02
46	4	September	3.2	500	121	68.7	-22	0.035	95	0	0.03	0	0.03	0.7	0.003	0.02
47	4	October	3.2	500	121	69.2	-20	0.044	94	0	0.03	0	0.03	1.2	0.003	0.02
48	4	November	3.3	500	121	69.6	-21	0.053	93	0	0.03	0	0.03	1	0.003	0.02
49	4	December	3.3	500	121	74	-21	0.061	92	0	0.03	0	0.03	1.4	0.003	0.021
50	4	January	3.3	500	121	75.8	-19	0.063	92	0	0.02	0	0.03	1.1	0.003	0.021
51	4	February	3.3	500	121	72.7	-17	0.059	92	0	0.02	0	0.03	1.8	0.003	0.021
52	4	March	3.3	500	121	68.2	-17	0.055	92	0	0.02	0	0.03	1.2	0.003	0.022
53	4	April	3.3	500	121	66.5	-16	0.047	93	0	0.02	0	0.03	1.2	0.003	0.022
54	5	May	3.3	500	121	70.4	-17	0.039	95	0	0.02	0	0.03	0.2	0.003	0.022
55	5	June	3.3	500	121	73.6	-18	0.034	95	0	0.02	0	0.03	0.7	0.003	0.022
56	5	July	3.3	500	121	71.8	-19	0.028	95	0	0.03	0	0.03	0.4	0.004	0.022
57	5	August	3.3	500	121	67.8	-20	0.028	95	0	0.03	0	0.03	0.6	0.004	0.022
58	5	September	3.3	500	121	68.7	-22	0.036	95	0	0.03	0	0.03	0.7	0.004	0.022
59	5	October	3.3	500	121	69.2	-20	0.044	94	0	0.03	0	0.03	1.3	0.004	0.023
60	5	November	3.3	500	121	69.6	-21	0.053	92	0	0.03	0	0.03	1.1	0.004	0.023
61	5	December	3.3	500	121	74	-21	0.062	91	0	0.03	0	0.03	1.5	0.004	0.023
62	5	January	3.3	500	121	75.8	-19	0.063	91	0	0.02	0	0.03	1.2	0.004	0.023
63	5	February	3.3	500	121	72.7	-17	0.059	92	0	0.02	0	0.03	1.9	0.004	0.024
64	5	March	3.3	500	121	68.2	-17	0.055	92	0	0.02	0	0.03	1.3	0.004	0.024
65	5	April	3.3	500	121	66.5	-16	0.047	93	0	0.02	0	0.03	1.3	0.004	0.024
66	6	May	3.3	500	121	70.4	-17	0.039	95	0	0.02	0	0.03	0.2	0.004	0.024
67	6	June	3.3	500	121	73.6	-18	0.034	95	0	0.02	0	0.03	0.7	0.004	0.024
68	6	July	3.3	500	121	71.8	-19	0.028	95	0	0.03	0	0.03	0.4	0.004	0.024
69	6	August	3.3	500	121	67.8	-20	0.028	95	0	0.03	0	0.03	0.6	0.004	0.025
70	6	September	3.3	500	121	68.7	-22	0.036	95	0	0.03	0	0.03	0.8	0.005	0.025
71	6	October	3.3	500	121	69.2	-20	0.044	94	0	0.03	0	0.03	1.4	0.005	0.025
72	6	November	3.3	500	121	69.6	-21	0.053	92	0	0.03	0	0.03	1.2	0.005	0.025
73	6	December	3.3	500	121	74	-21	0.062	91	0	0.03	0	0.03	1.6	0.005	0.025
74	6	January	3.3	500	121	75.8	-19	0.063	91	0	0.02	0	0.03	1.2	0.005	0.026
75	6	February	3.3	500	121	72.7	-17	0.059	91	0	0.02	0	0.03	2	0.005	0.026
76	6	March	3.3	500	121	68.2	-17	0.055	92	0	0.02	0	0.03	1.4	0.005	0.026
77	6	April	3.3	500	121	66.5	-16	0.047	93	0	0.02	0	0.03	1.4	0.005	0.027
78	7	May	3.3	500	121	70.4	-17	0.039	95	0	0.02	0	0.03	0.2	0.005	0.027
79	7	June	3.3	500	121	73.6	-18	0.034	95	0	0.02	0	0.03	0.7	0.005	0.027
80	7	July	3.3	500	121	71.8	-19	0.028	95	0	0.03	0	0.03	0.4	0.005	0.027
81	7	August	3.3	500	121	67.8	-20	0.028	95	0	0.03	0	0.03	0.7	0.005	0.027
82	7	September	3.3	500	121	68.7	-22	0.036	95	0	0.03	0	0.03	0.8	0.006	0.027

83	7	October	3.3	500	121	69.2	-20	0.044	94	0	0.03	0	0.03	1.5	0.006	0.027
84	7	November	3.3	500	121	69.6	-21	0.053	92	0	0.03	0	0.03	1.2	0.006	0.028
85	7	December	3.3	500	121	74	-21	0.062	91	0	0.03	0	0.03	1.7	0.006	0.028
86	7	January	3.3	500	121	75.8	-19	0.063	91	0	0.02	0	0.03	1.3	0.006	0.028
87	7	February	3.3	500	121	72.7	-17	0.059	91	0	0.02	0	0.03	2.1	0.006	0.028
88	7	March	3.3	500	121	68.2	-17	0.055	92	0	0.02	0	0.03	1.4	0.006	0.029
89	7	April	3.3	500	121	66.5	-16	0.047	93	0	0.02	0	0.03	1.5	0.006	0.029
90	8	May	3.3	500	121	70.4	-17	0.039	95	0	0.02	0	0.03	0.2	0.006	0.029
91	8	June	3.3	500	121	73.6	-18	0.034	95	0	0.02	0	0.03	0.7	0.006	0.029
92	8	July	3.3	500	121	71.8	-19	0.028	95	0	0.03	0	0.03	0.4	0.006	0.029
93	8	August	3.3	500	121	67.8	-20	0.028	95	0	0.03	0	0.03	0.7	0.007	0.029
94	8	September	3.3	500	121	68.7	-22	0.036	95	0	0.03	0	0.03	0.8	0.007	0.029
95	8	October	3.3	500	121	69.2	-20	0.044	94	0	0.03	0	0.03	1.6	0.007	0.03
96	8	November	3.3	500	121	69.6	-21	0.053	92	0	0.03	0	0.03	1.3	0.007	0.03
97	8	December	3.3	500	121	74	-21	0.062	91	0	0.03	0	0.03	1.8	0.007	0.03
98	8	January	3.3	500	121	75.8	-19	0.064	91	0	0.02	0	0.03	1.3	0.007	0.03
99	8	February	3.3	500	121	72.7	-17	0.059	91	0	0.02	0	0.03	2.2	0.007	0.031
100	8	March	3.3	500	121	68.2	-17	0.055	92	0	0.02	0	0.03	1.5	0.007	0.031
101	8	April	3.3	500	121	66.5	-16	0.047	93	0	0.02	0	0.03	1.5	0.007	0.031
102	9	May	3.3	500	121	70.4	-17	0.039	95	0	0.02	0	0.03	0.2	0.007	0.031
103	9	June	3.3	500	121	73.6	-18	0.034	95	0	0.02	0	0.03	0.8	0.008	0.031
104	9	July	3.3	500	121	71.8	-19	0.028	95	0	0.03	0	0.03	0.4	0.008	0.031
105	9	August	3.3	500	121	67.8	-20	0.028	95	0	0.03	0	0.03	0.7	0.008	0.032
106	9	September	3.3	500	121	68.7	-22	0.036	95	0	0.03	0	0.03	0.8	0.008	0.032
107	9	October	3.3	500	121	69.2	-20	0.044	94	0	0.03	0	0.03	1.6	0.008	0.032
108	9	November	3.3	500	121	69.6	-21	0.053	92	0	0.03	0	0.03	1.3	0.008	0.032
109	9	December	3.3	500	121	74	-21	0.062	91	0	0.03	0	0.03	1.8	0.008	0.032
110	9	January	3.3	500	121	75.8	-19	0.064	91	0	0.02	0	0.03	1.4	0.008	0.033
111	9	February	3.3	500	121	72.7	-17	0.06	91	0	0.02	0	0.03	2.3	0.008	0.033
112	9	March	3.3	500	121	68.2	-17	0.055	92	0	0.02	0	0.03	1.5	0.009	0.033
113	9	April	3.3	500	121	66.5	-16	0.047	93	0	0.02	0	0.03	1.6	0.009	0.034
114	10	May	3.3	500	121	70.4	-17	0.039	95	0	0.02	0	0.03	0.2	0.009	0.034
115	10	June	3.3	500	121	73.6	-18	0.034	95	0	0.02	0	0.03	0.8	0.009	0.034
116	10	July	3.3	500	121	71.8	-19	0.028	95	0	0.03	0	0.03	0.4	0.009	0.034
117	10	August	3.3	500	121	67.8	-20	0.028	95	0	0.03	0	0.03	0.7	0.009	0.034
118	10	September	3.3	500	121	68.7	-22	0.036	95	0	0.03	0	0.03	0.8	0.009	0.034
119	10	October	3.3	500	121	69.2	-20	0.044	94	0	0.03	0	0.03	1.7	0.009	0.034
120	10	November	3.3	500	121	69.6	-21	0.053	92	0	0.03	0	0.03	1.4	0.009	0.035
121	10	December	3.3	500	121	74	-21	0.062	91	0	0.03	0	0.03	1.9	0.009	0.035
122	10	January	3.3	500	121	75.8	-19	0.064	91	0	0.02	0	0.03	1.4	0.009	0.035
123	10	February	3.3	500	121	72.7	-17	0.06	91	0	0.02	0	0.03	2.3	0.009	0.035
124	10	March	3.3	500	121	68.2	-17	0.055	92	0	0.02	0	0.03	1.6	0.01	0.036
125	10	April	3.3	500	121	66.5	-16	0.047	93	0	0.02	0	0.03	1.6	0.01	0.036
126	11	May	3.3	500	121	70.4	-17	0.039	95	0	0.02	0	0.03	0.2	0.01	0.036

127	11	June	3.3	500	121	73.6	-18	0.034	95	0	0.02	0	0.03	0.8	0.01	0.036
128	11	July	3.3	500	121	71.8	-19	0.028	95	0	0.03	0	0.03	0.4	0.01	0.036
129	11	August	3.3	500	121	67.8	-20	0.028	95	0	0.03	0	0.03	0.7	0.01	0.036
130	11	September	3.3	500	121	68.7	-22	0.036	95	0	0.03	0	0.03	0.9	0.01	0.036
131	11	October	3.3	500	121	69.2	-20	0.044	93	0	0.03	0	0.03	1.7	0.01	0.037
132	11	November	3.3	500	121	69.6	-21	0.053	92	0	0.03	0	0.03	1.4	0.01	0.037
133	11	December	3.3	500	121	74	-21	0.062	91	0	0.03	0	0.03	1.9	0.01	0.037
134	11	January	3.3	500	121	75.8	-19	0.064	91	0	0.02	0	0.03	1.5	0.01	0.037
135	11	February	3.3	500	121	72.7	-17	0.06	91	0	0.02	0	0.03	2.4	0.011	0.038
136	11	March	3.3	500	121	68.2	-17	0.055	92	0	0.02	0	0.03	1.6	0.011	0.038
137	11	April	3.3	500	121	66.5	-16	0.047	93	0	0.02	0	0.03	1.6	0.011	0.038
138	12	May	3.3	500	121	70.4	-17	0.039	95	0	0.02	0	0.03	0.2	0.011	0.038
139	12	June	3.3	500	121	73.6	-18	0.034	95	0	0.02	0	0.03	0.8	0.011	0.038
140	12	July	3.3	500	121	71.8	-19	0.028	95	0	0.03	0	0.03	0.4	0.011	0.038
141	12	August	3.3	500	121	67.8	-20	0.028	95	0	0.03	0	0.03	0.8	0.011	0.038
142	12	September	3.3	500	121	68.7	-22	0.036	95	0	0.03	0	0.03	0.9	0.011	0.039
143	12	October	3.3	500	121	69.2	-20	0.044	93	0	0.03	0	0.03	1.8	0.011	0.039
144	12	November	3.3	500	121	69.6	-21	0.053	92	0	0.03	0	0.03	1.4	0.011	0.039
145	12	December	3.3	500	121	74	-21	0.062	91	0	0.03	0	0.03	2	0.012	0.039
146	12	January	3.3	500	121	75.8	-19	0.064	91	0	0.02	0	0.03	1.5	0.012	0.04
147	12	February	3.3	500	121	72.7	-17	0.06	91	0	0.02	0	0.03	2.4	0.012	0.04
148	12	March	3.3	500	121	68.2	-17	0.055	92	0	0.02	0	0.03	1.6	0.012	0.04
149	12	April	3.3	500	121	66.5	-16	0.047	93	0	0.02	0	0.03	1.7	0.012	0.04
150	13	May	3.3	500	121	70.4	-17	0.039	95	0	0.02	0	0.03	0.2	0.012	0.04
151	13	June	3.3	500	121	73.6	-18	0.034	95	0	0.02	0	0.03	0.8	0.012	0.041
152	13	July	3.3	500	121	71.8	-19	0.028	95	0	0.03	0	0.03	0.5	0.012	0.041
153	13	August	3.3	500	121	67.8	-20	0.028	95	0	0.03	0	0.03	0.8	0.012	0.041
154	13	September	3.3	500	121	68.7	-22	0.036	95	0	0.03	0	0.03	0.9	0.012	0.041
155	13	October	3.3	500	121	69.2	-20	0.044	93	0	0.03	0	0.03	1.8	0.012	0.041
156	13	November	3.3	500	121	69.6	-21	0.053	92	0	0.03	0	0.03	1.5	0.013	0.041
157	13	December	3.3	500	121	74	-21	0.062	91	0	0.03	0	0.03	2	0.013	0.042
158	13	January	3.3	500	121	75.8	-19	0.064	91	0	0.02	0	0.03	1.5	0.013	0.042
159	13	February	3.3	500	121	72.7	-17	0.06	91	0	0.02	0	0.03	2.5	0.013	0.042
160	13	March	3.3	500	121	68.2	-17	0.055	92	0	0.02	0	0.03	1.7	0.013	0.042
161	13	April	3.3	500	121	66.5	-16	0.047	93	0	0.02	0	0.03	1.7	0.013	0.043
162	14	May	3.3	500	121	70.4	-17	0.039	95	0	0.02	0	0.03	0.2	0.013	0.043
163	14	June	3.3	500	121	73.6	-18	0.034	95	0	0.02	0	0.03	0.9	0.013	0.043
164	14	July	3.3	500	121	71.8	-19	0.028	95	0	0.03	0	0.03	0.5	0.013	0.043
165	14	August	3.3	500	121	67.8	-20	0.028	95	0	0.03	0	0.03	0.8	0.013	0.043
166	14	September	3.3	500	121	68.7	-22	0.036	95	0	0.03	0	0.03	0.9	0.013	0.043
167	14	October	3.3	500	121	69.2	-20	0.044	93	0	0.03	0	0.03	1.9	0.014	0.043
168	14	November	3.3	500	121	69.6	-21	0.053	92	0	0.03	0	0.03	1.5	0.014	0.044
169	14	December	3.3	500	121	74	-21	0.062	91	0	0.03	0	0.03	2	0.014	0.044
170	14	January	3.3	500	121	75.8	-19	0.064	91	0	0.02	0	0.03	1.6	0.014	0.044

171	14	February	3.3	500	121	72.7	-17	0.06	91	0	0.02	0	0.03	2.5	0.014	0.044
172	14	March	3.3	500	121	68.2	-17	0.055	92	0	0.02	0	0.03	1.7	0.014	0.045
173	14	April	3.3	500	121	66.5	-16	0.047	93	0	0.02	0	0.03	1.8	0.014	0.045
174	15	May	3.3	500	121	70.4	-17	0.039	95	0	0.02	0	0.03	0.2	0.014	0.045
175	15	June	3.3	500	121	73.6	-18	0.034	95	0	0.02	0	0.03	0.9	0.014	0.045
176	15	July	3.3	500	121	71.8	-19	0.028	95	0	0.03	0	0.03	0.5	0.015	0.045
177	15	August	3.3	500	121	67.8	-20	0.028	95	0	0.03	0	0.03	0.8	0.015	0.045
178	15	September	3.3	500	121	68.7	-22	0.036	95	0	0.03	0	0.03	0.9	0.015	0.045
179	15	October	3.3	500	121	69.2	-20	0.044	93	0	0.03	0	0.03	1.9	0.015	0.045
180	15	November	3.3	500	121	69.6	-21	0.053	92	0	0.03	0	0.03	1.5	0.015	0.046
181	15	December	3.3	500	121	74	-21	0.062	91	0	0.03	0	0.03	2.1	0.015	0.046
182	15	January	3.3	500	121	75.8	-19	0.064	91	0	0.02	0	0.03	1.6	0.015	0.046
183	15	February	3.3	500	121	72.7	-17	0.06	91	0	0.02	0	0.03	2.6	0.015	0.047
184	15	March	3.3	500	121	68.2	-17	0.055	92	0	0.02	0	0.03	1.7	0.015	0.047
185	15	April	3.3	500	121	66.5	-16	0.047	93	0	0.02	0	0.03	1.8	0.016	0.047
186	16	May	3.3	500	121	70.4	-17	0.039	95	0	0.02	0	0.03	0.2	0.016	0.047
187	16	June	3.3	500	121	73.6	-18	0.034	95	0	0.02	0	0.03	0.9	0.016	0.047
188	16	July	3.3	500	121	71.8	-19	0.028	95	0	0.03	0	0.03	0.5	0.016	0.047
189	16	August	3.3	500	121	67.8	-20	0.028	95	0	0.03	0	0.03	0.8	0.016	0.047
190	16	September	3.3	500	121	68.7	-22	0.036	95	0	0.03	0	0.03	1	0.016	0.048
191	16	October	3.3	500	121	69.2	-20	0.044	93	0	0.03	0	0.03	1.9	0.016	0.048
192	16	November	3.3	500	121	69.6	-21	0.053	92	0	0.03	0	0.03	1.6	0.016	0.048
193	16	December	3.3	500	121	74	-21	0.062	91	0	0.03	0	0.03	2.1	0.016	0.048
194	16	January	3.3	500	121	75.8	-19	0.064	91	0	0.02	0	0.03	1.6	0.016	0.048
195	16	February	3.3	500	121	72.7	-17	0.06	91	0	0.02	0	0.03	2.7	0.017	0.049
196	16	March	3.3	500	121	68.2	-17	0.055	92	0	0.02	0	0.03	1.8	0.017	0.049
197	16	April	3.3	500	121	66.5	-16	0.047	93	0	0.02	0	0.03	1.8	0.017	0.049
198	17	May	3.3	500	121	70.4	-17	0.039	95	0	0.02	0	0.03	0.2	0.017	0.049
199	17	June	3.3	500	121	73.6	-18	0.034	95	0	0.02	0	0.03	0.9	0.017	0.049
200	17	July	3.3	500	121	71.8	-19	0.028	95	0	0.03	0	0.03	0.5	0.017	0.049
201	17	August	3.3	500	121	67.8	-20	0.028	95	0	0.03	0	0.03	0.8	0.017	0.05
202	17	September	3.3	500	121	68.7	-22	0.036	95	0	0.03	0	0.03	1	0.017	0.05
203	17	October	3.3	500	121	69.2	-20	0.044	93	0	0.03	0	0.03	2	0.017	0.05
204	17	November	3.3	500	121	69.6	-21	0.053	92	0	0.03	0	0.03	1.6	0.017	0.05
205	17	December	3.3	500	121	74	-21	0.062	91	0	0.03	0	0.03	2.2	0.017	0.05
206	17	January	3.3	500	121	75.8	-19	0.064	91	0	0.02	0	0.03	1.6	0.018	0.051
207	17	February	3.3	500	121	72.7	-17	0.06	91	0	0.02	0	0.03	2.7	0.018	0.051
208	17	March	3.3	500	121	68.2	-17	0.055	92	0	0.02	0	0.03	1.8	0.018	0.051
209	17	April	3.3	500	121	66.5	-16	0.047	93	0	0.02	0	0.03	1.9	0.018	0.051
210	18	May	3.3	500	121	70.4	-17	0.039	95	0	0.02	0	0.03	0.2	0.018	0.051
211	18	June	3.3	500	121	73.6	-18	0.034	95	0	0.02	0	0.03	0.9	0.018	0.052
212	18	July	3.3	500	121	71.8	-19	0.028	95	0	0.03	0	0.03	0.5	0.018	0.052
213	18	August	3.3	500	121	67.8	-20	0.028	95	0	0.03	0	0.03	0.9	0.018	0.052
214	18	September	3.3	500	121	68.7	-22	0.036	95	0	0.03	0	0.03	1	0.018	0.052

215	18	October	3.3	500	121	69.2	-20	0.044	93	0	0.03	0	0.03	2	0.018	0.052
216	18	November	3.4	500	121	69.6	-21	0.053	92	0	0.03	0	0.03	1.6	0.018	0.052
217	18	December	3.4	500	121	74	-21	0.062	91	0	0.03	0	0.03	2.2	0.019	0.053
218	18	January	3.4	500	121	75.8	-19	0.064	91	0	0.02	0	0.03	1.7	0.019	0.053
219	18	February	3.4	500	121	72.7	-17	0.06	91	0	0.02	0	0.03	2.8	0.019	0.053
220	18	March	3.4	500	121	68.2	-17	0.055	92	0	0.02	0	0.03	1.8	0.019	0.053
221	18	April	3.4	500	121	66.5	-16	0.047	93	0	0.02	0	0.03	1.9	0.019	0.054
222	19	May	3.4	500	121	70.4	-17	0.039	95	0	0.02	0	0.03	0.2	0.019	0.054
223	19	June	3.4	500	121	73.6	-18	0.034	95	0	0.02	0	0.03	0.9	0.019	0.054
224	19	July	3.4	500	121	71.8	-19	0.028	95	0	0.03	0	0.03	0.5	0.019	0.054
225	19	August	3.4	500	121	67.8	-20	0.029	95	0	0.03	0	0.03	0.9	0.019	0.054
226	19	September	3.4	500	121	68.7	-22	0.036	95	0	0.03	0	0.03	1	0.019	0.054
227	19	October	3.4	500	121	69.2	-20	0.044	93	0	0.03	0	0.03	2.1	0.02	0.054
228	19	November	3.4	500	121	69.6	-21	0.053	92	0	0.03	0	0.03	1.7	0.02	0.054
229	19	December	3.4	500	121	74	-21	0.062	91	0	0.03	0	0.03	2.3	0.02	0.055
230	19	January	3.4	500	121	75.8	-19	0.064	91	0	0.02	0	0.03	1.7	0.02	0.055
231	19	February	3.4	500	121	72.7	-17	0.06	91	0	0.02	0	0.03	2.8	0.02	0.055
232	19	March	3.4	500	121	68.2	-17	0.055	92	0	0.02	0	0.03	1.9	0.02	0.055
233	19	April	3.4	500	121	66.5	-16	0.047	93	0	0.02	0	0.03	2	0.02	0.056
234	20	May	3.4	500	121	70.4	-17	0.039	95	0	0.02	0	0.03	0.2	0.02	0.056
235	20	June	3.4	500	121	73.6	-18	0.034	95	0	0.02	0	0.03	1	0.02	0.056
236	20	July	3.4	500	121	71.8	-19	0.028	95	0	0.02	0	0.03	0.5	0.021	0.056
237	20	August	3.4	500	121	67.8	-20	0.029	95	0	0.03	0	0.03	0.9	0.021	0.056
238	20	September	3.4	500	121	68.7	-22	0.036	95	0	0.03	0	0.03	1	0.021	0.056
239	20	October	3.4	500	121	69.2	-20	0.044	93	0	0.03	0	0.03	2.1	0.021	0.057
240	20	November	3.4	500	121	69.6	-21	0.053	92	0	0.03	0	0.03	1.7	0.021	0.057
															0.0209	

Predicted cracking: Project K-3344-01(traffic).dgp

Pavement		Month	Cumulative Fatigue Damage									Percent slabs cracked	d at specific reliability	
mo	yr		Bottom-up					Top-down						
			Single	Tandem	Tridem	Quad	Total	S WB	M WB	L WB	Total			
1	0	December	0	0	0	0	0	0	0	0	0	0	0	6
2	0	January	0	0	0	0	0	0	0	0	0	0	0	6
3	0	February	0	0	0	0	0	0	0	0	0	0	0	6
4	0	March	0	0	0	0	0	0	0	0	0	0	0	6
5	0	April	0	0	0	0	0	0	0	0	0	0	0	6
6	1	May	0	0	0	0	0	0	0	0	0	0	0	6
7	1	June	0	0	0	0	0	0	0	0	0	0	0	6
8	1	July	0	0	0	0	0	0	0	0	0	0	0	6
9	1	August	0	0	0	0	0	0	0	0	0	0	0	6
10	1	September	0	0	0	0	0	0	0	0	0	0	0	6
11	1	October	0	0	0	0	0	0	0	0	0	0	0	6
12	1	November	0	0	0	0	0	0	0	0	0	0	0	6
13	1	December	0	0	0	0	0	0	0.0001	0	2E-04	0	0	6
14	1	January	0	0	0	0	0	0	0.0001	0	2E-04	0	0	6
15	1	February	0.0001	0	0	0	1E-04	0	0.0002	0	3E-04	0	0	6
16	1	March	0.0001	0	0	0	1E-04	0	0.0002	0	4E-04	0	0	6
17	1	April	0.0001	0.0001	0	0	2E-04	0	0.0004	0	7E-04	0	0	6
18	2	May	0.0001	0.0001	0	0	3E-04	0	0.0004	0	8E-04	0	0	6
19	2	June	0.0006	0.0001	0	0	7E-04	0	0.0005	0	0.001	0	0	6
20	2	July	0.0006	0.0001	0	0	8E-04	0	0.0006	0	0.001	0	0	6
21	2	August	0.0006	0.0002	0	0	8E-04	0	0.001	0	0.002	0	0	6
22	2	September	0.0007	0.0002	0	0	8E-04	0	0.0015	0	0.003	0	0	6
23	2	October	0.0007	0.0002	0	0	8E-04	0	0.0018	0	0.004	0	0	6
24	2	November	0.0007	0.0002	0	0	8E-04	0	0.0019	0	0.004	0	0	6
25	2	December	0.0007	0.0002	0	0	8E-04	0	0.002	0	0.004	0	0	6
26	2	January	0.0007	0.0002	0	0	9E-04	0	0.002	0	0.004	0	0	6
27	2	February	0.0007	0.0002	0	0	9E-04	0	0.002	0	0.004	0	0	6
28	2	March	0.0007	0.0002	0	0	9E-04	0	0.0021	0	0.004	0	0	6
29	2	April	0.0007	0.0003	0	0	0.001	0	0.0022	0	0.004	0	0	6
30	3	May	0.0008	0.0003	0	0	0.001	0	0.0022	0	0.004	0	0	6
31	3	June	0.0011	0.0003	0	0	0.002	0	0.0024	0	0.005	0	0	6
32	3	July	0.0012	0.0003	0	0	0.002	0	0.0024	0	0.005	0	0	6
33	3	August	0.0012	0.0003	0	0	0.002	0	0.0028	0	0.005	0	0	6
34	3	September	0.0012	0.0003	0	0	0.002	0	0.0032	0	0.006	0	0	6
35	3	October	0.0012	0.0004	0	0	0.002	0	0.0035	0	0.007	0	0	6
36	3	November	0.0012	0.0004	0	0	0.002	0	0.0036	0	0.007	0	0	6
37	3	December	0.0012	0.0004	0	0	0.002	0	0.0037	0	0.007	0	0	6
38	3	January	0.0012	0.0004	0	0	0.002	0	0.0037	0	0.007	0	0	6
39	3	February	0.0013	0.0004	0	0	0.002	0	0.0037	0	0.007	0	0	6
40	3	March	0.0013	0.0004	0	0	0.002	0	0.0038	0	0.007	0	0	6
41	3	April	0.0014	0.0004	0	0	0.002	0	0.0039	0	0.008	0	0	6
42	4	May	0.0014	0.0004	0	0	0.002	0	0.0039	0	0.008	0	0	6
43	4	June	0.0017	0.0005	0	0	0.002	0	0.004	0	0.008	0	0	6
44	4	July	0.0017	0.0005	0	0	0.002	0	0.004	0	0.008	0	0	6
45	4	August	0.0018	0.0005	0	0	0.002	0	0.0045	0	0.009	0	0	6
46	4	September	0.0018	0.0005	0	0	0.002	0	0.0049	0	0.009	0	0	6
47	4	October	0.0018	0.0005	0	0	0.002	0	0.0051	0	0.01	0	0	6

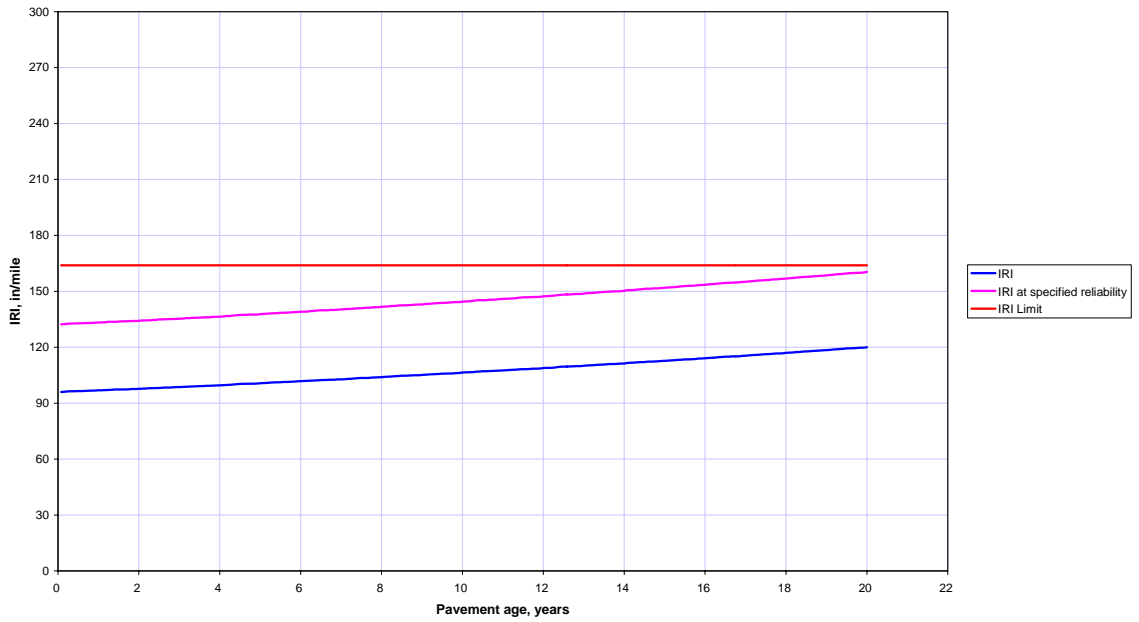
48	4	November	0.0018	0.0005	0	0	0.002	0	0.0052	0	0.01	0	6
49	4	December	0.0018	0.0005	0	0	0.002	0	0.0053	0	0.01	0	6
50	4	January	0.0018	0.0005	0	0	0.002	0	0.0053	0	0.01	0	6
51	4	February	0.0018	0.0005	0	0	0.002	0	0.0053	0	0.01	0	6
52	4	March	0.0018	0.0005	0	0	0.002	0	0.0054	0	0.01	0	6
53	4	April	0.0019	0.0005	0	0	0.003	0	0.0055	0	0.011	0.1	6.1
54	5	May	0.0019	0.0005	0	0	0.003	0	0.0055	0	0.011	0.1	6.1
55	5	June	0.0022	0.0006	0	0	0.003	0	0.0056	0	0.011	0.1	6.1
56	5	July	0.0023	0.0006	0	0	0.003	0	0.0056	0	0.011	0.1	6.1
57	5	August	0.0023	0.0006	0	0	0.003	0	0.006	0	0.012	0.1	6.1
58	5	September	0.0023	0.0006	0	0	0.003	0	0.0064	0	0.012	0.1	6.1
59	5	October	0.0023	0.0007	0	0	0.003	0	0.0067	0	0.013	0.1	6.1
60	5	November	0.0023	0.0007	0	0	0.003	0	0.0068	0	0.013	0.1	6.1
61	5	December	0.0023	0.0007	0	0	0.003	0	0.0068	0	0.013	0.1	6.1
62	5	January	0.0023	0.0007	0	0	0.003	0	0.0068	0	0.013	0.1	6.1
63	5	February	0.0024	0.0007	0	0	0.003	0	0.0069	0	0.013	0.1	6.1
64	5	March	0.0024	0.0007	0	0	0.003	0	0.0069	0	0.013	0.1	6.1
65	5	April	0.0025	0.0007	0	0	0.003	0	0.0071	0	0.014	0.1	6.1
66	6	May	0.0025	0.0007	0	0	0.003	0	0.0071	0	0.014	0.1	6.1
67	6	June	0.0028	0.0008	0	0	0.004	0	0.0072	0	0.014	0.1	6.1
68	6	July	0.0028	0.0008	0	0	0.004	0	0.0072	0	0.014	0.1	6.1
69	6	August	0.0028	0.0008	0	0	0.004	0	0.0076	0	0.015	0.1	6.1
70	6	September	0.0028	0.0008	0	0	0.004	0	0.008	0	0.015	0.1	6.1
71	6	October	0.0028	0.0008	0	0	0.004	0	0.0082	0	0.016	0.1	6.1
72	6	November	0.0028	0.0008	0	0	0.004	0	0.0083	0	0.016	0.1	6.1
73	6	December	0.0028	0.0008	0	0	0.004	0	0.0084	0	0.016	0.1	6.1
74	6	January	0.0029	0.0008	0	0	0.004	0	0.0084	0	0.016	0.1	6.1
75	6	February	0.0029	0.0008	0	0	0.004	0	0.0084	0	0.016	0.1	6.1
76	6	March	0.0029	0.0008	0	0	0.004	0	0.0084	0	0.016	0.1	6.1
77	6	April	0.003	0.0008	0	0	0.004	0	0.0086	0	0.016	0.1	6.1
78	7	May	0.003	0.0008	0	0	0.004	0	0.0086	0	0.016	0.1	6.1
79	7	June	0.0033	0.0009	0	0	0.004	0	0.0087	0	0.017	0.1	6.1
80	7	July	0.0033	0.0009	0	0	0.004	0	0.0087	0	0.017	0.1	6.1
81	7	August	0.0033	0.0009	0	0	0.004	0	0.0091	0	0.017	0.1	6.1
82	7	September	0.0034	0.0009	0	0	0.004	0.01	0.0095	0	0.018	0.1	6.1
83	7	October	0.0034	0.0009	0	0	0.004	0.01	0.0097	0	0.019	0.1	6.1
84	7	November	0.0034	0.0009	0	0	0.004	0.01	0.0098	0	0.019	0.1	6.1
85	7	December	0.0034	0.0009	0	0	0.004	0.01	0.0099	0	0.019	0.1	6.1
86	7	January	0.0034	0.0009	0	0	0.004	0.01	0.0099	0	0.019	0.1	6.1
87	7	February	0.0034	0.0009	0	0	0.004	0.01	0.0099	0	0.019	0.1	6.1
88	7	March	0.0034	0.0009	0	0	0.004	0.01	0.0099	0	0.019	0.1	6.1
89	7	April	0.0035	0.001	0	0	0.005	0.01	0.0101	0	0.019	0.1	6.1
90	8	May	0.0035	0.001	0	0	0.005	0.01	0.0101	0	0.019	0.1	6.1
91	8	June	0.0038	0.001	0	0	0.005	0.01	0.0102	0	0.019	0.1	6.1
92	8	July	0.0038	0.0011	0	0	0.005	0.01	0.0102	0	0.019	0.1	6.1
93	8	August	0.0039	0.0011	0	0	0.005	0.01	0.0106	0	0.02	0.2	6.3
94	8	September	0.0039	0.0011	0	0	0.005	0.01	0.011	0	0.021	0.2	6.3
95	8	October	0.0039	0.0011	0	0	0.005	0.01	0.0112	0	0.021	0.2	6.3
96	8	November	0.0039	0.0011	0	0	0.005	0.01	0.0113	0	0.022	0.2	6.3
97	8	December	0.0039	0.0011	0	0	0.005	0.01	0.0113	0	0.022	0.2	6.3
98	8	January	0.0039	0.0011	0	0	0.005	0.01	0.0114	0	0.022	0.2	6.3
99	8	February	0.0039	0.0011	0	0	0.005	0.01	0.0114	0	0.022	0.2	6.3
100	8	March	0.0039	0.0011	0	0	0.005	0.01	0.0114	0	0.022	0.2	6.3
101	8	April	0.004	0.0011	0	0	0.005	0.01	0.0116	0	0.022	0.2	6.3
102	9	May	0.004	0.0011	0	0	0.005	0.01	0.0116	0	0.022	0.2	6.3

103	9	June	0.0043	0.0012	0	0	0.006	0.01	0.0117	0	0.022	0.2	6.3
104	9	July	0.0044	0.0012	0	0	0.006	0.01	0.0117	0	0.022	0.2	6.3
105	9	August	0.0044	0.0012	0	0	0.006	0.01	0.0121	0	0.023	0.2	6.3
106	9	September	0.0044	0.0012	0	0	0.006	0.01	0.0125	0	0.024	0.2	6.3
107	9	October	0.0044	0.0012	0	0	0.006	0.01	0.0127	0	0.024	0.2	6.3
108	9	November	0.0044	0.0012	0	0	0.006	0.01	0.0128	0	0.024	0.2	6.3
109	9	December	0.0044	0.0012	0	0	0.006	0.01	0.0128	0	0.024	0.2	6.3
110	9	January	0.0044	0.0012	0	0	0.006	0.01	0.0128	0	0.024	0.2	6.3
111	9	February	0.0045	0.0012	0	0	0.006	0.01	0.0129	0	0.024	0.2	6.3
112	9	March	0.0045	0.0012	0	0	0.006	0.01	0.0129	0	0.025	0.2	6.3
113	9	April	0.0045	0.0012	0	0	0.006	0.01	0.013	0	0.025	0.2	6.3
114	10	May	0.0045	0.0012	0	0	0.006	0.01	0.013	0	0.025	0.2	6.3
115	10	June	0.0048	0.0013	0	0	0.006	0.01	0.0131	0.01	0.025	0.2	6.3
116	10	July	0.0049	0.0013	0	0	0.006	0.01	0.0132	0.01	0.025	0.2	6.3
117	10	August	0.0049	0.0013	0	0	0.006	0.01	0.0136	0.01	0.026	0.2	6.3
118	10	September	0.0049	0.0013	0	0	0.006	0.01	0.0139	0.01	0.026	0.2	6.3
119	10	October	0.0049	0.0013	0	0	0.006	0.01	0.0142	0.01	0.027	0.2	6.3
120	10	November	0.0049	0.0013	0	0	0.006	0.01	0.0142	0.01	0.027	0.3	6.4
121	10	December	0.0049	0.0013	0	0	0.006	0.01	0.0143	0.01	0.027	0.3	6.4
122	10	January	0.0049	0.0014	0	0	0.006	0.01	0.0143	0.01	0.027	0.3	6.4
123	10	February	0.005	0.0014	0	0	0.006	0.01	0.0143	0.01	0.027	0.3	6.4
124	10	March	0.005	0.0014	0	0	0.006	0.01	0.0144	0.01	0.027	0.3	6.4
125	10	April	0.0051	0.0014	0	0	0.006	0.01	0.0145	0.01	0.028	0.3	6.4
126	11	May	0.0051	0.0014	0	0	0.007	0.01	0.0145	0.01	0.028	0.3	6.4
127	11	June	0.0053	0.0015	0	0	0.007	0.01	0.0146	0.01	0.028	0.3	6.4
128	11	July	0.0054	0.0015	0	0	0.007	0.01	0.0147	0.01	0.028	0.3	6.4
129	11	August	0.0054	0.0015	0	0	0.007	0.01	0.015	0.01	0.029	0.3	6.4
130	11	September	0.0054	0.0015	0	0	0.007	0.01	0.0154	0.01	0.029	0.3	6.4
131	11	October	0.0054	0.0015	0	0	0.007	0.01	0.0157	0.01	0.03	0.3	6.4
132	11	November	0.0054	0.0015	0	0	0.007	0.01	0.0157	0.01	0.03	0.3	6.4
133	11	December	0.0054	0.0015	0	0	0.007	0.01	0.0158	0.01	0.03	0.3	6.4
134	11	January	0.0055	0.0015	0	0	0.007	0.01	0.0158	0.01	0.03	0.3	6.4
135	11	February	0.0055	0.0015	0	0	0.007	0.01	0.0158	0.01	0.03	0.3	6.4
136	11	March	0.0055	0.0015	0	0	0.007	0.01	0.0159	0.01	0.03	0.3	6.4
137	11	April	0.0056	0.0015	0	0	0.007	0.01	0.016	0.01	0.03	0.3	6.4
138	12	May	0.0056	0.0015	0	0	0.007	0.01	0.016	0.01	0.03	0.3	6.4
139	12	June	0.0059	0.0016	0	0	0.008	0.01	0.0161	0.01	0.031	0.3	6.4
140	12	July	0.0059	0.0016	0	0	0.008	0.01	0.0161	0.01	0.031	0.3	6.4
141	12	August	0.0059	0.0016	0	0	0.008	0.01	0.0165	0.01	0.031	0.3	6.4
142	12	September	0.006	0.0016	0	0	0.008	0.01	0.0169	0.01	0.032	0.3	6.4
143	12	October	0.006	0.0016	0	0	0.008	0.01	0.0171	0.01	0.032	0.3	6.4
144	12	November	0.006	0.0016	0	0	0.008	0.01	0.0172	0.01	0.033	0.3	6.4
145	12	December	0.006	0.0016	0	0	0.008	0.01	0.0173	0.01	0.033	0.3	6.4
146	12	January	0.006	0.0016	0	0	0.008	0.01	0.0173	0.01	0.033	0.3	6.4
147	12	February	0.006	0.0016	0	0	0.008	0.01	0.0173	0.01	0.033	0.3	6.4
148	12	March	0.006	0.0016	0	0	0.008	0.01	0.0173	0.01	0.033	0.3	6.4
149	12	April	0.0061	0.0017	0	0	0.008	0.01	0.0175	0.01	0.033	0.4	6.6
150	13	May	0.0061	0.0017	0	0	0.008	0.01	0.0175	0.01	0.033	0.4	6.6
151	13	June	0.0064	0.0017	0	0	0.008	0.01	0.0176	0.01	0.033	0.4	6.6
152	13	July	0.0064	0.0017	0	0	0.008	0.01	0.0176	0.01	0.033	0.4	6.6
153	13	August	0.0065	0.0018	0	0	0.008	0.01	0.018	0.01	0.034	0.4	6.6
154	13	September	0.0065	0.0018	0	0	0.008	0.01	0.0184	0.01	0.035	0.4	6.6
155	13	October	0.0065	0.0018	0	0	0.008	0.01	0.0186	0.01	0.035	0.4	6.6
156	13	November	0.0065	0.0018	0	0	0.008	0.01	0.0187	0.01	0.035	0.4	6.6
157	13	December	0.0065	0.0018	0	0	0.008	0.01	0.0188	0.01	0.036	0.4	6.6

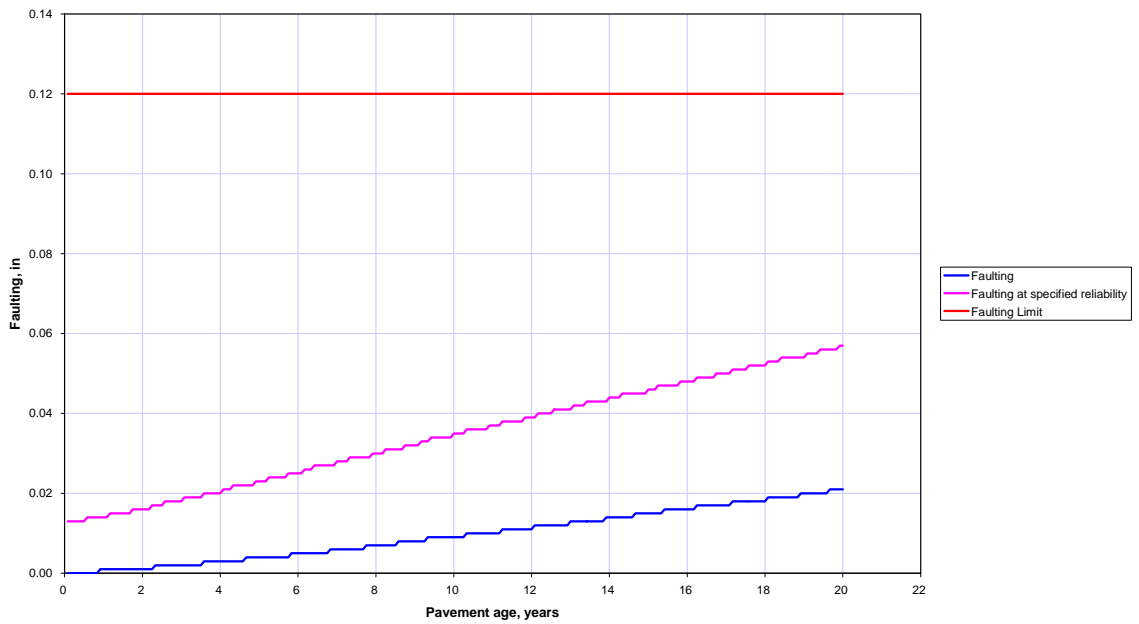
158	13	January	0.0065	0.0018	0	0	0.008	0.01	0.0188	0.01	0.036	0.4	6.6
159	13	February	0.0065	0.0018	0	0	0.008	0.01	0.0188	0.01	0.036	0.4	6.6
160	13	March	0.0065	0.0018	0	0	0.008	0.01	0.0188	0.01	0.036	0.4	6.6
161	13	April	0.0066	0.0018	0	0	0.008	0.01	0.019	0.01	0.036	0.4	6.6
162	14	May	0.0066	0.0018	0	0	0.008	0.01	0.019	0.01	0.036	0.4	6.6
163	14	June	0.0069	0.0019	0	0	0.009	0.01	0.0191	0.01	0.036	0.4	6.6
164	14	July	0.007	0.0019	0	0	0.009	0.01	0.0191	0.01	0.036	0.4	6.6
165	14	August	0.007	0.0019	0	0	0.009	0.01	0.0195	0.01	0.037	0.4	6.6
166	14	September	0.007	0.0019	0	0	0.009	0.01	0.0199	0.01	0.038	0.4	6.6
167	14	October	0.007	0.0019	0	0	0.009	0.01	0.0201	0.01	0.038	0.4	6.6
168	14	November	0.007	0.0019	0	0	0.009	0.01	0.0202	0.01	0.038	0.4	6.6
169	14	December	0.007	0.0019	0	0	0.009	0.01	0.0203	0.01	0.038	0.5	6.7
170	14	January	0.007	0.0019	0	0	0.009	0.01	0.0203	0.01	0.038	0.5	6.7
171	14	February	0.0071	0.0019	0	0	0.009	0.01	0.0203	0.01	0.038	0.5	6.7
172	14	March	0.0071	0.0019	0	0	0.009	0.01	0.0203	0.01	0.039	0.5	6.7
173	14	April	0.0072	0.0019	0	0	0.009	0.01	0.0205	0.01	0.039	0.5	6.7
174	15	May	0.0072	0.0019	0	0	0.009	0.01	0.0205	0.01	0.039	0.5	6.7
175	15	June	0.0075	0.002	0	0	0.01	0.01	0.0206	0.01	0.039	0.5	6.7
176	15	July	0.0075	0.002	0	0	0.01	0.01	0.0206	0.01	0.039	0.5	6.7
177	15	August	0.0075	0.002	0	0	0.01	0.01	0.021	0.01	0.04	0.5	6.7
178	15	September	0.0075	0.002	0	0	0.01	0.01	0.0214	0.01	0.04	0.5	6.7
179	15	October	0.0076	0.002	0	0	0.01	0.01	0.0216	0.01	0.041	0.5	6.7
180	15	November	0.0076	0.002	0	0	0.01	0.01	0.0217	0.01	0.041	0.5	6.7
181	15	December	0.0076	0.002	0	0	0.01	0.01	0.0218	0.01	0.041	0.5	6.7
182	15	January	0.0076	0.002	0	0	0.01	0.01	0.0218	0.01	0.041	0.5	6.7
183	15	February	0.0076	0.0021	0	0	0.01	0.01	0.0218	0.01	0.041	0.5	6.7
184	15	March	0.0076	0.0021	0	0	0.01	0.01	0.0219	0.01	0.041	0.5	6.7
185	15	April	0.0077	0.0021	0	0	0.01	0.01	0.022	0.01	0.042	0.5	6.7
186	16	May	0.0077	0.0021	0	0	0.01	0.01	0.022	0.01	0.042	0.5	6.7
187	16	June	0.008	0.0022	0	0	0.01	0.01	0.0221	0.01	0.042	0.5	6.7
188	16	July	0.008	0.0022	0	0	0.01	0.01	0.0221	0.01	0.042	0.5	6.7
189	16	August	0.0081	0.0022	0	0	0.01	0.01	0.0225	0.01	0.043	0.5	6.7
190	16	September	0.0081	0.0022	0	0	0.01	0.01	0.0229	0.01	0.043	0.6	6.9
191	16	October	0.0081	0.0022	0	0	0.01	0.01	0.0232	0.01	0.044	0.6	6.9
192	16	November	0.0081	0.0022	0	0	0.01	0.01	0.0232	0.01	0.044	0.6	6.9
193	16	December	0.0081	0.0022	0	0	0.01	0.01	0.0233	0.01	0.044	0.6	6.9
194	16	January	0.0081	0.0022	0	0	0.01	0.01	0.0233	0.01	0.044	0.6	6.9
195	16	February	0.0082	0.0022	0	0	0.01	0.01	0.0233	0.01	0.044	0.6	6.9
196	16	March	0.0082	0.0022	0	0	0.01	0.01	0.0234	0.01	0.044	0.6	6.9
197	16	April	0.0082	0.0022	0	0	0.011	0.01	0.0235	0.01	0.044	0.6	6.9
198	17	May	0.0082	0.0022	0	0	0.011	0.01	0.0235	0.01	0.044	0.6	6.9
199	17	June	0.0085	0.0023	0	0	0.011	0.01	0.0236	0.01	0.045	0.6	6.9
200	17	July	0.0086	0.0023	0	0	0.011	0.01	0.0237	0.01	0.045	0.6	6.9
201	17	August	0.0086	0.0023	0	0	0.011	0.01	0.024	0.01	0.045	0.6	6.9
202	17	September	0.0086	0.0023	0	0	0.011	0.01	0.0244	0.01	0.046	0.6	6.9
203	17	October	0.0086	0.0023	0	0	0.011	0.01	0.0247	0.01	0.047	0.6	6.9
204	17	November	0.0086	0.0023	0	0	0.011	0.01	0.0248	0.01	0.047	0.6	6.9
205	17	December	0.0086	0.0023	0	0	0.011	0.01	0.0248	0.01	0.047	0.6	6.9
206	17	January	0.0087	0.0023	0	0	0.011	0.01	0.0248	0.01	0.047	0.6	6.9
207	17	February	0.0087	0.0023	0	0	0.011	0.01	0.0249	0.01	0.047	0.6	6.9
208	17	March	0.0087	0.0023	0	0	0.011	0.01	0.0249	0.01	0.047	0.6	6.9
209	17	April	0.0088	0.0024	0	0	0.011	0.01	0.0251	0.01	0.047	0.6	6.9
210	18	May	0.0088	0.0024	0	0	0.011	0.01	0.0251	0.01	0.047	0.6	6.9
211	18	June	0.0091	0.0024	0	0	0.012	0.01	0.0252	0.01	0.048	0.6	6.9
212	18	July	0.0091	0.0024	0	0	0.012	0.01	0.0252	0.01	0.048	0.7	7

213	18	August	0.0092	0.0025	0	0	0.012	0.01	0.0256	0.01	0.048	0.7	7	
214	18	September	0.0092	0.0025	0	0	0.012	0.01	0.026	0.01	0.049	0.7	7	
215	18	October	0.0092	0.0025	0	0	0.012	0.01	0.0262	0.01	0.05	0.7	7	
216	18	November	0.0092	0.0025	0	0	0.012	0.01	0.0263	0.01	0.05	0.7	7	
217	18	December	0.0092	0.0025	0	0	0.012	0.01	0.0264	0.01	0.05	0.7	7	
218	18	January	0.0092	0.0025	0	0	0.012	0.01	0.0264	0.01	0.05	0.7	7	
219	18	February	0.0093	0.0025	0	0	0.012	0.01	0.0264	0.01	0.05	0.7	7	
220	18	March	0.0093	0.0025	0	0	0.012	0.01	0.0265	0.01	0.05	0.7	7	
221	18	April	0.0093	0.0025	0	0	0.012	0.01	0.0266	0.01	0.05	0.7	7	
222	19	May	0.0094	0.0025	0	0	0.012	0.01	0.0266	0.01	0.05	0.7	7	
223	19	June	0.0097	0.0026	0	0	0.012	0.01	0.0267	0.01	0.05	0.7	7	
224	19	July	0.0097	0.0026	0	0	0.012	0.01	0.0267	0.01	0.05	0.7	7	
225	19	August	0.0097	0.0026	0	0	0.012	0.01	0.0271	0.01	0.051	0.7	7	
226	19	September	0.0097	0.0026	0	0	0.012	0.01	0.0276	0.01	0.052	0.8	7.1	
227	19	October	0.0098	0.0026	0	0	0.012	0.01	0.0278	0.01	0.052	0.8	7.1	
228	19	November	0.0098	0.0026	0	0	0.012	0.01	0.0279	0.01	0.053	0.8	7.1	
229	19	December	0.0098	0.0026	0	0	0.012	0.01	0.0279	0.01	0.053	0.8	7.1	
230	19	January	0.0098	0.0026	0	0	0.012	0.01	0.0279	0.01	0.053	0.8	7.1	
231	19	February	0.0098	0.0026	0	0	0.013	0.01	0.028	0.01	0.053	0.8	7.1	
232	19	March	0.0098	0.0026	0	0	0.013	0.01	0.028	0.01	0.053	0.8	7.1	
233	19	April	0.0099	0.0026	0	0	0.013	0.01	0.0282	0.01	0.053	0.8	7.1	
234	20	May	0.0099	0.0026	0	0	0.013	0.01	0.0282	0.01	0.053	0.8	7.1	
235	20	June	0.0102	0.0027	0	0	0.013	0.01	0.0283	0.01	0.053	0.8	7.1	
236	20	July	0.0103	0.0027	0	0	0.013	0.01	0.0283	0.01	0.053	0.8	7.1	
237	20	August	0.0103	0.0027	0	0	0.013	0.01	0.0287	0.01	0.054	0.8	7.1	
238	20	September	0.0103	0.0028	0	0	0.013	0.01	0.0291	0.01	0.055	0.8	7.1	
239	20	October	0.0103	0.0028	0	0	0.013	0.02	0.0294	0.01	0.055	0.8	7.1	
240	20	November	0.0103	0.0028	0	0	0.013	0.02	0.0295	0.01	0.056	0.8	7.1	
							0.0131					0.0555		

Predicted IRI



Predicted Faulting



Predicted Cracking

